Raman Microscopic and Computational Studies of Artists' Pigments and Molecular Inorganic Compounds

By

Katherine Louise Brown

A thesis submitted in partial fulfilment of the requirements of the degree of Doctor of Philosophy

Christopher Ingold Laboratories
Department of Chemistry
University College London

University of London
October 2002

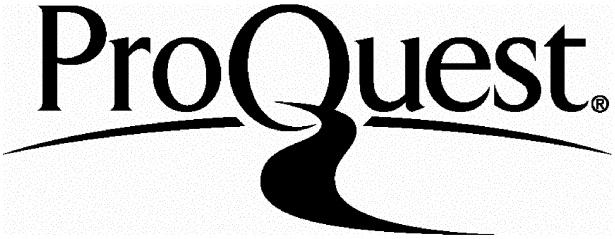

Abstract

This thesis is principally concerned with spectroscopic and computational studies of artists' pigments. Manuscripts, art and archaeological artefacts were examined by Raman microscopy, identifying the pigments and drawing conclusions for historical and conservation purposes.

Studies of Anglo Saxon and later manuscripts have shown the Insular palette triumvirate, assumed to be orpiment, red lead and verdigris, to contain red ochre and vergaut, but no verdigris. This remains unchanged until the introduction of lazurite in c.920 AD and vermilion in the 12^{th} century. Lazurite has been erroneously identified on the Lindisfarne Gospels, by the technique of Roosen-Runge. Raman microscopy shows the blue pigments to be exclusively indigo, casting doubt on analyses performed using Roosen-Runge's technique.

The Islamic manuscript palette was found to be remarkably consistent across a substantial geographical area over an extended period. It is also very similar to that of early Western manuscripts. Comparison of these results with existing literary sources has shown the latter to be highly inaccurate.

The palette of William Blake was examined and compared to results of analysis by False Colour Infrared Photography (FC-IP). The FC-IP technique was determined to be inappropriate for pigment identification.

Two significant artefacts were shown to be modern forgeries: a rare Assyrian fresco contains a modern green pigment, and the world famous Vinland map was found to have significant quantities of anatase in the yellow lines.

Density Functional Theory methods were applied to the mechanism of decay isomerisation of As_4S_4, which was partially clarified, and to the geometries of R_2SeX_2 (R = CF_3, CF_2H, CFH_2, CH_3, CH_2CH_3, $CH(CH_3)_2$, t-Butyl, X = F, Cl, Br, I, At). The most stable geometry was found to be determined by the polarity of the Se–X bonds and the steric and electron-withdrawal effects of the R-group on the C–Se bond strength.

Acknowledgements

This work would not have been possible without the help and support of a great many people.

My parents are responsible for my existence and have been paying the penalties, financial and otherwise, with great forbearance ever since! Thank you.

My thanks is certainly owed and gratefully given to my supervisors, Dr. Nikolas Kaltsoyannis for his constant encouragement and assistance, both intellectual and practical, and Professor Robin Clark for his contribution.

The majority of this thesis is concerned with the results of collaborations with a number of major institutions.

At the British Library, I could not even have begun without David Jacobs and the conservation staff of Studios D and C. Dr. Michelle Brown and Dr. Muhammad Isa Whaley gave me the freedom of their collections and access to some of the most singularly beautiful and significant objects I have ever seen.

At the Victoria and Albert Museum and the Tate Gallery I am indebted to Mike Wheeler, Noa Cahaner McManus, Piers Townsend and Dr. Joyce Townsend, all of whom cheerfully accepted the complete chaos that follows in my wake and made me feel welcome in their studios and laboratories.

In the USA, I have to thank Theresa Fairbanks-Harris, Amy Gerbracht and Juliet Desmond of the Yale Centre for British Art, and Bob Babcock of the Beinecke Manuscript and Rare Book Library. For this field trip the support of Renishaw PLC and especially Annette Zimmermann was essential.

At UCL, my friends and colleagues were a constant source of information, encouragement and entertainment especially Dr. Steve Firth, Dr. Tracey Chaplin and the occupants, past and present, of 132 and G25: Amanda, Dickon, Maria Rosa, Dirk, Aileen, Linnea, Emma, Simon and Natalie. Thanks guys!

Dr. Martin Gilbert has been a dear friend and advisor. He bravely read and commented on the entire document. That said, the mistakes are all mine!

Dr. Andrew Wills has been a tremendous source of help, advice and guidance. He has come to be a most greatly valued friend.

Contents

Figures

Tables

Glossary

Codicology	The study of manuscripts as cultural artefacts for historical purposes.
Colophon	An inscription at the beginning or end of a manuscript detailing facts relevant to its production such as the name of the scribe.
Divan	A collection of poetry.
Folio	A single sheet in a manuscript.
Gathering	A collection of folios bound together.
Gouache	Watercolour bound with gum.
Mandorla	An oval shaped decorative device.
Paleography	The study of the development of ancient writing.
Quire	A gathering of four sheets, folded once.
Recto	The side of the folio to be read first.
Sutra	A chapter in an Oriental manuscript.
Tempera	A painting medium in which the pigment is bound with egg.
Unvan	A decorated chapter heading.
Vergaut	A green pigment produced by combining blue and yellow pigments.
Verso	The side of the folio to be read second.

Note: Some dates have been given in both the Gregorian and the Islamic calender. In the Islamic calendar dates are given relative to the migration of the Prophet to Medina – the *hegira*, 16th July 622 AD. It is based on the lunar year and consequently has years roughly 11 days shorter than those of the solar year. To convert from hegira years (H) to the Gregorian calendar (C) use the following formula:

$H \times 32/33 + 622 = C.$

Pigments

The chemical formulae of the pigments found in this study are listed below. Reference Raman spectra may be found in appendix 6. [Bell, Burg]

Anatase	TiO_2
Azurite	$2CuCO_3.Cu(OH)_2$
Barytes	$BaSO_4$
Carbon	C_n
Chalk	$CaCO_3$
Gypsum	$CaSO_4.2H_2O$
Indigo	Indigotin, $C_{16}H_{10}N_2O_2$
Lazurite	$Na_8[Al_6Si_6O_{24}]S_n$
Litharge	PbO
Orpiment	As_2S_3
Pararealgar	As_4S_4
Prussian Blue	$Fe_4[Fe(CN)_6]_3.14\text{-}16H_2O$
Realgar	As_4S_4
Red Lead	Pb_3O_4
Red Ochre	Fe_2O_3
Verdigris	$Cu(CH_3COO)_2$
Vermilion	HgS
White Lead	$2PbCO_3.Pb(OH)_2$

Chapter 1: Introduction

Not all those who wander are lost

The Lord of the Rings
J. R. R. Tolkien
1954

This thesis represents the first major step in a significant undertaking in cross-disciplinary research, encompassing conservation, art history, spectroscopy and computational chemistry. Although seemingly unrelated, these areas are closely interconnected and initially shared a common direction: the scientific analysis and identification of materials used in the production of works of art and archaeological artefacts and the knowledge that this information reveals.

1.1: Raman Microscopy and the Analysis of Art and Artefacts

The scientific analysis of art and artefacts is important for several reasons, as is discussed in chapter 2. In terms of the conservation of an object, it is essential to know the nature of the materials from which it is composed. This in turn can lead to interesting studies of the nature and products of any decay and the application of methods to prevent or lessen the impact of that decay. Considerable historical information is also found in the identification of the materials themselves: which materials were used by the artisans manufacturing the object; were the materials known to be locally available, imported along trade routes or the product of novel manufacturing techniques? The movement of ideas and groups of people can be found in the spread of particular materials, using the record found in the artefacts themselves. Finally, authentication of art objects is made considerably easier if information about the nature of the materials from which they would be expected to be composed is available.

The ultimate aim of this work was the production of an historico-geographical map of the use of pigments globally through history, from prehistoric times to the present day. It is hoped that this map would provide considerable information to scholars. Variation

in the use of pigments historically and geographically would allow unprovenanced objects to be placed more accurately within the historico-geographical framework and would greatly assist in the authentication of newly discovered materials. Technological development within a culture could be assessed from the sophistication of the materials that it produced. The spread of materials and technologies with migratory patterns or trade and communication routes would be obvious from the development of the use of those materials.

Raman microscopy is now recognised as an excellent tool for the non-destructive analysis of materials related to the production of art objects, whether they are modern painting materials or ancient archaeological artefacts. Although less suitable for the analysis of organic materials, the identification of mineral pigments is very fast and can be achieved with no damage to the object in question.

The results in this thesis represent a first step in the development of such a map, considering the development of manuscript illustration in two major cultures, and applying existing knowledge of pigment use to authenticate materials of doubtful origin.

The theory and instrumentation for the analysis are presented in chapter 2. Thereafter the results of the analysis of a variety of materials are presented and discussed: Anglo Saxon and later manuscripts from the British Library in chapter 3, a range of Islamic material from the British Library and Victoria and Albert Museum in chapter 4. Chapter 5 contains a pigment analysis of the work of the English artist, William Blake, from the Tate Gallery, and a comparison with a pigment analysis of the same material by an alternative technique. The analysis and authentication of two significant pieces, Assyrian frescos from a private collection and the Vinland Map from Yale University, are described in chapters 6 and 7.

1.2: Computational Chemistry

Common to almost all the material studied by Raman microscopy is the theme of pigment degradation. The degradation of realgar (As_4S_4), in particular, has been the subject of a number of recent publications. To understand the processes occurring within the realgar molecule as it alters, an attempt was made to model the decay channel using computational techniques.

Density functional theory, and its specific application in the Amsterdam Density Functional program suite, is described in chapter 8. Attempts to model the decay of realgar into pararealgar are described in chapter 9. Chapter 10 contains an unrelated series of calculations of the structure and bonding of dihalogendiorganoselenium compounds – having already acquired the necessary computational resources and techniques they were used as far as possible!

1.3: Additional Parts

The majority of the material examined is of great visual interest so this thesis includes a number of appendices devoted to colour pictures. In the scientific analysis of works of art, context is everything; therefore for completeness an image of every work of art and every page of every manuscript that is discussed is located in the appropriate appendix. Appendices have been used to avoid disturbing the body of the text with inconvenient intrusions.

Since the work has been cross-disciplinary and the vocabulary required for the discussion of manuscripts particularly is not familiar to a scientific audience, a glossary has been included.

References are given in the format [REF] where REF represents the first four letters of the principal author's surname or some other major point of distinction such as the title of a computer program. For example, [Back] represents "The Lindisfarne Gospels, Janet Backhouse, 1992, Phaidon Press Ltd., London." All references are given together in one section.

Being granted access to the materials that I have examined has been an unprecedented privilege that I have enjoyed a great deal. The results that have been produced are uniquely situated at the arts/science interface and, I hope, will generate new insights for the scientist, conservator and historian alike.

Chapter 2: Raman Spectroscopy

To call up a demon you must learn its name.

Neuromancer
William Gibson
1983

This chapter is primarily devoted to describing Raman spectroscopy, the technique that forms the basis for the experimental work detailed in this thesis. After a brief description of the discovery of the Raman effect, a classical treatment of the underlying theory will be recounted followed by the current state of technological development. Finally the application of Raman microscopy to art and archaeology is discussed.

2.1: History

In 1921 the Indian scientist Chandrasekhara Raman began the investigations for which he would win the Nobel Prize in 1930. He had become interested in the phenomenon of light scattering through liquids whilst observing the intense blue colour of the Mediterranean Sea. [Long] He proposed that the sunlight was being scattered by the water molecules and began experiments to test this assertion. Following a discussion on the recently discovered Compton effect, Raman published a quantitative theory in 1927 that convinced him that an optical analogue must exist. In 1928, using only natural light and, by modern standards, very rudimentary equipment Raman and his student, K. S. Krishnan, discovered that it was possible for liquids and gases to scatter light at both the incident wavelength and at a modified one. A note to Nature followed [Rama] and the apparent simplicity of the effect and ease with which it could be seen soon engendered contributions from around the world.

2.2: Theory of the Raman Effect

Much of molecular spectroscopy is concerned with the interaction between incident electromagnetic radiation and the electronic dipole moment of a molecule. [Banw] This interaction only occurs (in the absence of higher order effects such as changes in the quadrupole moment) if there is a change in the electronic dipole moment of the molecule.

Molecular electron clouds may experience four different sorts of motion, three of which can change the electronic dipole moment of the molecule. Transitions between electronic states can alter the distribution of the electron cloud between nuclei. The molecule may rotate, changing the orientation of the electron cloud, and vibrate, a motion of the nuclei with respect to each other, which may disturb the electron cloud. Finally, a translation of the molecule's centre of mass may occur but this does not alter the electronic dipole moment as the centre of mass moves as a notional free particle.

The three internal degrees of freedom of the molecule by which the electronic dipole moment may be changed interact with the incident radiation field to produce complex spectra. The spectra are unlike those of the isolated atom where the interaction is effected solely by the motion of electrons with respect to the nucleus. The energies and timescales of these motions are sufficiently different that they can be considered separately, the Born-Oppenheimer approximation, even though they may be occurring simultaneously. [Banw] This is made possible by neglecting small terms in the solution to the Schrödinger equation and it means, in effect, that the electronic, vibrational and rotational motions can be considered independently. This approximation results in the total energy of the motions of the molecule being the sum of the energies of the individual motions

$$E_{tot} = E_{elec} + E_{vib} + E_{rot} \qquad (2.1)$$

For example, if we are considering the electronic energy of a diatomic molecule, the nuclei can be considered to be at equilibrium internuclear separation as though the molecule were not vibrating because they are very much more massive than the electrons. [Laid]

Raman spectroscopy can be used to probe the electronic, vibrational and rotational states of molecules. The classical treatment of Raman scattering below adequately describes the origin of vibration spectra, producing results that remain valid under quantum mechanical considerations. However, for the purposes of this work, rotational and electronic Raman spectra were not studied, so they will not be considered further here. The vibrations of diatomic molecules will first be treated classically and the quantum mechanical considerations will be introduced (section 2.2.2.).

2.2.1. The vibrations of diatomic molecules – a classical treatment

A diatomic molecule consists of two atoms of mass m_1 and m_2, at a distance r_1 and r_2 from their equilibrium centre of gravity, connected by a chemical bond. (Figure 2.1) [Ferr]

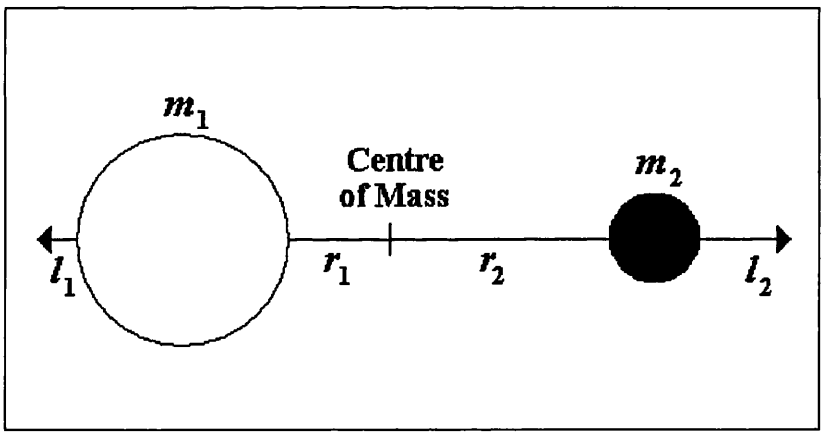

Figure 2.1: The vibration of a diatomic molecule.

If the atoms are displaced by l_1 and l_2 from their equilibrium positions, conservation of the centre of mass requires that

$$m_1 r_1 = m_2 r_2 \tag{2.2}$$

$$m_1(r_1 + l_1) = m_2(r_2 + l_2) \tag{2.3}$$

If these equations are combined then

$$l_1 = \left(\frac{m_2}{m_1}\right) l_2 \quad \text{and} \quad l_2 = \left(\frac{m_1}{m_2}\right) l_1 \tag{2.4}$$

Classically, the chemical bond is considered as a spring that obeys Hooke's law, [Laid] so the restoring force, f, is given by

$$f = -K(l_1 + l_2) \tag{2.5}$$

where K is the force constant.

Substituting (2.4) into (2.5) gives

$$f = -K\left(\frac{m_1 + m_2}{m_1}\right)l_2 = -K\left(\frac{m_1 + m_2}{m_2}\right)l_1 \tag{2.6}$$

Using (2.6) in Newton's equation of motion for each atom

$$m_1 \frac{\mathrm{d}^2 l_1}{\mathrm{d}t^2} = -K\left(\frac{m_1 + m_2}{m_2}\right)l_1 \tag{2.7}$$

$$m_2 \frac{\mathrm{d}^2 l_2}{\mathrm{d}t^2} = -K\left(\frac{m_1 + m_2}{m_2}\right)l_2 \tag{2.8}$$

multiplying (2.7) by $\left(\frac{m_2}{m_1 + m_2}\right)$ and (2.8) by $\left(\frac{m_1}{m_1 + m_2}\right)$ and adding gives

$$\frac{m_1 m_2}{m_1 + m_2}\left(\frac{\mathrm{d}^2 l_1}{\mathrm{d}t^2} + \frac{\mathrm{d}^2 l_2}{\mathrm{d}t^2}\right) = -K(l_1 + l_2) \tag{2.9}$$

In terms of the reduced mass μ and the total displacement x the equation of motion for the system becomes

$$\mu \frac{\mathrm{d}^2 x}{\mathrm{d}t^2} = -Kx \tag{2.10}$$

where $\mu = \frac{m_1 m_2}{m_1 + m_2}$, to which the solution is

$$x = x_0 \sin(2\pi v_0 t + \varphi) \tag{2.11}$$

where x_0 is the maximum displacement, φ the phase constant and v_0 the classical vibration frequency is given by

$$v_0 = \frac{1}{2\pi}\sqrt{\frac{K}{\mu}} \tag{2.12}$$

The potential energy of the system (V) is determined from

$$\mathrm{d}V = -f\,\mathrm{d}x = Kx\,\mathrm{d}x \tag{2.13}$$

Accordingly, by integration and substitution

$$\begin{aligned} V &= \tfrac{1}{2}Kx^2 \\ &= 2\pi^2 v_0^2 \mu x_0^2 \sin^2(2\pi v_0 t + \varphi) \end{aligned} \tag{2.14}$$

The kinetic energy (T) is

$$T = \frac{1}{2}m_1\left(\frac{dx_1}{dt}\right)^2 + \frac{1}{2}m_2\left(\frac{dx_2}{dt}\right)^2$$
$$= 2\pi^2 v_0^2 \mu x_0^2 \cos^2(2\pi v_0 t + \varphi) \qquad (2.15)$$

So E, the total energy, is given by

$$E = T + V$$
$$= 2\pi^2 v_0^2 \mu x_0^2 \qquad (2.16)$$
$$= \text{constant}$$

If V is plotted as a function of x the following parabolic potential is produced. (Figure 2.2) The potential $V = \frac{1}{2}Kx^2$, $E = T$ at $x = 0$ and $E = V$ at $x = \pm x_0$. This describes the vibrations of an harmonic oscillator.

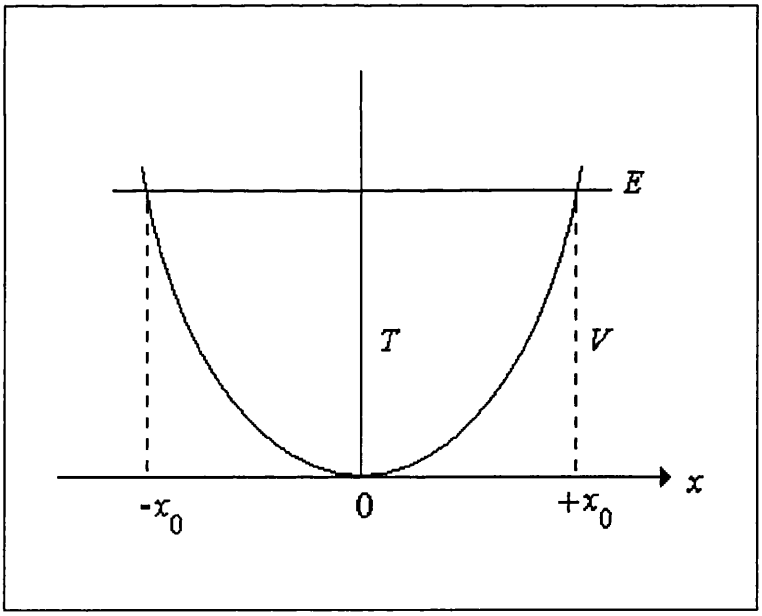

Figure 2.2: Potential energy diagram for a harmonic oscillator.

2.2.2. The vibrations of a diatomic molecule - a quantum mechanical description

A vibrating diatomic molecule can be treated as a single particle of reduced mass μ with potential energy given by (2.14) according to quantum mechanics. The one-dimensional time-independent Schrödinger wave equation is

$$\frac{d^2\psi}{dx^2} + \frac{2m}{\hbar^2}(E - V)\psi = 0 \qquad (2.17)$$

In terms of the reduced mass and displacement of a vibrating diatomic molecule, this becomes

$$\frac{d^2\psi}{dx^2}+\frac{8\pi^2\mu}{h^2}\left(E-\frac{1}{2}Kx^2\right)\psi=0 \tag{2.18}$$

If ψ is single valued, finite and continuous then the solution of this equation gives the eigenvalues

$$E_v = h\nu\left(v+\tfrac{1}{2}\right) \tag{2.19}$$

where v is the vibrational quantum number with values 0, 1, 2, 3,... and the vibrational frequency ν is given by

$$\nu=\frac{1}{2\pi}\sqrt{\frac{K}{\mu}} \tag{2.20}$$

Although the classical and quantum treatments of the simple harmonic oscillator give the same resultant vibrational frequency, certain differences should be noted. Classically $E = 0$ at $x = 0$ and the change in vibrational energy is continuous. In quantum mechanics the lowest energy state, $v = 0$, has energy $\frac{1}{2}h\nu$, the zero point energy. Further, the energy changes in discrete units of $h\nu$, with a selection rule $\Delta v = \pm 1$ dictated by the symmetry of the potential.

2.2.3. The effects of anharmonicity

A key consideration is that real molecules do not exactly follow Hooke's Law and so do not undergo simple harmonic motion. Molecules will dissociate at large internuclear displacement and their bonds are not perfectly elastic. The actual shape of the potential for an anharmonic vibrating diatomic molecule is described to a good approximation by the empirical Morse potential:

$$V = D_e\left(1-e^{-\beta x}\right)^2 \tag{2.21}$$

where D_e is the dissociation energy and β a measure of the curvature at the bottom of the well. [Banw] Solving the Schrödinger equation with this potential gives the eigenvalues

$$E_v = hc\omega_e\left(v+\tfrac{1}{2}\right)-hc\chi_e\omega_e\left(v+\tfrac{1}{2}\right)^2+... \tag{2.22}$$

where ω_e is the wavenumber corrected for anharmonicity and $\chi_e\omega_e$ is a measure of that anharmonicity.

It can be seen from (2.22) that the energy levels of the anharmonic oscillator are not equidistant but decrease in separation with increasing v.

In the harmonic oscillator potential a selection rule of $\Delta v = \pm 1$ applies. In the anharmonic case transitions involving $\Delta v = \pm 1, \pm 2, \pm 3, \ldots$ are allowed, although transitions of $\Delta v > 1$ are observed to be of rapidly diminishing probability. The $v = 0 \leftrightarrow 1$ transition is the strongest at room temperature as a result of Maxwell-Boltzmann statistics and is called the fundamental. The less intense transitions, $v = 0 \leftrightarrow \geq 2$, are called overtones.

2.2.4. The vibrations of polyatomic molecules

Diatomic molecules have only one mode of vibration dependant solely upon the internuclear separation. The positions and motions of a molecule containing N nuclei require 3N coordinates to describe them. Of these, the coordinates describing the rotations (3) and translations (3) can be neglected since they have no effect on the vibrations of the molecule, so for a polyatomic molecule there are 3N - 6 fundamental modes of vibration. In the case of linear molecules, only two rotational modes are distinguishable as rotation about the molecular axis has no effect and so there are 3N - 5 fundamental vibrational frequencies.

The independent normal modes of a polyatomic molecule may be illustrated with reference to carbon dioxide (CO_2). CO_2 is a linear tri-atomic molecule and as such it has four fundamental modes. (N = 3, 3N – 5 = 4). (Figure 2.3) Although the CO_2 molecule vibrates in a complex fashion, this vibration is entirely composed of combinations of the four normal vibrations. It should be noted that the pair of vibrations labelled v_2 are doubly degenerate as they have the same frequency but vibrate at 90° to one another.

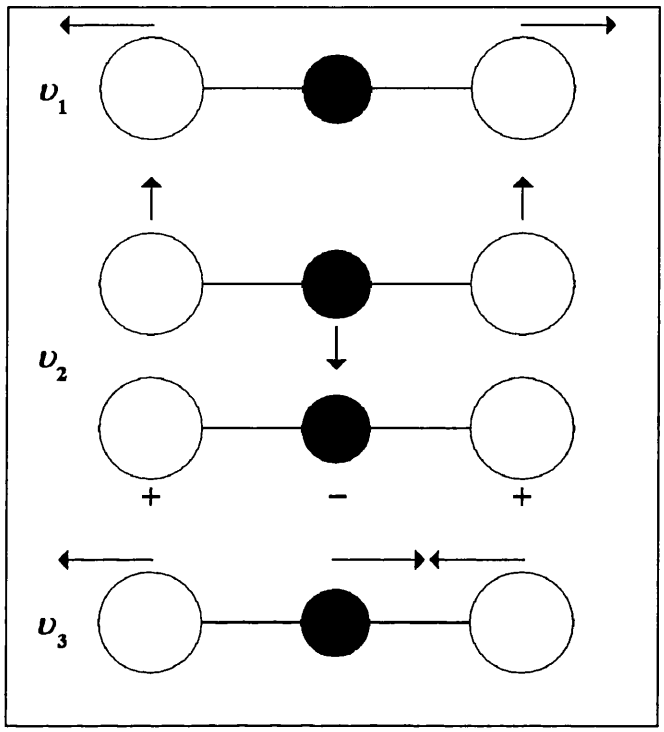

Figure 2.3: The four fundamental modes of vibration of CO_2. Motion into and out of the page is indicated by + and -.

2.2.5. The origin of the Raman effect

Scattering of light at a different frequency from that of the incident light is called the Raman effect. It arises from the interaction of the electric field of a photon with the electronic dipole moment of a molecule. When a sample is irradiated, scattered light is observed at the same frequency as the incident light (Rayleigh scattering), whilst Raman scattering is weaker (~10^{-5} of the incident beam) and of a different frequency. [Ferr]

The electric field strength of an electromagnetic wave is given by

$$\boldsymbol{E} = \boldsymbol{E}_0 \cos 2\pi \nu_0 t \tag{2.23}$$

where E_0, the maximum field strength, is the vibrational amplitude and ν_0 the frequency of the light. If a molecule is irradiated by this wave, an electric dipole moment $\boldsymbol{\mu}$ is induced in it

$$\boldsymbol{\mu} = \boldsymbol{\alpha} E + \tfrac{1}{2!}\boldsymbol{\beta} \cdot E^2 + \tfrac{1}{3!}\boldsymbol{\gamma} \cdot E^3 + \ldots \tag{2.24}$$

where α is the polarisability, β is the hyperpolarisability and γ is the second hyperpolarisability etc. [Lon1] Generally, the hyperpolarisabilities are sufficiently small to be neglected unless the electric field strength is very large.

Thus

$$\mu = \alpha E = \alpha E_0 \cos 2\pi \nu_0 t \tag{2.25}$$

where μ and E are vectors and α is the polarisability tensor.

If the molecule vibrates with frequency ν_1 then the nuclear displacement x is written

$$x = x_0 \cos 2\pi \nu_1 t \tag{2.26}$$

where x_0 is the vibrational amplitude – the maximum displacement from the equilibrium bond length. For small amplitude vibrations α is approximately linear with x and is given by

$$\alpha = \alpha_0 + \left(\frac{\partial \alpha}{\partial x}\right)_0 x - \frac{1}{2}\left(\frac{\partial^2 \alpha}{\partial x^2}\right)_0 x^2 \ldots \tag{2.27}$$

Combining (2.23) to (2.27), and disregarding high powers of x gives

$$\begin{aligned} \mu &= E_0 \cos(2\pi\nu_0 t)\left(\alpha_0 + \left(\frac{\partial \alpha}{\partial x}\right)_0 x_0 \cos(2\pi\nu_1 t)\right) \\ &\equiv E_0\alpha_0 \cos(2\pi\nu_0 t) + E_0 x_0 \left(\frac{\partial \alpha}{\partial x}\right)_0 \cos(2\pi\nu_0 t)\cos(2\pi\nu_1 t) \end{aligned} \tag{2.28}$$

By simple trigonometric substitution this becomes

$$\mu = E_0\alpha_0 \cos(2\pi\nu_0 t) + \tfrac{1}{2} E_0 x_0 \left(\frac{\partial \alpha}{\partial x}\right)_0 (\cos 2\pi(\nu_0 + \nu_1)t + \cos 2\pi(\nu_0 - \nu_1)t) \tag{2.29}$$

Classically, the first term represents an oscillating dipole radiating light at ν_0 - Rayleigh scattering. The second and third terms represent Raman scattering of frequency $\nu_0 + \nu_1$ (anti-Stokes) and $\nu_0 - \nu_1$ (Stokes), i.e. the frequency of the incident beam has been modulated by the molecular vibrational frequency.

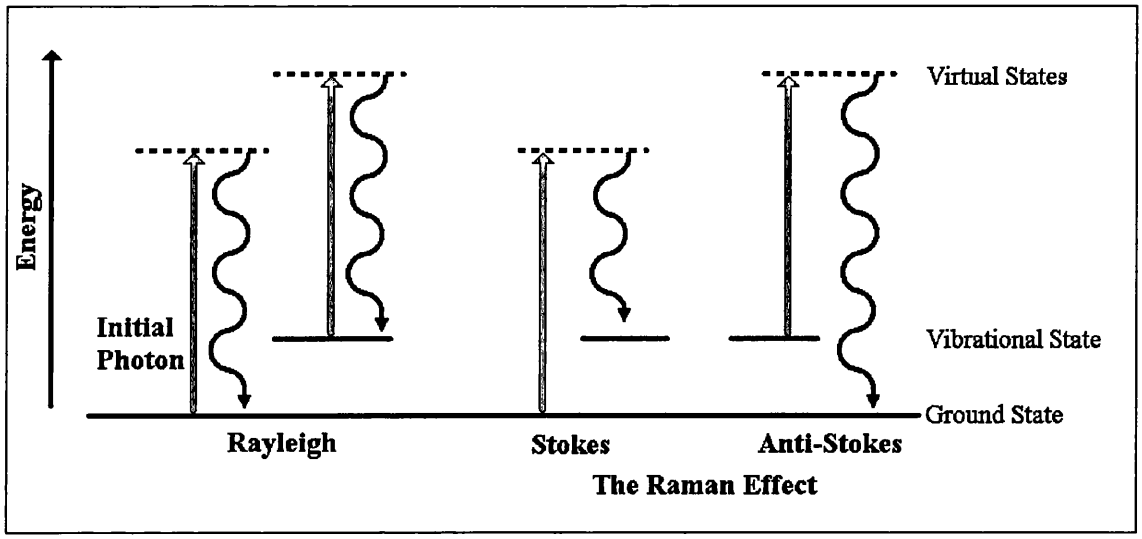

Figure 2.4: Scattering from the vibrational transitions of a molecule.

The mechanisms of Raman scattering are shown in figure 2.4. Stokes Raman scattering is considerably more intense than anti-Stokes as a consequence of Maxwell-Boltzmann statistics. Anti-Stokes scattering arises from the excited $\upsilon = 1$ level that has a smaller population than the $\upsilon = 0$ level in a molecule in thermodynamic equilibrium.

The intensity of Raman scattering also relates directly to the frequency of the exciting line. The intensity of scattering is proportional to the square of the amplitude of oscillation, which in turn is proportional to the square of the frequency of the oscillation. Since the frequency of the oscillation of the dipole is dictated by that of the exciting line the intensity therefore varies as the fourth power of the exciting frequency.

2.2.6. Selection rules and Raman activity

Not all possible vibrational transitions within a molecule are Raman active. The Raman effect only operates on internal modes for which the change of polarisability of the molecule at the equilibrium configuration is non-zero.

A dipole moment is induced in a molecule placed in an electric field, as discussed in section 2.2.5. The induced dipole moment

$$\mu = \alpha E \tag{2.30}$$

can be represented in matrix form by

$$\begin{bmatrix} \mu_x \\ \mu_y \\ \mu_z \end{bmatrix} = \begin{bmatrix} \alpha_{xx} & \alpha_{xy} & \alpha_{xz} \\ \alpha_{yx} & \alpha_{yy} & \alpha_{yz} \\ \alpha_{zx} & \alpha_{zy} & \alpha_{zz} \end{bmatrix} \begin{bmatrix} E_x \\ E_y \\ E_z \end{bmatrix} \tag{2.31}$$

This tensor is symmetric and real, with $\alpha_{xy} = \alpha_{yx}$, $\alpha_{xz} = \alpha_{zx}$ and $\alpha_{yz} = \alpha_{zy}$.
A vibration is Raman active if one of the components α_{ij} is altered during the vibration. This is can seen if a three-dimensional polarisability ellipsoid is plotted. [Lon1]

An ellipsoid which has its centre at the origin of a coordinate system, but whose axes are not coincident with the axes of the coordinate system may be represented by the equation

$$\alpha_{xx}x^2 + \alpha_{yy}y^2 + \alpha_{zz}z^2 + 2\alpha_{xy}xy + 2\alpha_{yz}yz + 2\alpha_{zx}zx = 1 \tag{2.32}$$

A line drawn from the origin to a point on the surface of the ellipsoid with coordinates x, y, z, has a length equal to $\alpha_E^{-½}$ where α_E is the polarisability in that direction. Along the principal axes of the ellipsoid, a, b and c, the direction of μ is the same as the direction of E. For these directions

$$\begin{aligned} \mu_a &= \alpha_a E_a \\ \mu_b &= \alpha_b E_b \\ \mu_c &= \alpha_c E_c \end{aligned} \tag{2.33}$$

where α_a, α_b, α_c are the polarizabilities along the principal axes a, b and c.

If the coordinate system is rotated so that the Cartesian axes x, y and z coincide with the principal axes of the polarisability ellipsoid then the polarisability tensor adopts a much simpler form

$$\alpha_{xy} = \alpha_{yz} = \alpha_{zx} = 0 \tag{2.34}$$

Equations 2.33 become

$$\begin{aligned} \mu_x &= \alpha_{xx} E_x \\ \mu_y &= \alpha_{yy} E_y \\ \mu_z &= \alpha_{zz} E_z \end{aligned} \tag{2.35}$$

The equation for the polarisability ellipsoid becomes

$$\alpha_{xx}x^2 + \alpha_{yy}y^2 + \alpha_{zz}z^2 = 1 \qquad (2.36)$$

with semiminor axis values of $\alpha_{xx}^{-½}$, $\alpha_{yy}^{-½}$ and $\alpha_{zz}^{-½}$.

Plotting $\alpha_i^{-½}$ for the extremes in the vibrations of a CO_2 molecule results in a diagram of the changes in the polarisability ellipsoid during those vibrations. (Figure 2.5)

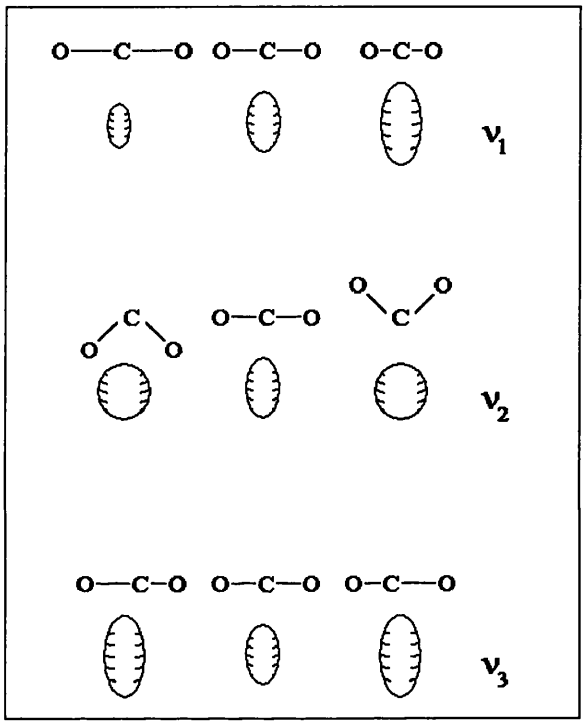

Figure 2.5: Variation in the polarisability ellipsoid of the three normal vibrations of CO_2.

A normal vibration is Raman active if the size, shape or orientation of the polarisability ellipsoid changes between the two extremes of the vibration. The ν_2 and ν_3 vibrations of CO_2 are not Raman active because, although changes in the size of the polarisability ellipsoids do take place, the size, shape and orientation are the same at two extremes of the vibrations in both cases.

In the case of H_2O (figure 2.6) all three normal vibrations are Raman active. In the ν_1 case the size of the polarisability ellipsoid has changed. For ν_2 it is the shape that changes between the extremes of vibration and for ν_3, the orientation.

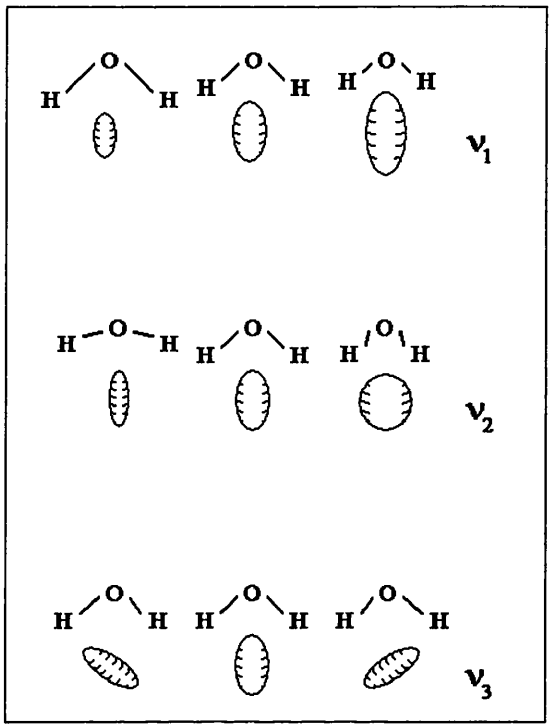

Figure 2.6: Variation in the polarisability ellipsoid of the three normal vibrations of H_2O.

2.2.7. Resonance Raman spectra

Resonance Raman spectra occur when the energy of the exciting radiation corresponds with that of an electronic transition of a chromophore within the molecule. The intensities of Raman bands originating in vibrations of this chromophore are selectively enhanced by a factor of as much as 10^5. Where a molecule contains two or more chromophores with different electronic bands, the exciting line can be selected to enhance vibrations specific to one or another.

2.3: Instrumentation and techniques

The recording of Raman spectra can be approached in a number of ways, using various techniques such as microscopy or Fourier transform methods. However, certain components are required regardless of the configuration used. These, and some common problems, will be discussed in this section.

2.3.1. Common techniques

To collect Raman spectra several components are required that are common to all commercially available Raman spectrometers and microscopes. These are: an excitation source, an illumination and light collection system, a monochromator (not in Fourier transform systems) and a detector.

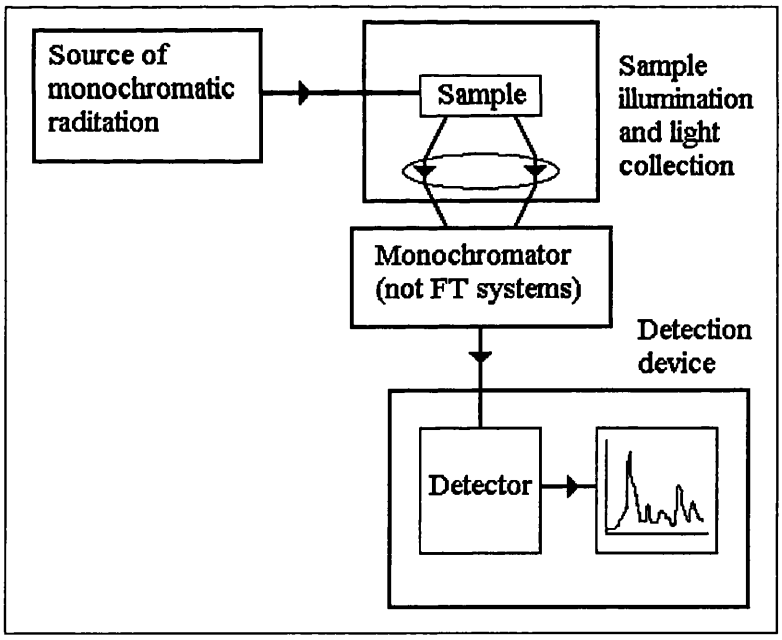

Figure 2.7: The components of a basic Raman spectrometer.

2.3.2. Excitation sources and sample illumination

The laser has become the principal excitation source for Raman spectroscopy, with both pulsed and continuous wave lasers being used, allowing time resolved and continuous spectroscopy. Lasers are particularly appropriate for vibrational spectroscopy since they are highly monochromatic and have small diameter beams, allowing them to be

easily focused and re-collimated after scattering. The availability of a range of different wavelengths permits appropriate selection to obtain most intense spectra.

To produce intense Raman spectra, the laser must be focused onto the sample and the scattered light collected as efficiently as possible. A number of different geometries have been used for the collection optics - 90°, 180° and oblique angle scattering geometries being commonly used. A Raman microscope uses the 180° scattering geometry to collect light. This is particularly useful for light scattered from or near the surface of opaque solid samples.

2.3.3. Scattered light detection

The detection of Raman scattered light is not a simple process given the extreme weakness of the Raman effect. Further problems are presented by stray light that may enter the spectrometer and particularly Rayleigh light scattered from the sample, which constitutes a far higher proportion of the collected light than that which has been Raman scattered. One of the most commonly used techniques for the removal of everything but the Raman scattered light is the use of a monochromator.

A monochromator uses a diffraction grating to separate the scattered light by its wavelength, allowing radiation of a particular wavelength to be selected and directed towards the detector. The use of two or more monochromators in series refines this process, narrowing the selected wavelength range with each successive diffraction grating, and allowing detection of Raman scattered light at very low wavenumber shifts. However, the problems of signal loss can become acute as the throughput decreases substantially with the addition of each monochromator.

An alternative method of selecting Raman from Rayleigh scattered light, which is becoming increasingly popular, is the use of holographic notch filters. As its name implies, a holographic notch filter makes use of the underlying principles of interference to reject a narrow band of wavelengths and transmit all other wavelengths, resulting in a 'notch' in the continuum transmission spectrum of the device. These are made from a sheet of photosensitive gelatin sandwiched between transparent substrates. A photo-induced reaction in the gelatin is generated by a suitable laser wavelength, producing

periodic changes in the refractive index of the material, which are written as a permanent hologram into the gelatin. Careful control of the hologram allows the very efficient reflection of a narrow band of wavelengths. If the filter is selected to match the exciting wavelength being used, and placed in the light path after scattering and before the detector, the Rayleigh scattered light is rejected so only the Raman scattered light reaches the detector.

After the Raman scattered light has been separated from the Rayleigh scattered light and dispersed into its component wavelengths it has to be detected and measured. C. V. Raman's experiments achieved this by the use of a photographic plate, whereby the presence of the different wavelengths was recorded as a line. This remained the principal form of detection for Raman spectroscopy before the advent of the photomultiplier tube. [Ferr]

Photomultipliers work by allowing incident photons to excite an electron from a photosensitive surface such as gallium arsenide. This electron is accelerated down a potential gradient and goes on to excite others, creating a cascade, until a measurable current is produced. This allows spectra to be measured electronically, facilitating the use of computers for data recording and analysis. However, using a single photomultiplier necessitates that only photons of one particular energy are counted at one time so spectra have to be scanned incrementally and hence the rate of data collection is slow.

Collection speeds can be increased by the use of a photodiode array, allowing multichannel detection simultaneously across a wide frequency range. The dispersed light emerging from the spectrometer produces a charge pattern along the focal plane of the array that is directly related to the intensity of the incident radiation. [Ferr]

Increasingly, modern instrumentation is coming to rely upon charge-coupled devices (CCDs) to effect detection of the Raman scattered light. The incident photons are detected by an array of cooled silicon diodes. This approach has the advantage of low readout noise, high quantum efficiency and a wide detectable wavelength range. [Eppe]

2.3.4. Calibration

The dispersion of light from a grating is dependent on environmental factors such as the temperature, humidity and carbon dioxide content of the air through which the scattered light has passed. For the purposes of standardisation and to aid theoretical calculations, the characteristic wavenumbers are referred to vacuum. In addition, systematic errors may be introduced by variations in the instrumentation, requiring the wavenumber calibration to be frequently checked.

A convenient calibration method uses the well-known emission spectrum of neon. [Burn] The difference between the emitted wavelengths of the neon lamp and the wavelength of the excitation source, the effective Raman shift, is found and then converted to wavenumbers in vacuum. This is accomplished by the use of Edlèn's empirical dispersion formula for light in air following the iterative methodology of Strey. [Edlè, Stre] The resulting wavenumber calibrated neon emission lines, corrected for standard vacuum, can then be compared with those recorded by the spectrometer. A calibration curve is then constructed by plotting the difference between the observed and corrected neon emission wavenumbers against the observed neon wavenumbers. This curve is then used to correct the observed Raman band wavenumbers to vacuum wavenumbers.

2.3.5. Fluorescence

A problem often found in the recording of Raman spectra, particularly those of organic molecules, is that of fluorescence. [Banw] This can obscure the Raman spectrum entirely and so can substantially reduce the chance of obtaining useful data. As previously discussed, the Raman effect occurs when light is scattered coincident with a vibrational transition in a molecule. Fluorescence arises when the molecule is excited into a higher electronic state. The molecule decays via radiationless transitions into the vibrational ground state of that electronic state. From there it decays to a lower electronic state by the emission of radiation. This process occurs rapidly – of the order of 10^{-8} s between absorption and emission. Fluorescence is a much stronger effect and the emitted photons have lower frequency than the exciting photon, swamping the Raman signal.

Fluorescence can be combated in a number of ways. Prolonged exposure of the sample to the laser beam can 'bleach' the cause of the fluorescence. This is most appropriate if the fluorescence is caused by an impurity. However, the sample itself may be fluorescent or burned by the laser. Other alternatives include the use of time-resolved pulsed lasers and detection systems to detect the faster Raman response ($\sim 10^{-12}$s) or the introduction of quenching agents that allow the excited states to decay via the quenching molecule rather than in the emission of radiation. However, the simplest alternative may be to change the exciting wavelength, moving the incident beam, and hence the Raman spectrum by the same amount, but leaving the fluorescence at its original wavelength. The use of near-IR lasers and FT-Raman systems is also proving effective in the avoidance of fluorescence.

2.3.6. Fourier Transform Raman spectroscopy

Fourier Transform Raman spectroscopy has a number of advantages over dispersive spectroscopy, not least in the reduction of the possibility of fluorescence. It is capable of rapidly collecting high-resolution spectra with good signal throughput characteristics, notwithstanding the ν^4 dependence of the strength of Raman scattering. [Ferr, Banw]

A Nd:YAG laser operating at 1064 nm is usually used as the excitation source, with InGaAs detectors cooled by liquid nitrogen. Unlike dispersive Raman spectrometers, the intensity of each wavelength in the spectrum is measured simultaneously. A Michelson interferometer is used to produce an interference pattern from the emitted radiation frequencies, which is deconvoluted into an emission spectrum by a computerised Fourier transformation algorithm. However, detection in this wavelength region is sensitive to blackbody emissions from samples heated to above about 200 °C. In addition, water absorbs in the near IR region as a result of overtones of the –OH stretching fundamentals and as such is not a suitable solvent.

2.3.7. Raman microscopy and fibre optic probes

The first Raman microscope was produced by Delhaye and Dhamelincourt in 1974. [Delh] Although their intention was to image samples using a selected Raman band, the

innovation of directing the exciting line onto the sample via a microscope was to prove a fundamental step in the Raman analysis of extremely small samples.

A modern Raman microscope works in much the same fashion as Delhaye's but, for the applications of this research, recording a full spectrum of a spot rather than imaging with a single Raman line. The exciting line is directed onto the surface via an optical microscope, allowing the laser to be focused onto a small area of the sample, facilitating the collection of the scattered light through the same lens. After the scattered light has been filtered to remove the Rayleigh component, it is dispersed off a diffraction grating onto a CCD detector.

Many Raman microscopes, and other Raman systems, operate with remote fibre optic probes. These allow the sample to be placed remotely from the spectrometer, with the exciting line directed to the sample via an appropriate fibre optic and focused with a lens at the probe head. The light is returned via a second fibre optic and coupled into the spectrometer. However, the extended light path in such instruments reduces both the available power in the exciting line and the intensity of the returning Raman signal. For weakly scattering samples the poor signal-to-noise ratio can cause the Raman signal to be obscured.

2.4: Instrumentation

The three different Raman instruments used to conduct this research are presented here, as is the mechanism for supporting manuscript materials during analysis.

2.4.1. Renishaw Raman Microscope System 1000

The majority of the Raman analysis constituting this research was conducted using a Renishaw Raman Microscope System 1000, equipped with 632.8 nm and 514.5 nm red helium-neon and green argon ion lasers, operating at powers of up to 4 mW at the sample. The system is configured with a Leica optical microscope with 5x, 10x, 20x and 50x objective lenses, allowing a minimum spot size of ~3 μm, and a slow-scan

CCD detector, thermoelectrically cooled to –70 °C. A schematic diagram of the system is shown in figure 2.8, below.

The resolution of the instrument is dependent on the width of the slits immediately prior to the diffraction grating and on the selection of the grating itself. A 1200 lines mm^{-1} grating was used throughout which, with a slit width of 10 μm, gives a resolution of approximately 1 cm^{-1}. In general, this configuration was used, although occasionally the slit width was increased to 20 μm. Collection times varied, appropriately to the sample, ranging from a few seconds to over an hour.

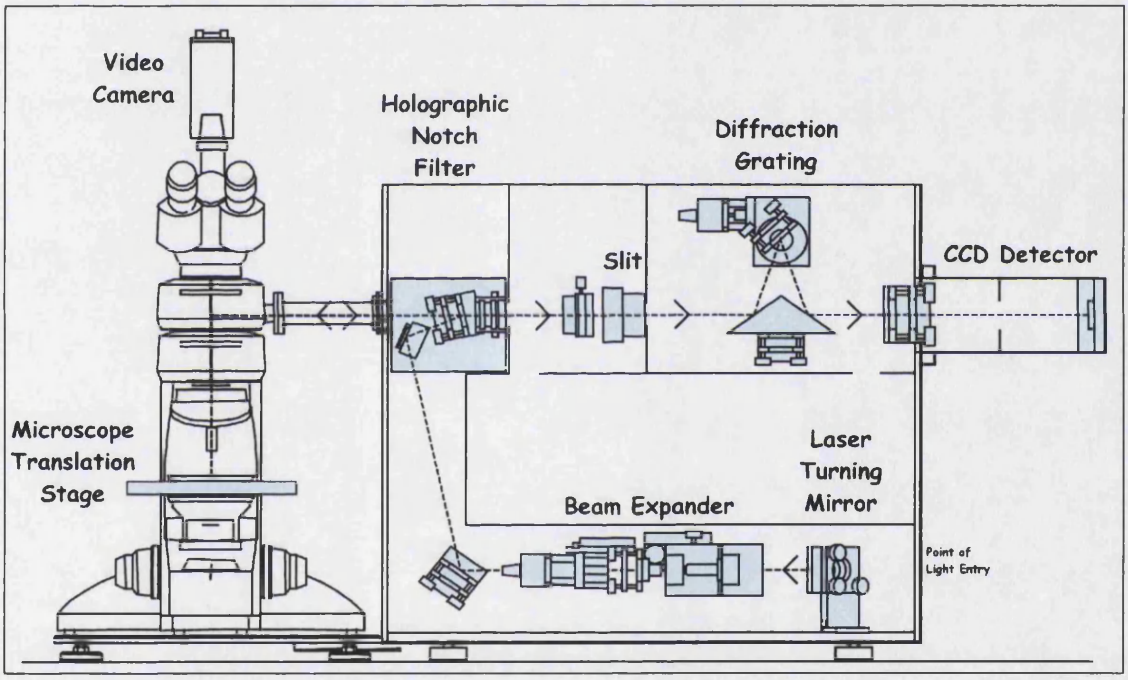

Figure 2.8: The Renishaw Raman System 1000 microscope. Schematic courtesy of Renishaw PLC.

The remote fibre optic probes couple directly into the Raman microscope. The fibre optic that carries the exciting radiation connects to the laser whilst that carrying the returning Raman signal is fed into the microscope at the translation stage; the end of the fibre is held in place on the stage, with the microscope focussed directly upon it. The holographic notch filter in the spectrometer box is removed since there is one situated in the probe head.

2.4.2. Renishaw Raman System 100

The analysis of the Vinland Map (chapter 7) was conducted using a Renishaw Raman System 100. This operates in a similar way to the System 1000, but without a microscope attachment. A 632.8 nm helium-neon laser was used, with a maximum power at the sample of 8 mW. Fibre optic probes are coupled directly onto the slit. The spectrometer has an 1800 lines mm^{-1} grating. A resolution of around 5 cm^{-1} was achieved due to the fixed slit width.

2.4.3. Bruker RFS 100/S FT-Raman microscope

A Bruker FT-Raman microscope was used for the analysis of a few of the works of William Blake that will be discussed in chapter 5. The instrument was equipped with a Nikon microscope and an Nd:YAG laser operating at 1064 nm. The Raman signal was detected with a liquid nitrogen cooled InGaAs detector.

Experiments were conducted at laser powers of ~2 mW at the sample, with a wavenumber resolution of either 4 or 8 cm^{-1}, using a 100x objective with accumulation times of up to 1000 seconds.

2.4.4. Supporting the artefact

If the artefact to be studied is small it can be placed directly on the microscope stage for analysis, with suitable external support and padding to ensure its safety. Larger objects such as manuscripts are often too heavy for the microscope stage to support them without drifting out of focus. In some cases the folios are too large to allow examination of anything but the edges of the pages; both the microscope and the spectrometer restrict the range of positions in which the manuscript can be placed. In addition, manuscripts are effectively constructed of two parts connected by a hinge. Both parts of the manuscript need to be fully supported whilst one folio is examined, with the added difficulties that many will not open to 180° and the binding often will not support the weight of the text block.

These difficulties can be partially overcome by the use of the remote probe, alleviating the problems of space but still requiring the manuscript to be fully supported and introducing the further problem of positioning and supporting the remote probe head at an appropriate angle to, and distance from, the page. In combination with conservation staff at The British Library, a solution was arrived at in the form of a book cradle. Modifications were made to a commercially available book support used for digital photography. Additional padding was added to protect the manuscript and substantial alterations made to the camera fixings. The camera arm was strengthened and an XYZ translation stage added to allow the probe head to be positioned adjacent to almost any area of the page and the laser brought into focus.

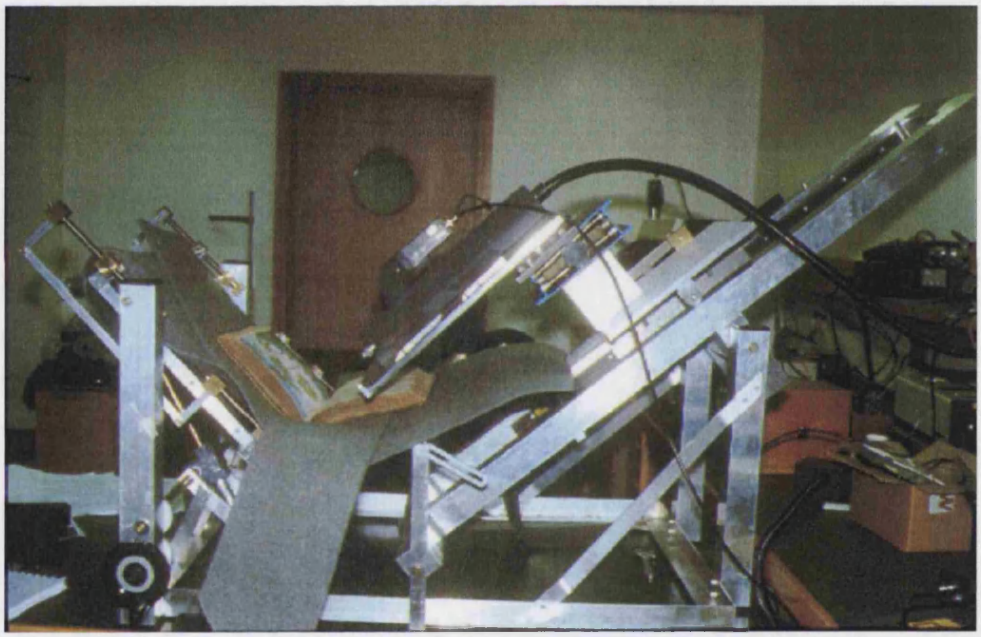

Figure 2.9: The book cradle and remote probe assembly.

2.5: Raman Microscopy in Art and Archaeology

The identification of materials used in works of art, archaeological artefacts and similar objects has become increasingly of interest to historians and conservation professionals. A long tradition of attempting to identify the palette of famous artists is being applied to a greater variety of objects of cultural significance. However, with the increasing desire for materials analysis has come a greater emphasis on non-destructive, but accurate, testing.

2.5.1. Why Raman microscopy?

In recent years, interest has been growing in the use of Raman microscopy as a technique for the analysis of fragile or valuable materials for a number of key reasons. Perhaps most important of these is its application *in situ*. Samples do not need be taken from an object to conduct a Raman analysis - an important consideration for delicate and fragile objects such as manuscripts that can be irreparably damaged by the removal of surface materials. Further, the technique is entirely non-destructive: laser irradiation at suitably low power does not damage the object under analysis.

Raman microscopy is unambiguous and extremely specific. Identification is aided by the very high spatial resolution (~1 μm) with which the sample may be selected, rendering a considerable degree of immunity from interference produced by adjacent materials. The technique is also extremely sensitive to very small samples (~$1x10^{-9}$ g), allowing the smallest components in admixture to be identified. [Best]

In addition, modern equipment is relatively portable. The ability to conduct analysis on site is particularly attractive to curators of valuable collections that cannot be removed from their home institutions without prohibitive expense and inconvenience.

2.5.2. Materials identification

As outlined earlier, the Raman spectrum produced by scattered photons can be treated as a fingerprint for each material; comparison of this spectrum with databases of previously collected spectra from standard samples allows its identification.

Where more than one pigment is present in admixture it is possible to separate them in one of two ways. By focusing exclusively on crystals of each pigment, one at a time, easily identified Raman spectra are produced that are separately indicative of each component of the mixture. Where the pigments are too finely mixed to allow this, a Raman spectrum from the mixture will contain peaks attributable to all of the materials. These can be separately identified, allowing the individual elements of the mixture to be established.

In recent years a number of databases of spectra applicable to the study of art and archaeology have been published. These include collections of spectra of ancient pigments, [Bell, Burg] modern pigments, [Vand] binding materials [Van1] and plant fibres. [Edwa]

2.5.3. What can be learnt?

Identifying the materials used in the construction of objects of historical importance is significant for a number of reasons. Little scientific analysis of this type of material has been attempted in the past as many techniques require sampling, detrimental to the preservation of the artefact. Unfortunately, this has meant that much of what is thought to be known about an object is taken from early descriptions of manufacturing technique, subject to interpretation errors, or is purely modern conjecture. For example, the Insular manuscript palette, chapter 3, does not rely exclusively on the use of verdigris for the production of green pigment as had previous been supposed.

Accurate identification of the structure of an historical artefact expands knowledge of the artefact itself and the period of its construction. Information can be obtained concerning why and how an object was made, the technological capabilities of the society that produced it, their trading links with other groups and the wealth and status of the individuals who commissioned the object. Evidence for these things can be found in the materials used, particularly in comparison with other artefacts from similar periods or geographical regions. For example, abrupt changes in the pattern of pigment use in the illustrations of a single manuscript can be indicative of periods of socio-economic change; perhaps new materials became available during production, or some upheaval prevented completion until a later date, or production was moved to a different location.

This kind of information can ascribe dates to objects, identify alterations such as over-painting in works of art, and detect forgeries since the date of first manufacture of many materials is known.

A full identification of the materials used in the production of any object of cultural significance has important consequences for the conservation and preservation of the

artefact. Recognition of the materials used in an object's construction allows appropriate, compatible repairs and treatments. Decorated manuscripts particularly benefit from analysis of the pigments used in their decoration since they are susceptible to degradation due to instability of the materials themselves and interactions with their environment. Appropriate care plans can be constructed to take full account of the effects of light, humidity and environmental contaminants, for example, on the object. Potential interactions between materials already present can be assessed. Finally, understanding what processes have occurred (by identification of the products), or may be going to occur, allows appropriate steps to be taken to optimise the environment of the object.

2.6: Experimental pigment identification

Although Raman microscopy is theoretically an ideal tool for pigment identification, the materials are rarely in an ideal condition. Often the pigments, binders or substrate are damaged, eroded or degraded in some way.

If pigments are mixed, often one element of the mixture will be identified and others will not. Possible causes for this include the presence of a pigment (often organic) with a very weak Raman signal, fluorescence and degradation producing unrecognisable Raman spectra (or no spectra at all).

Certain pigments can be recognised by distinctive decay patterns. Red lead decays through a series of other lead compounds with known spectra and its physical appearance changes distinctively. Decaying orpiment does not produce a discernable Raman spectrum in situ, but changes to a yellowish grey colour that renders any blue-yellow mixtures blue-grey rather than green. Similarly, lead white decays to lead sulphide, which is black.

The lack of discernible Raman spectra is a common feature amongst natural organic pigments which are rarely identifiable either in situ or under laboratory conditions. Unfortunately this is not a defining characteristic as a number of inorganic pigments can

be hard to identify in situ, amongst them red, yellow and green ochres and black pigments such as magnetite.

Verdigris, in particular, is extremely difficult to identify in situ. The exact chemical composition of the green pigment generally called verdigris is extremely variable, covering a range of copper acetates, $[Cu(CH_3COO)_2]_2 \cdot Cu(OH)_2 \cdot 5H_2O$, with varying levels of hydration, basicity and $[Cu(CH_3COO)_2]$ to $Cu(OH)_2$ ratio. All of these variations have slightly different Raman spectra, and some are extremely sensitive to thermally induced degradation. [Bell, Chap] Generally, all types of verdigris are characterised by a very intense band *c.* 2935 cm^{-1} and others at *c.* 2985, 1445, 1415, 1350 and 938 cm^{-1}. In the majority of cases additional bands may be found around *c.* 1550 cm^{-1} and at *c.* 1408 cm^{-1} or *c.* 1432 cm^{-1}. However, at room temperature spectral quality is low and compositional variations cause band mobility making conclusive identification difficult. For the purposes of this study, a green pigment is recorded as verdigris if it is clearly not malachite or any other well-characterised green pigment and has more than one band in the vicinity of 2935, 2985, 1550, 1445, 1432 or 1408 cm^{-1}. From a chemical point of view this is not a certain assignment. However, the historical methods of verdigris production have been many and varied and the nature of its decay is uncertain [Kühn] so for the purposes of distinguishing verdigris-type pigments from others it is more than sufficient.

2.7: Identification of Indian yellow by Ultra Violet examination

To unambiguously identify Indian yellow is troublesome because, contrary to published data, [Bell] Indian yellow does not easily produce a Raman spectrum; doubt exists as to whether the sample used for the database analysis is in fact genuinely Indian yellow. The pigment is believed to be produced from the residue of dried urine produced by cows fed exclusively on mango leaves. [Baer] As such its chemical composition is complicated. Further, it has not been commercially available since 1921 and its production is believed to have been outlawed in 1908. As a consequence, supplies of definite provenance are difficult to obtain.

One distinguishing feature of the material that is generally accepted to be Indian yellow is the distinctive fluorescence produced in response to a range of wavelengths, particularly at 535 nm in response to excitation at 435 nm. The fluorescence may also be observed with the use of an ultra violet lamp at around 365 nm, giving a distinctive yellow to orange-yellow colour. It is considerably stronger than fluorescence occurring from other materials present, distinguishing it from other materials. [Baer]

Identification of Indian yellow in this work is based on the fluorescence produced by an ultra violet lamp. An example of a digital photograph of a relevant folio, taken under these conditions, is included.

Chapter 3: Anglo Saxon and Later Manuscripts in the British Library

IMPORTANT NOTE

The Scots (originally Irish, but by now Scotch) were at this time inhabiting Ireland, having driven the Irish (Picts) out of Scotland; while the Picts (originally Scots) were now Irish (living in brackets) and vice versa. It is essential to keep these distinctions clearly in mind (and vice versa).

1066 And All That
W. C. Sellar and R. J. Yeatman
1933

The purpose of this chapter is twofold. First it recounts the early history of England from the Anglo Saxons to the Tudors and discusses the production and use of books within this cultural framework. It then goes on to describe each of the manuscripts analysed and discusses the results of the analysis in terms of this historical context.

3.1: England From the Rise of the Anglo Saxons to the Fall of the Plantagenets

Often turbulent, this period saw the creation of England as a nation and charts the rise and fall of several ruling dynasties with varied cultural influences from the Vikings to the Norman French.

3.1.1. The Ascendancy of Anglo Saxon Culture in England

From an inauspicious beginning as Germanic pirates and mercenaries in the 5th century, so rapid was the progress of Anglo Saxon culture that by the 1066 Norman Conquest Anglo Saxon England was renowned throughout the Western world for the sophistication of its cultural, legal, fiscal and ecclesiastical infrastructure. The conversion of the Anglo Saxons to Christianity, under the competing influences of the Roman and Celtic churches in the late 6th century, led to the transformation of the

earlier rich oral tradition into the well-developed literary culture that was crucial to the maintenance of so complex a social structure.[1]

The early 5th century saw the beginning of a geographical retreat by the British church that lasted until late in the 6th century. In the face of insurgences by Germanic pagan groups, this move into the highlands resulted in an active conversion of the Irish kingdoms. By the second half of the 6th century resistance to the Germanic advance had collapsed and small Anglo Saxon political units became established. Eventually Kent, Essex, Sussex, Wessex, East Anglia, Northumbria and Mercia became prominent; the majority of the indigenous population had retreated to Wales, Cornwall and southern Scotland or had migrated to Brittany.

The resurgence of Christianity, with the conversion of Anglo Saxon England, came on two fronts - the Celts from the Irish Kingdom of Dal Riada in Argyll and the Roman Church and the mission of St Augustine to Kent in 597. The contesting liturgical standpoint of these two groups (the principal differences of which were settled at the synod of Whitby in 664 in favour of Rome) was felt stylistically in work of the period. This is particularly seen in manuscripts such as the Lindisfarne Gospels (British Library Cotton Ms Nero D IV), with its heavy Celtic influence on the one hand and the Romanizing Stockholm Codex Aureus (Stockholm, Kungliga Biblioteket Ms A.135) on the other.

The similarity in the products of British and Irish culture during this period, until around 900 AD, gives rise to the term 'Insular' which could be applied to both of the aforementioned manuscripts. Although the separate groups retained their own culture there was considerable interaction between them and many elements of stylistic similarity. They were subject to the same artistic influences in the cultural exemplars from Mediterranean and Germanic countries, as well as Celtic, Antique and Oriental art. However, the interpretations of these exemplars were many and varied.

The 7th century saw the appointment of Archbishop Theodore of Tarsus to Canterbury, where he was Archbishop from 669 to 690. Theodore formalised the uniform

[1] For a brief history of England from the 5th Century until the demise of Anglo Saxon government see [Brow], [Hame], [Sell], [Blai], until the fall of the Plantagenets see [Hall], [Feil].

ecclesiastical structure of England during this period and with Hadrian, the African abbot of St Augustine's, established the school at Canterbury that brought the Mediterranean influence to the English educational curriculum. This curriculum was also adopted in Northumbria, particularly at Monkwearmouth and Jarrow, the institution that subsequently educated and was home to Bede for almost his entire life.

Irish and English religious also travelled widely to the Continent, founding monasteries such as Luxeuil, St Gall, Bobbio, Echternach and Fulda. These houses requested many works by scholars such as Bede and liturgical works from their parent monasteries, contributing considerably to Continental education. This culminated in the late 8th to 9th century Carolingian[2] renaissance under the Emperor Charlemagne. Assisted by Alcuin of York, one of the most learned churchman of the period, he succeeded in standardising both texts and scripts (with the production of the elegant and extremely legible Caroline miniscule) as part of an attempt to create political stability and cultural cohesion across his large and diverse empire.

The 8th century in England saw the rising ascendancy of Mercia; extending its authority throughout much of Southumbria[3]. The complex relations between this kingdom and the Carolingian empire are reflected in the Mediterranean and Oriental influences seen in the manuscripts and works of art produced in the south during this period.

By 830, however, a dissent-weakened Mercia had given way temporarily to Wessex supremacy. Relations with the Carolingian empire were of secondary importance in this period with the emergence of a new threat. Following a first attack at Lindisfarne in 793, it was but five years from the landing of the first great Viking army in 865 to the overthrow of all but the kingdom of Wessex.

The advance of the Vikings was only halted during the reign of Alfred the Great, by treaty drawn up between 886 and 890 with Guthrum, leader of the East Anglian Danes. This partitioned England into the Danelaw and the rest. Under Alfred, this included Wessex, south-western Mercia and the land south of the Thames. This new peace gave

[2] The Carolingian empire was established by Charlemagne who became emperor in 800, and was divided by the treaty of Verdun in 843. The Carolingian dynasty ruled in some areas until the late tenth century.
[3] Unlike Northumbria, the term Southumbria does not refer to a kingdom but to the parts of England immediately south of the River Humber.

Alfred leisure to pursue his other great interest – halting the perceived religious and cultural degeneracy of England, which he believed to be the cause of her current troubles. To this end he engaged English and Continental scholars to translate particularly apposite works from Old English and to rejuvenate scholarly pursuits in general. Thus Insular culture was preserved, but the influence of Continental trends more strongly felt, leading to the development of a new style of vernacular literature.

This regained prominence of art and literature was further indulged under Athelstan (925 – 939). The formation of diplomatic links with the Continent, afforded by the overthrow of the Danelaw and the formation of a single monarchy throughout England and into Scotland and Wales, granted him the opportunity to acquire many and varied works from a variety of sources.

The reign of King Edgar in the second half of the 10th century saw a massive reform of monastic habit with the uniform observance of the Rule of St. Benedict throughout the English church. Led by three reforming Archbishops, Dunstan of Canterbury, Aethelwold of Winchester and Oswald of Worcester and York, practice was formalised between 963 and 975 in the Regularis Concordia. Unfortunately the flourishing of the arts that this period of standarisation encouraged was once again constrained by a period of further disruption in the late 10th and early 11th centuries. The intervention of the Danes and the accession of Cnut came in 1016 as a result of poor rule by Ethelred II 'Unræd', the 'ill-advised', succession crises, conflict and an alliance with Normandy. The arts began to flower again, however, in the stability produced by Cnut's social contract, promising peace in return for allegiance and formalising England's position as part of a Scandinavian Empire.

Conflict began again following the death of Cnut, with only temporary peace found in the 1042 accession of Edward the Confessor. The short lived reign of his brother-in-law, Harold Godwine, Earl of Wessex, culminated in the Conquest in 1066 by William of Normandy and the end of the political identity of Anglo Saxon England, as recounted in the Bayeux Tapestry. This conclusion of the Anglo Saxon political period did not see a similar destruction of its cultural influence, however, with the English style a basis and stimulus for the development of culture, art and literacy throughout Europe.

3.1.2. England After The Norman Conquest

The imposition of Norman rule in England brought great change to the structure and organisation of day to day life, with the arrival of the feudal system. The subjugation of the English did not remove the threat of a Danish invasion, however, and the need for money to finance his army and the large number of outstanding property disputes caused William to send out his officials in 1086 to compile a survey of all the manors of England – the Doomsday book.

Even after William's death in 1087 at Mantes, fighting the French to hold the Dukedom of Normandy, peace did not follow. The elder of his sons, Robert, inherited the Dukedom of Normandy but was not able to hold it, and the second son, William Rufus, inherited the Kingdom of England. William Rufus and his son Henry both concluded that they would have no security in England with unrest in Normandy; many of the barons held land on both sides of the Channel. So to that end Henry finally took Normandy in 1106 leading to a period of stability that lasted until his death in 1135 and a continuing the close synergy with the Continent that was to last far longer.

Henry's son, also called William, had drowned in 1120 leaving no male heir. Henry had intended his daughter Matilda, who was married to Geoffrey Plantagenet of Anjou, to succeed. Within a fortnight of Henry's death, however, his nephew Stephen arrived from France to claim the throne. England was plunged into nearly twenty years of civil war as control passed between Stephen and Matilda. Stephen lost Normandy to Geoffrey but held England until his death in 1154. He was succeeded by Henry, the son of Geoffrey and Matilda and the husband of Eleanor of Aquitaine.

Henry II, the first Plantagenet king, inherited Anjou and Normandy from his father, Aquitaine from his wife and England from his uncle making him, at the age of twenty-one, one of the most powerful men in Europe. His reign was thirty-five years of relative peace although the court seldom spent long in one place or even in one country. His major achievement was the development of a countrywide system of law and local government, composed for the first time of trained officials, lawyers and judges. His sons were not such a success, however, with the popular Richard away Crusading for much of his reign, paid for by heavy taxation, and John, who succeeded him,

mismanaging the barons to such an extent that he was forced to sign the Magna Carta in 1215, accidentally enshrining the right of all freemen to be judged by their peers in the process.

During this period the gathering of scholars at Oxford and Cambridge, that would lead to the formation of England's first universities, began and the Franciscan friars arrived. They opened boarding houses for the students at Oxford, where Roger Bacon taught scientific method, and went out to preach to the poor. The men of the universities learned to be lawyers, climbing many social and intellectual ranks, and many worked in Westminster Hall. Soon after the formation of the first colleges at Oxford and Cambridge they built lodgings, the Inns of Court, between the commercial and political centres of London and Westminster.

Unfortunately, breaking his oath to observe the law, Richard plunged the country again into civil war and died, leaving the country to his son Henry III, who was nine years old. Peace was restored during the regency but when Henry came of age he tried to return to his father's style of government, angering the barons and the populace so much that civil war again ensued in 1258. Simon de Montfort became leader of a group calling for reform and defeated Henry, calling a Parliament in 1265 that included, for the first time, representation of the Commons. A few months later, however, he was killed in battle by Henry's son Edward.

Edward became king in 1272, commencing a period of considerable social reform. He checked the power of the barons and promoted trade. The language of government was gradually transferring from French to English and there was much more mixing between the classes as the younger sons of the nobility went into trade and the sons of villeins entered the universities, succeeding in the Church and at law. The Parliament, whilst not having any control, also expanded to include tradesmen and craftsmen alongside the Churchmen and nobility. England was prosperous, and apart from a continued campaign to invade Scotland, peaceful until Edward's death in 1307.

Edward II was not able to continue his father's work and war with the Scots and the barons again ensued. The Barons were defeated by the Commons in 1322 but Edward's peace was short-lived; he was murdered by his wife and her lover in 1327.

Edward III was overly fond of fighting and his failure to subdue the Scots turned him to a richer target. He declared war on France in 1337 – a war that was to last a hundred years. Perhaps surprisingly, given the expense, the war was popular with the freemen and Parliament voted him exceptional amounts of money. The regular meetings that were called increased its power, particularly giving a voice to the Commons who now sat separately from the barons in the Chapter house of Westminster Abbey.

For twenty years the war went very well. By 1360 Edward and his son, the Black Prince, had gained Calais, Ponthieu and south-west France in full sovereignty. Edward died in 1377 and was succeeded by Richard II, son of the Black Prince, who was eleven. His uncle, John of Gaunt, continued the war with France but all that remained of his father's conquest was Calais and a few towns in the west. It was not until 1397 that Richard regained control of his Parliament, but he overstretched himself and was forced to abdicate by the Commons in favour of John's son, Henry Bolingbroke, in 1399.

Henry IV and his son Henry V were both in a vulnerable position since they were not rightful hereditary rulers. Henry IV found himself having to submit to Parliament to retain his crown, considerably increasing their power over the monarchy. Henry V renewed the attacks on France to distract attention from his tenuous grip on the throne and in 1415, after victory at Agincourt, he married the daughter of the French king and was declared his heir.

By 1422 both he and the French king were dead and both kingdoms were in the hands of the infant Henry VI. The French united and by 1453 the English had been driven out of all but Calais. The Hundred Years War had ended and with it the close interaction between England and France. In its place came the Wars of the Roses which were to last a further thirty years.

Two factions were struggling for control of a Parliament which had grown steadily more powerful during the war with France. The Lancastrians were led by Margaret, Henry's queen, and the descendants of Henry IV's brother John, the Yorkists by the Duke of York, with a claim on the throne, and the Earl of Warwick. In 1453 Henry's son, Edward, was born and two years later war broke out.

After years of skirmishing, the Duke of York was captured and murdered at Wakefield by the Lancastrians. The new Duke was hastily crowned Edward IV by Warwick with a Yorkish victory at Towton in 1461 and Henry VI thrown into the Tower. By 1471, Henry's son, Edward, had been captured and killed and he himself murdered; York had supplanted Lancaster on the throne of England.

Only one Lancastrian claimant remained, Henry Tudor, Earl of Richmond, but he was still a child and living in France. Edward had much to do in restraining his quarrelling younger brothers, the Dukes of Clarence and Gloucester. Clarence was accused of treason and died in the Tower leaving Gloucester to become Protector on Edward's death in 1483. Edward's son Edward V was a boy of twelve and his brother younger still when Gloucester convinced Parliament that they were illegitimate and had himself crowned Richard III, soon after which the boys were murdered in the Tower.

In 1485 Henry Tudor landed at Milford Haven to march through Wales to Leicestershire. The Wars of the Roses ended on the battlefield at Bosworth where Richard died and Henry was crowned. Marrying Edward IV's daughter Elizabeth he united Lancaster and York in the House of Tudor; the age of the Plantagenets had ended.

3.2: The Creation and Ownership of the Book

In general, after the fall of the Roman Empire until the expansion of secular literacy in the 13th century, book production was predominantly the preserve of the monastic communities. However, there is considerable evidence that scribes and artists, as well as manuscripts, were considerably mobile within this milieu, travelling between scriptoria or as the entourage of distinguished churchmen or nobles, and further that writing was not solely the preserve of those within the community whose principal employment was book production. In general the members of monastic communities were educated and so many churchmen wrote but were not professional scribes. Only those who demonstrated considerable facility in this respect become lectors or scriptors, scholars or scribes.

There is also evidence that the female religious were involved in book production and fully able to read and write, as demonstrated by the request of Saint Boniface in 735 that the Abbess Eadburga of Minster-in-Thanet should produce for him a copy of the letters of St Peter, written in gold. [Back] Frequently, the care and teaching of children sent to monastic communities fell to such women and included instruction in reading and writing.

Commonly, the higher classes had much freer access to books than the general populace, often owning several although it is not clear whether they would have actually been able to read them without the assistance of their priest. Education was predominantly, but not entirely, the preserve of the ecclesiastically trained and was, therefore, also available to the lower freeborn classes should they decide to enter the church. However, the great majority of people saw books or writing only in the church or in courts of law, where they might see the great service books or have the King's writs read out to them.

The actual physical production of the book and its codicology varied but in general there were a number of consistent stages: the preparation of parchment, pricking and ruling out the sheets, writing, adding the rubrics (titles, headings etc.), decoration of the pages (creation of initials and miniatures), correcting the text, assembling the sheets into quires, sewing the quires together and binding. The precise working practice varied from institution to institution as might the number of scribes. A great Gospel may well have only a single scribe, for example, whilst another manuscript may involve the work of multiple hands. Later in the Anglo Saxon period the names of these scribes and craftsmen might be found recorded in colophons, but in general this was a practice found mostly in Irish manuscript production.

Similarly, the owners of early works were also not recorded; patron's names only appear to have been habitually noted in the manuscripts they commissioned from about the 9th century. From this information and other sources we do know that King Athelstan acquired and commissioned a number of books as did King Edgar and the reforming Bishops. Women were also amongst notable patrons: St Margaret of Scotland, who married to King Malcolm III of Scotland after the Norman conquest,

caused the creation of a number of manuscripts and Countess Judith of Flanders was known to own four Gospel books written by English scribes.

Books were created, therefore, for a number of purposes: for the religious community that produced them or other religious communities, for day to day use or for their libraries, for priests, for high ranking ecclesiastics or for high ranking secular figures – the personal possessions of royalty or nobility.

From evidence that remains, the texts themselves were many and varied. They included works from the scholars of antiquity such as Pliny and Cicero, the great writer of early Christianity – Saints Augustine and Gregory, and important scholars and poets – Prudentius and Isidore of Seville. Newer works by contemporary scholars were also commissioned, for example works of historiography by Bede, scientific thinking from Byrhtferth of Ramsey, medicinal knowledge and folk remedies, geographies, encyclopaedias, travellers' tales, maps, poetry and epics such as the poem Beowulf. Predictably, bibles, scriptures, lectionaries, missals and other religious works such as saints' Lives were a large part of the output of any scriptorium as well as more prosaic administrative documents including charters, royal writs, manumissions and records.

With the expansion of education, the standardisation of law courts and the creation of universities in the 12th and 13th centuries came a much greater demand for books. In a process repeated across Europe, book creation and consumption came out of the cloister and into the secular world. Particularly around the university in Paris, there is evidence of a street of booksellers and stationers selling second-hand books and other materials by the mid-13th century. [Hame] Around this time a significant advance in the production of bibles also took place with the compression of the complete text into one ordered and standardised volume. A medieval bestseller, such huge quantities were produced between about 1240 and 1280 that few were made after this date until the end of the middle ages – so many 13th century copies were available that there was no need to produce more.

Book production gradually became a trade like any other as the requirement for books grew. The range of material produced also increased dramatically with new texts on law, medicine and science required by the students to complement the existing works by

scholars such as Aristotle. It almost seems as though anyone who wanted could publish a book and great authors such as St. Thomas Aquinas and Peter Lombard produced a great many during this period.

It was also not uncommon for books to be produced in one place and illuminated in another. Bologna was a great centre for the teaching of law during the 13th and 14th centuries and so produced a great many texts. The principal Continental centre for illumination was Paris, however, so books were exported undecorated for sale through the northern university booksellers when the miniatures would be added.

Oxford became the great English centre of book production during this much more commercial period, with a thriving 13th century trade in Catte Street and flourishing commerce with the Continent. BL Royal Ms 10 E IV is a copy of the Decretals of Gregory IX with script in Italian, a prologue addressed to the University of Paris and English miniatures that may well have been produced in Oxford.

Students were not alone in this rising demand for books with a substantial increase in the aristocratic market. Romantic tales such as Lancelot du Lac, books of poetry and songbooks all find keen readers, along with scholarly works and theological and religious materials. A great many of the literary works were in French, the most widely spoken language on the Continent and still the mother tongue of much of the English aristocracy.

The single biggest revolution in secular book ownership was the production of the Book of Hours. Even those families who had never owned another book went out and purchased one of these. A compendium of devotional text intended to be read by the owner at various times throughout the day, each hour consisted of a short hymn, Psalms, a reading and a prayer. Decorated according to the depth of the pocket of the purchaser, they range from the very plain to the extravagant as might have been owned by the royal family or wealthy nobility. Children were taught to read with them, important family dates recorded in them and prayers for everyday occurrences such as childbirth and toothache added to the ends. So very many were made that about three hundred remain in the collection of the British Library alone, but to the people who purchased them they were very precious indeed. In many households they were the only book.

3.3: Anglo Saxon Manuscripts in the British Library

The British Library contains one of the world's foremost collections of Anglo Saxon period manuscripts originating both within the British Isles and abroad, exemplifying almost every significant script or school. However, although often well studied from a palaeographical point of view[4] somewhat less is known about the materials and methods used in their construction.

A great deal of information can be obtained from the study of finished and unfinished manuscripts (which are surprisingly common). For example visual examination can establish the source of the parchment – sheep, goat or calf, the way in which the parchment folios had been arranged, generally flesh side to flesh side and hair side to hair side or even which part of the animal the skin is from. Where the manuscript is unfinished, the order in which script and decoration were applied to the folio is clear from those pages which have been ruled and written and on which space has been left for the decorated initials, miniatures and borders to be added. [Haml] Further, where the illuminations are themselves unfinished the order in which the pigments have been applied can be clearly seen, for example as in British Library Add Ms 42555.

However, less is known about the materials used to compose these decorations. Information generally comes from one of three main sources. The most reliable of these are contemporary written materials such as pigment price lists or instructions to the artist about the colours of the composition. Recipe books compose a further written body of evidence but regrettably Anglo Saxon books of this type are extremely rare. Those manuscripts that are extant are predominantly later copies of earlier materials now lost or in the 'manuals for the education of gentlemen' vein of the Renaissance (for example [Thom], [Dodw]). Unfortunately, both these and the Anglo Saxon materials are subject to mistranslation and errors, on occasion because it simply is not certain what material is being referred to. A good example of this is found in Thompson's 1933 translation of Cennino D'Andrea Cennini's "Il Libro dell'Arte" [Thom p. 28]. It refers to a yellow colour called giallorino but it is far from clear what this is, except that it is of mineral character.

[4] For example in [Bish], [Brol], [Temp], [Alex] and numerous others.

The third major source of information is examination of the manuscript itself. Until very recently there were few non-destructive techniques that could provide an accurate identification of the materials. Samples of flaked pigments could be obtained from particularly friable illustrations for scientific analysis[5] but in general less exact techniques are relied upon, such as optical microscopy and ultra-violet and infrared photography.[6] All too often an identification made by visual inspection, before even these inexact techniques became available, becomes accepted as fact and uncritically reproduced even in current literature. Thus information that may be vital in ascribing a point or date of origin, for the greater understanding of the historical context of the work or for the planning of its long-term care, remains undiscovered and even unsought. For example, one of the standard catalogues of Anglo Saxon manuscripts [Temp, Nos. 49 and 66] mentions the use of a metallic red pigment on a number of folios of British Library MS Arundel 155 and British Library MS Cotton Cleopatra C VIII. As we shall see, Raman analysis demonstrates this to be nothing unusual but a degradation product of ordinary red lead that has been misinterpreted as a novel pigment.

Further to this, it has long been supposed that the traditional triumvirate of the Insular palette is composed of red lead, orpiment and verdigris, [Brow] all of which would have been conveniently available to the Insular scribe. However, the results of Raman analysis discussed below show this to be an erroneous assumption, the truth being rather more complicated.

[5] For a brief discussion of the advantages and disadvantages of neutron activation analysis see [Orna], the use of total reflection X-ray fluorescence, an elemental technique requiring a number of assumptions before identification can be made, is described in [Kloc], a discussion of the advantages of a number of techniques is found in [Cla1].

[6] For example, H. Roosen-Runge and A. E. A. Werner in [EQCL, Vol. 2]. The problem of different pigments producing similar false colours is demonstrated in [Moon], [Clar]

3.4: Tiberius Group Manuscripts

A group of manuscripts that will feature heavily in the forthcoming discussion are those of the 'Tiberius' group. They take their name from a copy of Bede's Historia Ecclesiastica (British Library Cotton MS Tiberius C.ii), the first noted exemplar of this type which was to be found in the old Cotton library on the set of shelves surmounted by a bust of the emperor Tiberius.

What exactly constitutes a Tiberius group manuscript is rather harder to define. They are all Southumbrian in origin, from Mercia, Wessex and Kent, and date from the late 8^{th} and early 9^{th} centuries – a period of considerable disruption. They are often written in varieties of miniscule script and decorated with fanciful zoomorphic beasts, forming ornamentation or display letters. The stylistic influences evident in these manuscripts are both Mediterranean and Irish in origin, suggesting continued contact with the Irish church that was still influential in Northumbria as well as the presence of Italian and other European exemplars. [Bro2]

Also contained within this group is the largest collection of evidence for female literacy in the period. Although the considerable political disruption must have influenced the survival rate of manuscript material, a substantial proportion of that which survives demonstrates creation or ownership by women – particularly in the Tiberius group prayerbooks some of which are discussed below.

3.5: Studies of Selected Anglo Saxon Manuscripts

In the following sections of this chapter each manuscript will be considered in turn, and its composition described. The results of studies by Raman microscopy will be presented and conclusions drawn. In some cases spectra could not be obtained from particular areas. These will be listed with the results of each folio.

Descriptions and background for the manuscripts was obtained from a number of sources. In general, there are a number of catalogues that feature as standard references

for this type of material.[7] Some manuscripts fall outside the remit of these lists and so other sources have been consulted.[8] In a very few cases, mostly with the Continental manuscripts, the only source of information has proved to be a two-line entry in a catalogue. Incredible though it seems, some of these manuscripts have been so little studied in recent times that we are only vaguely aware of what they are and when they were made; almost nothing is known at all. For the purposes of this study manuscripts of this type have been avoided as far as possible. Occasionally, however, they are all that has been made available.

3.5.1. Cotton Ms Nero D IV – The Lindisfarne Gospels

It is appropriate that this survey should start with one of the earliest surviving fully decorated manuscripts and certainly one of the most famous. For many, the Lindisfarne Gospels represents the pinnacle of artistic achievement in manuscript illumination. The work of one man, Eadfrith, Bishop of Lindisfarne, over a period of perhaps ten years, the exact date of its creation is the subject of considerable debate. Traditionally, the creation of the manuscript is ascribed to the translation of the relics of St. Cuthbert in 698 immediately before Eadfrith's succession. [Back] However, in a recent lecture Dr. Michelle Brown has discussed the association of the manuscript with the cult of St. Cuthbert and the attempts to establish a competing cult of Wilfrid at Ripon. The production of a splendid Gospel book for Wilfrid around 710 may well have been the catalyst for the production of a similar relic in honour of St. Cuthbert. On these and stylistic grounds, Brown proposes a somewhat later date for Lindisfarne between 710 and Bishop Eadfrith's death in 721. [Bro3]

A complete Gospel Book with four Gospels and Canon Tables, the Lindisfarne Gospels are a masterpiece of Anglo Saxon art. The text is from a Continental exemplar, probably a 6th century Neopolitan Gospel Book. [Alex, No. 9] Extensively and skilfully decorated, a full description and discussion of the stylistic implications of the illumination and its relationship to English and Continental exemplars is clearly far

[7] The following, from the same series, were found to be particularly useful [Alex], [Temp], [Morg], [Sand], [Scot] as well as the following exhibition catalogues [Bac1], [Webs]
[8] Other catalogues consulted include [Tho1], [Lowe] and [Addi]. Further information is also available from [Brow], [Bro1], [Dod1], [Hame], [Ham1]

beyond the scope of this work.[9] Briefly, however, the decoration consists of sixteen pages of arcaded Canon Tables (f. 10 – 17v), in pairs at each opening, and each Gospel is preceded by an Evangelist portrait (ff. 25v, 93v, 137v, 209v), a carpet page (ff. 26v, 94v, 138v, 210v) and an initial page (ff. 27, 95, 139, 211), with a further carpet page as a frontispiece to the manuscript (f. 2v) and a fifth initial page marking the beginning of the Christmas story in St. Matthews Gospel (f. 29). In addition, there are numerous large and small decorated initials marking prefaces, lists of chapters, festivals and key text passages. The most striking feature of both the carpet pages and the major initial pages is the fantastic complexity of the zoomorphic and interlace ornament, a striking contrast to the strong simplicity of the Evangelist portraits.

Previous analysis of the pigments was undertaken for the 1956 facsimile by Roosen-Runge and Werner [EQCL Vol II]. Using an optical microscope and comparisons with reconstructions from extant recipe books, their analysis concentrated on the colourings of the Evangelist miniatures. In summary, their results are presented below in Table 3.1.

The most important result from the optical analysis is the apparent identification of lazurite on f. 93v. The only known active source of lapis lazuli, the mineral from which the pigment lazurite is refined, during this period was the Badakshan mines in what is now north-east Afghanistan. [Gett] The presence of lazurite would represent the earliest known use of the pigment on a manuscript of English origin and would, by implication, prove the existence of a trade route from Badakshan, through the Mediterranean, to what Abbot Ceolfrith, in 716, described as 'the Ends of the Earth'. [Bro3]

In an attempt to verify the presence of lazurite in the decoration of the Lindisfarne Gospels, to prove the existence of this trade route and verify the accuracy of Roosen-Runge's technique, f. 93v – the Evangelist portrait of St. Mark was one of two folios selected for analysis. Since access to this manuscript is heavily restricted and time very limited only one other folio was studied. F. 139, the initial page of the Gospel of St. Luke, has not been studied by Roosen-Runge's techniques. However it does contain a variety of pigments and, particularly, three different shades of blue.

[9] The subject of a very many publications, masterful discussion and description can be found in [Bro3], [Back], [EQCL] and [Alex No. 9]. Cotton Nero D IV also features in virtually every other commentary on Anglo Saxon art.

Note: The immense complexity of the manuscript and the availability in advance of digital images of the relevant folios have made it desirable and possible to mark exactly which areas of the folio were examined on the illustration. This has not been possible in the majority of cases as permission to commission images was not obtained until after the analysis had been completed.

Colour	Pigments	Location
Red	Red Lead	Cushion, f. 25v
	Kermes and Grain – insect extracts	Cushion, f. 137v
Yellow	Orpiment	Halo, f. 25v
	Yellow Ochre	Lion, f. 93v
	Bile or Gall Yellow	Halos of symbol and servant, f. 25v
Blue	Lazurite	Cushion and Tunic, f. 93v
	Indigo/Woad	Bench, f. 25v
Green	Verdigris	Corner Ornament, top left and Matthew's Pallium, f. 25v
	Vergaut – Indigo and Orpiment	Bench Frame, f. 93v
Purple	Folium – extract of turnsole plant. pH varies the colour from red to blue.	Outer Frame, f. 137v Mark's Cloak, f. 93v Luke's Pallium, f. 137v Outer Frame, f. 25v Matthew's Tunic, f. 25v
Pink	Folium mixed with a white pigment such as White Lead, Chalk, Shell or Bone	Background, f. 25v Background, f. 93v Flesh Tones, f. 25v
Brown/Black	Ink – Iron Gall with added Carbon	Lion, f. 93v
White	Lead White	Hair, f. 25v

Table 3.1: The pigments identified by Roosen-Runge and Werner, Cotton Ms Nero D IV.

f. 93v The Evangelist Portrait of St. Mark

Area	Colour	Pigment
1	Orange	Red Lead
2	Blue	Indigo
3	Blue	Indigo
4	Blue	-
5	Blue	Indigo
6	Red	Red Lead
7	Pink	-
8	Yellow	Orpiment
9	Yellow	-
10	Yellow	-
11	Dark Green	Indigo, Trace Orpiment
12	White/Plain Parchment	Plain Parchment
13	Green	Possibly Verdigris
14	Blue	Indigo
15	Pink	-
16	Red	Red Lead
17	Dark Red	-
18	Yellow	Orpiment
19	Black	Probably Iron Gall, Trace Carbon
20	Green	Verdigris
21	Yellow	-
22	Green	Indigo/Orpiment
23	Pink	-
24	Black	Probably Iron Gall

Table 3.2: The pigments of the St. Mark Portrait – Cotton Ms Nero D IV f. 93v.

Spectra could not be obtained from some of the yellow areas, the pink or the dark red. The assignment of iron gall is made on the basis of there being no discernable Raman spectrum from a black or brown pigment, with some, occasionally considerable, fluorescence. Often small quantities of carbon are included in iron gall ink recipes, which may appear weakly in the spectrum. See figure A1.1, appendix 1.

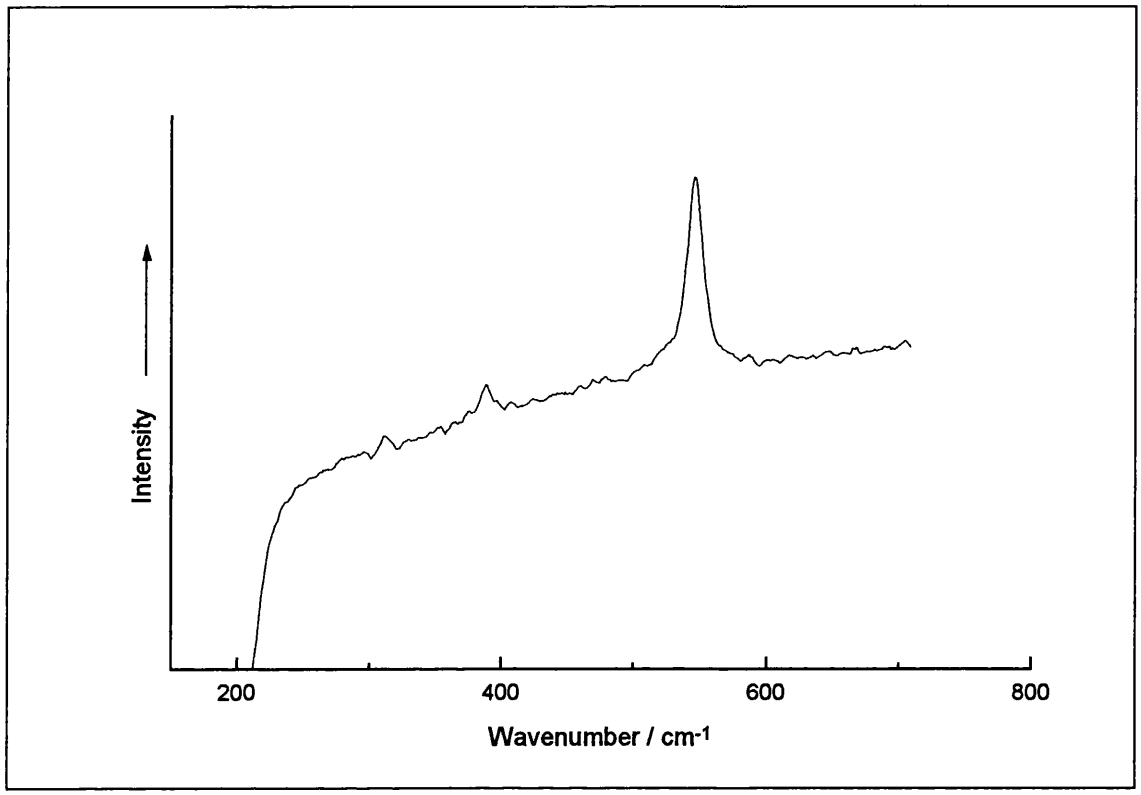

Figure 3.1: The Raman spectrum of red lead from sample area 1 of Cotton Ms Nero D IV. $\lambda_0 = 632.8$ nm, ~ 0.35 mW.

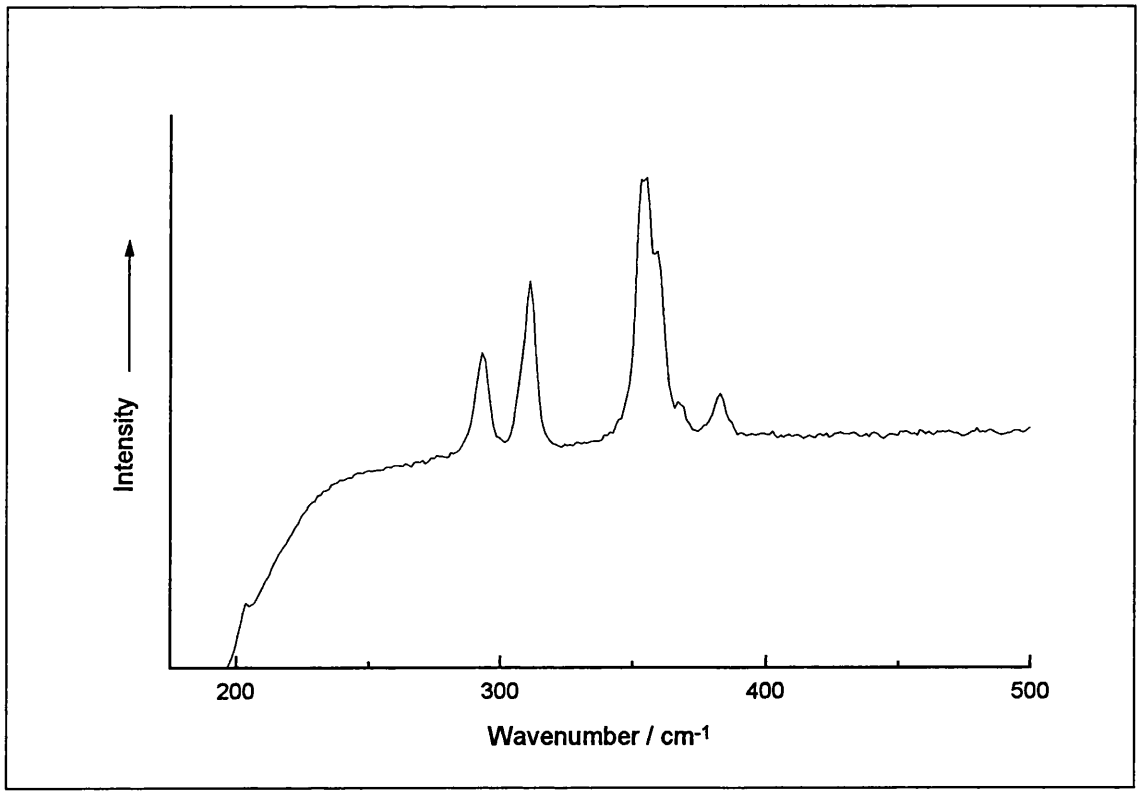

Figure 3.2: The Raman spectrum of orpiment from sample area 8 of Cotton Ms Nero D IV. $\lambda_0 = 632.8$ nm, ~ 0.35 mW.

f. 139 The Initial Page of the Gospel of St. Luke

Area	Colour	Pigment
25	Blue	Indigo
26	Yellow	Orpiment
27	Red	Red Lead
28	Green	Verdigris
29	Blue	Indigo
30	Blue	Indigo
31	Purple	-
32	Gold	-
33	Gold	-
34	Dark Green	Possibly Verdigris
35	Black	Probably Iron Gall
36	Brown-Black	Probably Iron Gall

Table 3.3: The pigments of the Initial page of the Gospel of St. Luke – Cotton Ms Nero D IV f. 139.

Spectra could not be obtained from the purple, the black and brown-black or the gold areas. See figure A1.2, appendix 1.

The results of the Raman analysis clearly show that the areas ascribed to lazurite by optical techniques in f. 93v did not give the Raman spectrum of lazurite but of the plant-derived organic compound indigotin – the source of colour for both indigo and woad.

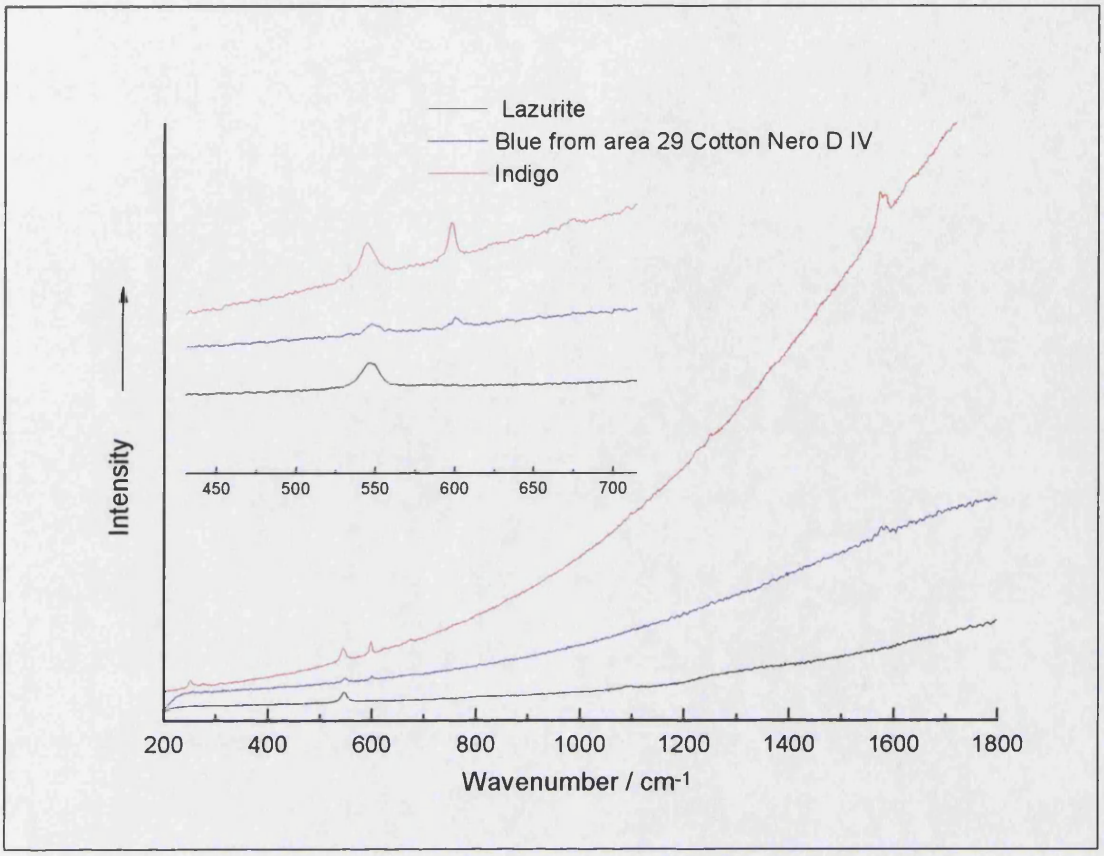

Figure 3.3: The Raman spectra of lazurite and indigo references and the blue sample from area 29 of Cotton Ms Nero D IV, indicating that the latter is indigo. Blue sample: λ_0 = 632.8 nm, ~ 0.35 mW. Lazurite and indigo: λ_0 = 632.8 nm, ~ 0.8 mW.

Contrary to accepted research [Bell] and with the advantage of modern instrumentation, it is in fact possible to obtain a Raman spectrum of indigo at visible wavelengths. The reference spectrum above was taken from a powdered sample of indigo, directly down the microscope, using a 20x lens and a laser power of approximately 0.8 mW. Twenty accumulations of 10 seconds were required with slits set at 10 μm.

As in f. 93v, the blue areas of f. 139 did not give the spectrum of lazurite but rather of indigo, this time clearly in more than one shade although no other substance was detected. Unfortunately, as the chromophore of indigo and woad is the same there is no way to distinguish between the foreign produced and the home-grown material.

The black and blue-black regions did not give Raman spectra in the case of f. 139 and only weak carbon for f. 93v suggesting the presence of an iron gall ink in both cases. The purple areas also did not give Raman spectra, perhaps implying the use of an organically derived pigment.

Interestingly, the analysis of these folios demonstrated that both verdigris and vergaut, the indigo and orpiment mixture, have been used in the green areas of the decoration. Orpiment has been used to colour some of the yellow areas although regions 9, 10 and 21 could not be identified. These could be either yellow ochre which is a poor Raman scatterer or an organic material such as the yellow gall that Roosen-Runge and Werner identified. The absence of any spectrum from the pink areas opposes the suggestion that these areas contain a white inorganic pigment in admixture with an organic red.

Verdigris is notoriously difficult to identify using the red helium-neon 632.8 nm laser, responding much better to green wavelengths. As it was not possible to analyse the manuscript directly with the 514.5 nm laser (in the absence of a suitable probe) to confirm the presence of verdigris, sweepings were taken from the gutter between f. 93v and f. 94. Quite frequently, due to the friable nature of many pigments, the gutter sweepings contain fragments of colour that have become detached from the page, becoming trapped as the manuscripts are seldom opened to their fullest extent. The sweepings were taken using new, clean paint brushes by David Jacobs, a Senior Conservator of the British Library. The sweepings were preserved on a glass slide and analysed using the microscope rather than the remote probe.

The gutter sweepings contained a large number of small particles, of various sizes, shapes and colours. Attempting to examine all of these would be extremely time consuming so a number were selected on the basis of size and colour. Verdigris was easily identified amongst this sample.

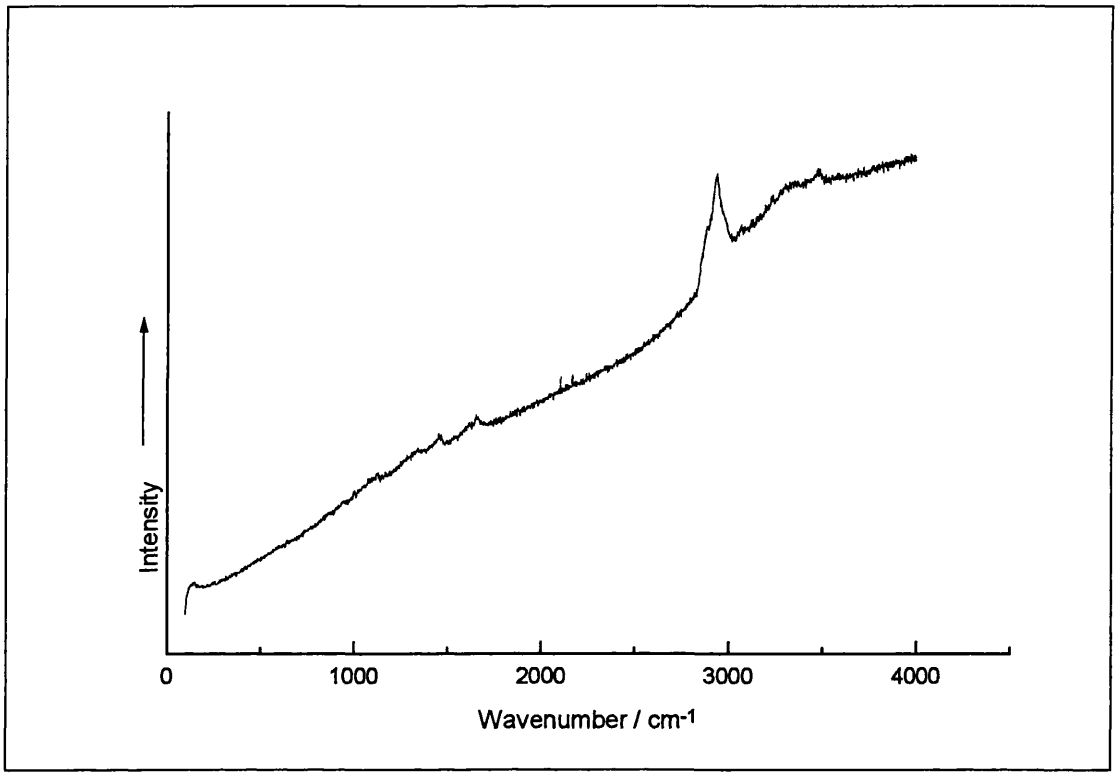

Figure 3.4: The Raman spectrum of verdigris from the gutter between ff. 93v and 94 of Cotton Ms Nero D IV. $\lambda_0 = 514.5$ nm, ~ 1.0 mW.

Although it is not possible using this technique to identify where the fragments have come from, or even to be absolutely certain that they originated as part of the illustration and have not been introduced by other means, the identification of verdigris in these sweepings gives a strong indication of the presence verdigris on the manuscript.

The absence of a spectrum from the gold painted areas on f. 139 adds considerable weight to the suggestion that these areas have been coloured with a paint composed of actual gold rather than a substitute, since gold has no Raman spectrum.

Two important conclusions can be drawn from this analysis. First, the optical microscopy techniques used for the previous analysis have proved inaccurate on two counts – the suggested presence of lazurite and the suggested presence of a white inorganic material in admixture in the pink pigment. Second, the absence of lazurite on a premium manuscript such as this suggests that the pigment was not available to Eadfrith at this time; the trading of lazurite had yet to reach Northumbria in the early 8th century.

3.5.2. Royal Ms 1 B VII

This is probably another Northumbrian manuscript, from the first half of the 8th century making it very nearly contemporary with the Lindisfarne Gospels. It has been argued that this is a copy of the same Continental exemplar that provided the text for the Lindisfarne Gospels, although with lower quality illumination. [Alex, No. 20]

The illumination consists of Canon Tables over twelve pages with major initials to the four Gospels and various smaller initials. The Canon Tables are decorated with interlace and human and zoomorphic heads although the palette throughout is limited to yellow, orange and green.

f. 9 The First Page of Canon Tables

Description	Colour	Pigment
LH Head	Yellow	Orpiment
Text, top line, top left	Red	Red Lead
LHS Central Top Decoration	Red	Red Lead
Centre, top left	Yellow	Orpiment
Bottom Centre	Red	Red Lead

Table 3.4: The pigments of the first page of Canon Tables – Royal Ms 1 B VII f. 9.

Spectra could not be obtained from the pale green areas. See figure A1.3, appendix 1.

f. 12 The Seventh Page of Illuminated Canon Tables

Description	Colour	Pigment
Centre Top	Green	Indigo, Orpiment
Centre Top, another area	Green	Indigo, Orpiment
Bottom Left	Green	Indigo, Orpiment
Bottom Right	Red	Red Lead
Bottom Right	Yellow	Orpiment

Table 3.5: The pigments of the seventh page of Canon Tables – Royal Ms 1 B VII f. 12.

See figure A1.4, appendix 1.

The pale green areas on f. 9 may not have produced Raman spectra for a number of reasons. The pigment used in these areas may have been one not suitable for Raman analysis, for example an organic material such as sap green, or large quantities of binder may be obscuring the spectrum. The simplest explanation, however, is that these areas are coloured with vergaut as are the other green areas, but are pale because very little pigment has been used thereby making it very difficult to obtain a Raman spectrum.

As discussed earlier, the yellow, red and green of the Insular manuscript are traditionally believed to be orpiment, red lead and verdigris. Here, again, general assumptions have proved to be extremely misleading. Vergaut, indigo/woad and orpiment, has been used in place of verdigris to provide the green colouring throughout. The argument for a 'traditional' triumvirate of pigments clearly cannot be applied to Northumbrian manuscripts at this time, although the palette used here is entirely consistent with the contemporary Lindisfarne Gospels.

3.5.3. Add Ms 40618

This pocket Gospel Book is an excellent example of Irish Insular book production, produced in South-East Ireland between 750 – 756 AD. Only one of its original miniatures remains, that of St. Luke (f. 21v). The initials (ff. 23 and 50) and Evangelist portraits, a second of St Luke and one of St John (ff. 22v and 49v), are later additions dating from a 10th century modernisation (c.920) for King Athelstan, probably at Winchester. Some of the original Irish decoration can still be seen below the replacement initial for St. Luke. Written in Irish cursive miniscule, developed in the condensing of text into a portable study format, the original parts of this manuscript represent an entirely new product of the close cultural synergy between Britain and Ireland from c. 550 to 900. With a range of influences including Celtic, early Christian, Germanic and Mediterranean art and culture this manuscript is representative of the beginnings of a style of decorated book production unique to Britain and Ireland that continued to develop throughout the Anglo Saxon period.

All decorated pages of this manuscript were analysed as they were few in number. They are presented here in the order they are found in the manuscript.

f. 21v The Original Miniature of St. Luke

Description	Colour	Pigments
Robes	Green	Orpiment, Verdigris
Block Pattern, RHS bottom	Yellow	Orpiment
Border	Red	Red Lead
Cloak Border	Red	Gypsum

Table 3.6: The pigments of the St Luke Miniature, Add. Ms. 40618 f. 21v.

Spectra could not be obtained from the purple areas or the darker red. See figure A1.5, appendix 1.

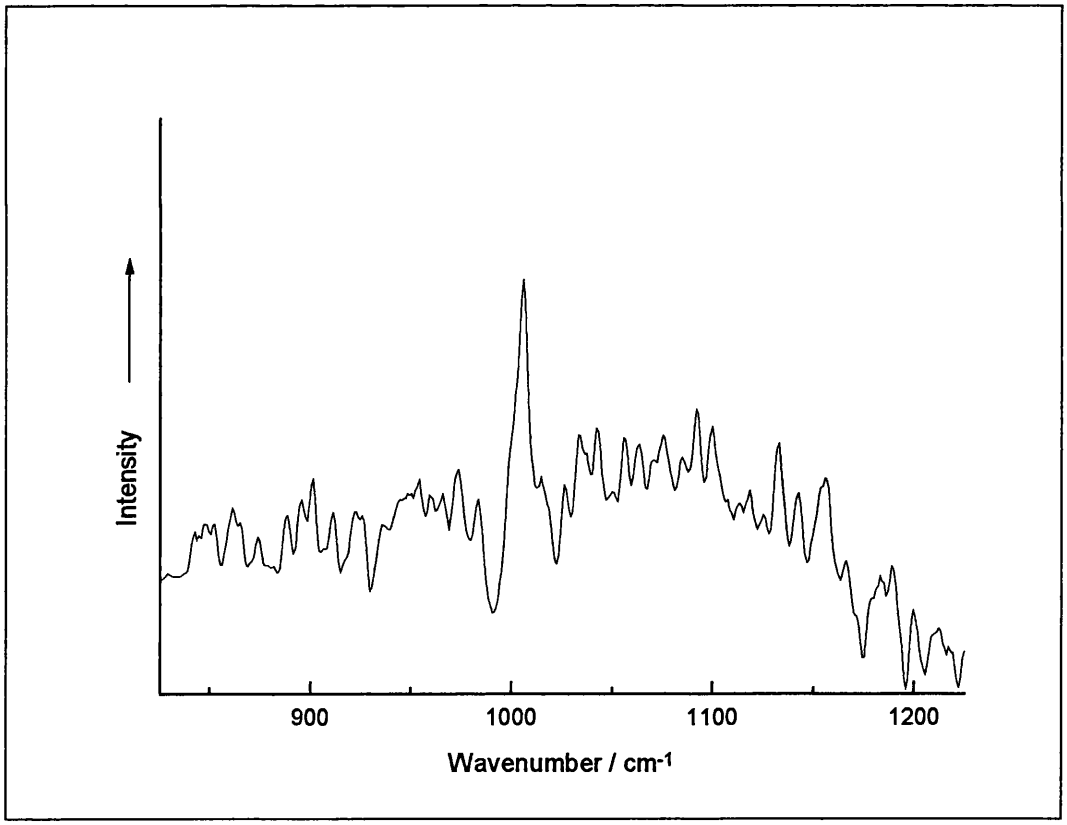

Figure 3.5: The Raman spectrum of gypsum from f. 21v of Add. Ms. 40618. λ_0 = 514.5 nm, ~ 1.0 mW.

f. 22v The Second Miniature of St. Luke

Description	Colour	Pigments
Drapes, top left	Blue	Lazurite
Background, RHS Saint	Yellow	Orpiment
Top Left Border	Red/Orange	Red Lead
LHS Border Grotesque	Yellow	Orpiment

Table 3.7: The pigments of the second St Luke Miniature, Add. Ms. 40618 f. 22v.

Spectra could not be obtained from green and dark red areas. See figure A1.6, appendix 1.

f. 23 Initial to the Gospel of St Luke

Description	Colour	Pigments
Border RHS of Q	Red	Red Lead
Shading, adjacent RHS Q	Blue	Lazurite
Shading Around Q, base	Red	Red Lead
Background	Blue	Lazurite

Table 3.8: The pigments of the Initial of the Gospel of St Luke, Add. Ms. 40618 f. 23.

See figure A1.7, appendix 1.

f. 49v The Miniature of St. John

Description	Colour	Pigment
Cloth LHS	Orange	Red Lead
Cloth LHS	Dark Red	Red Lead, Lead Degradation
Immediately Below Cloth LHS	Yellow	Orpiment
Outside Border LH Roundel	Orange	Red Lead, Lead Degradation
LHS Saint's Seat/Roof	Dark Red	Lead Degradation
Window Frame	Brownish	Red lead
Bottom of Building/Seat	Brown	Red Ochre
Bottom Left Corner, shading	Black	Weak Carbon
Footrest	Yellow	Orpiment
LHS Border	Blue	Lazurite
Bottom Left of Robe	Green	Orpiment

Table 3.9: The pigments of the St John Miniature, Add. Ms. 40618 f. 49v.

Spectra could not be obtained from some green and brown areas and the pink areas. See figure A1.8, appendix 1.

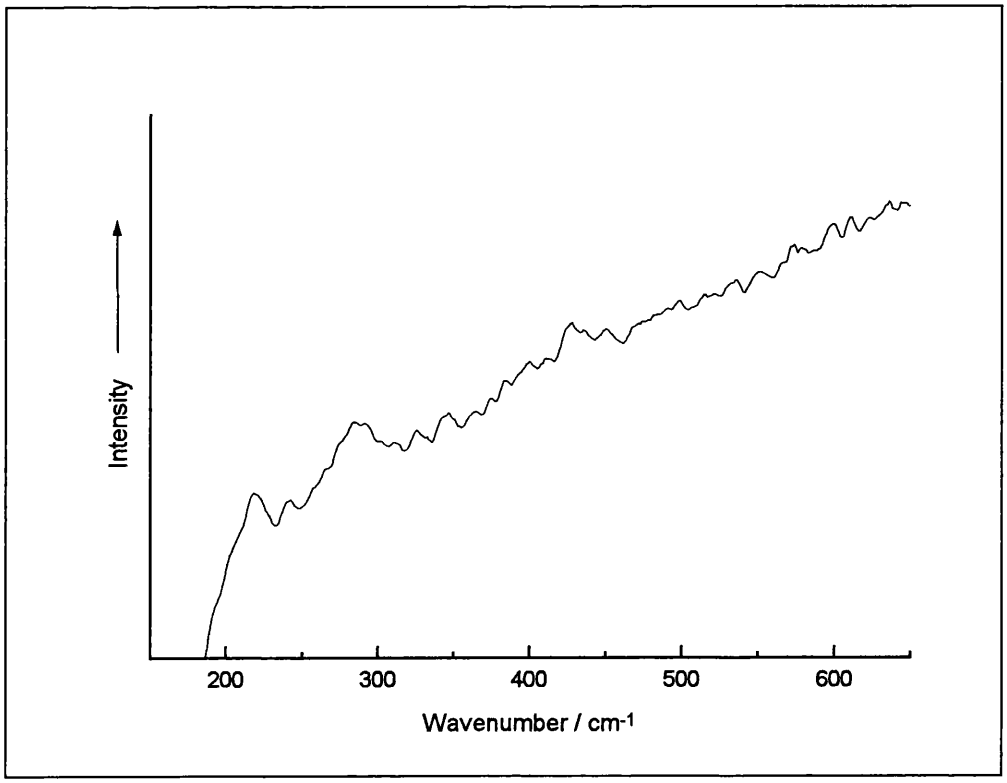

Figure 3.6: The Raman spectrum of red ochre from f. 49v of Add. Ms. 40618. λ_0 = 632.8 nm, ~ 0.35 mW.

f. 50 Initial to the Gospel of St. John

Description	Colour	Pigment
Flower RHS	Red	Red Lead
Dogs Head Grotesque	Red	Red Lead
Top Right Pattern	Blue	Lazurite
RHS Fill	Light Blue	Lazurite
RHS Centre Fill	Green	Orpiment

Table 3.10: The pigments of the Initial to the Gospel of St John, Add. Ms. 40618 f. 50.

See figure A1.9, appendix 1.

A number of areas failed to give spectra; they were dark red, purple, green, brown and pink in colour. The absence of any spectra at all would seem to imply that some of these colours are not produced from mixtures of mineral pigments, such as lazurite and red lead for purple and so forth. Raman microscopy is an excellent technique for the detection and analysis of such mixtures, producing spectra composed of features from some or all of the materials. Hence, a likely source for these pigments would be organic plant or animal materials which are considerably less amenable to analysis by Raman microscopy with visible radiation. In the case of the green areas, however, another possible explanation is that verdigris has been used as on f. 21v. Verdigris is notoriously difficult to identify and does not always produce a Raman spectrum even when it is present.

The only surviving 750AD miniature, that of St. Luke on the verso of f. 21, is distinctive in the elegant simplicity of its decoration and this is strongly reflected in the palette. Apart from the unidentified purple areas only orpiment, verdigris, red lead and gypsum (which was probably used as an extender, to increase the volume of a pigment rather than as a colour) are found, all of which could be of local derivation.

The later miniatures use a similarly limited palette, but to produce a greater range of colours. The use of verdigris may have been discontinued, perhaps being replaced with orpiment in combination with an unidentified blue pigment such as indigo. A number of key additions are also made. The use of red lead is far more extensive, and ochres

are found for brown areas but most important of all, a blue mineral pigment, lazurite, is introduced.

Until now the earliest use of lazurite in an English manuscript was thought to be the Lindisfarne Gospels but as we have seen this appears not to be the case. The 'updating' of Add Ms 40618 manuscript in around 920, which probably took place at Winchester, represents the earliest use of lazurite in an English manuscript that has been confirmed by Raman microscopy.

3.5.4. Cotton Ms Vespasian A1 – The Vespasian Psalter

Although earlier than Add Ms 40618, dating from the second quarter of the eighth century, this manuscript represents an altogether different style. An early example of the Tiberius group of manuscripts, it is composed in the Southumbrian Romanizing Uncial indicative of a Mediterranean influence. Produced at St. Augustine's, Canterbury or Minster-in-Thanet, the palette and illumination have a strong Mediterranean style – perhaps in response to manuscripts brought to Britain from Rome by Theodore of Tarsus in 669 which are likely to have provided exemplars for this work. Given that this manuscript predates Add Ms 40618, and certainly long predates its alterations, an examination of the blue pigments to ascertain the presence of lazurite is essential here.

Only one miniature survives, that of King David and his musicians (f. 30v), and two historiated initials – to Psalm 26, a D showing David and Jonathan holding spears and shaking hands (f. 31) and to Psalm 52, showing David rescuing a lamb from the lion (f. 53). Decorated initials still remain to most of the Psalms, those to Psalms 17 (f. 21v), 38 (f. 42), 68 (f. 64v), 80 (f. 79v), 97 (f. 93v), 109 (f. 110) and 118 (f. 115v) being elaborate and some decorated with birds, animals and interlace.

During the first half of the ninth century an interlinear gloss was added in the Mercian dialect of Old English, the earliest surviving translation of the psalms into English. Further material was incorporated into the book by Eadui Basan, one of the most famous artist-scribes who will be the subject of later discussion.

Initially the analysis of this manuscript was not a success. Only a handful of spectra from the many taken could be identified. The rest were essentially featureless, on large fluorescence backgrounds. A result this poor is very unusual in this type of material – the widespread use of mineral pigments generally makes analysis of most manuscripts relatively straightforward.

The paucity of results prompted further investigation of the manuscript's more recent history where an explanation for the anomaly was soon found. From the conservation records it would appear that a common consolidation treatment during the late 1970s was to thinly coat the manuscript with a layer of polyvinyl acetate (PVAc) in methanol, adhering the pigments more firmly to the page. Apart from the long-term effects on the preservation of the manuscript as a whole (see appendix 2), PVAc makes Raman analysis extremely difficult. In this particular instance it is so thinly applied as to make obtaining a spectrum of the PVAc itself almost impossible. Unfortunately even in these quantities it fluoresces hugely in response to visible laser irradiation, effectively preventing the spectra of many other materials also present from being detected. The results presented below relate to those materials that are strong Raman scatterers and could be detected through the PVAc layer.

Folio	Description	Colour	Pigments
f. 2v	Letter O Top Left	Black	Carbon
f. 3v	Rubric Letter P	Red	Red Lead
f. 30v	Centre of Chest	Red/Orange	Red Lead
f. 30v	Main Figure	Black	Carbon
f. 30v	'Floor'	Yellow	Orpiment
f. 30v	Centre Forehead LH Figure	White	White Lead

Table 3.11: The identifiable pigments - Cotton Ms Vespasian A 1.

No pigments in other areas could be identified. See figures A1.10, A1.11, A1.12, appendix 1.

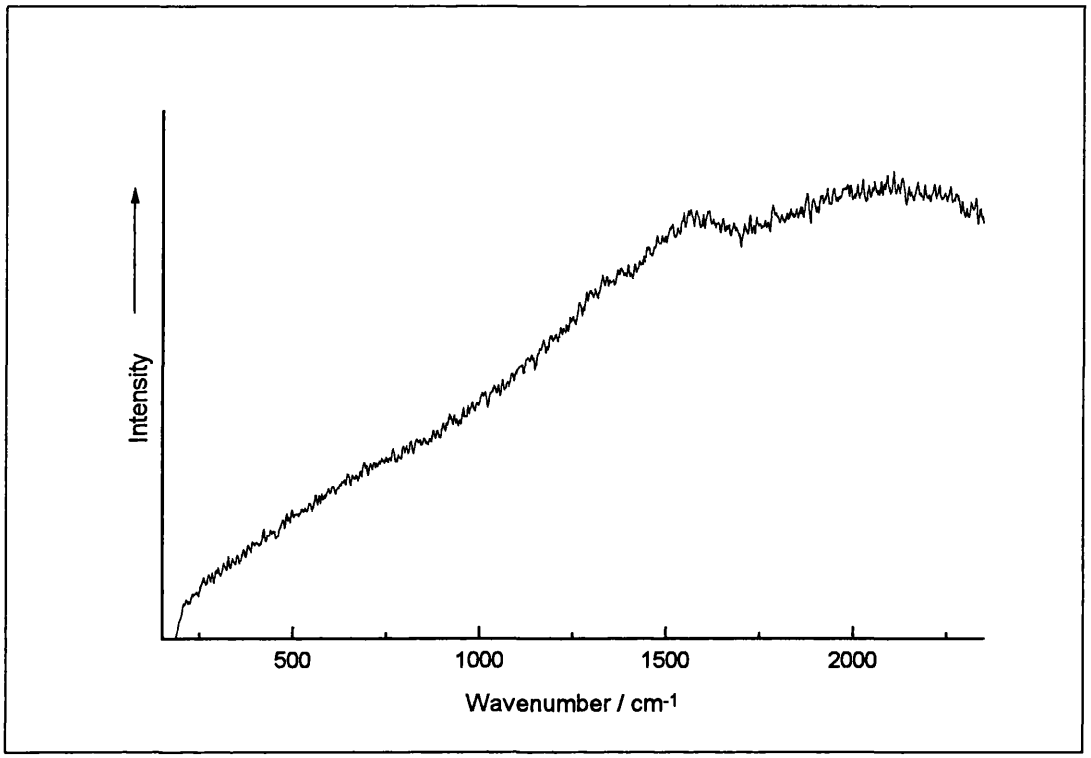

Figure 3.7: The Raman spectrum of carbon from f. 2v of Cotton Ms Vespasian A 1. λ_0 = 632.8 nm, ~ 0.35 mW.

The disappointingly few areas that gave spectra make it extremely hard to draw substantive conclusions about the palette of this manuscript. However red lead is again the dominant red pigment and white lead is seen here for the first time in white areas, which in the Irish pocket Gospel (Add Ms 40618) are left as plain parchment.

Notably, none of the blue areas examined gave identifiable Raman spectra. As lazurite is normally a strong Raman scatterer this can be interpreted in two ways. Either lazurite is there but is being obscured by the PVAc layer or the blue is actually a weaker scatterer such as the indigo that has been identified on other manuscripts of a similar date.

Also of interest is the green pigment that appears on ff. 2 and 2v. Folio 2 is itself possibly an 11th century replacement of the prefatory leaf although this is by no means certain. The green pigment is an offset of foliate decoration from another leaf that is no longer in position. A 13th century Beatus leaf (Cotton Ms Vespasian A 1 f. 1, now removed) had been placed with this manuscript by Robert Cotton during the 18th century but the offset does not match the decoration of this page. Neither does it match

that of the King David miniature that is now f. 30v but was probably originally a frontispiece.

3.5.5. Harley Ms 7653

An early Mercian prayer book made in the last decade of the 8th century, possibly from Worcester and again a member of the Tiberius group. It was used in private devotions and almost certainly produced for a woman; it has an unusually strong emphasis on female saints. Unfortunately it is in a somewhat fragmentary condition and much is missing, making it impossible to tell precisely what range of texts were included or whether there might have been a particular theme. This manuscript is not illustrated to the same extent as many of the others, having only coloured rubrication and decorated major initials.

Folio	Description	Colour	Pigment
1v	Text	Red	Red Ochre
1v	Text	Yellow	Orpiment
2v	Text	Green	Verdigris
6v	Text	Yellow	Orpiment
6v	Degraded Text	Red	Red lead
7	Text	Green	Verdigris

Table 3.12: The pigments of Harley Ms 7653.

Spectra could not be obtained from a number of red and green areas. See figures A1.13, A1.14, A1.15, A1.16, appendix 1.

It is interesting to note here that even in a relatively plain manuscript two different red pigments have been used on different pages. Unfortunately, as so little is known about the manuscript it is not possible to tell whether this is a result of the work of more than one scribe, perhaps with their own palette preferences.

The lack of spectra from red areas here may be attributable to one of two explanations. Either an organic red pigment, such as those used on the Lindisfarne Gospels, has been applied or the red areas have been coloured with red ochre. Although a spectrum was

obtained from red ochre on f. 1v, red ochre is not a strong scatterer so it is often difficult to obtain a spectrum when only a thin pigment layer has been applied.

3.5.6. Royal Ms 2 AXX – The Royal Prayer Book

The Royal Prayer Book is another Mercian devotional text although in this case there is a clear central theme – Christ as the healer of mankind. Again this book may have been owned by a woman, this time perhaps a physician, as many of the prayers are written for a female voice. The text recounts miracles from the Gospels, Roman and Celtic prayers and hymns and medical remedies and charms. From the first quarter of the 9th century and a member of the Tiberius group of manuscripts, an Irish influence is evident in both the style of text and of decoration.

The decoration is limited to rubrication, the initials of *Liber* in gold and silver (f. 1) and a zoomorphic initial (f. 17), with several smaller coloured initials.

Folio	Description	Colour	Pigments
f. 2	Solid Colour, LHS	Green	Verdigris
f. 4v	LHS Second Initial	Yellow	Orpiment
f. 4v	LHS Second Initial	Red	Red Lead
f. 4v	Letter O	Black	Probably Iron Gall
f. 17	Winged Biped	Green	Verdigris
f. 29v	Marginal C	Orange	Red Lead

Table 3.13: The pigments identified – Royal Ms 2 A XX.

See figures A1.17, A1.18, A1.19, A1.20, appendix 1.

It is interesting to note here that the marginal guides for the illuminators of the initials are in the same palette as the illumination itself.

The Irish stylistic influence also shows itself in the very simple palette of this manuscript, drawing on the common triumvirate of pigments found also in the original illustration of Add. 40618 (above). No attempt has been made to layer or shade the colours or produce complex decorative effects.

3.5.7. Royal Ms I E VI – The Royal Bible

This manuscript is probably of St. Augustine's, Canterbury origin and was created in the second quarter of the 9th century, only shortly before the beginnings of the Viking domination. It is a late example of the Tiberius group with Continental influence evident in the both the arcade framing of the opening words of St. Luke's Gospel, redolent of Carolingian Court School creations, and in the miniature of Christ Pantocrator surmounting the symbol of Luke - the bull - which was clearly modelled on a Continental exemplar, possibly Italian. [Alex, No. 32]

In its current format the manuscript comprises only a fragmentary Gospel book. A single detached folio is in the possession of the Cathedral Library at Canterbury (Additional Ms 16) and another single leaf in the Bodleian Library, Oxford is also believed to come from this manuscript (Ms Lat. bibl. b. 2(P)). However the large size of the manuscript and the quire numerations on the remaining part suggest that what remains came from a much larger Bible, rather than a distinctly separate Gospel book.
The Royal Bible is extensively decorated, although much has clearly been lost. It currently consists of decorated Canon Tables over five pages (ff. 4 – 6), an incipit page for the Gospel of St. Luke (f. 43) and initials at the chapter lists for St. Luke and St. John (ff. 42 and 68). The incipit pages of all but St. Luke's Gospel have been lost although illuminated display script is found on f. 1v, preceding St. Mark's Gospel on f. 30, St. Luke's on f. 44 and on the explicit page of St. Matthew's Gospel (f. 28v). All of these pages except for St. Matthew's explicit are in gold and silver on purple stained vellum. That of St. Matthew is in orange on plain vellum.

Purple pages such as these are somewhat unusual, extant generally only for selected folios of prestigious manuscripts. Only in a very few cases are entire manuscripts known to have been produced in gold or silver on purple, for example the 6th century manuscript of the four Gospels that was probably produced in Constantinople (of which British Library Cotton Ms Titus C. XV contains four folios).

The incipit page of St. Luke (f. 43) is also purple and illustrates his symbol and Christ the Evangelist as previously mentioned. The verso of the folio preceding St. Mark (f. 30v) also has its Evangelist portrait but in this case it is a later addition by an 11th

century artist. There is some evidence that parts of f. 43 were repainted in the same period that this addition was made.

A representative sample of the decorated pages were examined, including the Gospel miniatures and purple pages and other pages of particular interest.

f. 4 The first page of decorated Canon Tables

Description	Colour	Pigment
Bottom of Circle RHS	Yellow	Orpiment
Arcade Fill, below circle	Dark Red	Gypsum
Pattern, within circle	Light Red	Red Lead
Pattern, green border fill	White	Lead Degradation
Arcade Fill, top right	Blue/Purple	Lead Degradation
Dots, surrounding arcade	Red	Red Lead

Table 3.14: The first page of Canon Tables - Royal Ms I E VI f. 4.

See figure A1.21, appendix 1.

f. 4v The second page of decorated Canon Tables

Description	Colour	Pigment
Arcade Fill LHS	Red/Orange	Red Lead
Arcade Fill, second left top	Yellow	Orpiment
Arcade Fill LHS	Gold	Carbon, noise

Table 3.15: The second page of Canon Tables - Royal Ms I E VI f. 4v.

Spectra could not be obtained from green, black and blue areas on either page. The lack of a spectrum for the black ink implies the presence of iron gall ink. See figure A1.22, appendix 1.

f. 28v The Explicit Page of St. Matthew's Gospel

Description	Colour	Pigment
Coloured Text	Red/Orange	Red Lead

Table 3.16: The Explicit Page of St. Matthew's Gospel - Royal Ms I E VI f. 28v.

See figure A1.23, appendix 1.

f. 30v The Incipit Page and Evangelist Miniature of the Gospel of St. Mark, 11th century

Description	Colour	Pigment
Arcade Column Pediment	Red/Orange	Red Lead
Central Background	Yellow	Orpiment
Top Right Border	Yellow	Orpiment
Floor Beneath Saint	Blue/Grey	Indigo, Carbon
Hair	Brown	Red Lead

Table 3.17: The Evangelist Miniature of the Gospel of St. Mark - Royal Ms I E VI f. 30v.

Spectra could not be obtained from white, pink or some blue areas. See figure A1.24, appendix 1.

f. 43 The Incipit Page of the Gospel of St. Luke

Description	Colour	Pigment
Background to Bull	Yellow	Orpiment
Border decoration	Orange/Red	Red Lead
Border Decoration	Yellow	Orpiment
Solid Colour Around Bull	Green	Orpiment

Table 3.18: The Incipit Page of the Gospel of St. Luke - Royal Ms I E VI f. 43.

Spectra could not be obtained from the purple dye, black, brown and dark red areas. See figure A1.25, appendix 1.

Again this manuscript has not proved particularly amenable to analysis. The purple dye used on a number of the illustrated pages is rather fluorescent and has swamped the

signal from the surface pigment on a number of occasions, especially where the pigment layer is thin.

However, the standard pigments, red lead, orpiment and carbon, appear to have been used here with perhaps white lead for the 'white' areas as opposed to blank parchment in some places and orpiment in combination with another pigment for the green areas. The lack of a spectrum for the blue in this combination strongly suggests that it is not a mineral pigment such as lazurite or azurite. It is likely therefore that it is a plant or animal derived organic material of which the most likely is indigo/woad – a weak Raman scatterer that was found in the blue/grey areas of the 11th century additions.

The dark red areas, the purple dye and the pink are likely to be organically derived but whether plant, such as folium, or animal, such as murex or shellfish purple, cannot be ascertained.

The black pigment is highly likely to be iron gallo-tannate ink, since this is hard to detect by Raman spectroscopy.

3.5.8. Arundel Ms 155 – The Eadui Psalter

This is the first of a number of manuscripts known to have been written for Christ Church, Canterbury by Eadui Basan. It is established that he was working in the first half of the 11th century at Christ Church although he is known also to have spent time with King Cnut during the years of peace engendered by the allegiance to Scandinavia. Extant charters of his creation date from the second and third decades, allowing dates to be ascribed to his other works with comparative ease, including the Eadui Psalter and the Grimbald Gospels discussed here.

This particular manuscript can be dated reasonably precisely to the period between 1012 and 1023 as the original calendar, composed for use at Christ Church, includes the date of the martyrdom of St. Ælfheah in 1012 but not his translation from London to Canterbury in 1023 – this has been added later in a different hand.

The manuscript is composed of a calendar and tables, psalms, canticles, collects and prayers with 12th century additions. An interlinear gloss has been added to all but the 12th century parts, at times in Old English. The calendar (ff. 2–7v) is decorated in gold and various colours and followed by computistical tables (ff. 8v–11), for calculating moveable feasts, in similar style under arched frames in red outline. Outline drawings of St. Pachomius receiving the Easter tables from an angel, in red and black outline with green reinforcing, and St. Benedict with two monks, in black outline, are found on ff. 9v and 10.

Folio 12 contains the opening of Psalm 1 written in red and green with a decorated initial letter composed of gold panels, animal heads and scrolls, enclosed by a pair of heavy gold bands with climbing foliage. The opening initials to Psalms 51 (f. 53), 101 (f. 93) and 109 (f.105) are similarly decorated with initials and symbols of John and Luke for Psalm 51, green and gold lettering and a historiated initial of David slaying Goliath for Psalm 101 and blue lettering and a gold initial for Psalm 109. Initials to the other psalms are either red, blue, green or gold.

The two styles of illustration, the line drawings of f. 9v and the full painting of f. 93 are combined in a full page miniature (f. 133) of St. Benedict, in full colour, presenting his Rule to a group of line-drawn and tinted monks. At his feet is another monk, in full colour, believed to be a representation of Eadui Basan himself. Folios 136v – 170v are 12th century additions with initials in blue, red, green and buff and rubrics in blue and red.

The miniature of St. Benedict on f. 133 is particularly of interest since it had been subjected to pigment analysis previously. For her 1991 doctoral thesis, Sally Dormer conducted an examination of this illustration using Roosen-Runge's optical microscopy techniques. [Dorm] She identified a number of pigments (see table 3.24) some of which are not amenable to identification by Raman microscopy. Particularly the identification of folium, a plant-derived pigment of variable colour, or carmine and kermes from insects would not be possible – their absence only would be discoverable.

A selection of key folios from this manuscript have been studied, including f. 133. However the richness of the decoration is such that a complete study of every pigmented area is unfeasible.

ff. 2 and 3 First and Third Pages of the Calendar

Description	Colour	Pigment
f. 2 Text	Red, Silvery Degradation	Lead degradation
f. 2 Text	Green	Verdigris
f. 2 Text	Light Red	Red Lead
f.3 Text	Blue	Lazurite
f.3 Text	Black	Carbon

Table 3.19: The first and third pages of the Calendar - Arundel Ms 155 ff. 2 and 3.

See figures A1.26 and A1.27, appendix 1.

f. 9v From the Computistical Tables, with outline drawing of St. Pachomius receiving the Easter Tables from an Angel

Description	Colour	Pigment
Outline Drawing	Green	Verdigris
Text	Black	Probably Iron Gall, Trace Carbon

Table 3.20: From the Computistical Tables - Arundel Ms 155 f. 9v.

Spectra could not be obtained from the red rubrication, which was extremely fluorescent. See figure A1.28, appendix 1.

f. 12 The Opening of Psalm 1

Description	Colour	Pigment
Centre of B	White	White Lead, Gypsum
Centre of B	Orange	Lead Degradation
Bottom of Top Edge of B	Blue	Lazurite
Text	Red	Red Lead
Letter E	Green	Verdigris
Text	Pale Green	Verdigris

Table 3.21: The Opening of Psalm 1 - Arundel Ms 155 f. 12.

Spectra could not be obtained from the brown and pink areas. See figure A1.29, appendix 1.

f. 21v A Rubricated Page of the Psalms

Description	Colour	Pigment
Letter E	Dark Red	Red Lead
Letter E	Blue	Lazurite
Text	Black Ink	Probably Iron Gall, Trace Carbon

Table 3.22: A rubricated page - Arundel Ms 155 f. 21v.

See figure A1.30, appendix 1.

f. 133 Full Page Miniature of St. Benedict

Description	Colour	Pigment
Tinted Section RHS	Blue	Lazurite
Sky Above Heads	Orange/Red	Red Lead
Sky	Blue	Lazurite
Saint Benedict's Hair	Blue Grey	Indigo
Cope Fastening	Orange	Red Lead
Collar	White	White Lead
Bottom Right Arcade	Light Green	Verdigris

Table 3.23: The Miniature of St. Benedict - Arundel Ms 155 f. 133.

Spectra could not be obtained from the blue-green, the brown or the red tinted areas. See figure A1.31, appendix 1.

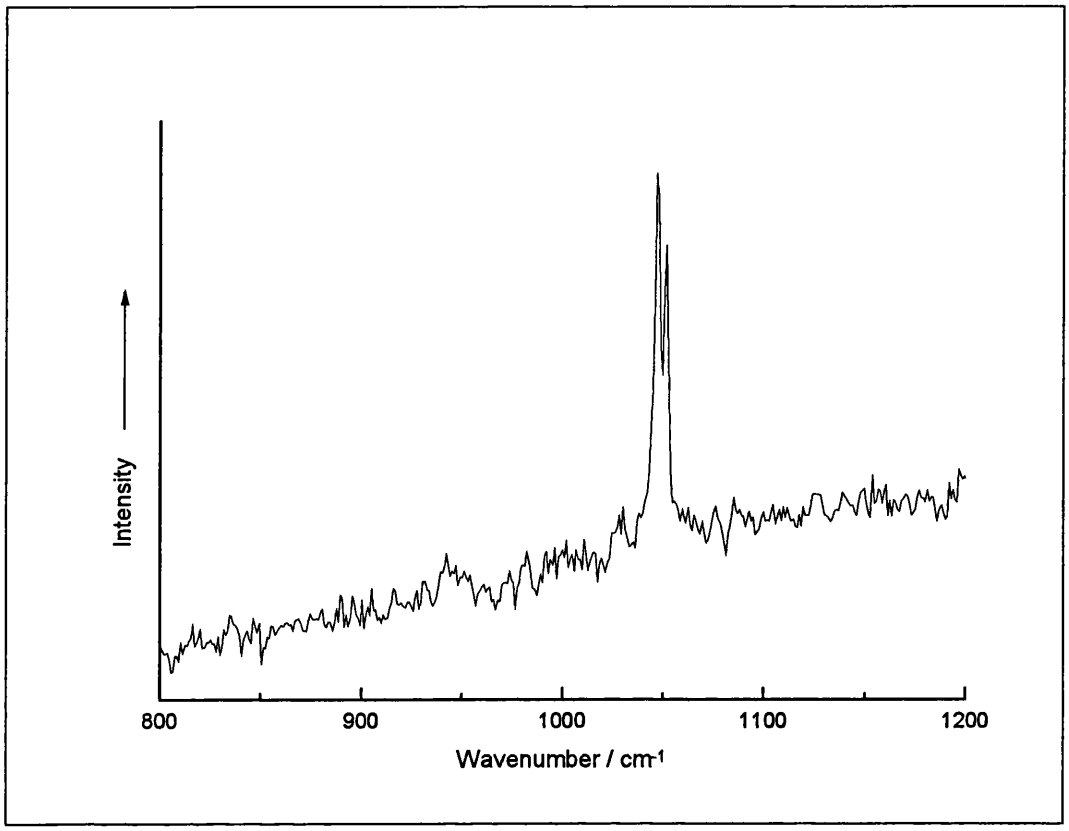

Figure 3.8: The Raman spectrum of white lead from f. 133 of Arundel Ms 155. λ_0 = 632.8 nm, ~ 0.35 mW.

Description	Colour	Pigment
Shadows	Red	Red Lead
Sky	Blue	Azurite
Cope Fastening	Orange	Red Lead
Saint Benedict's Hair	Blue-Grey	Azurite
Habit, prostrate monk	Red-Brown	Kermes
Arcade Infills	Green	Malachite
Tunic, monk with book	Red Tint	Carmine
Fill, behind prostrate monk	Green	Vergaut, Indigo/Orpiment

Table 3.24: The pigments of f. 133 identified by Sally Dormer.

Here it is particularly interesting to note that the Raman results totally contradict those of the optical examination as far as the blue pigments are concerned. Where Dormer has azurite, the spectrum of either indigo or lazurite has appeared. So while it would appear that although an extended palette of blues has been used, they are not as was initially supposed.

The greens, too, have proved more complex – Dormer identifies vergaut and malachite but only verdigris is identified by Raman microscopy. However, it is worth noting that not all of the same areas have been examined so there may yet be other pigments to discover by Raman microscopy. Brown and red-tinted areas that did not give spectra may have been coloured in an organic pigment such as folium, kermes or carmine, or a weakly scattering inorganic such as ochre.

f. 135v A Rubricated Page

Description	Colour	Pigment
Letter V	Blue	Lazurite
Text	Red	Red Lead
Text	Black	Probably Iron Gall

Table 3.25: A rubricated page - Arundel Ms 155 f. 135v.

See figure A1.32, appendix 1.

f. 147 Rubricated 12th Century Page

Description	Colour	Pigment
Small Initial	Green	Verdigris
Initial	Red	Vermilion
Initial	Blue	Lazurite
Initial	Beige	Trace Vermilion
Text	Black	Probably Iron Gall

Table 3.26: A 12th century addition - Arundel Ms 155 f. 147.

Spectra could not readily be obtained from the beige areas; vermilion is remarkably Raman active so it is very difficult to distinguish between vermilion that might have been used as part of the beige colouring and that which appears in very small quantities as accidental contamination. See figure A1.33, appendix 1.

The comparison of the optical and Raman microscopy results again demonstrates the inaccuracies of the optical technique. The blue areas that gave spectra all proved to be lazurite or indigo rather than the expected azurite. However, this does not preclude the presence of folium, carmine or kermes in the areas that did not give spectra.

The use of vermilion on the 12th century additional page is the first use of vermilion on a manuscript of English production found by this study. So far only red lead and ochre had been seen. Vermilion is produced in one of two ways; either mining the mineral form or a fairly rudimentary synthesis that has been known since at least as early as the end of the 7th century. The use of vermilion here represents either a spread in the trade of the mineral, since it is not found in the British Isles, or the synthetic form or the spread of the technology and knowledge required to allow the scribe to perform the synthesis for himself. [Get1]

3.5.9. Add. Ms 34890 – The Grimbald Gospels

This is another Eadui Basan manuscript, dated to approximately 1020, demonstrating considerable stylistic innovation. It uses plain backgrounds for its portrait miniatures, in contrast to earlier, more decorative surrounds and unusual compositions in the borders – particularly for the pages of St. John. Also unusual is the considerable use of silver in the decoration, which is now unfortunately considerably oxidised.

The pages preceding the Gospels are initialled in gold, with rubrics in red, blue and gold. Each Gospel begins with the customary Evangelist portrait and a decorated initial page with matching borders although those of Mark have been lost. (Matthew f. 10v-11, Luke f. 73v-74 and John f. 114v-115) The pages of Matthew and Luke are in acanthus-patterned Winchester borders, with medallions on four sides and gold and silver ornaments. Those of John are in similar style but the borders are filled not with foliage, but with figures and roundels containing choirs of angels and virgins. On either side of the portrait miniature the frame contains two medallions enclosing six apostles each whilst at the bottom two angels are portrayed holding a cloth containing naked figures – the souls of the departed. At the top of this and the text page are roundels supported by angels, showing the Trinity in Majesty on the one hand and the Virgin and Child on the other.

The considerable complexity of the Winchester style decoration of this manuscript makes it impossible to analyse completely. A representative sample of the colours and areas of each page has been selected on the basis of visual examination.

f. 1 A Text Page

Description	Colour	Pigment
Text	Black	Probably Iron Gall
Text	Red	Lead Degradation
Text, first line	Blue	Lazurite
Text, second line	Blue	Lazurite

Table 3.27: A text page - Add. Ms. 34890 f. 1.

Spectra could not be obtained from the ground visible below the gold initial. See figure A1.34, appendix 1.

f. 10v Evangelist Miniature of St. Matthew

Description	Colour	Pigment
Central Bezel, bottom left (adjacent to red lobe)	White	Red Lead, White Lead
Centre Bottom	Blue	Lazurite
Left of Centre Bottom	Green	Verdigris
Bottom Left Bezel	Yellow	Orpiment
Robe Above Leg	Grey	Indigo
Face of Saint	White	White Lead
Drapes, under Saint	Dark Blue	Lazurite

Table 3.28: The Evangelist Miniature of St. Matthew - Add. Ms. 34890 f. 10v.

Spectra could not be obtained from the red, pink and purple areas. See figure A1.35, appendix 1.

f. 73v Evangelist Miniature of St. Luke

Description	Colour	Pigment
Sleeve Drape, left arm	Blue	Lazurite
Box at Feet	Yellow	Orpiment
Central Bottom of Pattern	Grey	Indigo
Saint's Feet	White	White Lead
Bottom Left Bezel	Yellow	Orpiment
Centre Bottom	Yellow	Orpiment

Table 3.29: The Evangelist Miniature of St. Luke - Add. Ms. 34890 f. 73v.

Spectra could not be obtained from green, brown, purple or red areas. See figure A1.36, appendix 1.

f. 114v Evangelist Miniature of St. John

Description	Colour	Pigment
Bottom Centre	Blue	Lazurite
Adjacent Fold Pattern	White	Carbon, Lazurite
Below Robe	Green	Verdigris
Face	White	White Lead
Top of Plinth, LHS of two	Red	Lead Degradation
Scythe, bend	Yellow	Orpiment
RHS Plinth, by knee	Black	Carbon

Table 3.30: The Evangelist Miniature of St. John - Add. Ms. 34890 f. 114v.

Spectra could not be obtained from the brown areas. See figure A1.37, appendix 1.

The pigment mix of this manuscript is almost identical to that of British Library Ms Arundel 155, with the same use of verdigris, rather than a yellow/blue mixture, for the green areas, white lead for the white areas, red lead, lazurite and indigo. Again spectra cannot be obtained from some green, brown, pink and purple areas perhaps denoting the presence of organic pigments.

The Grimbald Gospels do represent a considerable stylistic advance in English manuscript production, perhaps a result of the freedom allowed by Cnut's temporary peace. However the similarity of the two palettes is striking, even with the stylistic differences. This provides strong evidence for an artistic preference for the use of particular materials in predetermined ways even as the nature of the product itself changes.

3.5.10. Cotton Cleopatra C VIII – Psychomachia, Prudentius

Aurelius Clemens Prudentius (348 – c.410) was a Spanish lawyer and civil servant but in his retirement devoted himself to the writing of Christian polemic and poetry. The Psychomachia (meaning 'Spiritual Combat') is an allegorical poem that uses the struggle between Christian virtues and pagan vices to represent the conflict between Christianity and paganism. This copy dates from the end of the 10th or the beginning of the 11th centuries and was again produced at Christ Church, Canterbury.

The manuscript is illustrated with a cycle of drawings of which eighty-two remain. They are in coloured outline with rectangular frames that they frequently overspill. The illustrations are by two artists working in similar styles. Hand I was responsible for ff. 1–16v and ff. 27v–33v while Hand II had charge of the mostly unfinished ff. 18–27. The opening of the prologue is in an apparently metallic red on a coloured band, while initials to sections and verses are in blue, red or green.

In the same binding is found some other material that is not a part of the Psychomachia. Nothing appears to be known about it except that it is probably Continental and from the late 11th or early 12th centuries. However, pages illustrated by each of the two hands of the Psychomachia and from the second manuscript have been examined.

f. 4 An Illustrated Page by Hand I

Description	Colour	Pigment
Letter N	Red	Red Lead
Line Drawing	Red	Red Ochre
Line Drawing	Black	Carbon
Line Drawing	Green	Verdigris
Text Initial	Green	Verdigris

Table 3.31: An illustrated page - Cotton Cleopatra C VIII f. 4.

See figure A1.38, appendix 1.

f. 18 An Illustrated Page by Hand II

Description	Colour	Pigment
Drawing	Green	Verdigris

Table 3.32: An illustrated page - Cotton Cleopatra C VIII f. 18.

Spectra could not be obtained from the yellow areas. See figure A1.39, appendix 1.

f. 28 A Second Illustrated Page by Hand I

Description	Colour	Pigment
Drawing	Blue	Lazurite, Carbon
Text	Blue	Lazurite

Table 3.33: An illustrated page - Cotton Cleopatra C VIII f. 28.

See figure A1.40, appendix 1.

f. 31 A Third Illustrated Page by Hand I

Description	Colour	Pigment
Sketch	Red	Red Ochre
Text	Red	Red Lead

Table 3.34: An illustrated page - Cotton Cleopatra C VIII f. 31.

See figure A1.41, appendix 1.

f. 38v A Page from the Second Manuscript

Description	Colour	Pigment
Text	Red	Vermilion
Text, Dark Area	Red	Vermilion

Table 3.35: A decorated page from the second manuscript - Cotton Cleopatra C VIII f. 38v.

Spectra could not be obtained from the purple letters. See figure A1.42, appendix 1.

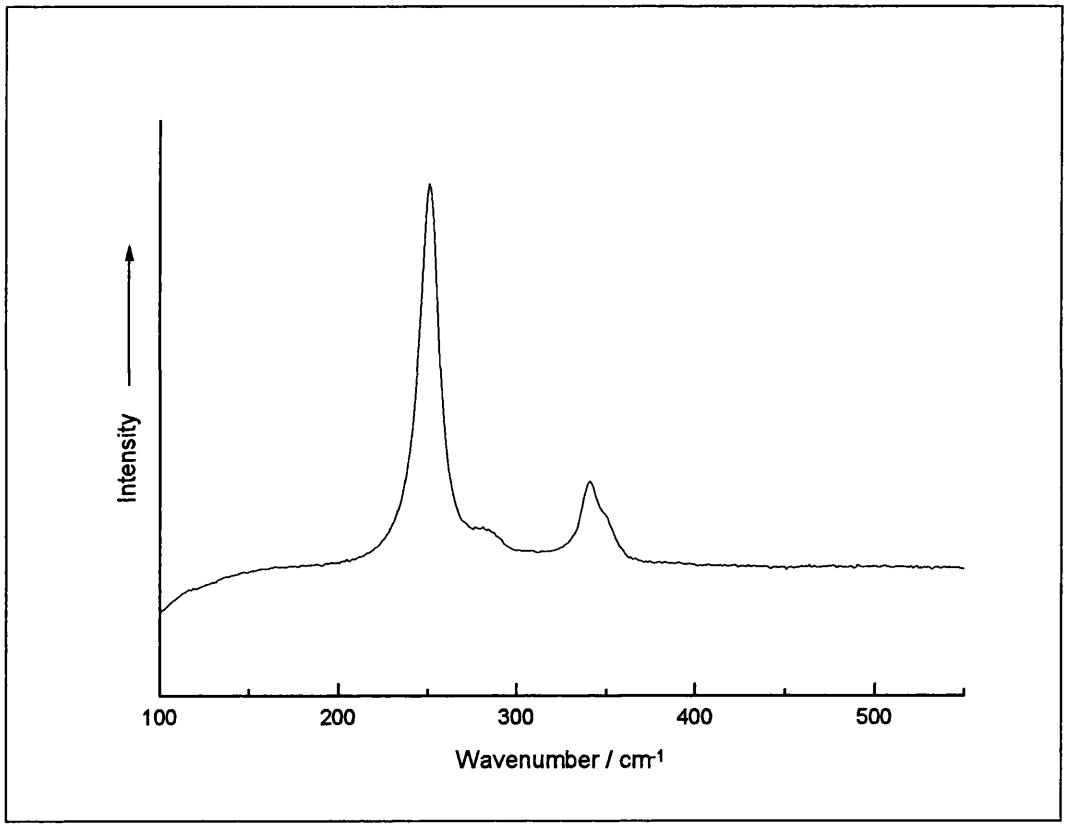

Figure 3.9: The Raman spectrum of vermilion from f. 38v of Cotton Ms Cleopatra C VIII. $\lambda_0 = 632.8$ nm, ~ 0.8 mW.

f. 48 Another Decorated Page from the Second Manuscript

Description	Colour	Pigment
Small Text	Red	Vermilion
Initial O	Red	Vermilion

Table 3.36: A decorated page from the second manuscript - Cotton Cleopatra C VIII f. 48.

See figure A1.43, appendix 1.

The palette of Hand II is apparently more limited than that of Hand I, with the use of only the same green pigment as Hand I and an unidentified yellow pigment. A clear distinction is made here between red pigments for drawing and those for the writing of text, red ochre and red lead respectively. However verdigris has been used for the green in both cases, perhaps suggesting that only one such pigment was available to the artists and scribe.

The red pigment used for the rubrication is completely different in the case of the second manuscript. The introduction of vermilion in preference to red ochre or red lead almost certainly dates this part of the manuscript to considerably later than the Psychomachia as we have seen from the consideration of contemporary material.

3.6: Later Manuscripts

The Anglo Saxon political period ended with the 1066 Norman conquest. However even in the closer union that followed, English art remained a school somewhat distinct from its Continental counterparts. Rather, the Normans excelled in administration and architecture than in applied arts such as carving and illumination. Their influence served instead to introduce English art to the Romanesque developments that had and were occurring on the Continent and to alter the script in which documents were written. This change is nowhere more clearly seen than in the introduction of a Bec hand and a more stilted style at Christ Church, Canterbury, which arrived with an infusion of Bec monks under the Norman Abbot Lanfranc who was determined to bring that somewhat relaxed house back into line. [Dod1]

The manuscripts discussed here date from the few centuries following the Norman conquest until the influence of the growing cloth trade, with the concomitant expansion in the dye industry, and the rise of the printing press irrevocably changed the nature of book production and decoration.

3.6.1. Add Ms 42555 – The Abingdon Apocalypse

The manuscript was produced for Abingdon Abbey in the years between about 1270 and 1275, at the beginning of the long period of prosperity under Edward I. It was left unfinished but, even in this incomplete state, was considered important enough to find its way into the possession of Queen Joan of Scotland in 1362.

This Apocalypse, in Latin with a French gloss, is unusual in that it is one of only a very few where both the text and the commentary are illustrated, resulting in 156 miniatures – approximately twice the usual number. These follow a number of themes including the Apocalypse itself and the Life of St. John. With the exception of ff. 64 and 64v the drawings are in one hand, often clearly visible from f. 30v onwards, and incorporate many elements of the new French influence. The earliest pages are coloured by an artist of considerable ability but the later pages are only partially completed by the artists, some of whom were rather less able. The roughest colouring may be later in date but stylistic analysis has not been possible due to the carelessness of the painting.

f. 5 St. John on Patmos

Description	Colour	Pigment
LHS Angel	Red/Orange	Vermilion
Lettering, in illustration LHS	Red	Vermilion
Top border	Orange	Vermilion, White Lead
Ground Under Gold, top right border	Pink	Chalk, Vermilion
Robe, RH figure	Dark Blue	Indigo
Finger, angel	White	White Lead
Ground, peacock tail	Pink	Vermilion, Chalk
Peacock Tail	Red	Vermilion
Peacock Tail	Grey	Carbon
Text	Red	Vermilion
RHS Principal Illumination	Green	Verdigris

Table 3.37: St John on Patmos – Add. Ms 42555 f. 5.

Spectra could not be obtained from the brown areas. See figure A1.44, appendix 1.

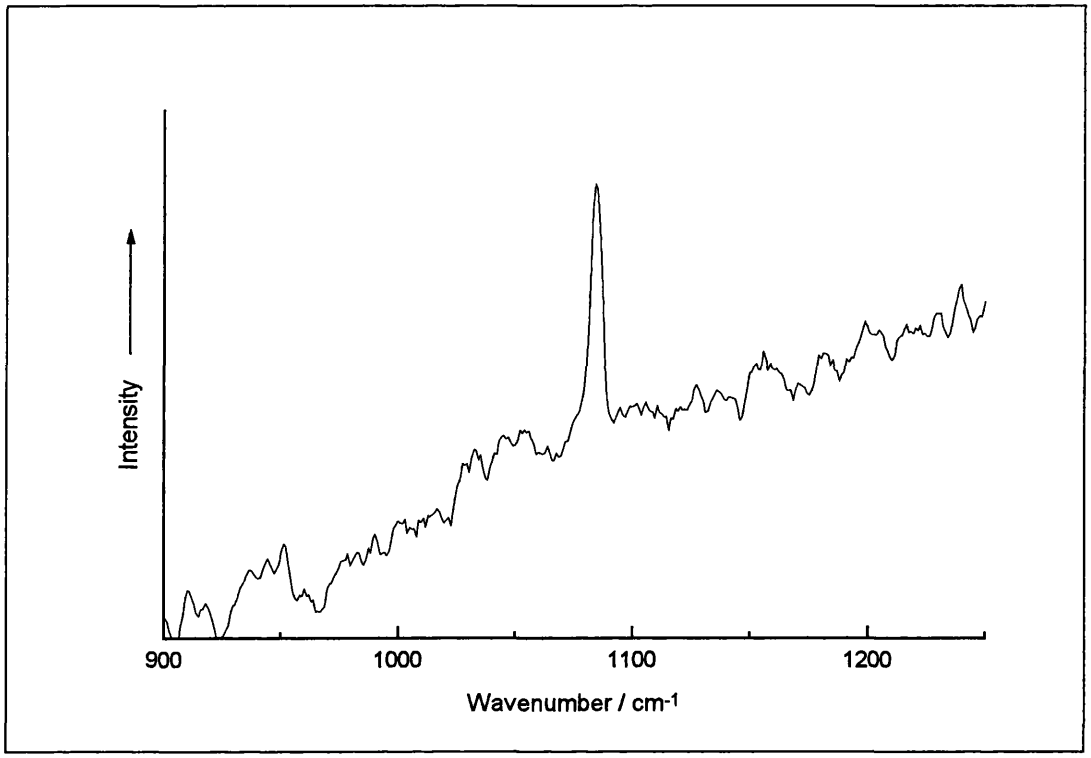

Figure 3.10: The Raman spectrum of chalk from the ground on f. 5 of Add Ms 42555. λ_0 = 632.8 nm, ~ 0.35 mW.

f. 6 Christ in Mandorla, with two supplicants flanked by Evangelist symbols and clerics

Description	Colour	Pigment
RH Border	Pale Blue	Lazurite
RH Border	Red	Vermilion
Bottom Border	Orange	Red Lead
Bottom, below text RHS	Red	Vermilion
Bottom, below text RHS	Blue	Lazurite
Hood	Green	Lazurite
Mandorla – lower background	Green	Verdigris
Text	Black	Probably Iron Gall

Table 3.38: Christ in Mandorla with Evangelist Symbols and Clerics – Add Ms 42555 f. 6.

See figure A1.45, appendix 1.

f. 18v St. John Shown the Celestial Host, with Christ in mandorla and Agnus Dei

Description	Colour	Pigment
Figure Third Row LHS	Yellow	Orpiment

Table 3.39: St. John with Christ and Agnus Dei – Add Ms 42555 f. 18v.

See figure A1.46, appendix 1.

f. 22 Moses Receiving the Law, with souls in peril on the sea

Description	Colour	Pigment
Sea RHS	Green	Verdigris
Flames	Red/Orange	Red Lead
Robe Central Figure	Blue	Lazurite
Top Border	Blue	Lazurite, Chalk
Ground Under Gold	Pink	Vermilion, Chalk
Below Text	Red	Vermilion

Table 3.40: Moses Receiving the Law With Souls in Peril on the Sea - Add Ms 42555 f. 22.

Spectra could not be obtained from some of the pink, black or blue areas. See figure A1.47, appendix 1.

This folio is particularly of interest as it contains a somewhat unusual representation of Moses with horns. This arises from a mistranslation of a passage in the text which should read "Moses came down from the mountain and he was radiant" rather than "...and he was horned" which has been illustrated.

f. 75 Decapitation of Martyrs, Christ and the heavenly host look on

Description	Colour	Pigment
Right Hand Figure	Green	Verdigris
Central Figure	Dark Blue	Lazurite
Robe	Blue Grey	Lazurite, Carbon
LH Main Figure	Orange	Red Lead
Sleeve	Yellow	Orpiment

Table 3.41: Decapitation of Martyrs – Add Ms 42555 f. 75.

Spectra could not be obtained from the pink areas. See figure A1.48, appendix 1.

This manuscript is slightly unusual in that it is possible to get good access to the ground, the surface preparation, normally concealed by the painting on top of it. Here the ground is principally composed of chalk with vermilion added as a colorant.

Another point of note here is the use of red lead for orange areas with vermilion for the red. Also of interest is the apparent use of lazurite in one of the green areas, although whether this is in combination with a yellow pigment to form the green or as an over-paint or shading it is impossible to tell.

3.6.2. Add Ms 24686 – The Alphonso Psalter

A London or East Anglian manuscript, the Psalter was produced in honour of the intended marriage of Prince Alphonso to Margaret of Holland. It can be dated very precisely as the betrothal took place in 1284 but Prince Alphonso died in August of that year, by which time only the text of the Psalms, Canticles and Litany and decoration of Psalms 1–25 were complete. Later, at the behest of his sister, Elizabeth de Bohun, the manuscript was updated with inserted Paris miniatures from the late 13th century. This was completed before the insertion of her obituary in 1316.

The decoration, as with the text, falls into a number of sections. First there are three full-page 14th century miniatures (ff. 2–3v), each in four compartments, of standing saints. This is followed by three similar pages (ff. 3v–4v), in six compartments, containing pasted-down 13th century French miniatures of the Passion and Resurrection on a 14th century background. Folios 5 through 10v contain a calendar with a strong East Anglian and Dominican influence, as evidenced in the choice of saints' days it commemorates, in red, gold, blue and black with early 14th century foliate decoration. Added around 1300, it includes obituaries for mostly female members of the English royal family in a number of hands.

The first gathering of Psalms (ff. 12–18v) have decorated initials in rose or blue against rose, blue or gold backgrounds, with geometric motifs, interlaced tendrils, grotesques or animals. Partial borders contain marginal scenes of mermaids, griffins and lions inter

alia, all extremely detailed and well executed. The decoration of the second gathering of Psalms (ff. 19–25v) is contemporary with the first and similar in design but without the decorated borders.

The rest of the manuscript has typical early 14th century decoration with large initials at the Psalter divisions (ff. 26v, 37v, 47v, 48, 58, 71v, 83v, 85 and 97), having foliate fillings and borders, and the Dominican-style Litany and Collects (ff. 132–136) that would be expected of a royal manuscript at this time.

f. 2 Early 14th C Miniatures of the Saints

Description	Colour	Pigment
Top right figure, robe RHS	Red	Red Lead
Block at Neck	White	White Lead
Robe, Centre	Blue/Grey	Lazurite
Sleeve, top left	Green	Verdigris
Robe Lining	Orange	Red Lead
Arm, bottom left	White	White Lead
Leaf, top right	Green	Verdigris
Top right figure	Dark Green	Verdigris
Halo	Blue	Azurite

Table 3.42: The 14th century miniatures – Add Ms 24686 f. 2.

Spectra could not be obtained from the pink areas. See figure A1.49, appendix 1.

f. 4 Late 13th C French Miniatures of the Passion

Description	Colour	Pigment
Top right robe, French	Orange	Red Lead
LHS French Top Border	Pink	White lead
Crown, top left, French	Green	Verdigris
Background Over-paint	Blue	Azurite

Table 3.43: The late 13th century miniatures - Add Ms 24686 f. 4.

Spectra could not be obtained from the pink areas, and some of the blue areas. See figure A1.50, appendix 1.

f. 8 A Decorated Calendar Page

Description	Colour	Pigment
Lettering	Red	Vermilion

Table 3.44: A decorated calendar page – Add Ms 24686 f. 8.

Spectra could not be obtained from the blue text. See figure A1.51, appendix 1.

f. 71v A Psalter Division Initial Page

Description	Colour	Pigment
Leaf	White	Chalk
Leaf, top left	Green	Verdigris
Border	Blue	Azurite
Border	Pink	White lead

Table 3.45: A Psalter division page – Add Ms 24686 f. 71v.

See figure A1.52, appendix 1.

f. 111v A Decorated Text Page

Description	Colour	Pigment
Text	Red	Carbon
Text Decoration	Dark Blue	Carbon
Leaves	Dark Green	Verdigris
Border	Blue	Azurite
Text	Blue	Azurite

Table 3.46: A decorated text page – Add Ms 24686 f. 111v.

See figure A1.53, appendix 1.

Here we see for the first time in this survey the use of azurite in the decoration of a manuscript, occurring in almost all facets of the decoration. The only place where it does not appear to occur is in the 13th century French miniatures – it is only found in the painting applied around and on the paste-downs, probably when they were inserted. Interestingly azurite is found in combination with lazurite on the 14th century miniatures

but indigo has not been used – perhaps suggesting a widening of the available palette and a move towards more costly materials.

Also of interest is the use of two different white pigments, white lead and chalk although the chalk only appears in the later illumination. Two red pigments have also been used – red lead and vermilion although the use of vermilion appears to be restricted to the text rather than the decoration.

3.6.3. Harley Ms 7026 – The Lovell Lectionary

The Lectionary was commissioned in or before 1408 for Salisbury Cathedral by John Lord Lovell (d.1408) and probably originates in the Benedictine Abbey at Glastonbury; their coat of arms is found in the upper border of f. 10. It is an unusual manuscript both because of its size, when complete it probably ran to more than one thousand folios of which a small portion remain, and because of the complexity of its decoration. Also bound with this manuscript are a number of decorated folios of text from a Missal, probably of London origin, dating from c. 1450 – 60.

Of particular significance is an unusual full page miniature (f. 4v) of a monk giving to or receiving from a figure, believed to be Lord Lovell, a book bound with a scene of the Coronation of the Virgin. It represents the first surviving image of a contemporary person that is likely to be a true portrait and is also considerably unconventional in style. The identity of the monastic figure remains uncertain, however. An inscription in the lower frame 'ffrater Johes Siferwas', the acknowledged illustrator of the Sherbourne Missal, has generally given rise to the belief that the figure in black is that of Siferwas himself. However, as no precedent exists for a Presentation scene between donor and illustrator, the monk may be either the abbot of the Benedictine abbey responsible for producing the book or one of the canons of Salisbury Cathedral accepting it.
In either case the construction of the scene is atypical with half-figures standing, Lord Lovell at a window, and shaking hands as the book is passed between them. Colour has been used very sparingly to emphasise the fine profile of Lord Lovell, in contrast to the darker background, with shading in white and grey.

Apart from Siferwas' frontispiece (Hand A), the hands of at least two other illustrators can be seen. Hand B (ff. 7, 9, 10, 12, 19, 20) draws somewhat lumpish figures without much decoration and predominantly shaded in black. His facial complexions lean towards the orange and are somewhat crudely applied. Hand C (ff. 5, 6, 7v, 9v, 10, 11, 20), which may again be Siferwas, has considerable mastery of perspective (particularly in f. 6) and produces work of unusual realism such as background trees and towns (f. 10 and 11). Complexions are shaded in browns and greens with less black outlining than is found in Hand B's work. Hand D completes the remaining pictures in the Lectionary. His backgrounds are more archaic in style with stippled gold designs. His figures are more angular in style than those of B although the representation of the faces is similar to B's. His depiction of the Nativity of the Virgin contains the first known use of shadow in English book illustration, with darkening of the floor tiles where the interior ceiling would affect the amount of light falling upon them.

The borders are, in this case, of equal illustrative importance to the miniatures. The basic structure is traditional and English with marginal scenes and English style decorative work such as oak and trefoil leaves, vines, and gold balls in support. The borders were produced by more than two hands – Border Hands A and B being restricted to the borders only, but illustrative Hand D making a reappearance. Border Hand A (ff. 5, 6, 7, 7v, 8, 9, 9v, 10, 11, 12, 19 and 20) was responsible for the most inventive designs with angels, dragons, human heads and coats of arms in roundels, ivy vines, acanthus and strawberries. Border Hand B is found mostly on the pages illustrated by Hand D (ff. 13, 14, 14v, 15, 16, 17, 18 and 18v) and is less inventive than Border Hand A relying mostly on traditional interface and leaf motifs. His use of colour is more dynamic than Border Hand A however. Hand D reappears on folio 18 where he is responsible for the marginal scenes, angels and Jesse tree.

Also of interest from a conservation point of view are the genealogical roundels of the Holand family that appear on the bottom of f. 4. They accompany a June 1600 inscription by Joseph Holland telling of his discovery of this fragment of the Lectionary commissioned by his predecessor John Holand, Lord Lovell. It appears that the ground under the gold layer that has been used to illustrate the page has bled, producing a vivid pink stain. It appears to be a relatively recent occurrence but the reasons for it are far from clear.

The immense complexity of this manuscript has meant that again only selected folios have been analysed. At least one example from each of the main illustrative hands and each of the border hands has been selected for analysis.

f. 4 Genealogical Inscription Page, June 1600

Description	Colour	Pigment
Text	Black	Carbon
Top Right	Red	Vermilion
Top Right, line between red and blue	White	White Lead
Bottom Line Text	Red	Vermilion
Bottom Circle	Blue	Carbon

Table 3.47: The genealogical inscription page - Harley Ms 7026 f. 4.

Spectra could not be obtained from the blue areas (illustration and circles), the pink staining, the gold rings, the black lines around them or the grey areas. See figure A1.54, appendix 1.

f. 4v The Presentation Miniature Frontispiece - Siferwas

Description	Colour	Pigment
Between Book and Hands	Orange	Vermilion
Robe, LH figure	Dark Red	Vermilion
LH Border, bottom	Dark Red	Vermilion
Collar LHS	White	Lead Degradation

Table 3.48: The Presentation Miniature frontispiece - Harley Ms 7026 f. 4v.

Spectra could not be obtained from the blue or the black areas. See figure A1.55, appendix 1.

f. 5 The Edict of Caesar Augustus – Hand C, Border Hand A

Description	Colour	Pigment
Tendrils LHS	Blue	Lazurite
Border LHS	Red	Vermilion
Coat of Arms LHS	Blue	Lazurite
Coat of Arms LHS	Red	Vermilion
Wolf	Grey	Lead Degradation
Figure, principal illumination	Dark Grey	Lazurite, Carbon
Background, principal illumination	Beige	Ochre
Figure, far RHS, principal illumination	Dark Blue	Lazurite, Carbon
Angel, bottom	Black	Carbon
Angel bottom	Red	Vermilion

Table 3.49: The Edict of Caesar Augustus - Harley Ms 7026 f. 5.

Spectra could not be obtained from some of the beige areas. See figure A1.56, appendix 1.

f. 7v The Adoration of The Magi - Hand C, Border Hand A

Description	Colour	Pigment
Border Top Left	Green	Orpiment

Table 3.50: The Adoration of the Magi - Harley Ms 7026 f. 7v.

See figure A1.57, appendix 1.

f. 12 The Presentation in the Temple - Hand B

Description	Colour	Pigment
LH Figure, central group	Powder Blue	Lazurite

Table 3.51: The Presentation in the Temple - Harley Ms 7026 f. 12.

Spectra could not be obtained from the pink areas. See figure A1.58, appendix 1.

f. 13 The Corpus Christi Procession – Hand D, Border Hand B

Description	Colour	Pigment
RHS Border	Green	Orpiment
LHS Border	Blue	Lazurite
Dog	Beige	Ochre

Table 3.52: The Corpus Christi Procession - Harley Ms 7026 f. 13.

See figure A1.59, appendix 1.

f. 21 A Decorated Text Page From the Additional Missal Fragment

Description	Colour	Pigment
Flower	Green	Verdirgis
Flower	Yellow	Lead Tin Yellow Type I
Bottom RHS	Blue	Azurite
Bottom RHS	White	White Lead
Bottom Left	Pink	Lead Degradation

Table 3.53: A decorated text page from the additional missal fragment - Harley Ms 7026 f. 21.

See figure A1.60, appendix 1.

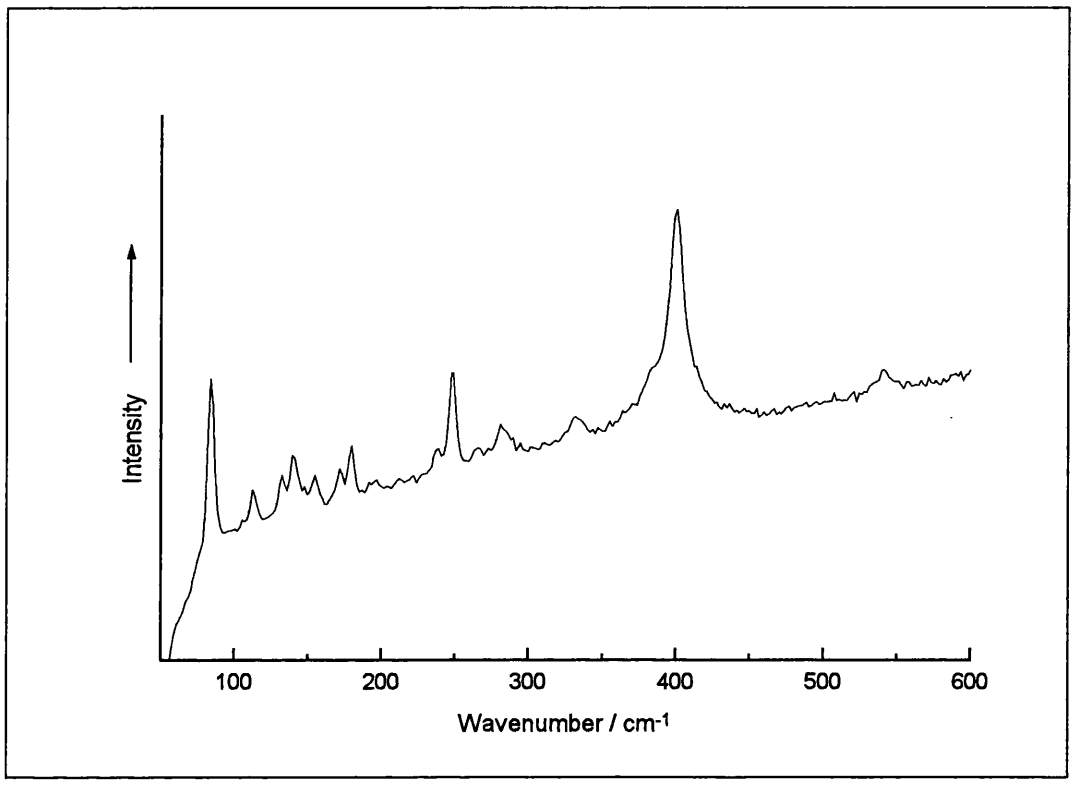

Figure 3.11: The Raman spectrum of azurite from f. 21 of Harley Ms 7026. $\lambda_0 = 514.5$ nm, ~ 1.0 mW.

As has been seen, the artists have between them used a full and extensive palette. A complete analysis has not been attempted - areas often being selected on the basis of colour alone to cover as wide a range as possible, as is particularly the case with the blue pigments. However, it can be seen that the palette is consistent across the range of artists. Orpiment, lazurite and ochre appear consistently, with vermilion and white lead also featuring in Siferwas' work. The green areas have given the spectrum of orpiment indicating the use of a yellow and blue mixture. As a spectrum was not obtained the likely blue pigment is an organic such as indigo or woad.

In contrast, the later additional folios use a somewhat different palette. Azurite (figure 3.11) is used for the blue pigment with a return to the use of verdigris for the green. Most notably, orpiment has been supplanted for the first time in this study by lead tin yellow type I. With its roots firmly in coloured glasses and potters' glazes, this pigment has been known since antiquity [Küh1] but does not seem to appear as a painter's pigment in easel paintings or book illumination until the early 14th century. More colourfast and less detrimental to its surroundings than orpiment, lead tin yellow does

not seem to have reached as far as Glastonbury from its Continental roots when the main part of this manuscript was constructed.

3.7: The Continental Schools of Manuscript Production – three exemplars

As we have seen, the influence of Continental exemplars on the stylistic development of Anglo Saxon manuscripts is well documented. Therefore, in such a study as this, it is logical to consider the influence of foreign production methods on the availability and choice of materials. Unfortunately, the difficulties that have been encountered by many workers in identifying the materials used in the decoration of manuscripts, discussed above, has made a serious consideration of the use, variety and availability of pigments on a Continental scale extremely difficult.

The manuscripts discussed below are exemplars of Italian and French manuscript production. Of varying date, they are all decorated to a greater or lesser extent although none of them even approaches the complexity of, for example, the Royal Bible discussed above. The selection was eclectic and based on availability since the condition of the manuscript had to be taken into account but, in general, they can be considered 'ordinary' manuscripts – typical of the majority of simply decorated manuscripts from their particular region and time.

3.7.1. Add Ms 31031 – Moralia in Job

A commentary on the Book of Job by Gregory the Great, this manuscript dates from the middle of the 8th century. It originates in Merovingian Gaul, possibly Laon, an area of Northern France with an active school of manuscript production.

It does not contain any miniatures, only rubricated text with occasional decorated initials.

f. 1 A Decorated Initial Page

Description	Colour	Pigment
1st Line of Rubric	Red	Red Lead
2nd Line of Rubric	Red	Red Lead
1st Line of Rubric	Green	Verdigris
2nd Line of Rubric	Green	Verdigris
Decorated Initial	Green	Verdigris

Table 3.54: A decorated initial page - Add 31031 f. 1.

See figure A1.61, appendix 1.

f. 5v A Rubricated Page

Description	Colour	Pigment
Text	Green	Verdigris

Table 3.55: A rubricated page - Add 31031 f. 5v.

Spectra could not be obtained from the yellow text. See figure A1.62, appendix 1.

This manuscript has an extremely limited palette, consisting of only verdigris, red lead and a yellow pigment that is likely to be either a weakly scattering ochre or an organic pigment such as yellow gall.

3.7.2. Add Ms 33241 – Gesta Cnutonis; The Acts of Cnut

An 11th century manuscript of Norman French manufacture, very little is known about it. The palette of the illumination is limited: simply red in two shades, yellow, green and blue.

f. 1 Blank First Page, with pigment migrating through

Description	Colour	Pigment
Staining Through Page	Green	Verdigris

Table 3.56: Pigment staining through to the blank page - Add Ms 33241 f. 1.

See figure A1.63, appendix 1.

f. 1v Queen Emma Receiving the Encomium From Its Scribe

Description	Colour	Pigment
Arches	Green	Verdigris

Table 3.57: Queen Emma Receiving the Encomium - Add Ms 33241 f. 1v.

Spectra could not be obtained from the blue or yellow areas. See figure A1.64, appendix 1.

f. 2 A Decorated Text Page

Description	Colour	Pigment
Top line	Orange	Red Lead
Text lines	Darker Red	Vermilion
Text line	Blue	Lazurite
Text Line	Green	Verdigris

Table 3.58: A decorated text page - Add Ms 33241 f. 2.

Spectra could not be obtained from the yellow areas, and the blue areas in the illustrations. This would imply the presence of a weakly scattering yellow pigment such as ochre or an organically derived material. The blue pigment is also likely to be organic rather than mineral in origin. See figure A1.65, appendix 1.

3.7.3. Add Ms 16413

An Italian manuscript from Benvevente, it contains extracts from the works of the Church Fathers, early theological writers and Acts of Councils. It was written in the 10^{th} century in Lombardic script.

f. 23v An Illuminated Page

Description	Colour	Pigment
Bottom centre, Saint's medallion	Red	Red Lead
Saint's Halo	Blue	Lazurite
Central Fill, letter E	Yellow	Orpiment Degradation
Text	Black	Probably Iron Gall

Table 3.59: An illuminated page - Add Ms 16413 f. 23v.

Spectra could not be obtained from the purple areas. See figure A1.66, appendix 1.

f. 29 A Rubricated Page

Description	Colour	Pigment
Rubric	Orange	Red lead
Shading, letter S	Yellow	Orpiment Degradation
Text Highlight	Green	Verdigris

Table 3.60: A rubricated page - Add Ms 16413 f. 29.

See figure A1.67, appendix 1.

A variation between the French and Italian palettes appears to be exemplified by these manuscripts. Although the Italian manuscript uses orpiment the French examples seem to be consistent in their avoidance of it, preferring instead an as yet unidentified pale yellow. Additionally they appear not to have used lazurite, with an organic blue that is likely to be indigo instead. The presence of lazurite in the Italian manuscript should not come as a surprise, however, since the majority of lazurite imported into Europe probably came via the great trading centre at Venice. [Gett] In general, however, there are no outstanding differences between contemporary Continental and English manuscripts.

3.8: Conclusions

First, it has long been believed that a particular triumvirate of pigments forms the basis of the Insular palette. It would be expected, therefore, that these pigments, red lead, orpiment and verdigris, would be found on most if not all manuscripts of Insular production. However, from the results of this study that is clearly not the case. The Insular triumvirate appears to be an Irish practice since it is found in the Irish pocket Gospel (Add Ms 40618) and in the Irish-influenced Royal Prayer Book (Royal Ms 2 A XX) although even in the case of the Gospel it has been augmented by other pigments, such as the unidentified purple and red. Further, elements of it appear in almost all Insular manuscripts with red lead and orpiment proving to be two of the most widely used pigments. It is in the production of green pigments that the differences arise, with

two of the earliest manuscripts studied, Cotton Ms Nero D IV and Royal Ms 1 B VII, being decorated with vergaut instead of or in addition to verdigris. Later in the Insular period red ochre also makes an appearance (Harley Ms 7653) in addition to red lead, and white lead is sometimes used instead of plain parchment for white or flesh areas (Cotton Ms Vespasian A1, Royal Ms 1 E VI).

In a number of cases pigments could not be identified. The colours concerned were common to almost all of the manuscripts: purple, pink, dark red, pale yellow, blue, green, brown and black. The brown and black pigments are probably, in many cases, iron gallo-tannate inks from which it is almost impossible to obtain a Raman spectrum using visible laser radiation. On some occasions the browns and certain of the reds and yellows may be derived from ochres or earth colours. These are pigments that get their colour from an iron based chromophore, Fe_2O_3, but are only weakly Raman scattering and so hard to detect. It is most likely that the other unidentified pigments are organic in origin – plant or animal derivatives such as folium or Tyrian purple for example. These often fluoresce in response to visible laser radiation and tend to have weak Raman spectra and hence are almost impossible to identify.

Another impediment to the identification of pigments on manuscripts has been found to be the action of old conservation treatments. In this case, the use of PVAc on Cotton Ms Vespasian A 1 has made it impossible to identify all but the strongest Raman scatterers. The effect of PVAc on the manuscript itself has also been detrimental (see appendix 2). Further work is clearly needed to assess the impact of previous conservation on the long-term preservation of manuscripts and, particularly in this case, to attempt to identify more of the surface pigments and how they have been affected.

It is interesting to note that the English manuscript palette underwent no significant changes for a substantial period. Consisting of red lead, red ochre, orpiment, indigo or woad, verdigris, carbon, iron gall and various organics, there are no additions during the Insular period (to 900 AD). Closer interactions with the Continent after the overthrow of Danelaw see the introduction of lazurite in 920 AD (Add Ms 40618, more of this later) and vermilion on the 12th century additions to Arundel Ms 155 – the first significant alterations to the pre-existing palette. Later still comes the arrival of azurite in the late 13th – early 14th century Alphonso Psalter (Add Ms 24686) and lead tin

yellow type I, a derivative of the glass and ceramics industry, in the parts of Harley Ms 7026 dating from the 1450s. Curiously, although both parts of this manuscript are extensively and intricately decorated, red lead does not appear to have been used; a complete reversal of the Insular trend.

The Continental manuscripts studied appear to have an even simpler palette than the English ones of comparable date and with few exceptions the palette is the same. The principal differences are the avoidance of orpiment, in favour of another, unidentified yellow, in the French material and the earlier appearance of vermilion. However, the extremely small size of the sample and the inclination towards simply decorated manuscripts means that further studies are required to understand this topic completely.

The most important issue raised by this study is that of the use of lazurite in manuscript illumination. A great deal has been written on the use of lazurite[10] and its presumed availability from the creation of the Lindisfarne Gospels early in the 8th century. Its superior colouring properties of would make it the obvious choice for the works of Opus Dei that manuscripts were and so it was long assumed that the great majority were produced using lazurite or, where funds did not permit, cheaper azurite.

The discovery that lazurite does not appear in any of the manuscripts studied until 920, and azurite not until nearly 400 years after that, is significant for two reasons. The first, and perhaps the most important, of these relates to the results of previous analyses conducted on this type of material. Due to the delicate nature of manuscripts, non-sampling techniques will always be the preferable method of materials' analysis. It is particularly unfortunate, therefore, that the results of a method that is relatively simple and hence popular should be called into question. However, without doubt the results of Raman analysis have shown that the technique devised by Roosen-Runge has not correctly identified the blue pigments on Cotton Ms Nero D VI or, when applied by Sally Dormer, the blue and green pigments on Arundel Ms 155. Regrettably, this casts doubt on the conclusions drawn about manuscripts analysed following this method and further work is certainly needed.

[10] [Dodw] [Dorm] [EQCL] [Gett] [Thom]

The absence of lazurite on a manuscript such as the Lindisfarne Gospels is also significant from a socio-historical viewpoint. It is logical to assume that, had costly and highly prized lazurite been available to Bishop Eadfrith for his great work he would surely have used it. Its absence must therefore imply that trade routes through to the Mediterranean were not as well developed or easily travelled as previously believed. The re-dating of the first use of lazurite on an English manuscript, demonstrated by Raman microscopy, to 920AD is far more in keeping with the period of increased intercourse with the Continent that would have brought such innovation to England.

Chapter 4: Islamic Manuscripts

وَمِنَ ٱلنَّاسِ مَن يُجَٰدِلُ فِى ٱللَّهِ بِغَيْرِ عِلْمٍ وَلَا هُدًى وَلَا كِتَٰبٍ مُّنِيرٍ

And among men there is he who disputes about Allah without knowledge and without guidance and without an illuminating book

Chapter 22, Verse 8
The Holy Qur'an
Translated by M. H. Shakir
1983

Due to its great geographical and historical extent, the styles and concepts captured by "Islamic Art" are many and varied. The characteristic love of knowledge and learning that infused most early Islamic scholarship was responsible for a thriving system of manuscript production that, in turn, preserved a great deal of the most highly regarded Classical literature. Although a great deal has been lost – the history of the Islamic nations being every bit as turbulent and marked by conflict as that of the Western world - what remains represents a pinnacle of artistic and cultural achievement but in a form very different from that found in the West.

4.1: Islamic manuscript production and decoration

The rise of Islam, from the 7th century to the present day, has encompassed many different cultural groups. These differences and their assimilation into a fluctuating cultural framework have engendered a pattern of development in the decorative arts that is often extremely complex.

A particularly contentious area is that of the representation of living beings. Although there is no formal statement in the Qur'an prohibiting the use of such images, the initial social and psychological reluctance, in the face of the rich religious imagery of the Mediterranean, gradually acquired theological justification. Various passages in the

Qur'an describing how only God has the power to give life, the omnipotence of God and the strict opposition to idols eventually led to the representation of life being regarded as sinful idolatry. [Grab] Although this prohibition was applied with varying stringency through different periods and regions, it did have an effect on the development of Islamic art. Calligraphy became the sacred art form for the expression of faith – in religious manuscripts the attention paid to, and hence extremely high standard of, the calligraphy often far outweighs that of the decoration surrounding it. This restriction of acceptable themes in religious art under Islam also led to a flowering of the secular arts not seen elsewhere. For example, early Western art is dominated by the representation of devotional themes whereas freedom of expression was found outside the constraints of religious works in Islam.

The broad geographical area, stretching from Mongolia to Morocco, encompassed by Islam had a great, and greatly varying, stylistic influence over the nature of its art. For example, the Mongol invasions of the 13th century brought with them the influences of Chinese art that fused with Persian and Arab styles to eventually develop a definitive Mongol Islamic style during the Ilkhanid period. [Canb] The influence of Chinese decorative arts can still be clearly seen in 15th century Persian painting, where Chinese floral and animal motifs were universally popular and incorporated at almost every opportunity. In India, the influence of existing Jain manuscript painting from western India can be seen in the predominantly Persian influenced Islamic art from the region in the 15th century. The fusion of influences from both cultures led eventually to the formation of the Sultanate school in India, which is stylistically distinct from material produced in Persia. [Los1]

The cross-cultural fusion that occurs with successive and repeated conflicts and conquests often makes the precise origin and date of a manuscript extremely hard to ascertain, particularly given the lack of geographical boundaries between neighbouring groups. Conflicting opinions often exist with regard to specific manuscripts, making this an ideal area for the introduction of scientific analysis. A full study of the palette and materials of manuscripts of known provenance can contribute to the establishment of a benchmark against which questioned material may be compared.

4.2: Three Sultanate manuscripts

The years of the Delhi Sultanate were a period of social and political change, with a variety of cultural influences. To provide a context for the Sultanate manuscripts studied in this chapter within the upheavals and population migrations, a summary of the few hundred years of history encompassing their creation is required.

Islam was first brought to India in the 8th century but it did not become firmly established until much later under the Turkish rule of Mahmud of Ghazni, who conquered the Punjab at the beginning of the 11th century. [Vaug] Ghazna was a significant administrative centre, second only to Baghdad in the Islamic world at this time. Hindustan was a great source of treasure and slaves and a fertile recruiting ground for troops so significant numbers of people, particularly craftsmen, were moved between the two regions. Lahore became the principal city of the new administration, which lasted over 150 years.

The demise of Ghaznavid rule began in 1181 when Muizz al-Din Ghuri began a series of conquests that brought all of Hindustan under Muslim rule. After his death in 1206, the governor of Lahore, Qutb al-Din Aibak, who had been Ghuri's slave, seized control to establish the first of five dynasties of the Sultanate of Dehli. The 'Slave Sultans' retained power until 1290, at which time a struggle between the old Turkish administration and Indian-born Muslims led to the succession of Jalal ud-Din Firuz Khalji. He was followed by his nephew Ala al-Din Khalji in 1296. By this time the attacks of the Chaghatai Mongols had became almost overwhelming and the Delhi army had doubled in size. The need for greater resources led Khalji to look further afield. In 1298 he conquered Gujarat, the Deccan and as far south as Madurai, annexing these kingdoms in 1316.

In 1320, following a civil war, Ghiyath al-Din Tughluq established a new dynasty, building a huge fort in Delhi and invading Khorasan to rid himself of the Mongols. After his death in 1325 the empire began to weaken, with a number of provinces declaring independence during the rule of his son Muhammed. Muhammad's successor Feroz Shah (1351–88) was the last of the Delhi Sultans to be invested in Cairo by the Abbasid caliph. The Tughluqs eventually fell in 1414, following the sack of Delhi in

1398 by Timur. Slaughtering many, he destroyed Delhi's political and cultural pre-eminence. The governor of Multan, Sayyid Khizr Khan, eventually took control in 1414, in the name of the Timurid Shah Rukh, and established the Sayyid dynasty which lasted until 1451. During this time, with Delhi no longer dominant, a number of new regional states developed. Vernacular languages became the new medium of Islamic culture, alongside Arabic and Persian, and led to a great flowering in Islamic art under fresh cultural influences.

The Sayyids were followed by the Lodis, who retained power until 1526. They reabsorbed Jaunpur, which had become a separate state in 1359 and extended the Delhi Sultanate from the Punjab to Bihar. However, the Delhi Sultanate came to an end in 1526 with the Battle of Panipat, which was won by Babur, a descendant of Timur, marking the beginning of the Mughal period.

The sack of Delhi in 1398 by the Transoxanian-Turkish leader Timur Lenk is perhaps the reason why so few Arabic and Persian manuscripts survive from the first two centuries of Muslim rule in India. [Lost] In addition their identification is greatly impeded by the lack of a distinctly Indian Islamic style. Illuminated manuscripts from at least the first two hundred years of Islamic rule in Delhi would, at their best, be indistinguishable from Iranian work since the finest scholars of the Islamic world flocked to Delhi to provide its rulers with the pinnacle of their achievement. Only after Timur's action are the book arts in Indian left sufficiently free of external Muslim influences that the development of a home-grown style begins.

The three manuscripts that were selected for Raman analysis form an interesting group. All three are fundamentally in the Iranian Shiraz style of the 15th and early 16th centuries. They use the same page layout – horizontal rectangular, or occasionally square, paintings in bands across the page framed by columns of text. However, these manuscripts have no provenance and are linked only by similarities in their appearance. Further, in each case there are indications that their origin is not in Shiraz but in Sultanate India. All three date from after the sack of Delhi, a period where the influence of Persian artistic traditions might have been expected to have lessened, suggesting that the local artists remained influenced by Persian training even in the face of great changes that followed Timur's act of cultural and political destruction.

4.2.1. OR 1403

The Shahnama is the most famous work of Persian literature. Completed by Firdasui in 1009–1010 at the request of Mahmud of Ghazni, the Book of Kings is an epic poem recounting the history of what is now Iran almost from the beginnings of civilisation.

A great many copies of this manuscript were produced in high court style in the ateliers of the rulers of Persia. No expense was spared and premium materials were used. Innumerable lesser copies were also made for regional rulers and lesser patrons, of which this manuscript is one. [Lost]

In a provincial Shirazi style with Timurid influences, the painting of its miniatures is naïve suggesting a considerable distance from Shiraz itself. A number of pieces of evidence seem to point to a provincial Indian origin. First, the text of the preface is unusual. It predates the text prepared by Prince Baisunghur of Herat for his edition of 1430, which has been used almost universally since, although this manuscript is actually dated 1438. Instead, this version includes the information that Firdausi took refuge in India at the court of the King of Delhi, whilst fleeing his patron Mahmud. The king favoured him, eventually sending him back to his birthplace of Tus, showered with rich gifts. The absence of this information in any other version, and the partiality in its portrayal of the Delhi Sultan suggests an Indian origin for the manuscript.

The illustration itself shows some evidence for an Indian origin. The illumination is ambitious but apparently uses poor quality materials and is crude when compared to Shirazi work. Sprays of leaves, characteristic of Shiraz, have been used, but details have been added in red. The typical delicate arabesques that would be expected in the borders of Persian illumination at this time are completely absent. In addition, although the artist uses the high horizon of sophisticated Persian painting, he has no comprehension of composition in three dimensions, failing to take advantage of the increase in space available to him.

Finally, it is believed that the yellow pigment used in the illustration of this manuscript is Indian yellow, a colour derived from the urine of cows fed on mango leaves. At the time of its discovery by Europeans in the 18th century, Indian yellow was made in one

small Indian village. Although its production and use may previously have been more widespread, at no time is it known to have been used in Persian painting.

A selection of the ninety-four illustrated pages was assessed by Raman microscopy and ultra-violet light (UV) examination. UV examination is used as it is the only non-sampling technique that can conveniently identify Indian yellow.

f. 8 Two Seated Figures Studying a Book

Description	Colour	Pigments
Dress	Red	Vermilion
Trousers, at ankle	Yellow	Orpiment

Table 4.1: The pigments OR 1403 f. 8.

See figure A3.1, appendix 3.

f. 9v Dancing Figures

Description	Colour	Pigments
Dress	Yellow	Pararealgar
Border	Blue	Lazurite
Tambourine	White	White Lead
Figure	Purple	Lazurite
Face	Flesh	Vermilion, White Lead
Hair	Black	Carbon
Pipes	Yellow	Orpiment
Leaves	Green	Orpiment, Indigo
Beard	Black	Carbon
Hair, dancer	Black	Carbon
Small Figure	White	White Lead
Second Figure	White	White Lead
Figure	Red	Vermilion
Flower	Orange	Red Lead, Orpiment
Grass	Green	Orpiment
Turban	White	White Lead
Beard	White	White Lead

Table 4.2: The pigments of OR 1403 f. 9v.

Spectra could not be obtained from the black sash on the principal figure, some green and the purple areas. See figure A3.2, appendix 3.

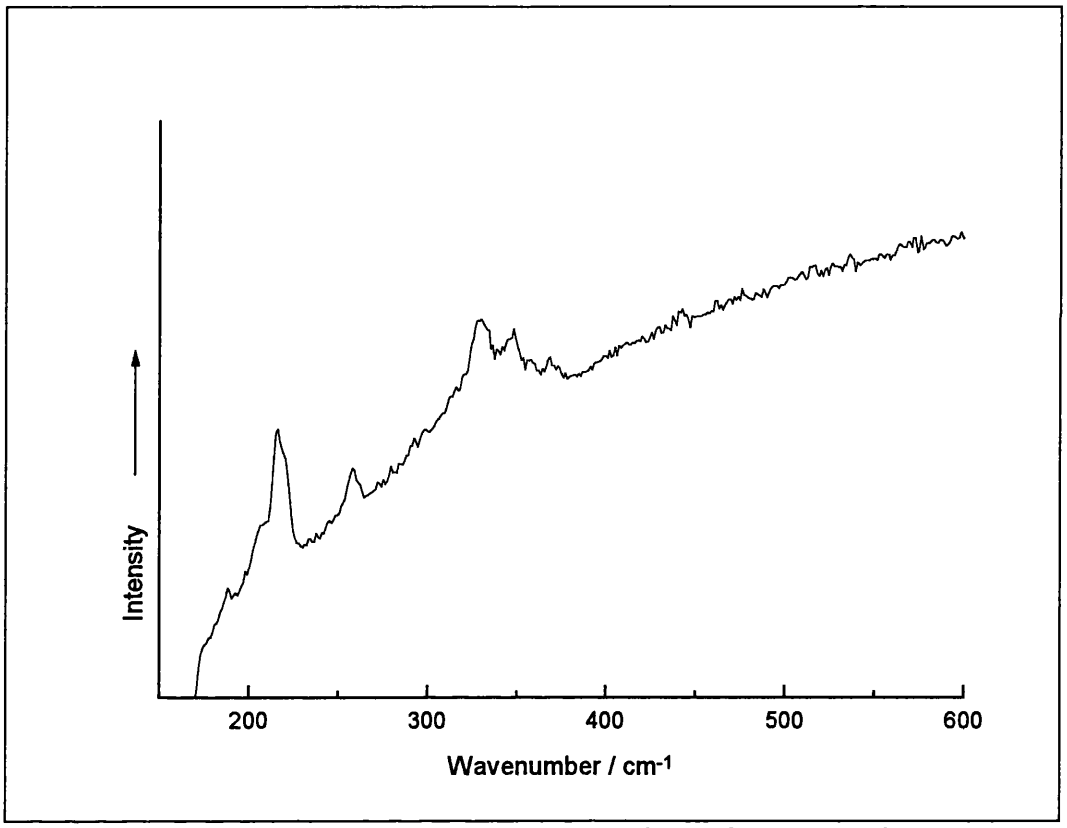

Figure 4.1: The Raman spectrum of pararealgar from f. 10 of OR 1403. $\lambda_0 = 632.8$ nm, ~0.35 mW.

f.10 A Teacher and Students

Description	Colour	Pigments
Beard	White	White Lead
Turban	White	White Lead
Carpet	Orange	Red Lead
Carpet Border	Red Brown	Vermilion
Mouth, LH figure	Red	Vermilion
Top Figure LHS	Red/Orange	Vermilion
Figure	Yellow	Pararealgar
Principal Figure Robe	Dark Green	Orpiment
Background Pattern	Blue	Lazurite
LH Figure Robe	Green	Orpiment

Table 4.3: The pigments of OR 1403 f. 10.

Again, spectra could not be obtained from the black sash. The purple, pink, brown, grey and degraded purple areas also did not give spectra. See figure A3.3, appendix 3.

f.13 A Ruler Addressing Two Subjects

Description	Colour	Pigment
Carpet	Red	Vermilion
Drape	Yellow	Orpiment
Central Figure	Blue	Lazurite
LH Figure	Blue	Lazurite
Turban LH figure	White	White Lead
Background	Blue/Green	Orpiment, Indigo

Table 4.4: The pigments of OR 1403 f. 13.

Spectra could not be obtained from the green or purple areas. See figure A3.4, appendix 3.

f. 425 Two Men and an Elephant

Description	Colour	Pigment
Robe	Orange	Red Lead
Sky	Blue	Lazurite
Tree Top	Orange	Orpiment, Indigo
Tree, bottom	Green	Orpiment
Tree Trunk	Orange/Brown	Orpiment, Vermilion

Table 4.5: The pigments of OR 1403 f. 425.

The purple, grey and gold coloured areas did not give spectra. See figure A3.5, appendix 3.

A number of areas did not give Raman spectra. These were pink, purple, grey or brown in colour and, in general, the absence of spectra is likely to indicate an organic origin for the pigments. The absence of spectra from certain green areas may be indicative of the presence of an organic pigment, or perhaps the degradation of inorganic pigments such as orpiment or the presence of a green inorganic pigment like verdigris which is problematic. The absence of spectra from gold coloured areas strongly suggests the presence of gold, which has no Raman spectrum.

The black sashes on ff. 9v and 10 appear to be later additions – they are not as well drawn as other parts of the miniatures and do not appear to be an integral part of the figures. Close examination shows the pigment to be shiny and not a cohesive part of the surface of the illustration, which had been burnished after completion. The other black pigments found on the miniatures are carbon but the sashes have no Raman spectra, suggesting an iron gallo-tannate ink which would be unlikely if they were contemporary with the rest of the miniature.

Analysis by UV examination did not indicate the presence of any Indian yellow, contrary to expectation. All of the yellow pigments were found to be orpiment or pararealgar. Pararealgar is a light-induced degradation product of realgar but is commonly found with orpiment. It was possibly used deliberately as a yellow pigment in its own right, or mistaken for orpiment by the artist. However, the lack of Indian yellow does not imply that the manuscript could not have been made in India, rather it neither confirms nor denies textual or other clues.

4.2.2. OR 13836

The Sharafnama is the first part of the Iskandarnama or Book of Alexander the Great, that describes his many campaigns. Written by the poet Nizami, this copy was made for Nusrat Shah, Sultan of Bengal in 1531–2 by Hamid Khan. [Lost]

Stylistically it resembles a 15th century Shirazi manuscript with elements that suggest 14th century Iranian influences. However, this manuscript is sufficiently distinct from those of Shiraz to suggest a period of independent stylistic development in Bengal. Many of the architectural details are distinctly Indian, traceable to buildings extant in Gaur and Pandua, and other particularly Sultanate features include the positioning of people in rows, women with round faces and long braids and the representation of the horses. The triangular panels of illumination on either side of obliquely written verses found on many pages are also unlike Shirazi manuscripts.
A number of the illustrated folios were examined.

f. 5 Double Page Unvan

Description	Colour	Pigment
Top Left Corner	Blue	Lazurite
Top Left Corner	Red	Vermilion
Flower, top left	Pale Blue	Lazurite

Table 4.6: The pigments of OR 13836 f. 5.

Spectra could not be obtained from the pink areas. See figure A3.6, appendix 3.

f. 17v Battle Scene

Description	Colour	Pigment
Horse Cloth, bottom right	Pale Blue	Lazurite
Trouser, bottom right	Red/Orange	Vermilion
Horse Cloth, bottom right	Dark Blue	Lazurite
Cloth, bottom right	Blue/Green	Indigo
Soldier, mounted right	Yellow	Orpiment
Horses Neck, right	White	Chalk
Trousers	Dark Green	Orpiment, Indigo
Cloth	Light Green	Orpiment, Indigo

Table 4.7: The pigments of OR 13836 f. 17v.

Spectra could not be obtained from the pink and dark red areas. See figure A3.7, appendix 3.

f. 21v A Ruler Addressing His Subjects

Description	Colour	Pigment
Clothing	Dark Blue	Lazurite
Clothing	Yellow	Orpiment
Clothing	Orange	Vermilion
Walls	Pink	Vermilion, Chalk
Panel, left	Dark Blue	Lazurite
Bird	Black	Carbon
Sleeves	Pale Blue	Lazurite, Chalk
Face	Flesh Tone	Vermilion, Chalk
Tree	Dark Green	Orpiment, Indigo
Tree	Light Green	Orpiment, Indigo

Table 4.8: The pigments of OR 13836 f. 21v.

Spectra could not be obtained from the gold areas. See figure A3.8, appendix 3.

The range of pigments used here is very similar to those of OR 1403. Again the pinks and dark reds have not produced Raman spectra, probably indicating the presence of organic material. The lack of spectra from the gold areas is likely to be indicative of the use of gold rather than a substitute.

4.2.3. OR 11676

This manuscript is thought to be the first illustrated copy of Javami' al-Hikayat, a collection of anecdotes, tales and notices by Nur ad-Din Muhammad 'Aufi. [Lost] 'Aufi was Bokharan by birth and travelled extensively before settling in Sind and Gujarat under the patronage of Nasir ad-Din Qubacha. However the consolidation of centralised Turkish rule in India led to the destruction of Qubacha's power base and the capture of his fortress in 1228. 'Aufi transferred to Delhi, where he remained thereafter, dedicating the collection of anecdotes that he had already begun to Iltutmish's Vizier, al-Junaydi.

This copy is dated 1439–40 but has no other provenance. Again it appears to be mainly Shirazian in style, but on this occasion with no Timurid influences. Instead it appears to

be related to an earlier Muzaffarid school of Shiraz. A number of features suggest an Indian origin for this manuscript, not least the apparent confusion of the artist between a tent and a royal parasol, with a figure on f. 40v generally believed to be firmly holding a guy rope, convinced that it belongs to a parasol rather than a tent. [Lost] The depiction of architecture in the illustrations appears somewhat un-Persian and aspects of the illumination itself seem Indian. The use of un-outlined leaf patterns with red highlights is old-fashioned and, as in OR 1403, the expected arabesques are entirely absent.

The twelve original miniatures are in the almost square 14th century format, towards the bottom of the page. Spaces left for a further ten were filled in the 16th century in the Bokharan style. In the 18th century, another three miniatures were added in an archaic Mughal style, indicating that the manuscript was almost certainly in India at this time. In addition the margins and side panels were filled with Mughal-style flora and fauna decoration.

If the twelve original miniatures are regarded as Indian, along with the final three then that is strong evidence to suggest that the manuscript was in India from 1440 to the 18th century. Although the 16th century illustrations are in Bokharan style, there is evidence to suggest that Bokhara-trained artists were working in India at this time. [Lost] Further, the inscription on f. 430v in the Bokharan style refers to a 'mighty Sultan who rules over all peoples, the master of the kings of the Turks and the Arabs and the Persians' suggesting, perhaps, an Indian origin. [Lost]

A selection of folios with miniatures of all of the various types were examined by Raman spectroscopy and UV.

f. 2 Decorated Page, patterned margins, original 14th century style

Description	Colour	Pigment
Border, LHS (not remargin)	Blue	Lazurite
Border, LHS	Pale Green	Indigo
Lozenge, top LHS border	Red	Red Lead
Border, top left	Black	Carbon
Border, left	Green	Verdigris
Flower, bottom left lozenge	Dark Red	Red Lead
LH panel, LH edge	Pale Green	White Lead, Verdigris
Flower Centre, LHS	Green	White Lead, Verdigris
Flower, top panel	Darker Green	Verdigris, Lazurite, White Lead

Table 4.9: The pigments of OR 11676 f. 2.

UV examination did not reveal the presence of any Indian yellow. See figure A3.9, appendix 3.

f.4v The Court of a King, Mughal style, 18th century

Description	Colour	Pigment
Quiver, far right figure	Red	Vermilion, Red Lead
Skirt, far right figure	White	White Lead
Second right figure	Yellow	White Lead
Platform foot, second left	Red	Vermilion
Platform base	Green	Indigo
Boots	Blue	Carbon, White Lead
Face, third from left	Flesh	Vermilion, White Lead
Background	Blue/Purple	Indigo

Table 4.10: The pigments of OR 11676 f. 4v.

Spectra could not be obtained from the purple areas, the black beard and the orange ground. UV examination indicated that the yellow pigment was Indian yellow. See figure A3.10, appendix 3.

f. 5 A Decorated Sutra Heading, from the original 14th century style illustration, with 18th century archaic Mughal-style floral decoration

Description	Colour	Pigment
Spot, centre bottom flower	White	White Lead
Leaves	Dark Green	Indigo
Top of Middle Border	Blue	Lazurite
Green Flower, lower centre	Green	Lazurite, Carbon
Red and white flower	Red	Red lead, White Lead
Detailing, top blue border	White	White Lead, Lazurite, Carbon
Gold Border	Gold	Carbon
Flower, top left	Dark Red	Red Lead
Additional Margin, top	Blue	Lazurite
Border, top panel, bottom left	Dark Green	Verdigris
Flower, top panel	Dark Green	White Lead, Verdigris

Table 4.11: The pigments of OR 11676 f. 5.

Spectra could not be obtained from the yellow areas, but UV examination indicated the presence of Indian yellow in the floral additions. A carbon spectrum has been obtained from the gold border. This may be derived either from an accidental contamination from a carbon based pigment elsewhere on the page, or in an under-drawing, or from an outside source such as soot. See figure A3.11, appendix 3.

f. 113 Men Meeting in a Mosque, original 14th century style

Description	Colour	Pigment
Background, LHS	Green	Lazurite, White Lead
Clothing, right hand figure	Brown	Orpiment, Red Lead
Carpet Border, bottom	Green	Lazurite
Figure, second from left	Dark Brown	Orpiment, Carbon
Robe, LHS	Red	Vermilion
Figure, LHS	Blue	Lazurite, White Lead
Turban	White	White Lead
Face, LHS	Flesh	Red Lead, White Lead
Beard	Black	Carbon, Lead Degradation
Carpet	Pale Blue	Lazurite
Sleeve	Brown	Orpiment
Carpet Border	Dark Blue	Lazurite
Sleeve	Dark Brown	Vermilion, Orpiment
Sword	Orange	Vermilion, Red Lead

Table 4.12: The pigments of OR 11676 f. 113.

Spectra could not be obtained from the gold areas.

UV examination indicated the presence of Indian yellow in the sword blade and at the neck of the kneeling figure. However, visually this appears to be a later retouching, so perhaps a pigment was introduced here that is not used elsewhere on the illustration. See figure A3.12, appendix 3.

f. 344 Men at a Well, Bokharan style, 16th century

Description	Colour	Pigment
Grass, LHS	Light Green	White Lead, Verdigris
Leaves, tree	Dark Green	Orpiment, Verdigris
Figure, LHS	Dark Blue	Lazurite
Boots	Black	Carbon
Turban	White	White Lead
Turban, detail	Red	Vermilion
Flower	Orange	Red Lead
Tree Trunk	Brown	Carbon, Red Lead
Sleeve, second figure from the left	Red	Vermilion
Figure	Brown/Beige	White Lead, Orpiment

Table 4.13: The pigments of OR 11676 f. 344.

Spectra could not be obtained from the gold and pink area. UV examination did not reveal the presence of Indian yellow. See figure A3.13, appendix 3.

f. 405v A Garden Pavilion, Bokharan style, 16th century

Description	Colour	Pigment
Floor Tiles	Pale Green	Indigo, Verdigris, White Lead
Figure, LHS	Orange	Red Lead
Carpet, RHS	Dark Blue	Lazurite
Figure, RHS	Pale Blue	Lazurite, White Lead
Trellis, RHS	Red	Vermilion
Clothing, man LHS	Beige	Orpiment, White Lead
Flower	Pink	Vermilion
Figure, LHS	Yellow	Orpiment

Table 4.14: The pigments of OR 11676 f. 405v.

Spectra could not be obtained from the purple areas. UV examination indicated that no Indian yellow was present. See figure A3.14, appendix 3.

This manuscript contains an interesting range of illustrative styles from different periods and regions, a variation that is reflected in the pigment use to some extent. Although

created in the 15th century, the original decoration reflects a previous period with its 14th century style. The palette is relatively simple with both vermilion and red lead, carbon, orpiment and lazurite. However, the greens are rather more complex and extensively mixed. Some are composed of indigo in mixture with an unidentified yellow pigment that may be organic or a weakly scattering ochre. Others are primarily verdigris, but with sophisticated shading and toning in white lead and lazurite. As with the other Sultanate manuscripts examined, no Indian yellow was found on the 15th century decoration.

The second selection of illustrations was added in the 16th century in Bokharan style. Although Bokhara is in modern Uzbekistan there is evidence to suggest that Bokharan artists were working in India at this time [Lost] so an Indian origin for the decoration is by no means precluded. The range of pigments is essentially the same as that of the original illustrations although it does not contain indigo – the only blue pigment is lazurite. Again the verdigris is toned with white lead and orpiment. Both red lead and vermilion are used for red and orange pigments, and carbon for black areas. Unfortunately the purple pigment could not be identified.

The final pieces of decoration were completed in the 18th century, but in an archaic Mughal style. It is here for the first time that Indian yellow has been used on the manuscript, with the characteristic fluorescence occurring in the yellow-pigmented areas. The rest of the palette remains remarkably similar to the previous two painting styles, with the re-introduction of indigo alongside lazurite, and white lead, red lead, vermilion and carbon. The green colours here are not verdigris, however, but have been obtained by mixing indigo with a yellow pigment. This yellow pigment is not Indian yellow but has not been identified. It may be an organic pigment, like the purple materials that have also eluded identification, or an ochre which scatters only weakly. In some areas the black pigment could not be identified, suggesting the presence of an iron gallo-tannate ink.

Throughout the manuscript, the gold areas did not give Raman spectra. This generally indicates the presence of gold, rather than a gold or yellow coloured substitute since these generally have Raman spectra. [Bell]

4.2.4. Conclusions

There are very few differences between the palettes of these three manuscripts. Although the earliest illustrations in each manuscript are separated by one hundred years all three artists have made use of vermilion, orpiment, lazurite and carbon as principal pigments. However, one or two differences do occur. OR 1403 and OR 11676 both use white lead for the white-pigmented areas whilst OR 13836 uses chalk. The Shahnama, OR 1403, is the only manuscript to make use of pararealgar, a light induced degradation product of realgar, as a yellow pigment. This may or may not be deliberate and is in addition to the orpiment that appears on all three manuscripts.

It is in the generation of the green pigments that the three manuscripts most differ, however. Both OR 1403 and OR 13836 make extensive use of indigo and orpiment mixtures to produce a range of green colours. In OR 11676 a similar range is provided by combinations of verdigris, indigo, lazurite and orpiment. This is the only appearance of lazurite in mixture on the original illustrations of all three manuscripts. It may be significant that OR 1403 and OR 13836 make use of indigo and orpiment in mixture and both contain textual evidence of an Indian origin, whilst OR 11676 uses verdigris in mixture and has a Sultanate designation that is purely stylistic.

A comparison between the materials used in these manuscripts and those known to have Persian, Mughal or Turkish origins can be found at the end of this chapter

4.3: Mughal Manuscripts

The word Mughal means Mongol in Persian and Arabic; the great Mughal dynasty was founded by Babur, a descendant of both Timur Lenk and Gengis Khan. [Vaug] Mughal rule in India began in 1526 when Babur won the battle of Panipat, defeating the Lodi ruler and putting an end to the Delhi Sultanate. [Hatt] His son, Humayun, was not so fortunate and was driven to Persia by Shir Shah Suri in 1540, only regaining his territory in 1555. In 1556, at the age of 14, Akbar inherited the newly regained kingdom, after his father died from falling down the steps of his beloved library. In a reign that lasted until 1605 he expanded Mughal control to include territories stretching

from Kabul and Kashmir to Bengal, through Khandesh, Malwa, Rajasthan and Gujarat to the northern borders of the Deccan. He operated a policy of tolerance and reconciliation between Hindus and Muslims, encouraging marriage alliances and cultural interchange between the two groups.

Although almost certainly dyslexic, Akbar was a considerable patron of the decorative arts. [Vaul] He amassed some 24,000 volumes in an extensive library and commissioned a considerable number from the court atelier under the Persians Mir Sayyid 'Ali and Khwaja' Abd al-Samad. Artists were gathered from a variety of different schools, those of the Sultanate courts, Persian, Hindu and Jaina craftsmen all finding employment. [Lost] His exposure to this variety, and work from a great many other sources including European artists, began a transformation in the style of illustrative work that incorporated the elegance of Persian work with the vitality and flair for natural forms of the Indian artists. [Tops] Patronage of the arts was continued by his successors, Jahangir (1605–27) and Shah Jahan (1628–58) who led innovation in portraiture and the depiction of personality as well as commissioning high quality studies of flora and fauna. At the same time Shah Jahan's armies campaigned to regain the lands of Balkh and Badakhshan that the Mughals claimed as part of their dynastic inheritance. Aurangzeb deposed his father in 1658 and abandoned these campaigns, concentrating instead on the Deccan which he subdued in 1687. He was less interested in the arts than his predecessors had been, leading to a marked decline in the cultural production of the Mughal empire although the empire itself was to survive a succession of weak rulers and conflicts until the British deposed the last Mughal emperor in 1857.

4.3.1. The Great Hamzanama

The Hamzanama is the story of the Amir Hamza, which has 360 tales. [Hill, Emme] This copy of the manuscript was commissioned by the Mughal Emperor Akbar in 1561/1562, and was produced in the court atelier under Mir Sayyid 'Ali and Khwaja' Abd al-Samad over a period of fifteen years, completed around 1577. It was originally composed of 14 volumes of 100 folios each, painted in the style of Mughal miniatures but on a grander scale, each folio measuring approximately 70 x 55 cm. The pieces are known to have been completed by a large team of craftsmen under the leadership of the two renowned Persian artists, in a fusion of Persian and Indian court styles. Of the

approximately 1400 folios created about 150 survive, distributed in public and private collections throughout the world. The Victoria and Albert Museum has 28 of these, acquired in two groups.

The first of these came to the museum in 1883, collected by C. Purdon Clarke during an expedition to India in 1882. [Whee] They were found in a tea-shop over a bridge in Srinagar, Kashmir – some of them reputedly tacked over the windows to keep out the rain. Two more were given to the museum in 1921 by Lt.-Gen. Egerton, also acquired in Srinagar in 1913.

The folios are composed in a laminate structure of alternating cloth and paper, held together by a layered paper border. In general, the paintings are in opaque watercolour or gouache on the thick, tightly woven canvas outer layer. In some cases however they have been painted directly onto the more loosely woven intermediate canvas with concomitant weaker adhesion of the pigment and accelerated degradation of the image. The calligraphy on the verso is written on the gold-flecked paper layer.

Three separate folios were examined by Raman microscopy and by UV. In general the folios are in reasonable condition but with some fading and flaking, and in the case of IS 1508-1883, the apparently deliberate scraping of the pigments from the faces of the figures. In IS 1513-1883 a rectangular area of apparently brighter colouration of the trees has occurred on the left side.

4.3.2. Three folios from the Hamzanama

IS 1505-1883: Hamza, approached by fairies who implore his aid in quelling the dragon said to be troubling his kinsmen the Genii, in the Caucasus mountains

Area	Colour	Description	Pigment
1	Blue/Green	Border RHS	-
2	Retouching?	Border RHS	White Lead, Orpiment
3	Yellow/Green	Leaves, tree LHS	Orpiment
4	Green	Wing feather	Orpiment
5	Green	Leaves, tree top right	Orpiment
6	Blue/Green	Border top right	-
7	Light Green	Roof decoration	White Lead, Verdigris
8	Blue	Lost	Lost
9	Orange	Clothing, bottom right	Red Lead
10	Light Blue	Border, bottom right	Indigo
11	Blue	Clothing, bottom right	Lazurite
12	Black	Doorway, RHS	-
13	Ground underneath gold	Building, bottom right	Red Lead
14	Orange	Border, top right	Red Lead
15	Grey	Roof, RHS	Indigo
16	Pink	Rocks, RHS	Vermilion, Red Lead
17	Peach	Pavilion, top	Red Lead, White Lead
18	Red	Pavilion, top	Red Lead
19	White	Pavilion, top	White Lead
20	Dark Blue	Pavilion Decoration, top	Lazurite
21	Beige	Pavilion Supports	-
22	Orange Ground	Under White, winged figure	Red Lead
23	Red	Sleeve, winged figure	Vermilion
24	Dark Green	Leaves, trees centre right	Orpiment
(25	?	-	Lazurite, Indigo)
26	Light Blue	Wings, winged figure	-
27	Dark Green	Grass, centre	White Lead

28	Pale Green	Pavilion Decoration, base	White Lead, Verdigris
29	Pink	Demon, LHS	-
30	Yellow	Winged Figure, top	Orpiment, Red Lead
31	Flesh	Flesh	Red Lead, White Lead
32	Flesh	Flesh	Red Lead, White Lead
33	Flesh	Flesh	Red Lead, White Lead
34	Blue	Border	Indigo
35	Black	Lines	Lazurite, Carbon

Table 4.15: The pigments of IS 1505-1883.

UV examination indicated that no Indian yellow was present. Spectra could not be obtained from the blue/green, beige, light blue and pink areas. See figure A3.15, appendix 3, where the numbered sample areas are indicated.

IS 1508-1883 The Murder of Qibad, in his sleeping pavilion

Area	Colour	Description	Pigment
1	Red	Covering, central figure	Vermilion
2	Red/Orange	Bed Plinth	Red Lead
3	Blue	Bed Plinth decoration	Lazurite
4	Pale Blue	Clothing, central figure	Lazurite, White Lead
5	Yellow	Clothing, LH figure	Orpiment
6	Flesh	Face, LH figure	Vermilion, Red Lead, Orpiment.
7	Over-painted Flesh	Face, figure RHS	Red Lead, Orpiment
8	Pink	Knee, horseback figure	Red Lead, White Lead
9	White	Horse, RHS	White Lead, Indigo
10	White	Turban, RHS figure by horse	White Lead
11	Pink	Bottom Step, pavilion	Red Lead, Orpiment
12	White	Top Step, pavilion	Red Lead, Orpiment, White Lead
13	Grey	Jar Lid, LHS	Lazurite
14	Pink	Top Step, pavilion	Orpiment, Vermilion

15	Yellow, metallic	Sword, cross piece	Orpiment
16	Purple	Clothing, RH figure	Lazurite
17	Faded Yellow	Pavilion, roof curtain	-
18	Black	Under Sleeping Figure	-
19	Black	Pattern, carpet RH pavilion	Orpiment
20	Dark Green	Grass, RH pavilion	Indigo
21	Lighter Green	Leaves, plant RH pavilion	Indigo, Orpiment
22	Green	Base of Pavilion	Verdigris
23	Light Green	Leggings, RH figure	-
24	Peach	Curtaining, around pavilion	White Lead, Red Lead, Orpiment
25	Pink	Trousers, figure bottom right	White Lead
26	Green	Border, RHS	Verdigris
27	Dark Green	Grass, RHS top	-
28	Light Green	Leaf, plant top RHS	Orpiment
29	Dark Green	Border, LHS	Orpiment
30	Blue Red Green White	Border	Lazurite Vermilion, Red Lead - -

Table 4.16: The pigments of IS 1508-1883.

Spectra could not be obtained from some of the black and faded yellow areas and from some of the green and white areas. UV examination indicated that no Indian yellow was present. See figure A3.16, appendix 3.

IS 1513-1883 Amar Ayaz Witnessing The Death Of Qamir

Area	Colour	Description	Pigment
1	Red	Leggings, central figure	Vermilion
2	Pale Green	Leggings, central figure	Verdigris
3	White	Trousers, central figure	White Lead
4	Orange	Trousers, central figure	Red Lead
5	Pink	Rock, LHS foreground	Red Lead, White Lead, Orpiment
6	Green, bright area	Leaves, tree LHS	Orpiment
7	Green, faded – 'white' bit	Leaves, tree LHS	Orpiment
8	Green	Border, LHS	Verdigris
9	Green	Leggings, central figure	Verdigris
10	Dark Green	Grass, foreground, centre	-
11	Light Green	Border, RHS	White Lead, Verdigris
12	Light Green	Leaves, tree LHS	Indigo, Orpiment
13	Grey, faded from green	Leaves, tree LHS	Indigo, Vermilion
14	Peach	Rock, LHS bottom	Orpiment, Red Lead
15	Blue	Sky, RHS	Lazurite
16	White	Clouds, RHS	Lazurite, White Lead
17	Orange	Border, top RHS	-
18	Brown	Tree Branch, top centre	Ochre, Indigo
19	Green	Leaves, tree top centre	Indigo, Orpiment
20	Dark Green	Tree, LHS	Indigo, Orpiment
21	Blue	Clothes, LH figure	Lazurite
22	Red	Shirt, LH figure	Vermilion
23	Purple	Sleeve, left foreground figure	-
24	White	Scarf, left foreground figure	White Lead, Indigo
25	Blue	Left Shoe, central figure	Lazurite
26	Green	Grass, central foreground	Indigo, Orpiment
27	Black	Outline, scarf central figure	Carbon, White Lead

(28	-	Lost	Lost)
29	Black	Doorway	-
30	Yellow, metallic	Sword Hilt, central figure	-
31	White	Sword Blade	White Lead
32	Dark Green	Leaves, central tree	Indigo
33	Dark Green	Leaves, central tree	Indigo
34	Brown	Rocks, centre LHS	Red Lead or Lazurite
35	Pale Blue	Clothes, RH top figure	-
36	Pink	Rock, centre	White Lead
37	Flesh	Flesh	Red Lead, White Lead
38	Flesh	Demon Flesh	Red Lead, White Lead
39	Flesh	Flesh	Red Lead, White Lead
40	Red	Border	Red Lead

Table 4.17: The pigments of IS 1513-1883.

Spectra could not be obtained from some of the orange, purple, black, yellow and blue areas. UV examination indicated that no Indian yellow was present. See figure A3.17, appendix 3.

4.3.3. Conclusions

Although there is no reason to believe that all three folios were produced by the same artist or artists, being produced under an atelier system, it is striking that there are almost no differences in the palettes of the three pieces. The use of vermilion, red lead, white lead, verdigris, orpiment, indigo and lazurite are universal, with only very occasional differences in their application; sometimes one artist chooses a particular combination over another to achieve an effect where a colleague has chosen differently for a similar area. The only notable difference in the palette is the appearance of ochre in IS 1513-1883. However, ochre is a poor scatterer and hence may be producing falsely negative results in other folios.

The brighter areas of IS 1513-1883 (samples 6 and 12) appear to be those areas in which fading has not taken place. Orpiment is commonly used in combination with blue pigments, in this case indigo, and is well known for its tendency to fade from yellow to

grey on long-term exposure to light. Spectra of orpiment result from both the unfaded areas and some of the faded areas (7, but not 13). It is likely, therefore, that those areas that appear bright have been covered and have not faded, rather than having been retouched.

In general it appears that, although a large number of people were involved in the production of the Hamzanama, a high degree of standardisation of materials existed across all of the craftsmen, with no substantive differences between the palettes of the three folios.

4.3.4. The Akbarnama, folio IM2-1896-65

The Akbarnama is an historical chronicle written between c. 1590 and 1598 by the court historian Abu'l Fazl. [Emme] It includes a detailed account of the reign of the Emperor Akbar. The emperor himself probably commissioned the copy from which this folio comes. The miniatures were painted by some of the finest artists of the age, between about 1586 and 1589. The manuscript has been broken up, probably in the 19th century, and the pages are separated.

This single sheet from the Victoria and Albert Museum was examined with Raman microscopy and UV light.

Area	Colour	Pigments
1	Red	Vermilion
2	Orange	Red Lead
3	Dark Blue	Lazurite
4	Bright Yellow	-
5	Light Blue	Indigo
6	White	White Lead
7	White	White Lead
8	Black	Indigo
9	Pink	Vermilion, Red Lead, White Lead
10	Grey	Carbon
11	Grey	Carbon
12	Blue	Lazurite
13	Brown	Vermilion
14	Black	Carbon, Lead Degradation
15	Flesh	Red Lead
16	Flesh, pale	Red Lead, White Lead
17	Green	-
18	Green	Verdigris
19	Green	-
20	Yellow/Green	Orpiment
21	Dark Green	-
22	Dark Green	-
23	Yellow	White Lead
24	Light Green	White Lead, Lazurite
25	Blue	Lazurite, Carbon

Table 4.18: The pigments of IM2-1896-65.

Spectra could not be obtained from some of the green areas. This may be attributable to weakly scattering verdigris or the presence of organic pigments that do not give discernable Raman spectra. Areas of this folio fluoresce in response to UV light, indicating the presence of Indian yellow. See figures A3.18 and A3.19, appendix 3.

4.3.5. Conclusions

In drawing comparisons with the Hamazanama – a manuscript of similar date and origin, but on cotton not on paper, it is interesting to observe that the palette is almost identical. The most remarkable difference comes in the appearance of Indian yellow, detected by UV light, which does not appear on the Hamazanama. However, even with the introduction of an alternative yellow, orpiment has still been used. It would appear, therefore, that there is no substantial difference in the palette used for painting on cloth and that for painting on paper. Although the Hamazanama is unusual in terms of its size and scale, it appears to have used an entirely standard palette.

4.4: Persian Manuscripts

Persian artists have a long tradition of manuscript illustration, dating from well before the beginning of the 14th century. [Canb] Although Iran has been invaded a great many times, imposing considerable ethnic and linguistic diversity, changes in artistic style were fused into a distinctive ethic that is characteristic of almost all Persian art, with intense, radiant colouring and precise execution.

The beginning of the modern era in Persian was marked by the coming to power of the Safavids in 1501, ending 250 years of fragmented domination by Mongols, Timurids and Turkmen. [Hat1] In 1499 Ismail attempted to seize power in Iran. With a following of fanatical Qizilbash he advanced from the Caspian Sea, across eastern Anatolia to Tabriz. The Turkman Aq Qoyunlu ruling Iran fled as Ismail advanced, so Safavid rule was established in Tabriz by 1501. By 1512, Iraq, the rest of Persia and the whole territory of the Aq Qoyunlu had been added to Ismail's rule.

Safavid dominance in Persia created unrest amongst the Qizilbash of Ottoman Anatolia – they revolted against the Sultan in 1512, leading the Ottoman Emperor Selim to put down the uprising and tackle the Safavids. In 1514 the Ottoman Turks inflicted a terrible defeat on the Persians at Chaldiran; the technological advance of guns gave them an unassailable advantage. Eastern Anatolia fell permanently to Ottoman Turkish

hands and the sack of Tabriz had long term effects on manuscript arts as, amongst other loot, the Turks carried off both artists and manuscripts.

Artistically Ismail favoured the Turkman idiom and the vibrancy of composition that it engendered continued throughout the Safavid period. His son, Tahmasp, was brought up initially in the intellectual environment of Herat. After his father's death in 1524, he moved to Tabriz but was still too young to rule which left considerable time for the pursuit of aesthetic interests. This continuing support of the royal atelier contributed significantly to the development of a distinctly Safavid painting style, with a fusion of the Turkman vibrancy of palette and form with the structured finesse of the style of Herat.

Unfortunately the fractious rule of a collection Qizilbash emirs engendered a series of conflicts between 1524 and 1537 with the Uzbeks, and between 1530 and 1555 with the Ottomans in the west. Even the overthrow of his regent in 1533 was insufficient to stabilise the situation and Tahmasp lost Mesopotamia and Baghdad to the Ottomans. Rather than engaging them in further battle, however, Tahmasp overstretched Ottoman lines of supply with a scorched earth policy that forced them to retreat, allowing the Safavids to reclaim the territory.

Although Tahmasp's artists were primarily occupied with a number of large manuscript projects they also painted occasional single-page works, a growing trend in Islamic painting that would eventually come to eclipse the long-standing tradition of manuscript illumination. Of all of his artists, two of the most highly regarded were the father and son, Mir Musavvir and Mir Sayyid 'Ali. It is indicative of Tahmasp's declining interest in the arts that, in the mid-1540s, when the Mughal emperor Humayun returned to India he was able to take these two and many others with him. By 1556 Tahmasp's declining interest had become the Edict of Sincere Repentance and the secular arts were outlawed; of the court artists who did not emigrate to India, many went to the court of Tahmasp's nephew, Sultan Ibrahim Mirza, at Mashad. As he aged, however, Tahmasp's stance on painting relaxed and a school developed in the new capital of Qazvin, chosen when Tabriz was under threat from the Ottomans in 1548.

Tahmasp was succeeded in 1576 by his second son, Ismail II. His cruelty resulted in his death through poisoned opium in 1577, leaving only Muhammed Khudabanda, Tahmasp's eldest son, who had previously been passed over as he was half blind. Various groups rebelled during this period, allowing the Ottomans to invade again in 1578, taking much of northern and western Iran over ten years. The Uzbeks besieged Herat and in 1587, the people of Khurasan rallied behind the governor of Mashhad and Abbas the adolescent son of Muhammed Khudabanda. They marched on Qazvin where the Shah promptly abdicated.

The reign of Muhammed Khudabanda was not a golden period for court manuscript production under the Safavids. With poor eyesight, he could not be expected to appreciate the decorative arts and many of the court artists of Qazvin left to seek employment elsewhere. They moved to India or Ottoman Turkey, or stayed in Persia at centres such as Herat or Mashhad. Increasingly, however, they turned to the creation of single page works, lacking wealthy patronage for the production of extravagant manuscripts. Also, for the first time, illustrations that were only partly painted or tinted were produced. This trend lasted until well into the 17th century, presumably because these works were cheaper to produce.

Shah Abbas inherited a run-down and almost bankrupt kingdom in 1587, under attack from both the Ottomans and the Uzbeks. However, by 1598 he had repulsed the Uzbeks and turned on the Ottomans, recapturing all of the lands lost or ceded, by 1624. Deposing the Qizilbash, he put all their assets into the royal coffers and used them to encourage commercial production and trade. He created a new capital at Isfahan in 1598, which became the new cultural and economic hub. He also encouraged the production of craft objects, including manuscripts and paintings, for export.

Isfahan had been a cultural centre before the arrival of the court but the range and volume of its work increased. Single page portraits were still fashionable but the variety of subjects expanded to include ordinary people as well as courtiers. Manuscript illustration continued but the gathering of a collection of single page works into albums became more popular, with the style of work clearly influenced by the steadily increasing flow of European visitors.

Great as Abbas' achievements had been, he instigated the eventual decline of the Safavids after his death in 1629 as his sons had been brought up confined to the harem and were uneducated, neglected and often unbalanced. From this time onwards all Safavid princes were raised in this way; their disinclination to govern and the resulting neglect of the social, military and administrative structures made the eventual overthrow of the last Safavid puppet Shah, by General Nadir in 1736, inevitable. Persia had been ruled for some time by a succession of army commanders in the name of various, mostly juvenile, Safavid princes. Nadir Shah overthrew both the occupying Afghans and Ottomans and began a series of conquests of his own which culminated in the sack of Delhi and the seizing of the famous Peacock Throne of the Mughal emperors. In 1747, however, he was murdered and the empire collapsed, eventually falling to the Qajars, Turkman nomads from the northwest, in 1794.

4.4.1. OR 11837

Majālis al-'ushshāk, attributed to Sultān Husain ibn Mansūr ibn Bāikarā. A collection of biographies of holy men, this version was created around 1560 AD/1124 AH. It has seventy-nine miniatures in large format. A single sheet was made available for analysis during conservation. [Mere, Tit1]

f.148 Maulānā Husain Khvārazm, being read to by a youth

Description	Colour	Pigment
Standing Figure 3	Dark Blue	Lazurite
Turban	White	White Lead
Turban decoration	Red	Vermilion
Centre Figure 2	Orange	Red Lead
Figure	Light Blue	Lazurite
Figure 1	Purple	Lazurite
Figure 1	Yellow	Orpiment
Head-dress, woman in window	White	White Lead

Table 4.19: The pigments of OR 11837 f. 148.

Spectra could not be obtained from any of the green or pink areas. See figure A3.20, appendix 3.

Although only a very small section of this manuscript was analysed, the palette is unexceptional. Of interest is the appearance of lazurite in the production of the purple pigment – suggesting a pigment mixture rather than the use of a purple organic material. The lack of spectra from the green and pink areas can probably be attributed to the presence of organic pigments or, in the case of the green pigment, verdigris or a copper derivative, which are hard to identify.

4.4.2. OR 7315

This is a Persian version of the Turkish manuscript 'Ajā'ib al-makhlūkāt by Zakariyyā ibn Muhammad ibn Mahmūd al-Kazvini. This is an extensively illustrated encyclopaedia dating from the early 17th century. [Mere, Tit1]

f. 11v Pegasus

Description	Colour	Pigment
Background	Blue	Lazurite
Spot	White	White Lead
Animal	Pink	White Lead

Table 4.20: The pigments of OR 7315 f. 11v.

See figure A3.21, appendix 3.

f. 12v Draco

Description	Colour	Pigment
Background	Blue	Lazurite
Dragon	Pink	Vermilion
Dragon's Head	Yellow	Orpiment
Dragon's Back	Black	Lazurite, Carbon

Table 4.21: The pigments of OR 7315 f. 12v.

See figure A3.22, appendix 3.

f. 26v Angels That Support God's Throne

Description	Colour	Pigment
Wing, RHS	Red/Orange	Vermilion
Background, RHS	Blue	Lazurite
Clothing, RHS	Yellow	Orpiment
Bird Figure	Orange	Red Lead

Table 4.22: The pigments of OR 7315 f. 26v.

Spectra could not be obtained from the flesh coloured areas, the brown and the green. See figure A3.23, appendix 3.

f. 30 Hārūt And Mārūt Hanging Upside-Down

Description	Colour	Pigment
Background	Black	Carbon
Figure	White	White Lead
Rocks	Yellow	Orpiment
Rocks, RHS wall	Orange	Red Lead
Rocks, RHS wall	Green	Verdigris
Tree	Red	Vermilion
Flowers	Yellow	Orpiment

Table 4.23: The pigments of OR 7315 f. 30.

See figure A3.24, appendix 3.

Again, this manuscript makes use of a standard palette. Here verdigris has been identified in more than one area, owing to its state of preservation and the thickness with which it has been applied. Spectra were not obtained from brown, flesh-toned and green areas. In the case of the brown and flesh this is likely to be due to the use of organic materials. The green is probably verdigris or a related degradation product.

4.4.3. OR 13935

This is the Persian version of a Turkish cosmographical treatise by Zakaiyyā ibn Muhammad al-Qazvini. [Wale] As such its origins may lie in the neighbouring Ottoman Empire or in Persia itself. It is dated to 1665 AD/1075 AH and has numerous illustrations, of which a selection was examined.

f. 1v A Decorated Page

Description	Colour	Pigment
Rectangular Panel, RHS	Pale Blue	Lazurite
Flower, RHS	Red	Red Lead
Centre of flower	White	White Lead, Chalk
Small flower	Dark Blue	Lazurite
Leaves	Yellow/Brown	Orpiment

Table 4.24: The pigments of OR 13935 f. 1v.

Spectra could not be obtained from the black outlines. See figure A3.25, appendix 3.

f. 15v Conjoined Twins

Description	Colour	Pigment
Clothes, far left figure	Red	Vermilion
Clothes, far right figure	Yellow	Orpiment
Trousers, third left figure	Red	Red Ochre
Grass	Green	Orpiment, Lazurite
Sky	Blue	Lazurite

Table 4.25: The pigments of OR 13935 f. 15v.

Spectra could not be obtained from the black tarnished areas. See figure A3.26, appendix 3.

f. 17 Winged Figures, holding a disc of concentric circles

Description	Colour	Pigment
Centre of Disc	Orange	Vermilion
5th Ring of Disc	Pink	Vermilion
Wing, RHS figure	Yellow	Orpiment
Shoulder, RHS figure	Red/Brown	Red Lead
RH Wing, LH figure	White	White Lead
Sky	Pale Blue	Indigo

Table 4.26: The pigments of OR 13935 f. 17.

Spectra could not be obtained from the dark green, beige, blue, black and grey areas - these appeared quite degraded. See figure A3.27, appendix 3.

f. 43v Winged Figure Holding a Trumpet, upper image

Description	Colour	Pigment
Skirt	Orange	Red Lead
Underskirt	Yellow	Orpiment
Foreground	Green	Orpiment, Indigo
Horizon	Light Green	Orpiment, Indigo
Lines on Blue Wings	Red	Red Ochre
Top Right Wing	Black	Indigo
Coat, degraded	Orange	Red Lead
Background	Dark Green	Orpiment

Table 4.27: The pigments of OR 13935 f. 43v.

Spectra could not be obtained from the beige hat and trumpet or the degraded purple areas. See figure A3.28, appendix 3.

f. 273 Man with a Torch, lower image

Description	Colour	Pigment
Trousers	Yellow	Orpiment
Clothing	Orange	Red Lead
Wheel	Blue	Lazurite
Turban	White	Chalk, White Lead

Table 4.28: The pigments of OR 13935 f. 273.

Spectra could not be obtained from the green pigment. See figure A3.29, appendix 3.

f. 306v Two Men in Combat

Description	Colour	Pigment
Jacket	Orange	Red Lead
Jacket	Yellow	Orpiment
Belt	Green	Orpiment
Hat	Black	Carbon
Sky	Dark Blue	Lazurite or Indigo
Background	Light Blue	Indigo

Table 4.29: The pigments of OR 13935 f. 306v.

Spectra could not be obtained from the beige areas. The identity of the pigment used to colour the sky is not clear as the principal bands of lazurite and indigo are at the same wavenumber. The spectral quality was sufficiently low that no other bands could be located. However, red lead, which also has a similar principal peak wavenumber, can be excluded on the grounds of its colour. See figure A3.30, appendix 3.

In general the condition of the illustrations in this manuscript is not ideal. Many of the pigments are degraded and discoloured which impedes identification. The black pigments that could not be identified fall into one of two types. The inks are likely to be iron gallo-tannate which is extremely difficult to identify by Raman microscopy. The tarnished black areas are probably silver tarnished to black; the resulting material is a very weak scatterer. The usual collection of unidentifiable organics probably accounts for the majority of the other samples that gave no spectra. One or two, for example the blue pigments, may be inorganic pigments that we would normally identify, but affected

either by the degradation of lead white, with which they may be mixed, or an organic binder. A couple of notable uses of pigments have occurred here, however. Firstly, verdigris has not been identified on the manuscript. The only identifiable greens have been composed of mixtures of blue indigo and yellow orpiment. Somewhat unusually, chalk appears in mixture with white lead in some of the white areas and extensive use has been made of red ochre as well as vermilion and red lead.

4.4.4. ISL 3442

Rather later than the other manuscripts, this is a Shahinshahnama from 1810 AD/1225 AH. It is an imitator of the Shahnama created in honour of Fath 'Ali Shah, King of Persia from 1797–1834 AD by poet Fath 'Ali Khan Kashi. [Ethe] Again, a single sheet was made available for analysis during conservation.

f. 354 Men in Battle

Description	Colour	Pigment
Bottom Right Figure	Pink	White Lead
Horse Bottom Right	Red	Vermilion
Sky	Light blue	White Lead
Horse	White	White lead

Table 4.30: The pigments of ISL 3442 f. 354.

Spectra could not be obtained from the purple or dark blue areas. See figure A3.31, appendix 3.

Few of the pigments of this folio were analysed and none of the results were unexpected. The difficulty in analysing the blue element of the sky can probably be attributed to small quantities of indigo, which is a weaker scatterer than lazurite and so may not have been detected.

4.4.5. Conclusions

This group of manuscripts have mixed origins and dates, which is not reflected in their palette. Even the identifiable palette of the early 19th century manuscript does not

deviate from the usual range of pigments. The only notable exceptions are found in the palette of OR 13935, which uses indigo and orpiment in admixture, chalk and red ochre. Doubt exists as to whether this manuscript, although in Persian, originates in Persia or neighbouring Ottoman Turkey. The lack of a clear distinction suggests that local variation in materials was rare in this region during this time.

4.5: Ottoman Turkish Manuscripts

Originating from the Turkman tribes in Anatolia, displaced by the Mongols in the 13th century, the Ottomans became the longest surviving Islamic dynasty. [Hat2] The first Ottoman ruler, Osman (c. 1300–26) extended his rule towards Byzantium, leaving his son Orkhan (1326–59) to conquer various Byzantine cities in Anatolia, turning them into important trading centres, and to annex the neighbouring Turkman lands to the east. His successors, Murad I (1359–89) and Bayazid I (1389–1402), soon controlled the trade routes into Constantinople and soundly defeated the Christian armies at the Battle of Kosovo in 1389 and at Nicopolis in 1396. Bayazid I expanded into the east until his army was destroyed by Timur, at the Battle of Ankara. He was captured and died leaving his four sons to fight until the succession of Mehmed I (1413–21).

From the reign of Orkhan, Ottoman rulers concentrated primarily on military security. Mehmed I was less expansionist and conflict was generally avoided until Murad II (1421–51) besieged Constantinople and annexed Serbia. Mehmed II Fatih (the Conqueror, 1451–81), his son, was the most distinguished of the Ottoman rulers, laying siege to and taking Constantinople in less than two months. He renamed the city Istanbul and made it his capital, resettling people from all over his empire there and giving tax concessions to artists and craftsmen. Mehmed II also employed many writers who worked on the copying of Turkish, Persian and Arabic manuscripts. A great many illuminated Koranic manuscripts were produced for the new Mosque complexes. He rebuilt the city and allowed the settlement of different religious groups with considerable cultural autonomy, encouraging a period of sustained artistic development. His son Bayazid II (1481–1512) concentrated on strengthening the economy and restricting the Europeanisation that had begun to appear throughout the empire. He was also fond of book arts, employing numerous native and Persian artists in the court

studio. However, his son Selim I Yavuz (the Grim, 1512–20), who put down in writing that he wanted to rule the whole world, [Hat2] overthrew his father and managed to double the size of the empire. To secure his throne he committed various acts of murder, allowing only Suleyman, of all his five sons, to live. Following the Battle of Chaldiran in 1514 he deported craftsmen and traders to Istanbul, particularly from Tabriz. The artists were put to work copying classical literary works on a large scale. Suleyman II (1520–66) is called by Europeans, 'the Magnificent' and by Turks, 'the Law-giver'. He codified the complex, flexible system of public law that supported the power and organisation of the state. The death of the Hungarian King at the Battle of Mohacs in 1526 brought Suleyman into direct conflict with the Hapsburgs who occupied central Hungary in 1528. By 1533 Suleyman and Charles V were confronting each other in Hungary, the Mediterranean and elsewhere.

By the time Suleyman came to power the court studio employed 41 painters and a number of bookbinders. To create a cultural base to match its political power, massive quantities of books were seized or purchased from the libraries at Tabriz and Buda and those of the Aq-Qoyunlu and Timurid rulers. Embassy gifts from the Safavids brought in considerable numbers of valuable manuscripts; in 1576 alone 18 Korans, 61 volumes of poetry and numerous albums of paintings were gifted. Also during this time the studio began to prepare extravagant editions of works by the Ottoman rulers and historical epics in cooperation with the leading scholars.

Unfortunately, Suleyman's decline into the harem before his death in 1566 left political control in the hands of his Grand Vizier, who became the leading political influence in an empire often run by the elite, with no effective control by government. Corruption, nepotism and assassination brought economic near-collapse. Reforms led by various Grand Viziers were only partially successful, whilst on the frontiers the Ottomans came under increasing pressure from the Hapsburgs. By the early 18th century, alliances between the Hapsburgs and the Russians cost the Ottomans the better part of the Balkans, the Crimea, Bessarabia and Podolia.

Under external, European, influences Selim III (1789–1807) began a radical restructuring of the treasury, legislation and the military, bringing opposition from the Janissaries and the elite and leading to his eventual execution in 1808. Mahmud II

(1808–39) continued his reforms but the work of both men was marked by considerable military losses and declarations of independence from Egypt, Bulgaria, Serbia, Romania and Greece. Further European style reforms were pushed through under successive Ottoman rulers, with varying success. A parliament was instituted and a range of rights guaranteed but Abdulhamid (1876–1909) used a state crisis in 1877 to suspend the reforms and the parliament, provoking resistance from the nationalist Young Turk Movement. They seized power, backed by the military, in 1908. Mehmed V replaced his brother as sultan but defeat in the 1914–18 war lead to the dismantling of the empire under his successor Mehmed VI in 1920. The sultan was deposed in 1922 by Mustafa Kamal 'Ataturk'. He transformed the empire into the republic that became modern Turkey.

4.5.1. OR 7073

The Divan, or poetry collection, of Ahmed Pasa, dating from early in the 16th century. [Titl] Originally it had four contemporary miniatures of good quality but these have been deliberately almost completely destroyed except for the first, which shows the Kâbe at Mecca.

f. 3v Unvan

Description	Colour	Pigment
Pattern	Red	Vermilion
Background	Blue	Lazurite

Table 4.31: The pigments of OR 7073 f. 3v.

Spectra could not be obtained from the grey areas. See figure A3.32, appendix 3.

f. 90 The Kâbe

Description	Colour	Pigment
Paving	Blue/Grey	Lazurite, White Lead

Table 4.32: The pigments of OR 7073 f. 90.

See figure A3.33, appendix 3.

f. 108v An Interior Scene

Description	Colour	Pigment
Background	Blue	Lazurite

Table 4.33: The pigments of OR 7073 f. 108v.

Spectra could not be obtained from the turquoise areas, the degraded red and purple pigments or the green. See figure A3.34, appendix 3.

f. 149v A Landscape, with trees

Description	Colour	Pigment
Tree trunk	Brown	Vermilion
Tree, top right	Green	Lazurite

Table 4.34: The pigments of OR 7073 f. 149v.

See figure A3.35, appendix 3.

The damaged condition of this manuscript made it particularly hard to analyse. The surface has been scraped and damaged in many areas, removing the majority of the pigment, and the remaining pigment is often discoloured and degraded. Spectra could not be obtained from some of the green areas, although those that were productive yielded lazurite. Spectra could not be obtained from a number of the degraded areas – either through lack of pigment or degradation of the pigment itself. An unusual turquoise colour resisted analysis and is probably organic in origin.

4.5.2. OR 7354

An unattributed Turkish translation of the Perisan book of stories and fables, Kalilah va Dimnah. [Titl] This copy was made in the late 16th century. Each folio is ornamented and it contains four miniatures.

f. 1 An Illuminated Page

Description	Colour	Pigment
Flower, LHS	Blue	Lazurite

Table 4.35: The pigments of OR 7354 f. 1.

Spectra could not be obtained from the red or black areas. See figure A3.36, appendix 3.

f.6v The Fox that Outwitted the Launderer's Ass

Description	Colour	Pigment
Donkey	Brown	Vermilion
Flower, bottom right by pile of cloth	Red	Red Lead
Flower, bottom left	Yellow	Orpiment
Leaf, flower bottom left	Green	Orpiment
Dog	Beige	White Lead
Grass	Dark Green	Orpiment
Saddle Cloth	Blue	Lazurite
Background Mountains	Blue	Indigo

Table 4.36: The pigments of OR 7354 f. 6v.

Spectra could not be obtained from the red/orange rock, the green background, the white turban or the black pool. The black of the water is probably degraded silver. See figure A3.37, appendix 3.

f. 9v The Man who Thought his Baby had been Attacked, with his wife

Description	Colour	Pigment
Figure, RHS	Red	Vermilion
Shutter, RHS	Yellow	Pararealgar
Furniture, centre	Orange	Vermilion
Border, top with pattern	Orange	Vermilion, Orpiment
Background, degraded	Pink	Red Lead, Lead Degradation
Turban	White	White Lead
Figure, LHS	Blue	Lazurite
Background, centre window	Dark Green	Orpiment
Leggings	Blue	Lazurite

Table 4.37: The pigments of OR 7354 f. 9v.

Spectra could not be obtained from some of the black and green areas. Unusually, pararealgar was detected on this folio and will be discussed later. See figure A3.38, appendix 3.

f.13 The Cat That Was Caught in the Snarer's Net

Description	Colour	Pigment
Leaf	Green	Orpiment, Indigo
Trunk	Light Green	Orpiment, White Lead
Plants, bottom	Dark Green	Orpiment
Trousers	Grey/Beige	White Lead, Lead Degradation
Coat	Purple	Lazurite
Grass	Dark Green	Orpiment
Rock, LHS	Blue	Indigo
Leaf	Red	Red Lead

Table 4.38: The pigments of OR 7354 f. 13.

Spectra could not be obtained from the pink mountains. See figure A3.39, appendix 3.

f. 19 The King Talking to a Bird

Description	Colour	Pigment
Jacket, LHS	Blue	Lazurite
Trees, centre	Green	Orpiment, Indigo
Jacket, centre	Yellow	Orpiment
Rock	Grey	White Lead
Ground	Cream	Orpiment, White Lead
Grass	Green	Indigo, Orpiment

Table 4.39: The pigments of OR 7354 f. 19.

See figure A3.40, appendix 3.

The palette of this manuscript is similar to that of the previous one. It also makes use of mixtures of yellow and blue pigments rather than verdigris as a source for green colourings. The yellows of this manuscript are also of interest as pararealgar makes a re-appearance here. It is used only in one area rather than extensively, and may have been mistaken for orpiment, which features elsewhere. The failure of a number of areas to give spectra may be attributed to a number of reasons. The two blacks are probably iron gall ink and degraded silver as before. The white area is likely to be white lead that has been affected by degradation. The reds, oranges, greens and pinks are either organic or pigments in such low concentration as to preclude obtaining spectra.

4.5.3. OR 405

The tragic story of Leila and Mecnun, a traditional story told in Turkish by Fuzuli. This is probably one of his last compositions, referring to himself in the epilogue as one whose life is nearly spent. [Rieu] This copy dates to 1664 and has 26 single page and one double page miniatures. [Titl]

f. 2v Unvan

Description	Colour	Pigment
Lower Section	Blue	Lazurite
Later Addition, top	Blue	Lazurite
Central Section	Green	Malachite, Verdigris
Bottom Section, adjacent to flower	White	White Lead, Chalk
Patterning	Red	Red Lead
RHS Border	Pink	Vermilion
Line, around text	Red	Vermilion

Table 4.40: The pigments of OR 405 f. 2v.

See figure A3.41, appendix 3.

f. 3v Unvan

Description	Colour	Pigment
Pattern	White	White Lead
Background	Dark Blue	Lazurite
Pattern	Pale Blue	White Lead, Indigo

Table 4.41: The pigments of OR 405 f. 3v.

See figure A3.42, appendix 3.

f. 11 The Prophet Rides Through the Heavens, Escorted by Angels

Description	Colour	Pigment
Saddle Cloth	Green	Verdigris
Horse	White	White Lead
Wings	Yellow	Orpiment
Background	Pale Blue	Lazurite
Clothes, bottom figure	Purple	Litharge

Table 4.42: The pigments of OR 405 f. 11.

See figure A3.43, appendix 3.

f. 19 Leila and Mecnun at School

Description	Colour	Pigment
Box, centre	Blue	Indigo, Lead Degradation
Hair	Black	Carbon
Background, top	White	White Lead
Lower Table	Red	Vermilion
Bottom of Robe, LHS	Orange	Red Lead
Face, bottom, LHS	White	White Lead
Central Figure	Pale Blue	Indigo
Cloth, centre bottom	Brown	Ochre
Headscarf, LHS	Yellow	Pararealgar, Orpiment

Table 4.43: The pigments of OR 405 f. 19.

Spectra could not be obtained from the pale green, dark green, purple and beige areas. See figure A3.44, appendix 3.

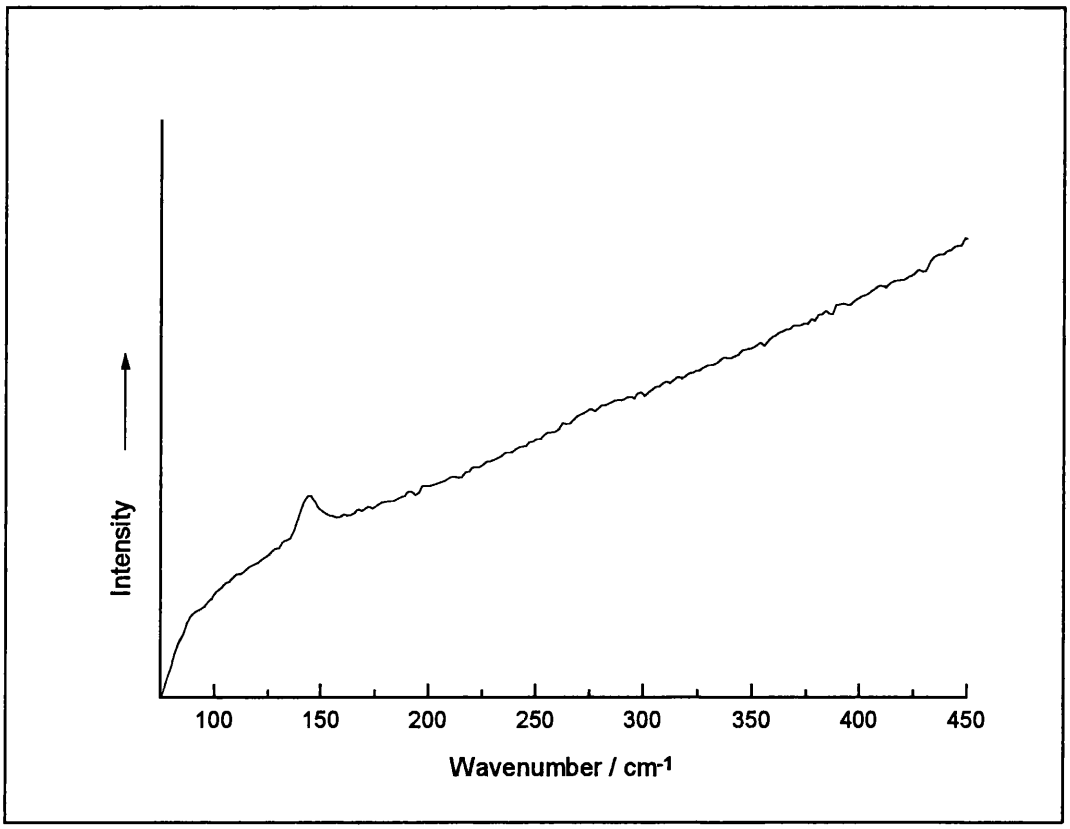

Figure 4.2: The Raman spectrum of litharge, taken from f. 11 of OR 405. $\lambda_0 = 632.8$ nm, ~0.35 mW.

f. 30 Mecnun Visited in the Desert

Description	Colour	Pigment
Clothing, RH figure	Purple	Indigo
Turban	Orange	Red Lead
Dress	Red/Orange	Red Lead
Feet, woman	White	White Lead

Table 4.44: The pigments of OR 405 f. 30.

See figure A3.45, appendix 3.

f. 83 Leila Visiting Mecnun in the Desert

Description	Colour	Pigment
Background	Yellow	Orpiment
Camel	Brown	Orpiment
Load on Camel	Green	Verdigris
Background	Yellow	Orpiment
Jacket, LH figure	Red/Brown	Vermilion, White Lead
Leggings	Orange	Red Lead
Load on Camel	Dark Brown	Indigo, Orpiment, Vermilion
Roof	Red	Red Lead
Figure, RH	Pink	Red Lead, White Lead
Background	Grey	Indigo

Table 4.45: The pigments of OR 405 f. 83.

Spectra could not be obtained from the purple/grey background or the yellow/brown cape. See figure A3.46, appendix 3.

This manuscript differs from the others of Turkish origin in that its green pigments are derived from verdigris rather than blue/yellow mixtures. Pararealgar appears here in admixture with orpiment. In all likelihood this is as an accidental contaminant since realgar, from which it is derived, is often found with orpiment in nature. Pararealgar and orpiment are sufficiently similar in colour as to make mixing them ineffectual. [Bona] Litharge (PbO) is also seen here for the first time in a purple coloured area. Litharge is a red pigment that occurs in its own right and as a product of the decay of

red lead. It may be that its use here occurs as an accidental or deliberate substitute for red lead, or as a product of the decay of red lead after the completion of the illustration. Chalk and ochre are both found on this manuscript, which also distinguish it from the other Ottoman Turkish works discussed here.

4.5.4. Conclusions

The palette of all three manuscripts is reasonably consistent, making use of indigo, lazurite, orpiment, red lead, vermilion and white lead. Again the principal difference is found in the production of green colours, with mixed blue and yellow for the first two manuscripts and verdigris and its derivatives for the rather later OR 405. Both OR 7354 and OR 405 make use of pararealgar as a yellow pigment although this may be as an accidental substitution for orpiment, especially in OR 405 where orpiment appears in the same area as the pararealgar.

OR 405 also contains two other differences: the use of chalk with white lead in a white area, and the appearance of litharge in a purple. This last may also be an accidental application since litharge occurs nowhere else, and is a common part of the decay chain of red lead.

4.6: Conclusions

Although this collection of manuscripts originates in different regions and at different dates, the palette across all of the manuscripts is remarkably similar. It also bears a startling resemblance to that of the Anglo Saxon manuscripts examined in chapter 3. The blue pigments are lazurite and indigo, the reds vermilion and red lead, white lead is the principal white pigment and the greens are provided by verdigris and mixtures of blue and yellow. Although technological constraints were certainly in operation, a range of alternative pigments exists of which very little, or nothing, is seen. For example, azurite, malachite, realgar, barytes, gypsum, lead tin yellow and massicot have been known since antiquity but appear in both Eastern and early Western work sparingly or not at all.

A number of slight differences do exist between different regions and periods, however, which allows some conclusions to be drawn about the more contentious manuscripts in this study: the Sultanate manuscripts OR 1403, OR 13836 and OR 11676 and the nominally Persian manuscript OR 13935.

4.6.1. Sultanate manuscripts

This group of manuscripts is fundamentally Persian in style, but elements of the decoration and, in some cases, textual evidence point to an Indian origin. All three date from after the sack of Delhi by Timur Lenk, when the Persian artistic influence might be expected to have lessened in India.

In comparison with the results of the analysis of Persian material (disregarding OR 13935 for the moment) a number of differences are striking. The Sultanate manuscripts OR 1403 and OR 13836 use indigo and orpiment in mixture to form a green pigment. This is in common with the Mughal Hanzanama. The Persian manuscripts in this study use verdigris, as does the Mughal Akbarnama. In Sultanate OR 11676 verdigris is also used for the original illustrations but, unlike the Persian material, it is mixed with indigo and lazurite.

The 16th century illustrations in Sultanate OR 11676 originate from around the same time as Sultanate OR 13836. In common with OR 13836, no verdigris is used. However, the 18th century illustrations revert to verdigris with indigo and lazurite, which is similar to some of the Mughal material that they seek to imitate.

A clear distinction exists between the indigo and orpiment greens of OR 1403 and OR 13836 and the verdigris of the Persian manuscripts. This distinction is less clear for the original illustrations of OR 11676 since although verdigris is used, it is not used in a way that is found in Persian work. The 16th century illustrations are similar to the other Sultanate material – showing no Persian influence, while the use of verdigris in the 18th century illustrations could be attributed to emulation of the Mughal style, which made use of both sources of green pigment.

The use of blue pigments, both alone and in admixture, is similarly varied. All of the Sultanate material uses lazurite as an unmixed blue pigment and indigo in mixtures. This is similar to the Persian material, which uses unmixed lazurite as the only source of blue pigment. However, no indigo is seen on Persian material. Mughal material uses both indigo and lazurite alone and indigo in admixture. Only OR 11676 also uses lazurite in admixture in both the 1439 and 18th century illustrations.

Pararealgar occasionally appears in both the Sultanate and Turkish material but this is possibly due to an accidental substitution in both cases, rather than evidence for a Turkish influence. Orpiment and pararealgar are frequently found together in nature and are similar in appearance. The limited use of pararealgar, in some cases in mixture with orpiment, suggests more that it has been introduced accidentally rather than chosen over the far more common orpiment.

In general, the influence of Persian artists is not seen in the choice of blue and green pigments for the Sultanate manuscripts. The use of verdigris in Sultanate OR 11676 suggests that the influence of Persian artists may have been stronger in this manuscript than in the others. Two possible explanations for this are immediately obvious. It may be that the manuscript was produced by a Persian or Persian-trained artist, in India; alternatively, the manuscript was produced in Persia itself, by a Persian or Sultanate artist, in the Sultanate style. Either case may have influenced the selection of materials. Similarly, the selection of lazurite for the unmixed blues in the Sultanate manuscripts may be due to Persian influence, but the mixing of pigments and use of indigo certainly is not.

Further research should ascertain whether the production and use of blue and green pigments can serve as a specific marker for the identification of foreign influence in Sultanate manuscript production. At present there are insufficient data to draw more than tentative conclusions as to the origins of these manuscripts, based on pigment use alone. However, the findings of this study do seem to support the non-Persian origin suggested by stylistic and textual evidence.

4.6.2. The origin of OR 13935

Or 13935 differs from the other Persian manuscripts in its use of a mixed green over verdigris and the presence of both ochre and chalk. An Ottoman Turkish origin is suggested as an alternative and these characteristics are shared with some of the Ottoman Turkish material.

As was discussed in the preceding section, mixed greens do not appear on Persian material. However, they do appear in Ottoman Turkish material, as does verdigris.
Red ochre was found on both Ottoman Turkish and Mughal material. This is a very common pigment and is readily available. It has been used since the earliest times and might be expected to have been more prevalent. However, it is not a strong Raman scatterer so it is possible that it may have been present on other manuscripts but not detected. Nevertheless, the far greater extent to which red lead has been used suggests that it was preferred over any alternative. Ochre is present in far more significant quantities on OR 13935 than on any of the Ottoman Turkish or Mughal material so any apparent similarity may be spurious.

Chalk is also a common pigment but is only found here on one example of Ottoman Turkish and one of Sultanate work, apart from OR 13935. Clearly, white lead, with its superior covering power, is favoured considerably. Chalk has been used so sparingly that its presence may be accidental and undue significance should not be attached to it.

The appearance of litharge in one of the Turkish manuscripts is more likely to be by accident than design. Litharge is a by-product of the formation of red lead and a product of its decay, but is very similar in its physical appearance.

There is insufficient evidence to say with certainty that the origin of OR 13935 lies in Ottoman Turkey and not in Persia. The identification of a distinctly non-Persian mixed green does contribute strongly to doubt regarding a suggested Persian origin. However, further research is needed since the number of manuscripts studied here is too small to detect defining elements.

4.6.3. A comment on the literary sources

In general, the palette of the materials studied is very much what would be expected from a study of modern and contemporary sources on oriental art. However, one or two assertions in the literature are not reflected in the results found by this study. In a widely referred to text on Mughal Painting, Moti Chandra suggests that the most popular white pigment of the Mughal period was zinc white. [Chan] Although he acknowledges that it became commercially available only in the 18th century he implies that a source must have been available since his discussions with modern painters in the traditional style suggest that only zinc white was used. Other authors [Port, Suma] maintain that the technical literature of the period or inherited tradition describes the use of chalk or talc in oriental miniature painting. None of these assertions is confirmed by the present results.

Chandra also describes the use of Indian yellow by Mughal painters, an opinion reiterated by other scholars. [Roge] Studies of the contemporary technical literature suggest that it was not. [Port] UV examination has revealed its presence on the Akbarnama of the late 16th century and archaic Mughal additions made to OR 11676 in the 18th century. It is not found on any of the Delhi Sultanate work, where its presence had been alleged, or on the Persian and Turkish manuscripts studied. Chandra further goes on to state that orpiment was not used in Mughal painting, but Raman microscopy has shown it to be the most common yellow pigment on all of the Islamic materials analysed.

Examination of the contemporary technical literature has suggested the use of both cobalt-based blues and azurite. [Port] However, such descriptive manuscripts are notoriously difficult to translate, with the same name often used for more than one material, or precise meanings for words long lost. Chandra states that lazurite cannot have been used extensively on Mughal work because of the considerable expense. [Chan] The only two blue pigments found during this analysis have been lazurite and indigo, strongly indicating that his sources may not be reliable.

As with the results of the studies on Western manuscripts presented in chapter 3, misconceptions about the materials used in the production of Islamic art abound. The

contemporary descriptions of materials and working practices were sometimes even deliberately obscure to protect the artists' secrets and are prone to misinterpretation. Modern works on the subject seem to rely on modern working practices and misconceptions. This cannot fail to have an effect on scholars' assessment and perception of the material, both from a conservation and a curatorial point of view. The importance of obtaining repeatable, testable and objective scientific evidence, to ensure accurate identification of materials, is clear. This work provides a first step towards completing that requirement.

Chapter 5: The Work of William Blake, in the Tate Gallery

In eternity all is vision.

Laocoön
William Blake
c.1820

The work presented in this chapter was conducted in collaboration with Noa Cahaner McManus, formerly of the Tate Gallery, to whom I am particularly indebted for the false colour photographs.

William Blake was born in Soho, London in November 1757 and died in August 1827 after a long and productive career, spent mostly in obscurity and relative poverty. [Butl, Vau2] The son of a hosier, he apprenticed as a printmaker and engraver, which provided him with a livelihood throughout his life as well as influencing the technique of a large body of his work.

Artist, poet and philosopher, Blake's work has a uniquely visionary quality that was quite out of keeping with his contemporaries, such as Turner, Constable and Reynolds. A large portion of his work relates to a quasi-religious philosophical system of his own devising and is particularly related in his illuminated books: Songs of Innocence and of Experience, Visions of the Daughters of Albion, The Book of Urizen, The Book of Los and The Book of Ahania. Interpreting Blake's vision is a part of this research, as explored by others, to whom the descriptions of his work herein are owed. [Particularly Butl, also Vau1, Bind]

Very little is known with any certainty about Blake's choice of materials, although he is known for his disregard for accepted technique and tendency to develop methods of his own. [But1] He worked in a number of formats, in combination or separately: pencil; pen; chalk; various washes; watercolour; line engraving; relief etchings printed, sometimes in colour, and finished in pen, watercolour or gouache; straightforward colour printing with a variety of finishes; tempera, which he called fresco although this is not the Renaissance practice. His techniques, and use of colour in particular, appear to be governed by what was immediately available rather than any grand vision. His

tempera technique is especially troublesome since it relied on binding the colours with glue, which tends to yellow as it ages. [Butl, Town]

The purpose of this study is twofold: to establish as far as possible the palette used by Blake in a range of his work including the watercolours and large prints and to compare the results of this analysis with that of the technique of false colour photography and hence attempt to adjudge its effectiveness.

5.1: False Colour Photography

False colour infrared photography (FC-IP) is a technique that is widely used by conservators as a means of identifying pigments without requiring sampling. Photographs of the work are taken with special film that is sensitive in the infrared. The resulting pictures are compared with images of pigment samples obtained in the same way. Differences in the response of the materials in the infrared provide more information to aid in their identification. Unfortunately, there is doubt about its effectiveness and reliability. [Moon, Clar] The technique is sensitive to experimental procedure, such as the temperature and storage conditions of the film, the illumination of the samples, filtration, contrast, developing procedure and so forth. These many variables cause considerable problems when attempting to obtain reproducible results.

In this case Kodak Ektachrome Professional Infrared EIR Film 2236 has been used to photograph works of art, recording radiation in the visible range and up to 900 nm in the infrared. [Caha] The colours produced using false colour film do not correspond to the colours of the objects photographed. Materials exhibit specific infrared signatures that can be captured on such film, emphasising the differences between two pigments that may appear to be the same colour to the naked eye. If the FC-IP appearance of particular pigments is known then the interpretation of FC-IP images of works of art can be accomplished.

It was not possible for FC-IP images to be taken of all of the work available for examination by Raman microscopy. The results of those that were analysed are presented after the Raman microscopy results below.

5.2: The Results of Analysis by Raman Microscopy

In all, the pigments of fourteen of Blake's major works were examined by Raman microscopy with varying degrees of success. These included works from a period of approximately fifty years from c.1780 to c.1830 in a range of techniques including watercolour, colour print and relief etching and a tempera, 'fresco', painting.

5.2.1. An Allegory of the Bible, T01128

c.1780–85. Pen and watercolour over pencil.
The subject of this work is unidentified, hence the rather general title by which it is known. The relative strength of colour in areas previously covered by a mount suggest that the pigments have faded. [Butl]

Description	Colour	Pigment
Floor, LHS	Blue	Carbon, Prussian Blue
Dress, figure second left, foreground	Blue	Prussian Blue
Child's Leg	Pink	Vermilion

Table 5.1: The pigments of An Allegory of the Bible.

Spectra could not be obtained from elsewhere on the painting – attempts were made to analyse the dark pink, yellow, brown and blue/grey. Its faded condition makes analysis difficult. See figure A4.1, appendix 4.

5.2.2. Age Teaching Youth, N05183

c.1785–90. Pen and watercolour.
A number of interpretations can be placed on this scene. One in keeping with Blake's personal morality is the casting of the old man as repression and false witness with the boy in the foreground Nature uninspired, suggested by the leaf and tendril motif of his dress. The girl points to heaven, representing imagination, as if to contradict the codified knowledge of books. [Butl]

Description	Colour	Pigment
Eye, seated figure	Black	Carbon
Middle of Back	Blue	Prussian Blue, Carbon
Sky	Pale Blue	Prussian Blue, White Lead
Lower Leg, middle	Pink	Vermilion
Foreground, RHS	Blue/Green	Prussian Blue

Table 5.2: The pigments of Age Teaching Youth.

Spectra could not be obtained from red, yellow and green areas. This is in part due to the thin application of pigment in watercolour technique; these particular pigments may be organic in origin. See figure A4.2, appendix 4.

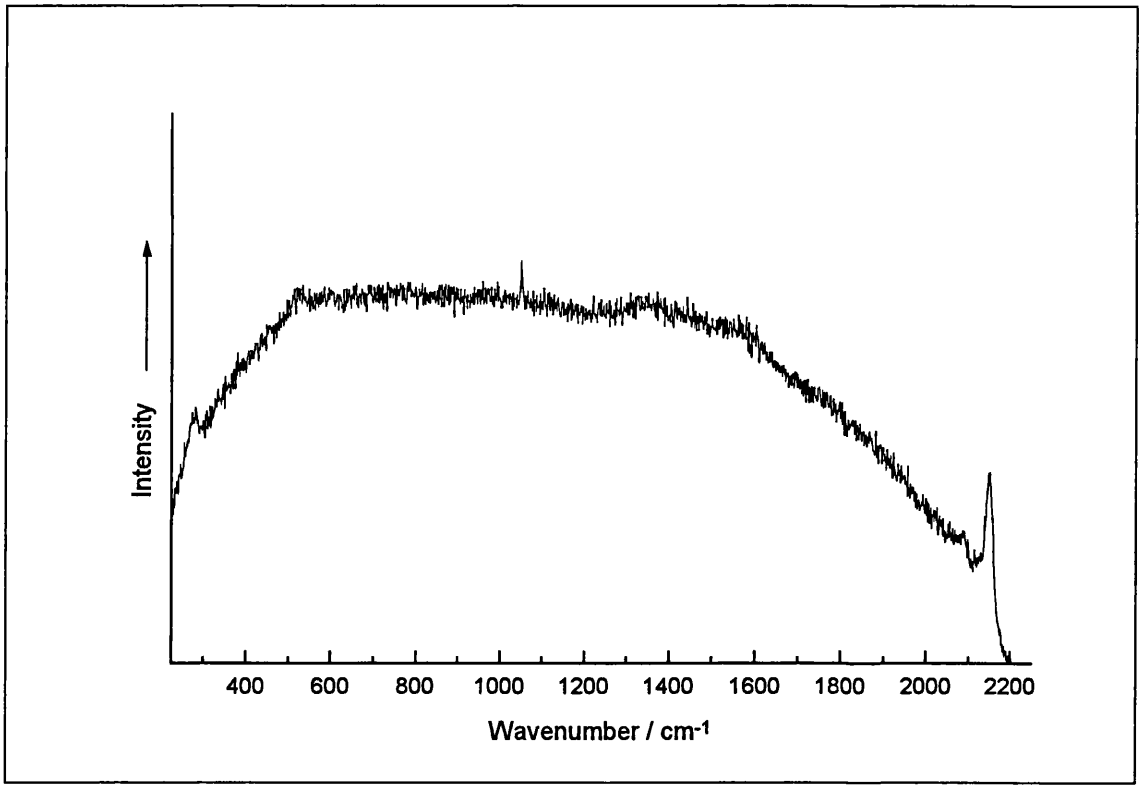

Figure 5.1: The Raman spectrum of Prussian blue, with white lead from Age Teaching Youth. $\lambda_0 = 632.8$ nm, ~ 0.35 mW.

5.2.3. Los and Orc, T00547

c.1792-3. Pen and watercolour.

A product of Blake's private mythology, Orc is the son of Los and Enitharmon. Los embodies the creative imagination, Enitharmon his inspiration and Orc energy and the idea of revolution. Los becomes jealous of Orc's love for his mother, causing Orc to come to hate him. Los chains Orc to the mountainside with the Chains of Jealousy, representing the restraint of natural passion. When they come to release him, Los and Enithamon realise that Orc's limbs have become entrapped in the rock and they are too late. [Butl, Tate]

Description	Colour	Pigment
Foreground, inside left leg, standing figure	Orange/Yellow	Trace vermilion
Rock, RHS	Blue	Indigo
Top Right, background	Blue/Black	Indigo
LHS, middle	Dark Blue	Indigo

Table 5.3: The pigments of Los and Orc.

Spectra could not be obtained from black or flesh coloured areas. Both colourants may be organic (a very dark blue for example, in the case of the apparently black pigment), making them hard to identify. See figure A4.3, appendix 4.

5.2.4. Visions of the Daughters of Albion, Plate 4, N03374

1793/c.1795. Colour-printed relief etching finished in ink and watercolour.

Visions of the Daughters of Albion is an allegory of the sinfulness of subjecting love to bonds of orthodox morality. Blake's target specifically is the suffering that sexual convention brings to the women of England. Plate 4 illustrates the lines: [Vaug, Butl]

"Why does my Theotormon sit weeping upon the threshold;
And Oothoon hovers by his side, persuading him in vain."

Description	Colour	Pigment
'Flame', lhs, top middle above figure	Blue	Prussian Blue, Carbon
Cloud, RH edge, above sun	Red	Vermilion, Red Ochre
Rock, LHS	Red	Vermilion
Left Leg, seated figure	White	Lead White
'Flame', above head	Dark Blue/Black	Carbon
Edge of Sun	Yellow	Chalk, White Lead

Table 5.4: The pigments of Visions of the Daughters of Albion, Plate 4.

See figure A4.4, appendix 4.

5.2.5. Satan Exulting Over Eve, T07213

1795. Colour print finished in pen and watercolour.

The subject of this print is clearly Biblical, from Genesis, although Milton's Paradise Lost, where Eve tells Adam of eating a fruit from the tree and being swept up into the clouds, may also have been an inspiration. [Tate, But1]

Description	Colour	Pigment
Snake	Blue	Carbon
Flame, above snake	Red	Vermilion

Table 5.5: The pigments of Satan Exulting Over Eve.

Spectra could not be obtained from some of the blue and red areas, and the orange areas, possibly due to fluorescence from organic materials such as binders. The blue pigment here gave the spectrum of carbon, a black material. It is likely that carbon was added to darken a blue pigment that has not given a Raman spectrum. See figure A4.5, appendix 4.

5.2.6. God Judging Adam, N05063

1795. Colour-printed relief etching finished in ink and watercolour.
This is the second pull of this particular subject, the other two being at the Metropolitan and Philadelphia Museums of Art. Its subject is clearly Biblical and it reflects Blake's negative attitude towards the God of the Old Testament, with the figure of God resembling Urizen, the tyrannical law-maker in Blake's own mythology. [Tate, Butl]

Description	Colour	Pigment
Flame, RHS behind God's seat	Red	Vermilion
Flame, RHS behind God's seat	Yellow/Grey	Chalk, White Lead
Flames, top right	Orange/Red	Vermilion, White Lead, Chalk
Ground, in front of hoof	Blue	Prussian Blue, Chalk
Background, top left	Yellow	Chalk
Background, top right	Yellow	Chalk, White Lead

Table 5.6: The pigments of God Judging Adam.

Spectra could not be obtained from the black areas. This may indicate the presence of an unidentifiable organic material. See figure A4.6, appendix 4.

5.2.7. Newton, N05058

1795/c.1805. Colour print finished in ink and watercolour.
The watermark on the paper of this print is 1804, requiring the print to have been pulled after this date although Blake himself dates the work to 1795. Sir Isaac Newton was seen as a towering figure in British scientific rationalism. Blake's negative image is again heavily influenced by his personal morality. Newton is measuring out the image of the Trinity, a triangle, at his feet. Blake saw imagination as God in Man and the single rational vision exemplified by Newton's reasoning as the cause of war and moral decay. [Butl, Tate]

Description	Colour	Pigment
Flowers, bottom LHS	Red	Vermilion
Front Foot, second toe	Flesh	White Lead, Vermilion
Foreground, middle	Blue	Prussian Blue, Chalk
Foreground, below paper	Yellow	Yellow Ochre
Rocks, top left	Dark Blue	Carbon
Bottom Right, foreground	Blue	Prussian Blue

Table 5.7: The pigments of Newton.

Spectra could not be obtained from orange, black or green areas, again due to the presence of fluorescent material. Again the spectrum of carbon is derived from a component of the blue material. See figure A4.7, appendix 4.

5.2.8. Pity, N05062

c.1795. Colour print finished in ink and watercolour.

This print is generally agreed to be an illustration of Shakespeare's Macbeth, Act 1, Scene VII

"And pity, like a naked new-born babe,
Striding the blast, or heav'n's cherubim hors'd
Upon the sightless couriers of air,
Shall blow the horrid deed in every eye;
That tears shall drown the wind - ..."

However, what interpretation should be placed on the individual figures is not clear. [Butl, Vaug]

Description	Colour	Pigment
Right Shoulder, prone figure	Pink	Vermilion
Background, above prone figure	Dark Blue	Prussian Blue
Background, above legs of prone figure	Dark Blue	Prussian Blue
Legs, top figure	White	White Lead
Hair, foreground top figure	Yellow	Chalk
Foreground, bottom right corner	Red	Red Ochre
Mid-ground, right hand side	Black	Carbon
Lips, prone figure	Red	Vermilion

Table 5.8: The pigments of Pity.

Spectra could not be obtained from green, yellow and some black areas. See figure A4.8, appendix 4.

5.2.9. The Night of Enitharmon's Joy, formerly called Hecate, N05056

c.1795. Colour print finished in ink and watercolour.

Long believed to be a representation of Hecate, the Infernal Goddess, who is referred to by Shakespeare both in Macbeth and A Midsummer Night's Dream, this print has been recently re-identified as a product of Blake's own mythology. [Butl, Tate] It illustrates lines from the illuminated book Europe where Enitharmon sets out her false religion that imposes a separation between male and female, represented behind her.

Description	Colour	Pigment
Owl, left eye	Red	Vermilion
Owl, right eye	Blue	Chalk, Prussian Blue
Background Edge, middle RHS	Black	Carbon
Rock, above owl	Brown	Carbon
Left Wing, familiar	Blue	Prussian Blue, Carbon, Chalk
Right Foot, central figure	Flesh	Vermilion, White Lead
Foreground, below foot	Green	Carbon, Chalk

Table 5.9: The pigments of The Night of Enitharmon's Joy.

Spectra could not be obtained from the yellow areas. See figure A4.9, appendix 4.

5.2.10. The Body of Christ Borne to the Tomb, N01164

c.1799–1800. Tempera on canvas.
This is the only one of Blake's tempera works analysed in this study. It is somewhat yellowed and indistinct, attributable to the use of glue as both a binder and a varnish. [Butl] The picture is clearly Biblical in inception and belongs to a series of some 50 pictures on Biblical subjects produced for Thomas Butts, one of Blake's most consistent patrons.

Only one area gave a Raman spectrum, although several areas were attempted. The blood on the body of Christ was found to be vermilion. Blake's habit of using carpenters' glue in his tempera made this work particularly uncooperative to Raman analysis since the glue fluoresces. Vermilion is known for its strong Raman spectrum, a likely reason why this pigment alone was detectable. See figure A4.10, appendix 4.

5.2.11. The River of Life, N05887

c.1805. Pen and watercolour.
Also produced for Thomas Butts, as part of a series of watercolours of Biblical theme, this picture is an illustration of Revelation, XXII, 1–2.

"He showed me a river of water of life, clear as crystal, proceeding out of the throne of God and of the Lamb, in the middle of its street. On this side of the river and on that was the tree of life, bearing twelve kinds of fruits, yielding its fruit every month. The leaves of the tree were for the healing of the nations."

Additional figures of Blake's invention have been added, Christ leading two children to the Divine Sun, St. John the Divine, haloed by the sun, and the figures pertaining to Innocence on the left bank and Experience on the right. [Butl, Tate]

The picture appears to be considerably faded, indicated by a darker blue area at the bottom that may have been covered by a previous mount.

Description	Colour	Pigment
River, bottom edge	Blue	Prussian Blue

Table 5.10: The pigments of The River of Life

Spectra could not be obtained from any other areas of the painting due to the very thin application of pigment. See figure A4.11, appendix 4.

5.2.12. Dante and Virgil Penetrating the Forest, N03351

1824–7. Pencil, pen and watercolour.
Commissioned by John Linnell, Blake began a series of illustrations to Dante's Divine Comedy in 1824. The main series consists of 102 watercolours in varying stages of completion as well as sketches and engravings.

This is an illustration of the Inferno 11, 139–42. Dante finds himself lost in the forest and pursued by bears; he meets Virgil who offers to lead him to safety, through Hell and Purgatory to Paradise. [Tate, Butl]

The choice of colours in this painting is typical of those used in the Divine Comedy series. However, it is not certain whether the blue colouring of the forest is a deliberate selection or the product of a fading blue and yellow mixture.

Description	Colour	Pigment
Sky, top right	Pale Blue	Prussian Blue
Ink, bottom left	Black	Carbon

Table 5.11: The pigments of Dante and Virgil Penetrating the Forest.

Spectra could not be obtained from other areas of the painting. See figure A4.12, appendix 4.

5.2.13. The Pit of Disease: The Falsifiers, N03362

1824–7. Pen and watercolour.
This is the illustration to Inferno XXIX, 46–84 and XXX, 49–99, the tenth trench of the eighth circle of hell. Here falsifiers are punished with innumerable diseases. Dante is represented in red and Virgil in blue, representing feelings and imagination respectively. [Butl]

The only spectra were obtained from the flames in the background, which were identified as vermilion. Spectra could not be obtained from other areas. See figure A4.13, appendix 4.

5.2.14. Dante and Virgil Approaching the Angel who Guards the Entrance of Purgatory, N03367

1824–7. Pencil, pen and watercolour
This is an illustration of Purgatorio, IX, 73–105, where Dante and Virgil, ascending the Mountain of Purgatory, approach the angel who guards the gate. The three steps, marble, stone and porphyry, represent sincerity, contrition and love. [Butl]

Description	Colour	Pigment
Horizon, above figures	Red	Vermilion
Sky	Blue	Indigo
Sea	Dark Blue	Indigo
Ink, top right	Black	Carbon
Paint, top right	Black	Carbon

Table 5.12: The pigments of Dante and Virgil Approaching the Angel who Guards the Entrance of Purgatory

Spectra could not be obtained from the red clouds or a bright blue in the sky. See figure A4.14, appendix 4.

5.3: False Colour Infra Red Photography Results

From an examination of the false colour images of the pigment samples (figures A4.15, A4.16, A4.17, A4.18, appendix 4) a number of important factors are immediately obvious. Great similarities exist between the carbon-based black pigments, making them almost indistinguishable. The white pigments are also extremely difficult to distinguish, with only the false colour image of chalk apparently showing some hint of pinkness, the others remaining white.

The yellow pigments suffer from a similar lack of colour, being mostly tinted similar pale yellows in false colour. The exceptions to this are yellow ochre, which appears brown, mars yellow (which is very similar to yellow ochre) which appears a darker brown and massicot, which appears blue. The green pigments produce a slightly greater range of colours under false colour conditions. However, many of these are still hard to distinguish since they are varying shades of blue with the exception of green earth, viridian and cobalt green, which appear pink. The blue pigments similarly all appear blue or pink to red, with a range of red shades from the dark red of indigo to the paler pink of cerulean blue. The red pigments appear predominately yellow, with the exception of mars red, red earth and brazilwood, which appear brown. The brown pigments appear a variety of shades of dark brown and black.

The common occurrence of particular false colours, arising from a number of different pigments, creates considerable difficulties in distinguishing between them. The natural light colour of the pigment must be taken into account when making pigment assignments.

The results of false colour analysis of a selection of the Blake works studied above are presented below. The results of false colour analysis have only been considered in areas that were analysed by Raman microscopy, whether or not a Raman spectrum was obtained, to enable comparison.

5.3.1. Age Teaching Youth

Description	Colour	Possible False Colour Identification	Raman Identification
Eye, seated figure	Black	Black Carbon	Carbon
Back, seated figure	Blue	Blue Blue Verditer, Prussian Blue, Azurite, Manganese Blue	Prussian Blue, Carbon
Sky	Bright Blue	Blue Blue Verditer, Prussian Blue, Azurite, Manganese Blue	Prussian Blue, White Lead
Leg, seated figure	Flesh tone	Greyish	Vermilion
Foreground, RHS	Blue/ Green	Dark Blue/Black Blue Verditer, Prussian Blue, Azurite, Manganese Blue	Prussian Blue
Seated Figure, pattern on clothes	Red	Orange/Yellow	No spectrum
Curl of Hair, seated figure, top, middle	Yellow	Greyish. Massicot, Mars Yellow, Yellow Ochre	No spectrum

Table 5.13: The results of false colour analysis of Age Teaching Youth

For the false colour image see figure A4.19, appendix 4.

Several possible pigments have been identified, particularly for the blues and yellows, but it is not clear from the false colour results which have been used. The false colour technique has also failed to identify the white pigments found in mixture.

5.3.2. Los and Orc

Description	Colour	False Colour Identification	Raman Identification
Foreground, inside left leg, standing figure	Yellow/ Orange	Pale Pink Orpiment, Saffron, Naples Yellow, Cadmium, Barium, Indian Yellows	Trace Vermilion
Rock RHS, by head of prone figure	Dark Blue	Red Indigo, Smalt, Lazurite, Cobalt Blue	Indigo
Top Right Background, sky	Blue/ Black	Red Indigo, Smalt, Lazurite, Cobalt Blue	Indigo
Blue, far LHS, middle	Blue/ Grey	Red Indigo, Smalt, Lazurite, Cobalt Blue	Indigo
Left Foot, standing figure	Flesh Tone	White/Pink Chalk	No spectrum
RHS, background	Black	Black Carbon	No spectrum

Table 5.14: The results of false colour analysis of Los and Orc.

For the false colour image see figure A4.20, appendix 4.

Here again, the false colour technique has suggested a number of possible pigments. However, no conclusive identification of the blues has been possible.

5.3.3. Visions of the Daughters of Albion, Plate 4

Description	Colour	False Colour Identification	Raman Identification
"Flames" LHS, top, above flying figure	Blue/ Black	Dark Blue/Black Prussian Blue, Blue Verditer,	Prussian Blue, Carbon
Cloud, RH edge, above sun	Red	Orange/Yellow Any Except Brazilwood	Vermilion, Red Ochre
Rock, LHS	Red	Orange/ Red Brazilwood	Vermilion
Left Leg, seated figure	White	White	Lead White
"Flame", above head of seated figure	Dark Blue/ Black	Black Prussian Blue, Blue Verditer, Carbon	Carbon
Edge of Sun	Yellow	White/Yellow, pale, Orpiment, Saffron, Naples, Cadmium, Barium, Indian Yellows, any white	Chalk, White Lead

Table 5.15: The results of false colour analysis of Visions of the Daughters of Albion, Plate 4.

For the false colour image see figure A4.21, appendix 4.

It should be noted here that the false colour results were particularly misleading. The red pigment on the rock, LHS, has been identified as brazilwood by false colour techniques, since this is the most likely visual identification. However, the results of Raman microscopy actually demonstrate the pigment to be vermilion. A possible cause of this discrepancy is the effect that differing concentrations of pigment have on the colour and tone of the false colour images; higher concentrations of pigment result in stronger colours. This is not a limitation shared by Raman microscopy.

5.3.4. God Judging Adam

Description	Colour	False Colour Identification	Raman Identification
Flame, RHS behind God's seat	Red	Brownish Yellow Almost all reds, browns and yellows	Vermilion
Flame, RHS behind God's seat	Yellow/ Grey	Off-White	Chalk, White Lead
Flames, top right	Orange/ Red	Brownish Yellow Almost all reds, browns and yellows	Vermilion, White Lead, Chalk
Ground, in front of hoof	Blue	Bright Blue Prussian Blue, Azurite, Blue Verditer, Manganese Blue	Prussian Blue, Chalk
Background, top left	Yellow	Pale pink Chalk	Chalk
Background, top right	Yellow	Pale pink Chalk	Chalk, White Lead

Table 5.16: The results of false colour analysis of God Judging Adam.

For the false colour image see figure A4.22, appendix 4.

The false colour photography has failed to identify the white pigments, with the exception of chalk, and struggles particularly with the red and orange colours.

5.3.5. Newton

Description	Colour	False Colour Identification	Raman Identification
Flowers, bottom LHS	Red	Pale Pink Brazilwood	Vermilion
Front Foot, second toe	Flesh	Pale Pink Brazilwood	Vermilion, White Lead
Foreground, middle	Blue	Bright Blue Prussian Blue, Azurite, Blue Verditer, Manganese Blue	Prussian Blue, Chalk
Foreground, below paper	Yellow	Off White A range of whites, yellows and reds	Yellow Ochre
Rocks, top left	Dark Blue	Dark Blue/ Black Prussian Blue, Blue Verditer, Carbon	Carbon
Bottom Right, foreground	Blue	Bright Blue Prussian Blue, Azurite, Blue Verditer, Manganese Blue	Prussian Blue

Table 5.17: The results of false colour analysis of Newton.

For the false colour image see figure A4.23, appendix 4.

The false colour results here suffer particularly from their inability to distinguish elements of mixtures such as vermilion and white lead. The colour derived by the false colour photography is affected by the presence of all the pigments in the mixture, altering the resulting shade.

5.3.6. Pity

Description	Colour	False Colour Identification	Raman Identification
Right Shoulder, prone figure	Pink	Pale Blue No identification possible	Vermilion
Background, above prone figure	Dark Blue	Black Prussian Blue, Azurite, Blue Verditer, Manganese Blue	Prussian Blue
Background, above legs of prone figure	Dark Blue	Black Prussian Blue, Azurite, Blue Verditer, Manganese Blue	Prussian Blue
Legs, top figure	White	Pale Bluish No identification possible	White Lead
Hair, top figure	Yellow	Off White Any white pigment	Chalk
Foreground, bottom right corner	Red	Dark Blue/Black Indian Red	Red Ochre
Midground, RHS	Black	Black Carbon	Carbon
Lips, prone figure	Red	Brown/Orange Not Brazilwood	Vermilion

Table 5.18: The results of false colour analysis of Pity.

For the false colour image see figure A4.24, appendix 4.

There are clear discrepancies between the results of the FC-IP and the results of the Raman microscopy. The identification of vermilion is proving to be particularly difficult on this work, appearing both brown/orange and pale blue under false colour conditions.

5.3.7. The Pit of Disease: The Falsifiers

Description	Colour	False Colour Identification	Raman Identification
Flames, by blue	Red	Yellow/Brown Almost all reds, browns and yellows	Vermilion

Table 5.19: The results of false colour analysis of The Pit of Disease: The Falsifiers.

For the false colour image see figure A4.25, appendix 4.

Only one area generated a Raman spectrum for comparison; the false colour results are entirely inconclusive.

5.3.8. Dante and Virgil Approaching the Angel who Guards the Entrance of Purgatory

Description	Colour	False Colour Identification	Raman Identification
Horizon, above figures	Red	Pale Pink Chalk	Vermilion
Sky, top left	Blue	Blue Prussian Blue, Azurite, Blue Verditer, Manganese Blue	Indigo
Sea	Dark Blue	Dark Red, Indigo, Smalt, Lazurite, Cobalt Blue	Indigo
Ink Printing, top right	Black	Black Carbon	Carbon
Paint, top right	Black	Black Carbon	Carbon

Table 5.20: The results of false colour analysis of Dante and Virgil Approaching the Angel who Guards the Entrance of Purgatory.

For the false colour image see figure A4.26, appendix 4.

The false colour analysis of the sky has produced a completely anomalous result – appearing blue when it has been identified as indigo by Raman analysis

5.4: William Blake's Palette

A number of pigments eluded identification for various reasons. Some were applied very thinly, making identification difficult, and others were either fluorescent themselves or contained within a fluorescent medium which obscured any Raman spectrum that might have arise from the pigment. Of those that were identified, most striking is the similarity of the palette across the range of work, produced at a range of dates throughout Blake's career.

The only tempera piece examined proved remarkably resistant to analysis: the only pigment that could be identified was vermilion, which has a strong Raman spectrum. In the main these difficulties can be attributed to the use of glue as a binding medium and varnish thereby insulating the pigments in a layer of complex organic material that is fluorescent in response to visible wavelengths.

The other works examined were produced in watercolour or a combination of watercolour and colour print. The watercolour palette is very simple. The blues are either Prussian blue or indigo, although both do not appear to occur on the same work. The black, and dark shading, is provided by the use of carbon, either alone or in admixture with other pigments, particularly the blues. The red pigment is vermilion and the white, found only in admixture, is white lead. A number of pigments eluded identification, particularly a number of dark reds that are likely to be organic in origin. Likely candidates for the unidentified yellows are thinly applied yellow ochre, a poor Raman scatterer, or organic pigments such as gamboge. The same yellows would have occurred in the green pigments that could not be identified, since they are blue/green mixes. The blues that Blake favoured – indigo and Prussian blue, are strong colours and so would have to have been applied very lightly to make green, so their identification by Raman microscopy is difficult.

Unfortunately it is extremely difficult to distinguish between the printed and watercolour pigments on the colour prints so the palette must be treated across the works as a whole. However, a few differences do exist between these works and the watercolours which may be attributable to the use of alternative pigments for printing. Prussian blue remains the blue pigment of choice; indigo was not found on the colour prints. The principal red pigment is still vermilion but red ochre is also found in some areas. However, red ochre is hard to detect by Raman microscopy so its presence may have been overlooked in the watercolours. Carbon and white lead appear as before, but the addition of chalk is made, often in admixture. In addition yellow ochre was identified in a few areas. Again, greens, yellows, reds and oranges eluded identification. This may be attributed to the use of organic pigments or, perhaps, the introduction of a binding medium to aid the printing process.

In general, Blake's palette was not extensive, and did not reflect the visionary quality of the work he produced - all of the pigments identified were freely available and of traditional standing. Even the newest of them, Prussian blue, had been available since 1704 and was in common use. [Cla1]

5.5: False Colour Infrared Photography as a Technique for Pigment Identification

The difficulties in producing consistent false colour images in varying experimental conditions have been fully discussed by others [Moon, Clar] and need not be repeated here. What is immediately apparent from the false colour images of the pigment swatches is the difficulty in distinguishing between different pigments due to the similarity of their false colours. For example, indigo and lazurite/ultramarine blue appear a very similar pink/red shade that makes them indistinguishable and the white pigments have almost no false colour at all.

A further problem is introduced by the concentration of the pigment. A very thin wash of pigment will appear pale and a thicker one dark. This can serve to make the pigments indistinguishable from one another in false colour in the same way that it occurs under natural light – which is why pigment analysis is attempted in the first place!

Further problems are introduced by the use of mixed pigments. Although the introduction of a white pigment does not change the false colour, except to lighten it, the inclusion of a pigment with a strong false colour must produce an image composed of the colours of both pigments with no obvious means of differentiating between them.

Some conspicuous differences do exist between the false colours of pigments that appear very similar under normal conditions. For example, indigo and Prussian blue are nearly indistinguishable to the naked eye. However, indigo appears red and Prussian blue still blue under false colour conditions. This suggests that FC-IP may have application in distinguishing between a choice of two similarly coloured pigments, if there are sound reasons to believe that one or other of them had been used. Unfortunately, the results above suggest that FC-IP may not be even this reliable since Raman microscopy has identified indigo where the false colours have appeared both red and blue. FC-IP is clearly an inferior technique to Raman microscopy and is of limited utility in practice.

Chapter 6: Assyrian Frescos

I'm a professional cynic
But my heart's not in it

Country House,
Blur,
1995

Two pieces of Assyrian fresco, from the 7th/8th century BCE were lent from a private collection for pigment analysis. Two adjoining pieces in relatively good condition, they depict a warrior being trampled under the hooves of a horse; apparently part of a much larger scene. The frescos had no documented provenance, and presented a rare opportunity to study early fresco pigments in situ.

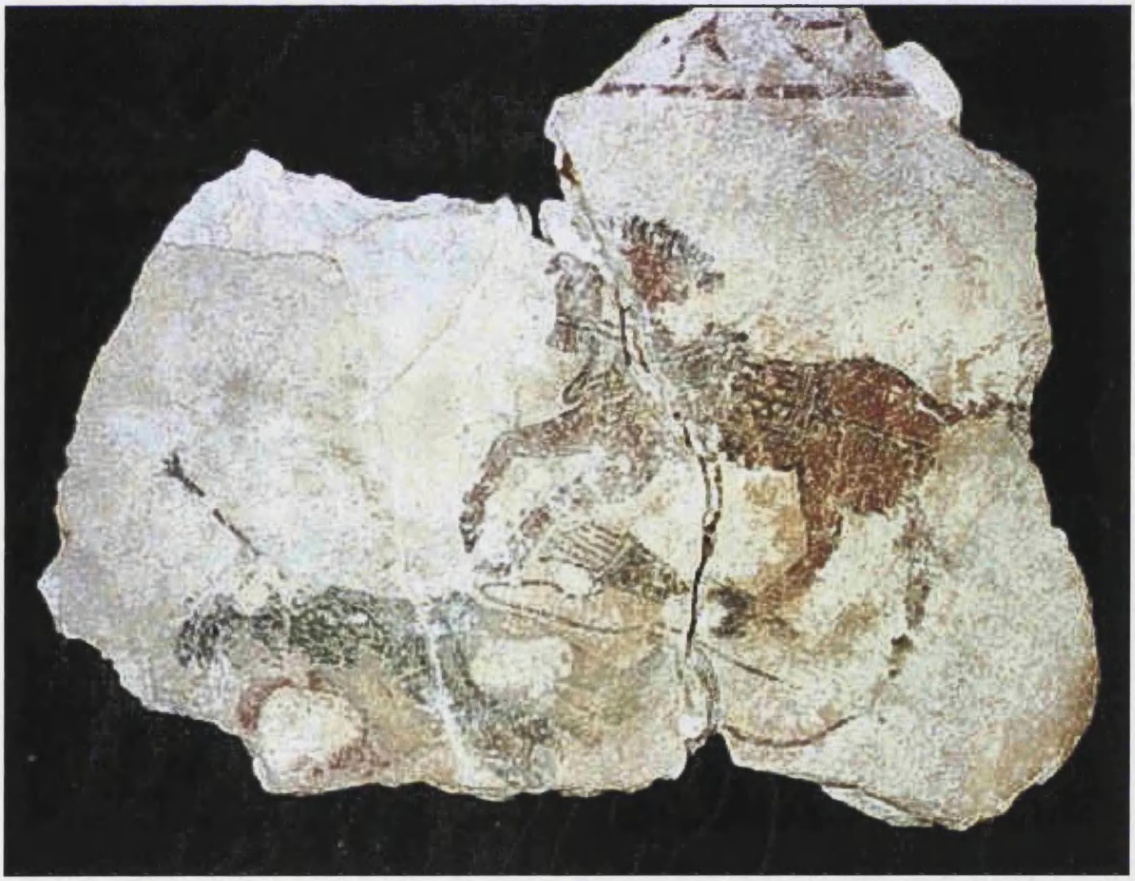

Figure 6.1: The two adjoining sections of Assyrian fresco.

6.1: The Pigment Analysis

The fresco is composed of four colours, red, black, beige and green on an off-white susbstrate. Areas in all colours and the substrate were examined.

6.1.1. The red pigment

Red pigment was found in a number of areas – the horse, its saddlecloth and the border at the top of the pieces. The pigment was identified as red ochre in all cases. (Figure 6.2)

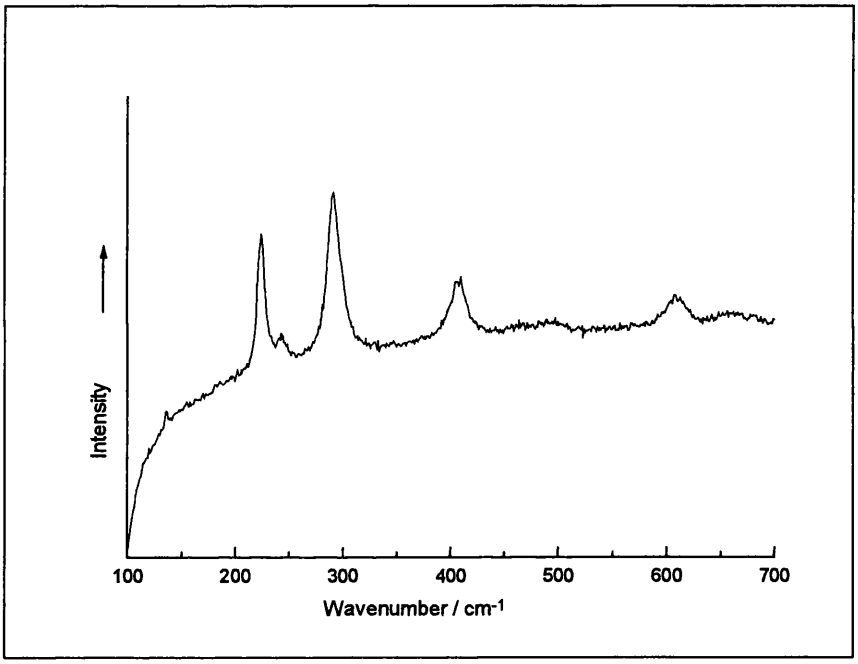

Figure 6.2: The Raman spectrum of red ochre from the body of the horse. λ_0 = 632.8 nm, ~ 0.35 mW.

The red areas also contain carbon and the minerals chalk ($CaCO_3$) and barytes ($BaSO_4$). (Figure 6.3) The carbon may have been added to vary the colour of the pigment or may simply be the result of environmental contamination from fires for heating and lighting. The chalk and barytes are either used as fillers, or alternatively were natural contaminants of the pigment in the ground from which it was extracted.

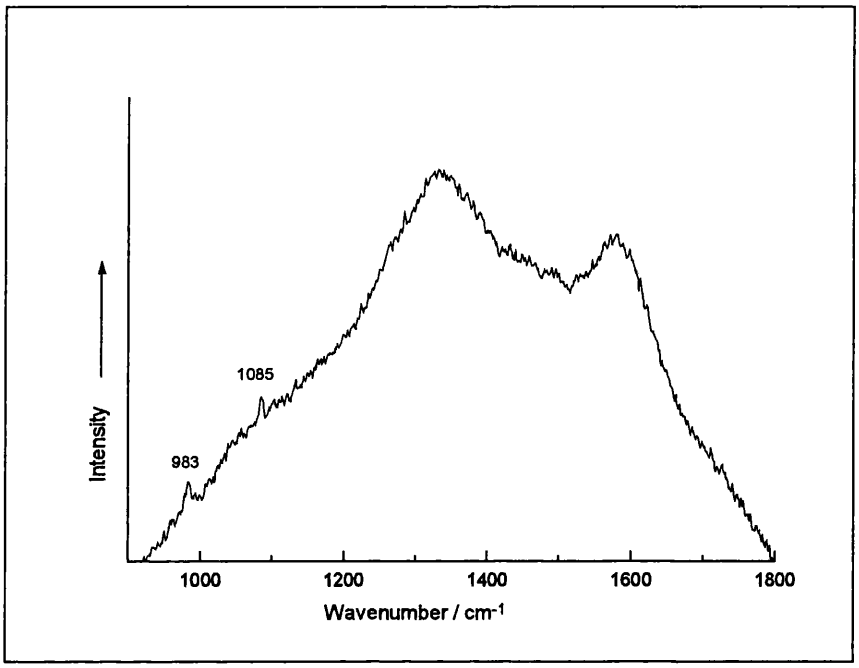

Figure 6.3: The Raman spectra of carbon, chalk and barytes from the red pigment on the body of the horse. $\lambda_0 = 632.8$ nm, ~ 0.35 mW.

6.1.2. The black pigment

A black pigment line was used to outline the horse and colour its mane and tail. The same black pigment was used to pick out details on the bridle and saddlecloth and appears on the hair and quiver of the prone figure.

The black pigment was found to be composed of carbon, with some traces of chalk. (Figure 6.4) The presence of chalk may be attributable to some form of contamination during construction, or the material from the substrate showing through.

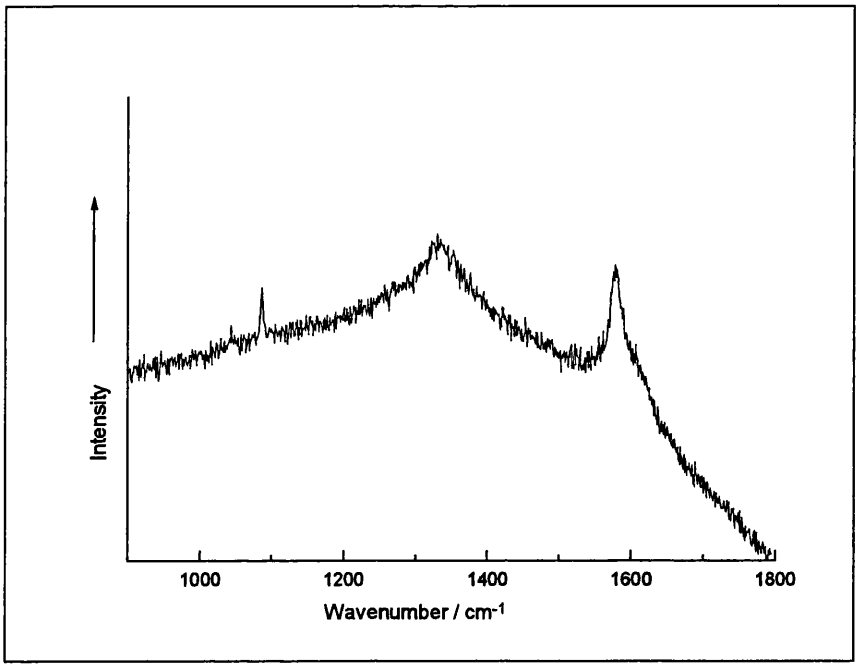

Figure 6.4: The Raman spectra of chalk and carbon from the black pigment on the hair of the prone figure. $\lambda_0 = 632.8$ nm, ~ 0.35 mW.

6.1.3. The beige pigment

Both the background and the saddlecloth on the horse were painted in a pale beige pigment. This was found to be composed of chalk. (Figure 6.5)

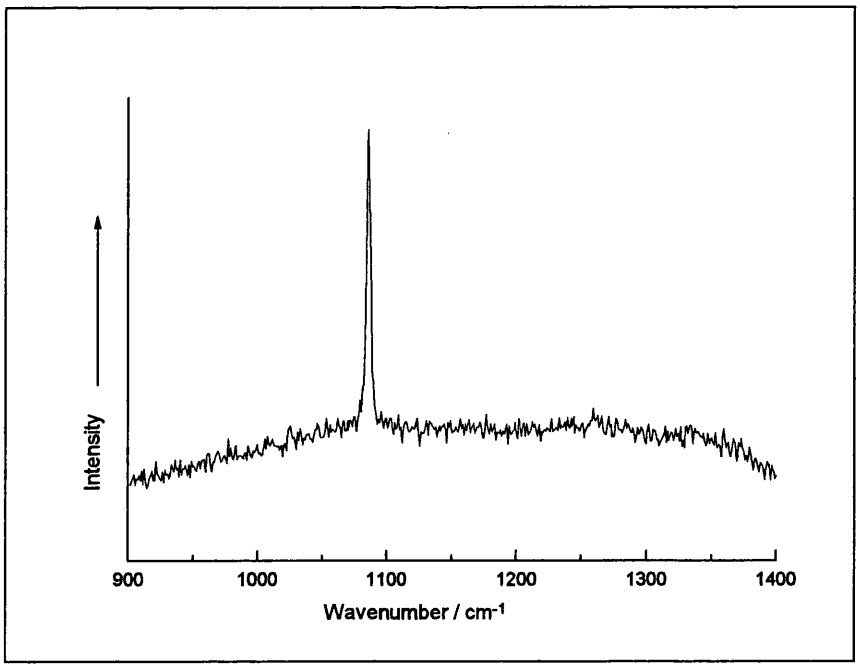

Figure 6.5: The Raman spectrum of chalk from the beige pigment on the saddlecloth on the horse. $\lambda_0 = 632.8$ nm, ~ 0.35 mW.

6.1.4. The substrate

The substrate has the visual appearance of some form of plaster composite. It was found to contain quantities of chalk and silicon-based minerals. (Figure 6.6)

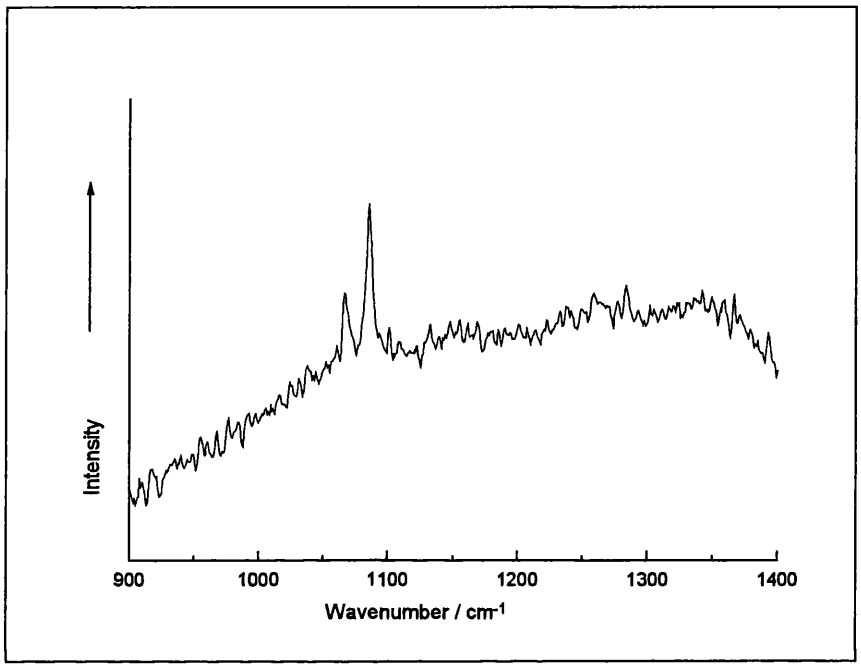

Figure 6.6: The Raman spectra of chalk and silicon-based materials from the substrate of the frescos. $\lambda_0 = 632.8$ nm, ~ 0.35 mW

6.1.5. The green pigment

The green pigment which appears on the clothing of the figure proved to be impossible to identify conclusively. Although it was only used in one area of the fresco, it was used extensively and appears contemporaneous with the other pigments – it is not a retouching of a faded or damaged area.

It had an unusual spectrum, with a considerable number of features, that was not particularly amenable to analysis with visible wavelengths. Using the FT-Raman instrument at 1064 nm a much clearer spectrum was obtained. (Figure 6.7) This is not a spectrum that has been recorded in any of the standard pigment references and so was unknown to us.

Fortunately some synthetic pigments from the early to mid 20th century were being studied at the same time and one of these, Naphthol Green B, was found to bear a strong resemblance to the unknown pigment. (Figure 6.7) Although it is clearly not an identical material, the similarity with the unknown pigment is sufficiently striking to indicate that they come from a closely related family of materials.

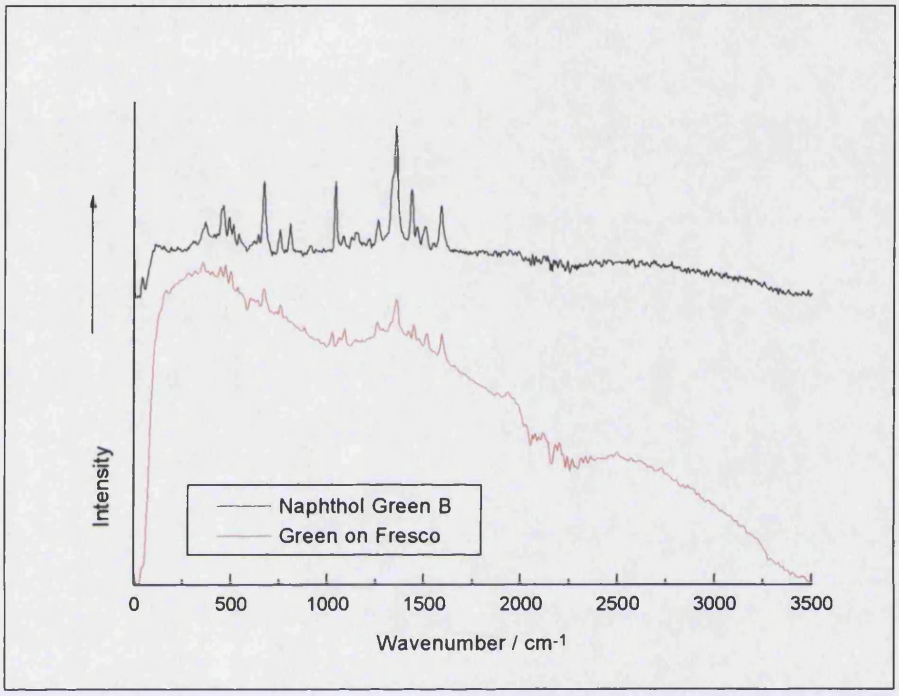

Figure 6.7: The Raman spectra of the unknown green and Naphthol Green B. λ_0 = 1064 nm, ~ 1.00 mW

6.2: Naphthol Green B

Naphthol Green B was patented in 1945. [USPa] It comes from a family of nitroso dyes that were not synthesised until after the work of William Perkin in the 1850s.

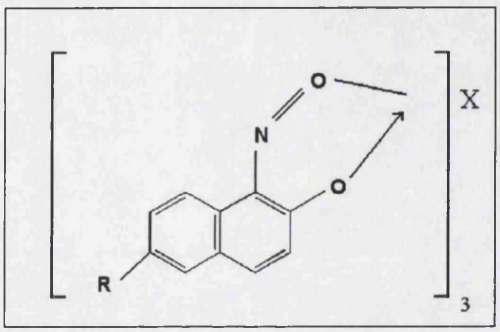

Figure 6.8: A typical nitroso dye structure.

These chelate compounds range in colour from dull green to brown according to their composition: X = Fe(III), Co(III), Cr(III) or Ni(III). Naphthol Green B has X = Fe(III) and R = NaO_3S. [Krah] (Figure 6.8)

6.3: Conclusion

Although the majority of the pigments found on this piece are easily obtained natural materials, as one would expect from a work of this supposed date, the presence of a modern synthetic material raises a number of questions. The green pigment does not have the appearance of a later addition to the piece – it appears to be an integral part of the structure of the work and as such it certainly does not belong on an Assyrian work of art!

The only possible unfortunate conclusion that can be drawn is that the piece is a modern forgery purporting to be a far older, rare work of art. Raman microscopy has been shown to be an excellent technique to enable the definite identification of such material, an aid to the scholar and the collector alike.

Chapter 7: The Vinland Map and the Tartar Relation

Hmm... If I remember my atlas,
We live in a big, purple country.
The Authoritative Calvin and Hobbes,
Bill Watterson,
1990

The Vinland Map and Tartar Relation, held in the Beinecke Rare Book and Manuscript Library of Yale University, are extremely significant documents. They have been at the centre of controversy since they first came to light in 1957. Sometime after 1959, when they were first offered for sale, both were purchased and later given to Yale University by an unknown benefactor who was discovered to be the philanthropist Paul Mellon. Unfortunately, they have no provenance and their whereabouts have been far from certain, even in relatively recent times.

7.1: The Manuscripts

When Vinland Map and the Tartar Relation first came to the attention of modern scholars they were bound together in a modern calf binding, having reputedly come from the collection of a private individual in Europe. [Skel] Now separated, they had clearly not originally been bound in this format as worm holes in the Tartar Relation did not match the position of those in the Vinland Map, as would be expected had the documents been side-by-side at the time of the worm holes' creation. Shortly after their initial discovery, a second manuscript was discovered. This was a part of Vincent of Beauvais' 'Speculum Historiale', a well known historical document of which many copies exist. However, closer examination revealed that the paper was identical to that of the Tartar Relation and worm holes at the front matched those of the Vinland Map, whilst those at the back matched the Tartar Relation. It appears that, for a time at least, this volume of the Speculum Historiale may have bound with the Vinland Map and the Tartar Relation. This implies, perhaps, that the Vinland Map, Tartar Relation and Speculum Historiale share the same provenance although it provides no evidence as to how long the manuscripts were together or the date of the formation of the worm holes.

7.1.1. The Tartar Relation

The Tartar Relation consists of a previously unknown account of the expedition of Friar John de Plano Carpini to the Mongols in 1245 – 47. Three other accounts of this expedition are known, having been issued in 1247. The story also appears in abridged form in the final book of the Speculum Historiale. The Tartar Relation is written in an Upper Rhineland cursive book hand, which dates from the first half of the 15th century – in this particular case a date in the 1440s has been judged most appropriate. It is composed of a single quire of sixteen leaves, of which the outer and inner sheets (1, 8, 9 and 16) are parchment – the rest being paper. The paper itself can also be dated to around 1440 by examination of the watermarks. The manuscript is written in a brown/black ink with rubrication in red.

7.1.2. The Vinland Map

The Vinland Map is a world map on parchment measuring 28 cm by 40 cm, which includes, significantly, representations of Iceland, Greenland and the north-eastern coast of North America ("Vinland"). (Figure 7.1) The map is not in good condition, apparently suffering from considerable pigment loss, which is unsurprising for a manuscript of its postulated age. The parchment is in reasonable condition and clean, with an additional strip of parchment securing the spine and small squares of parchment patching over a number of small holes. The ink lines appear to be composed of two parts, a yellowish line which strongly adheres via absorption to the parchment and an apparently overlaid black line from which >90% of the black pigment appears to have flaked off; indeed in some places the black has been almost entirely lost. (Figure 7.2)

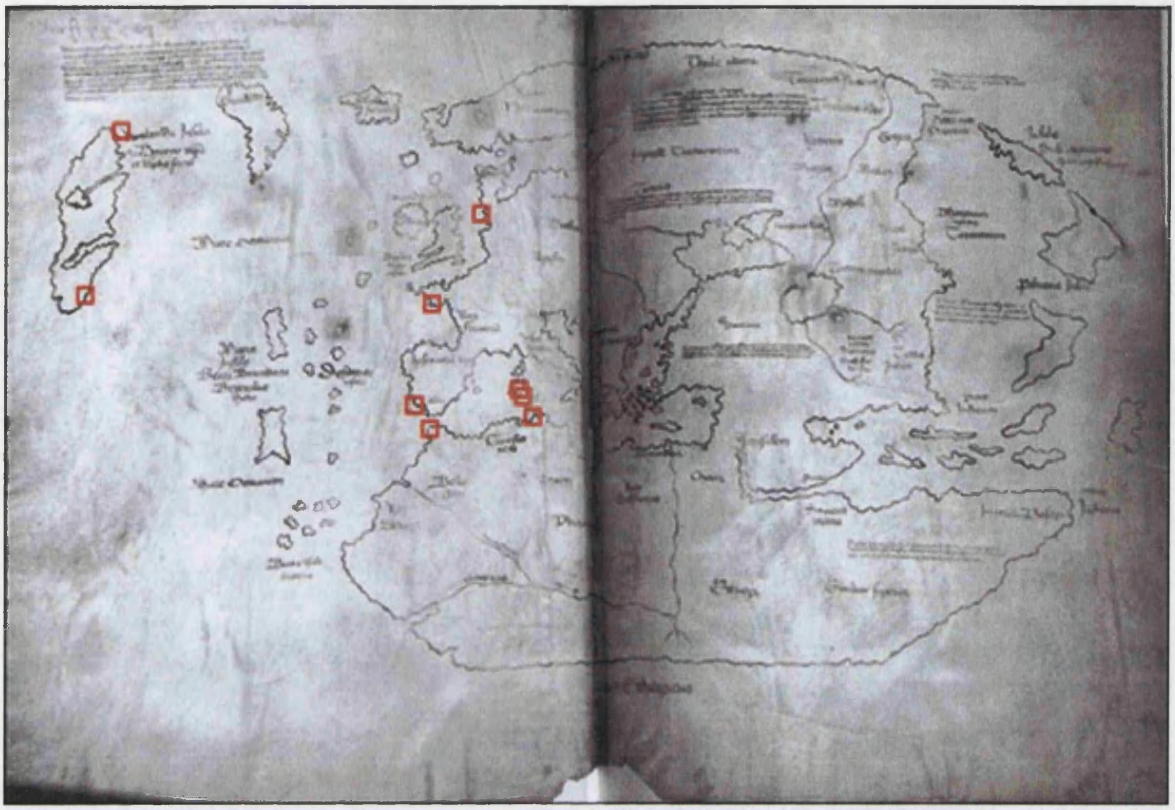

Figure 7.1: The Vinland Map, courtesy of Jim Siebold, Cartographic Images, awww.henry-davis.com/MAPS. The red boxes indicate those areas from which Raman spectra were obtained.

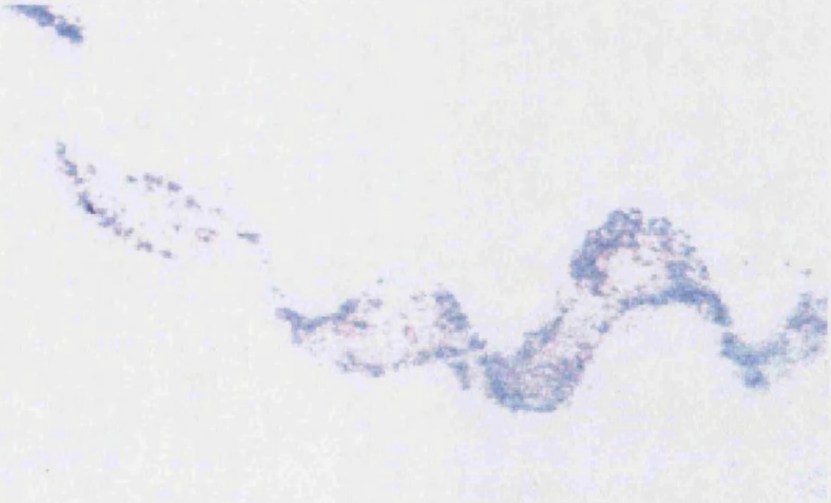

Figure 7.2: Photo-micrograph of the ink on the Vinland Map. Although the quality of this image is poor, the black line and yellow under-layer can clearly be seen.

On 11th October 1965, tactfully the day before Columbus Day, facsimiles and transcriptions of both documents were published. [Skel] These were accompanied by claims, based on cartographical, paleographical and philological analysis, that the

Vinland Map was drawn from two different prototypes and created around 1440, possibly during the great ecclesiastical Council of Basle in Switzerland, thereby predating by some 50 years the discovery of America by Columbus.

It is now well known that the Vikings did indeed reach the new world – evidence of their settlement has been discovered in Newfoundland (L'Anse aux Meadows) and elsewhere. [Ings, Wall] However, the sudden appearance of a manuscript with a clear depiction of part of the north Atlantic seaboard, but no apparent origin or provenance, was destined to cause controversy.

7.2: Previous Studies

Over several years, attempts to verify the suggested origin of the map have been made with the sanction of Yale University. However, their conclusions have not been in agreement with one another. Polarised light microscopy (PLM), micro-X-ray diffraction (XRD) and scanning electron microscopy (SEM)/energy dispersive X-ray analysis (EDX) by McCrone Associates [Mccr, Mcc1, Mcc2] have, in 1974 and 1991, indicated the presence of anatase, the least common form of titanium dioxide found in nature, in the yellow lines. Transmission electron microscopy (TEM) of the anatase on the Vinland Map showed it to be in the form of uniform, well-rounded, single crystals c. 0.1 - 0.3 μm across and with a narrow size distribution, a characteristic of synthetic calcined anatase but not of the mineral; the latter, when ground, form irregular, jagged particles of widely varying dimensions. Since off-white cream-yellow anatase could not be synthesised until c. 1920, and white anatase until c. 1923, McCrone concluded that the implication of this discovery is that the Vinland Map itself must be post c. 1920 (though the parchment may be earlier). Subsequent analyses by Cahill et al. using particle-induced X-ray emission (PIXE), another elemental technique, have also led to the detection of titanium on the map. However, they conclude that (a) the anatase is not confined to the lines on the Vinland Map and (b) titanium (to a maximum of 10 ng cm^{-2}, c. 0.0062% by mass) and other heavy elements are present only in trace amounts in the inks. [Cahi] Cahill et al. therefore concluded that the Vinland Map should be re-evaluated, an opinion they re-affirm in 1995, going so far as to suggest that the sampling method used by McCrone Associates is inherently flawed. [Cah1] However,

the interpretation given to the PIXE results has been robustly challenged by McCrone. [Mcc3]

The results of a small-sample carbon-dating study have recently been published [Dona] but relate only to the age of the parchment not the date of creation of the map, whilst palaeographical studies seem to support or cast doubt on any or all of the proposed dates, being the subject of considerable scholarly disagreement. [Wall, Mcna, Towe]

Various explanations have been put forward for the possible presence of anatase on the map, including accidental environmental contamination from house paints containing titanium dioxide. Olin, as reported by Washburn and Lambert, suggested in the 1970s and reiterated in 2000, that anatase could have been formed during the medieval production of iron-based inks from iron/titanium ores (ilmenite, $FeTiO_3$, being the principal ore of titanium) and incorporated into the ink during the production process. [Wash, Lamb, Olin] However, the procedure outlined is known to yield finely divided, almost amorphous, anatase which is unresolved by PLM and which gives very broad powder diffraction lines by XRD. [Mccr, Mcc1, Mcc2] To convert this material to the form apparently identified on the Vinland Map by McCrone via PLM and TEM would require a calcination step (800 – 1000 °C) unknown in the 15th century.

The black pigment in the ink has also not previously been identified, but several possibilities have been considered including carbon black and iron gallotannate. McNaughton has proposed that a printing ink based upon chromite ($FeCr_2O_4$) was used. [Mcna] This black material must be heated to c. 90 °C in order to be fixed to a substrate; in the absence of such treatment the black fraction may flake off, an apparent explanation of the deterioration of the Vinland Map.

7.3: Analysis of the Documents by Raman Microprobe Spectroscopy

Both the Vinland Map and the Tartar Relation were examined by Raman microprobe spectroscopy. For this study it was unfortunately not possible to gain access to a Raman microscope such as that used in other studies discribed in this thesis. Instead a spectrometer coupled to remote fibre-optic probes, with inherently poorer spatial and spectral resolution and poorer signal/noise ratios, was used. Fibre-optic-based systems have the advantage of permitting the investigation of a greater range of sites on an awkwardly shaped or large object [Cla2] but can suffer from excessive vibration caused by the difficulty in positioning unwieldy, delicate and often surprisingly heavy manuscripts and art objects. For a full description of the instrument used, a Renishaw System 100, see chapter 2.

7.3.1. The analysis of the Vinland Map

A number of areas were selected for analysis. The plain parchment samples were chosen on the basis of their distance from both the inked lines and the edges of the document – coming principally from the centre of the continental land masses or the oceans. Those containing ink were selected on the basis of the visually-assessed density of the pigment – thereby increasing the likelihood of successfully focusing on the ink itself.

Analysis of blank areas of the parchment resulted in essentially featureless Raman spectra. Regions of the Vinland Map which yielded Raman spectra are indicated in figure 7.1. Analysis of the black ink on six areas of the map and its legends gave rise in each case to a poorly defined but nevertheless characteristic Raman spectrum of carbon (figure 7.3), the broad bands attributable to defect and graphitic carbon being evident at ~1325 and ~1580 cm^{-1}. [Bell]

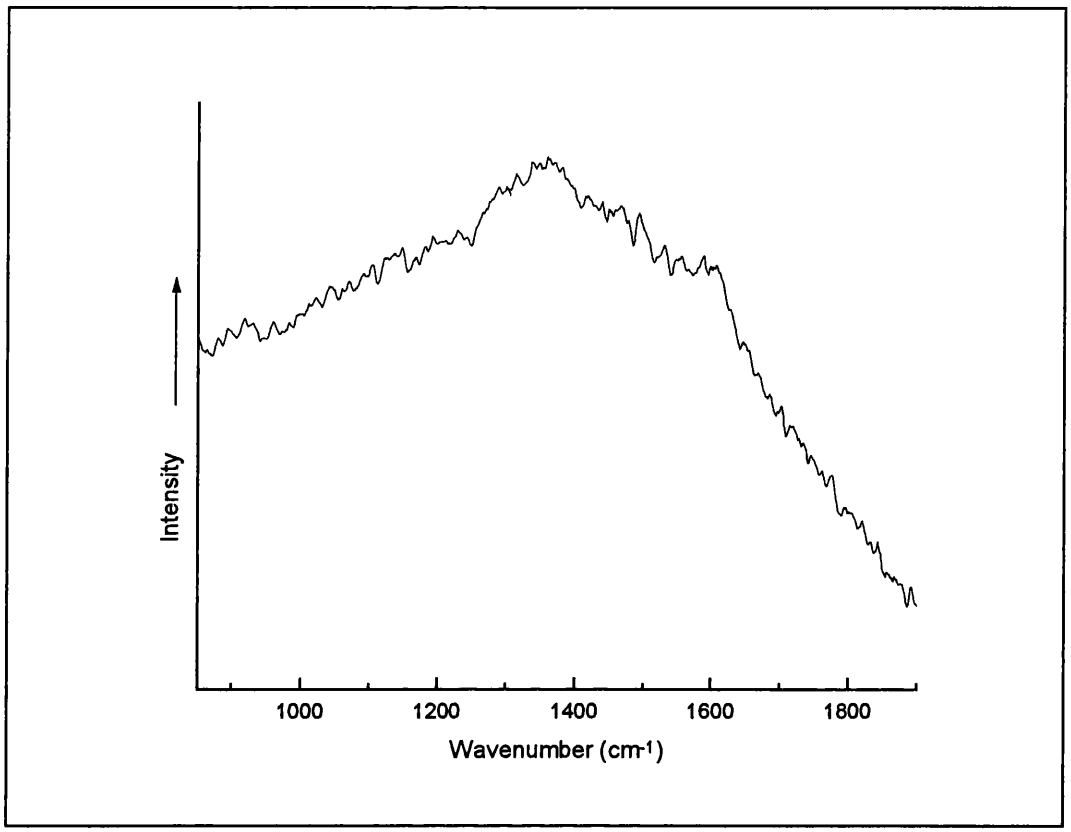

Figure 7.3: The Raman spectrum of carbon, taken from the black ink on the Vinland map.

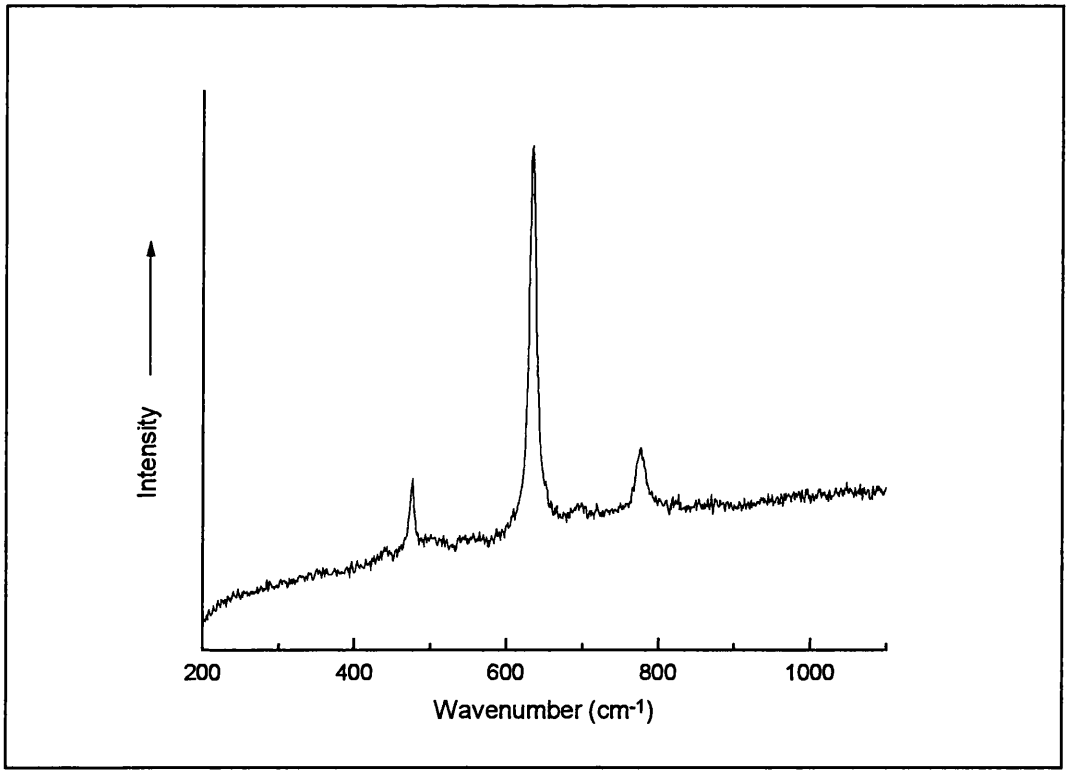

Figure 7.4: The Raman spectrum of Chromite ($FeCr_2O_4$), taken from a reference sample.

Chromite ($FeCr_2O_4$), which is a reasonably good scatterer (figure 7.4), was not detected in any of the lines on the map. Further, no residue of ilmenite, (figure 7.5) which may have been expected from an imprecise medieval recipe for making iron gall ink, was found in the lines on the map.

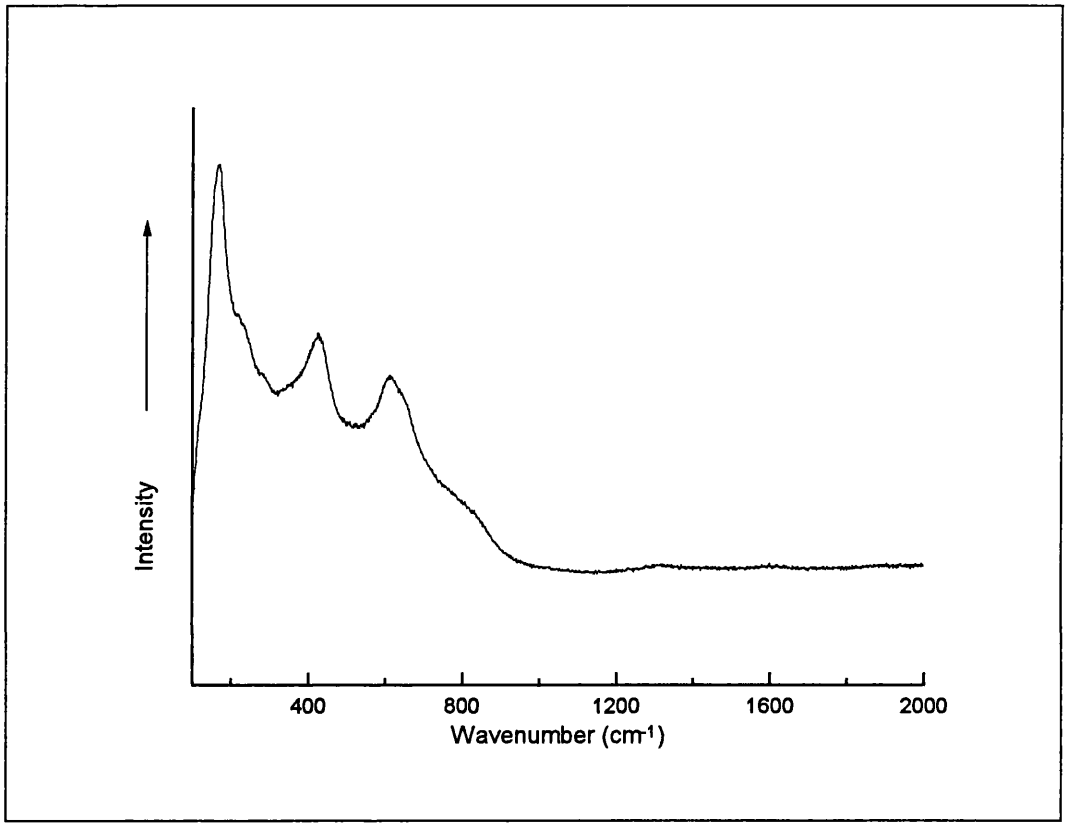

Figure 7.5: The Raman spectrum of Ilmenite ($FeTiO_3$), taken from a reference sample.

Anatase was found to be present in the yellow lines in five areas, traces also being found in places where the black ink coincides with the yellow lines. The most intense band characteristic of anatase (at 143 cm^{-1}) is clearly present despite the proximity of the low wavenumber cut-off of the notch filter assembly of the fibre optic probe. [Burg] The weak broad band which is evident at c. 398 cm^{-1} is also characteristic of anatase (figure 7.6) and, among other features, distinguishes it from rutile, its polymorph.

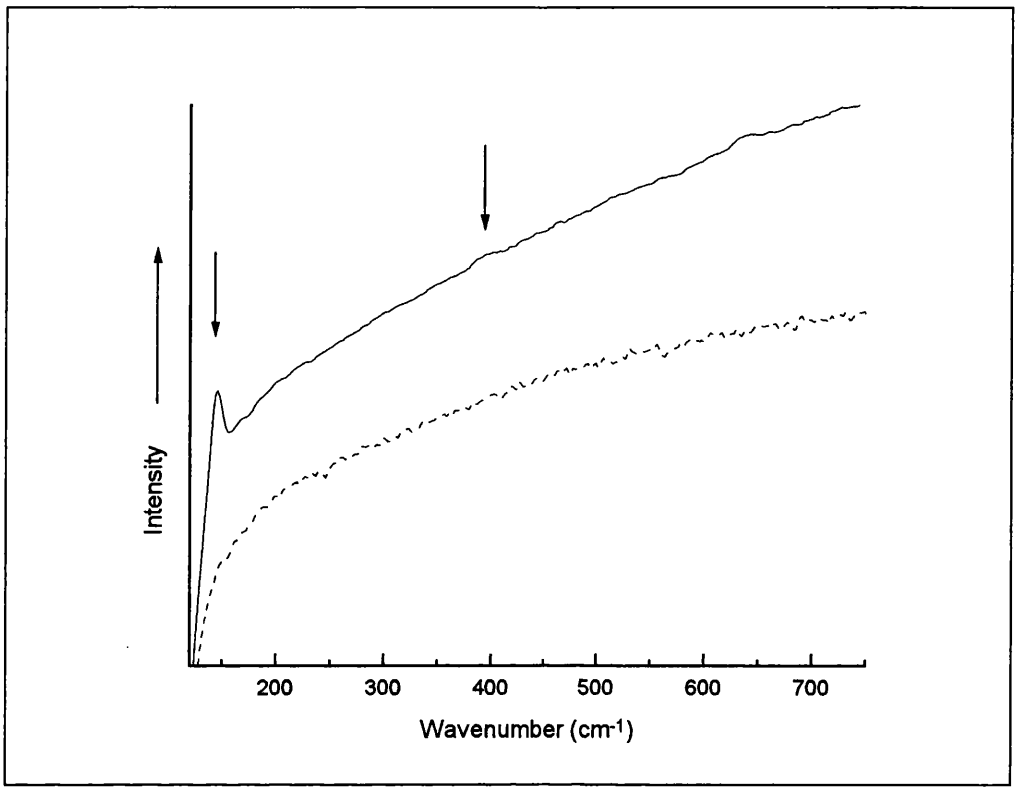

Figure 7.6: Anatase and plain parchment from the Vinland Map; solid line, anatase in yellow line; dotted line, plain parchment.

Spectra taken from the yellow areas were extremely fluorescent, suggestive of the presence of organic materials on the parchment surface, possibly gelatin as proposed by McCrone. [Mcc3]

7.3.2. The analysis of the Tartar Relation

As discussed previously, the Tartar Relation is written in a brown/black ink with a red rubrication. The ink of the rubric was found to be vermilion (figure 7.7), with the three characteristic bands of HgS at 252, 282 and 343 cm^{-1}. [Bell] The black ink gave only a very weak spectrum of carbon, suggestive of its presence in only very small amounts, together with intense fluorescence. This fluorescence may be caused by the presence of a variety of organic materials such as binders but is commonly found as a feature of an iron gallotannate ink.

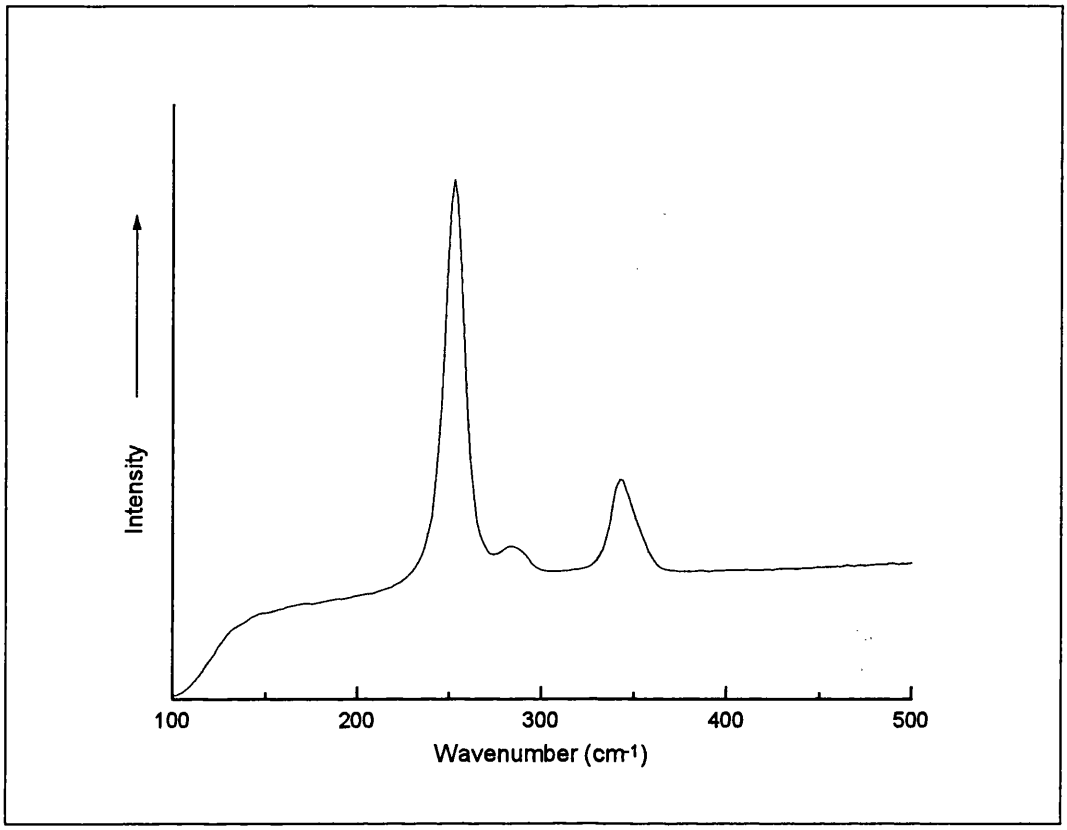

Figure 7.7: The Raman spectrum of vermilion from the rubrication of the Tartar Relation.

7.4: Discussion

The rubrication of the Tartar relation was found to be composed of vermilion which is entirely in keeping with expectation for works of the mid-fifteenth century, the accepted date for this manuscript.

The weakness of the carbon signals in the spectra of the ink on the Tartar Relation shows that the ink contains very little carbon and this observation, along with the fluorescence and the general appearance of the ink (brown-black), is suggestive of an ink which is essentially composed of iron gallotannate. The black ink on the Vinland Map, however, is not of the same composition as it is carbon based. This would seem to suggest that the two documents were not produced by the same hand in the same time frame.

Olin's suggestion of ilmenite as a source for the production of anatase would, moreover, appear to be irrelevant since the dominant pigment in the black ink on the Vinland Map is here identified to be carbon rather than iron gallotannate, ilmenite or chromite.

Anatase was identified in the yellow lines and, in some cases, in the vicinity of the black ink, presumably from the underlying yellow line. It was not found elsewhere on the surface, as would be expected if its presence were to be attributed to outside contamination from, for example, dust from white ceiling paint, which may contain detectable quantities of anatase. This strongly indicates that anatase was a deliberate component, with organic binders in the yellow lines. Anatase is comparatively rare and is the least abundant of the three polymorphs of titanium dioxide (anatase, brookite and rutile) which are present in the earth's crust. [Trea] When found in nature, it is usually as black or dark grey tetragonal crystals, less often as brown or indigo crystals, and very rarely as yellow crystals. It is important to emphasise that anatase was detected solely in the ink lines and not elsewhere on the parchment, i.e. it is not uniformly distributed over the surface of the map and so must be an integral part of the yellow line. Moreover, the results relate to material at the surface only and not to that within the body of the parchment, since the laser beam is unlikely to penetrate more than c. 1 μm.

It is generally accepted that, prior to the development of the printing press, manuscripts were written in either carbon-based or iron gallotannate inks. A common means of differentiating between them is the erosion of the parchment or paper substrate by iron ions leeching from the iron gallotannate inks. This causes considerable discolouration and embrittlement of both paper and parchment, often leading to brown or yellow staining and, sometimes, considerable loss of the fabric of the manuscript. This trait is not evident in manuscripts produced with carbon-based inks, which are inherently more stable than iron gallotannates. Had the Vinland Map been drawn in a medieval iron gallotannate ink, a yellowing at the borders of the ink such as that seen on the map might have been expected. Knowing that such yellowing is a common feature of medieval manuscripts, a clever forger may seek to simulate the degradation by the inclusion of a yellow line in his rendering of the map. However, it has been shown that (a) the black ink on the Vinland Map is carbon-based making the natural occurrence of such a feature impossible and (b) that the Vinland Map shows no evidence of embrittlement of the parchment or associated parchment loss. Furthermore the presence

of anatase in a genuine medieval ink is extremely unlikely and has not been detected on any other such manuscript examined by Raman spectroscopy. It seems that the appearance of yellow borders to the black ink on the Vinland Map is only possible if the Vinland Map had been produced by laying down on the parchment first a yellow line, followed by the black ink. The presence in this yellow line of quantities of anatase indicates that the Vinland Map is a 20th century product.

7.5: Conclusions

The inks used for the construction of the Tartar Relation are entirely appropriate for the date assigned to it. However, one of those used to draw the Vinland Map is not. The presence of a yellow line containing anatase, closely associated with a stable carbon ink, strongly suggests that the Vinland Map is a modern forgery.

Chapter 8: Density Functional Theory

The good thing about a spear is that almost everybody could understand it. It had basically one feature: the pointy end. Our brains were fully equipped for this level of complexity.
The Dilbert Principle
Scott Adams
1996

The calculations of molecular geometries, energies and vibrations have been conducted using the Amsterdam Density Functional (ADF) expression of Density Functional Theory. The central principle of Density Functional Theory (DFT) is the absolute reliance of the ground-state electronic energy on the ground-state electron density. This is embodied in the equations of Hohenberg and Kohn. [Hohe, Jens]

8.1: The Hohenberg-Kohn Theorems

The fundamental theorems of Hohenberg and Kohn [Hohe] are central to DFT but are, in essence, relatively simple. The ground state charge density ρ is sufficient to describe the ground state properties of the system. Further, for any trial charge density ρ_{trial}, $E_0 \leq E[\rho_{trial}]$.

The electron density is calculated from the square of the wave function, found by solving the Schrödinger equation integrated over N-1 electron coordinates. The electron Hamiltonian for an M nuclei, N electron system is given by

$$\hat{H} = -\sum_{i=1}^{N}\frac{1}{2}\nabla_i^2 - \sum_{i=1}^{N}\sum_{A=1}^{M}\frac{Z_A}{|\boldsymbol{R}_A - \boldsymbol{r}_i|} + \sum_{i=1}^{N}\sum_{j>1}^{N}\frac{1}{|\boldsymbol{r}_i - \boldsymbol{r}_j|} + \sum_{A=1}^{M}\sum_{B=A}^{M}\frac{Z_A Z_B}{|\boldsymbol{R}_A - \boldsymbol{R}_B|} \qquad (8.1)$$

Under the Born-Oppenheimer approximation the last term is constant. The Hamiltonian is determined by the number of electrons and the potential created by the nuclei. Thus the ground state wave function and energy are also determined by these quantities.

If the existence of two different external potentials V_{ext} and V'_{ext}, that produce the same electron density ρ, is assumed then the existence of two different Hamiltonians $\hat{H}$ and $\hat{H}'$ is implicit. These Hamiltonians have corresponding different lowest energy wave

functions, Ψ and Ψ' respectively. If Ψ' is considered an approximate wave function for $\hat{H}$ and the variational principle applied (which simply states that the expectation value of the energy derived from an approximate wavefunction will be an upper bound to the true value pertaining to the accurate wavefunction) then

$$\left\langle \Psi' \middle| \hat{H} \middle| \Psi' \right\rangle > E_0 \tag{8.2}$$

$$\left\langle \Psi' \middle| \hat{H}' \middle| \Psi' \right\rangle + \left\langle \Psi' \middle| \hat{H} - \hat{H}' \middle| \Psi' \right\rangle > E_0 \tag{8.3}$$

$$E_0' + \left\langle \Psi' \middle| V_{ext} - V_{ext}' \middle| \Psi' \right\rangle > E_0 \tag{8.4}$$

$$E_0' + \int \rho(\boldsymbol{r})(V_{ext} - V_{ext}')d\boldsymbol{r} > E_0 \tag{8.5}$$

Considering Ψ an approximate wave function for $\hat{H}$' yields

$$E_0 - \int \rho(\boldsymbol{r})(V_{ext} - V_{ext}')d\boldsymbol{r} > E_0' \tag{8.6}$$

Combining the two final equations (8.5 and 8.6) yields

$$E_0' + E_0 > E_0' + E_0 \tag{8.7}$$

thereby demonstrating that the initial assumption, of the existence of two potentials that produce the same electron density, is incorrect. The electron density and the nuclear potential are exclusively related, hence so are the Hamiltonian and the energy.

This allows the Schrödinger equation to be rewritten in terms of the functionals of the charge density, giving

$$E[\rho] = T[\rho] + V_{ee}[\rho] + V_{ne}[\rho] \tag{8.8}$$

where T is the kinetic energy, V_{ee} the electron-electron repulsion energy and V_{ne} the nucleus-electron attraction energy.

If the variational principle is applied to the electron density, given an approximate electron density ρ' which integrates to the number of electrons, N,

$$\int \rho'(\boldsymbol{r})d\boldsymbol{r} = N \tag{8.9}$$

then the energy given by this density sets an upper limit on the exact ground state energy provided that the exact functional is used

$$E_0[\rho'] \geq E_0[\rho] \tag{8.10}$$

However, the form of the functional connecting the electron density and the exact ground state energy is not known. DFT attempts to produce functionals that accurately connect these two quantities.

8.2: The Kohn-Sham Equation

The largest contribution to the evaluation of the ground state energy is the determination of the kinetic energy term in the energy expansion (eq. 8.8). Kohn and Sham [Kohn] realised that if an explicit functional to determine the kinetic energy could not be found, a large part of it could still be calculated accurately, leaving a small remainder to be approximated combined with the non-classical electron exchange and correlation energies.

An arbitrary electronic system experiences an external potential $v(\boldsymbol{r})$. The same external potential is applied to a fictitious state of non-interacting electrons, described by a single determinantal wavefunction

$$\Psi_{\text{non-int}} = \frac{1}{\sqrt{n!}}\left|\phi_1\phi_2\ldots\phi_n\right| \tag{8.11}$$

where ϕ_i are the n lowest eigenstates of the one-electron Hamiltonian

$$\hat{h}_{\text{non-int}}\phi_i = \left(-\frac{1}{2}\nabla^2 + v(\boldsymbol{r})\right)\phi_i = \varepsilon_i\phi_i \tag{8.12}$$

If the electron system is an atom or a molecule then there are n ϕ_i one electron spin-orbitals, giving a charge density of

$$\rho(\boldsymbol{r}) = \sum_i^n \left|\phi_i(\boldsymbol{r})\right|^2 \tag{8.13}$$

The kinetic energy of the non-interacting system is given by

$$T_{\text{non-int}} = \left\langle \Psi_{\text{non-int}} \left| \sum_i^n \left(-\frac{1}{2}\nabla_i^2\right) \right| \Psi_{\text{non-int}} \right\rangle = \sum_i^n \left\langle \phi_i \left| -\frac{1}{2}\nabla^2 \right| \phi_i \right\rangle \tag{8.14}$$

Although $T_{\text{non-int}}[\rho]$ is not the same as the kinetic energy of the interacting system, Kohn and Sham realised that the non-interacting system of electrons is equivalent to a real system experiencing a modified external potential. $T_{\text{non-int}}[\rho]$ is the kinetic energy of such a real system of interacting electrons.

The energy of the interacting system can be written

$$E[\rho] = T_{\text{non-int}}[\rho] + J[\rho] + V_{\text{ne}}[\rho] + E_{\text{xc}}[\rho] \tag{8.15}$$

where J is the classical Coulomb energy and E_{xc} is the exchange-correlation energy, given as V_{ee} in equation 8.8.

The exchange-correlation energy is given by

$$E_{xc}[\rho] = (T[\rho] - T_{non\text{-}int}[\rho]) + (V_{ee}[\rho] - J[\rho]) \tag{8.16}$$

However, this definition includes terms that are not easily evaluated. It contains electron exchange and correlation, and a portion of the kinetic energy of the system – the difference between the non-interacting energy of the reference system and the real energy of the interacting electrons. Various forms of E_{xc} will be discussed below.

The electronic energy of the non-interacting system is given by

$$E_{non\text{-}int}[\rho] = T_{non\text{-}int}[\rho] + V_{ne}[\rho] \tag{8.17}$$

where V_{ne} is the nucleus-electron attraction energy for a given charge density and nuclear potential field

$$V_{ne} = \int \rho(\boldsymbol{r}) v(\boldsymbol{r}) d\boldsymbol{r} \tag{8.18}$$

Combining the previous two equations gives

$$E_{non\text{-}int}[\rho] = T_{non\text{-}int}[\rho] + \int \rho(\boldsymbol{r}) v(\boldsymbol{r}) d\boldsymbol{r} \tag{8.19}$$

The total energy for the non-interacting system of electrons depends on the charge density which can be found by solving the one-electron Hamiltonian (eq. 8.12) and substituting for ϕ_i into the charge density equation (8.13).

The total electronic energy of the real system of electrons is given by the substitution of the nucleus-electron attraction energy into the total energy

$$E[\rho] = T_{non\text{-}int}[\rho] + J[\rho] + E_{xc} + \int \rho(\boldsymbol{r}) v(\boldsymbol{r}) d\boldsymbol{r} \tag{8.20}$$

The charge density for this system can be found using the Kohn-Sham effective potential, the modified external field, v_{eff} to replace $v(\boldsymbol{r})$ in the one-electron eigenvalue equation

$$\hat{h}\phi_i = \left(-\frac{1}{2}\nabla^2 + v_{eff}(\boldsymbol{r})\right)\phi_i = \varepsilon_i \phi_i \tag{8.21}$$

where v_{eff} is given by

$$v_{\text{eff}}(\boldsymbol{r}) = v(\boldsymbol{r}) + \int \frac{\rho(\boldsymbol{r}')}{|\boldsymbol{r} - \boldsymbol{r}'|} d\boldsymbol{r}' + v_{\text{xc}}(\boldsymbol{r}) \tag{8.22}$$

in which v_{xc} is called the exchange-correlation potential and is defined as

$$v_{\text{xc}}(\boldsymbol{r}) = \frac{\delta E_{\text{xc}}[\rho]}{\delta \rho(\boldsymbol{r})} \tag{8.23}$$

Combining the effective potential with the kinetic energy gives the one-electron Kohn-Sham equation

$$\left(-\frac{1}{2}\nabla^2 + v(\boldsymbol{r}) + \int \frac{\rho(\boldsymbol{r}')}{|\boldsymbol{r} - \boldsymbol{r}'|} + v_{\text{xc}}(\boldsymbol{r}) \right) \phi_i = \varepsilon \phi_i \tag{8.24}$$

The form of the exchange-correlation potential is the principal difference between various DFT methods. Given the exact form of the potential, the Kohn-Sham equation is rigorously correct and determines the exact charge distribution and wavefunction.

8.3: Local Density and Local Spin Density Approximations

The origins of DFT lie some time in advance of the work of Hohenberg and Kohn, in earlier efforts by Thomas, Fermi and Dirac to use the electron density to describe the properties of atomic and molecular systems. [Koch]

The Thomas-Fermi model considers only the kinetic energy of the electrons, treating the nuclear-electron and electron-electron interactions entirely classically. They use a simple expression for the kinetic energy based on the constant density uniform electron gas

$$T[\rho(\boldsymbol{r})] = \frac{3}{10}(3\pi^2)^{2/3} \int \rho^{5/3}(\boldsymbol{r}) d\boldsymbol{r} \tag{8.25}$$

Combined with the classical expressions for the potentials this gives the Thomas-Fermi expression for the energy of the atom

$$E[\rho(\boldsymbol{r})] = \frac{3}{10}(3\pi^2)^{2/3} \int \rho^{5/3}(\boldsymbol{r}) d\boldsymbol{r} + \int \rho(\boldsymbol{r}) v(\boldsymbol{r}) + J[\rho] \tag{8.26}$$

The energy given by this equation is entirely in terms of the electron density and so it is a genuine density functional. However, it completely neglects exchange and correlation effects and so is only of limited use. The introduction of an exchange term,

$$E_x[\rho] = -C_x \int \rho^{4/3}(\boldsymbol{r})\mathrm{d}\boldsymbol{r} \tag{8.27}$$

where

$$C_x = \frac{3}{4}\left(\frac{3}{\pi}\right)^{\frac{1}{3}} \tag{8.28}$$

first derived by Block but associated with Dirac, [Jens] improved the accuracy of the Thomas-Fermi-Dirac model. However, neither the Thomas-Fermi nor the Thomas-Fermi-Dirac models predict bonding, effectively precluding its existence.

Both of these models assume that the density locally can be treated as a slowly varying function – the Local Density Approximation (LDA). The difference between these different DFT methods lies in the way in which the exchange term is treated. The Thomas-Fermi method ignores it completely, the Thomas-Fermi-Dirac model treats it very simply. The Local Spin Density Approximation (LSDA) allows the spin of the electrons to be considered which is particularly important in open shell systems and in the presence of magnetic fields. Here the α and β electron densities are not equal, so the electron density becomes

$$\rho(\boldsymbol{r}) = \rho_\alpha(\boldsymbol{r}) + \rho_\beta(\boldsymbol{r}) \tag{8.29}$$

and the exchange energy becomes

$$E_x^{\mathrm{LSDA}}[\rho] = -2^{1/3} C_x \int \left[\rho_\alpha^{4/3} + \rho_\beta^{4/3}\right]\mathrm{d}\boldsymbol{r} \tag{8.30}$$

8.4: Correlation Energy

In general the exchange and correlation parts of the exchange-correlation energy are treated separately. The correlation energy of a uniform electron gas has been calculated for a number of different densities by Monte Carlo methods. [Jens] Analytic interpolation formula, such as that of Vosko, Wilk and Nusair [Vosk] and Perdew and

Wang, [Perd] have been developed to allow the use of Monte Carlo results in DFT calculations. These interpolate between unpolarised and spin polarised limits.

However, the LSDA underestimates the exchange energy by ~10%, an error which is larger than the entire correlation energy. In addition electron correlation is over estimated by a factor ~2, leading to over-binding as bond strengths are over-estimated. [Jens]

8.5: Gradient Corrected Methods

The accuracy of L(S)DA methods alone is insufficient for some chemical applications – particularly the calculation of energies. A significant improvement was brought in the 1980s by extensions to the local approximation that considered the gradient of the electron density. [Koch] This allows the inhomogeneity of the electron density to be taken into account – the LDA becomes the first term of a Taylor expansion of the uniform density and better approximations of the exchange-correlation functional are arrived at through consideration of the next lowest terms of the series

$$E_{xc}^{GEA}[\rho_\alpha,\rho_\beta]=\int \rho\varepsilon_{xc}(\rho_\alpha,\rho_\beta)d\boldsymbol{r}+\sum_{\sigma,\sigma'}\int C_{xc}^{\sigma,\sigma'}(\rho_\alpha,\rho_\beta)\frac{\nabla\rho_\sigma}{\rho_\sigma^{4/3}}\frac{\nabla\rho_{\sigma'}}{\rho_{\sigma'}^{4/3}}d\boldsymbol{r}+.... \quad (8.31)$$

where E_{xc}^{GEA} is the gradient expansion approximation energy functional for exchange-correlation, ε_{xc} is the exchange-correlation energy of the uniform electron gas and σ, σ' represent α or β spin.

It applies to systems where the density is not uniform but slowly varying. However although more developed theoretically, in general it does not improve the accuracy of calculations of real molecules, resulting in the development of alternative gradient corrections collectively known as generalised gradient approximations (GGA) and generally written

$$E_{xc}^{GGA}[\rho_\alpha,\rho_\beta]=\int f(\rho_\alpha,\rho_\beta,\nabla\rho_\alpha,\nabla\rho_\beta)d\boldsymbol{r} \quad (8.32)$$

In general, E_{xc}^{GGA} is split into exchange and correlation contributions and approximations for the two terms are sought separately from a combination of theoretical and semi-empirical techniques.

8.6: Amsterdam Density Functional

The density functional calculations were performed with versions 2.3, 1999.02 and 2000.02 of the Fortran based program Amsterdam Density Functional (ADF).[1] Among other capabilities it facilitates the calculation of energies, optimised geometries and vibrational frequencies.

ADF uses a fragmentary approach – basic atoms with the required properties are calculated and used to construct molecular orbitals. The basic atoms are spherically symmetric and spin restricted; they do not constitute a particularly good model of a real atom as they are designed to be computationally convenient.

8.6.1. Basis sets

ADF uses Slater Type Orbitals (STOs) as basis functions to construct the basic atoms. [Slat, Jens] These have the form

$$\chi_{\varsigma,n,l,m}(r,\theta,\varphi) = NY_{l,m}(\theta,\varphi)r^{n-1}e^{-\varsigma r} \tag{8.33}$$

where N is a normalisation constant, $Y_{l,m}$ are the spherical harmonic functions and ς is the orbital exponent given by

$$\varsigma = \frac{(Z-s)}{n} \tag{8.34}$$

where Z is the atomic number, n is the orbital's principal quantum number and s is a screening constant.

As STOs do not have any radial nodes, nodes in the radial part of the orbital are constructed from linear combinations of STOs. However, they do demonstrate the appropriate cusp at the nucleus and fall-off behaviour with increasing distance from the nucleus.

The minimum basis set contains only sufficient functions to contain all the electrons of the neutral atom. This is a single s-function for hydrogen and helium, two s-functions

[1] ADF is licensed by Scientific Computing and Modelling NV, who request the inclusion of the following references: [teVe, ADF]

(1s and 2s) and one p-function ($2p_x$, $2p_y$ and $2p_z$) for the first row of the periodic table. For second row atoms three s-functions (1s, 2s and 3s) and two sets of p-functions (2p and 3p) are required.

Double zeta (DZ) type basis sets have double the number of basis functions; first row elements would now have four s-functions (1s, 1s', 2s and 2s') and two p-functions (2p and 2p'). This allows different exponents to be applied to each set of p-orbitals, for example, describing the differences in the electron distribution in different directions more accurately. However, since only the valence orbitals are involved in bonding, only these orbitals need to be expanded, producing a split valence basis.

This extension of the angular momentum functions can be expanded into triple, quadruple and further basis sets. However, the addition of higher angular momentum functions than that of the valence electrons, polarisation functions, is also important to describe the difference between the electron distribution along and perpendicular to a bond, for example. So p-orbitals may be used to polarise s-orbitals, d-orbitals to polarise p-orbitals, f-orbitals for d-orbitals and so forth.

ADF 2.3 – 2000.02 uses a choice of five different basis sets:

Type I: Single zeta, without polarisation.

Type II: Double zeta, without polarisation, triple zeta for the 3d shells of the first row transition metals, 4f shells of the Lanthinides and 5f of the Actinides.

Type III: As Type II, but with a polarisation function up to Ar and for the 4p series Ga to Kr.

Type IV: Triple zeta, with a polarisation function up to Ar and for Ga to Kr.

Type V: Triple zeta, with two polarisation functions to Ar.

Increasing complexity of the basis sets should lead to a more accurate representation of the system in question. However, the increased basis set complexity necessitates an increased computational effort.

8.6.2. Frozen cores

The use of split valence basis sets allows the non-valence electron core of an atom to be 'frozen' so that these electrons are not directly involved in the calculations of the electron density. In heavier elements this can make a significant difference to the size of the calculation since the computational load increases as approximately the third power of the number electrons. [Jens, teVe]

The frozen core orbitals in ADF are solutions of a large-basis all-electron calculation on the isolated atom, which are expressed as an auxiliary set of STOs, distinct from the valence set.

8.6.3. Relativistic effects

Since the electrons in heavy elements are moving at an appreciable fraction of the speed of light, relativistic effects must be taken into account in calculations concerning elements from approximately the fifth period of the periodic table onwards.

This leads to two effects – spin-orbit coupling and the modification of the electronic wavefunctions and energies. The latter can be split into an orbital contraction and an indirect orbital expansion. The orbital contraction has two contributory parts: the relativistic modification of the orbital itself and the change in the nature of the Hamiltonian in transferring from the non-relativistic to the relativistic picture. [Bae1]

Contrary to popular argument, Baerends et al. demonstrated that the orthogonalisation of valence orbitals on the contracted inner core orbitals leads, in fact, to an expansion of these valence orbitals. However, the relativistic modification of the Hamiltonian causes the admixing of higher bound and, especially, continuum orbitals leads to an overall orbital contraction.

The increased screening of the nuclear charge that results from the contraction of the outer core s and p electrons allows an expansion of the valence d and f orbitals of similar radial distribution.

ADF uses the Dirac equation

$$\left[c\boldsymbol{\alpha}\cdot\hat{\mathrm{p}}+\beta mc^2\right]\Psi = i\frac{\partial\Psi}{\partial t} \tag{8.35}$$

where $\boldsymbol{\alpha}$ and β are 4 x 4 matrices and $\hat{\mathrm{p}}$ is the momentum operator, to compute relativistic frozen core potentials and densities. The Dirac equation treats time and space to the same differential order – a requirement of special relativity that is not met by Schrödinger's equation. ADF computes a fully relativistic atom, with spin-orbit coupling and double group symmetries, using a fully relativistic Hamiltonian. The resulting relativistic core potentials can be utilised in the zero order regular approximation (ZORA),[2] considering only Darwin (due to the electron making a high-frequency oscillation around its mean position) and mass-velocity (due to dependence of electron mass on velocity) corrections [Jens] or with spin-orbit coupling added.

ZORA is an expansion of the Dirac equation in terms of

$$\frac{E}{\left(2mc^2-\mathrm{V}\right)} \tag{8.36}$$

resulting in the ZORA Hamiltonian

$$\begin{aligned}\hat{\mathrm{H}}_{\mathrm{ZORA}} &= (\sigma\cdot\hat{\mathrm{p}})\frac{c^2}{2mc^2-\mathrm{V}}(\sigma\cdot\hat{\mathrm{p}})+\mathrm{V}\\ &= \sum_{\mathrm{i}} p_{\mathrm{i}}\frac{c^2}{2mc^2-\mathrm{V}}p_{\mathrm{i}}+\frac{mc^2}{\left(2mc^2-V\right)^2}\sigma\cdot(\nabla V\times\hat{\mathrm{p}})+V\end{aligned} \tag{8.37}$$

where σ are Pauli spin matrices, which gives a more accurate description of relativistic effects than the Pauli formulism, which suffers, counter-intuitively, from variational collapse on expansion of the basis set and restriction of the frozen core. [teVe]

8.6.4. Mulliken population analysis

The principal result of DFT calculations is the electronic wavefunctions and their associated energy. However, various other properties may be derived. Amongst these is the assignment of the electrons to various molecular orbitals and their charge to particular atoms. One method of accomplishing this in ADF is to use Mulliken population analysis. [Jens, Mull]

[2] SCM request the inclusion of the following references [vanL, van1, van2].

The electron density at a position $\boldsymbol{r}$, of a single molecular orbital containing one electron is the square of the molecular orbital

$$\rho_{\mathrm{i}}(\boldsymbol{r}) = \phi_{\mathrm{i}}^2(\boldsymbol{r}) \tag{8.38}$$

If the molecular orbital (MO) is expanded as a set of normalised, non-orthogonal basis functions, this is written

$$\begin{aligned} \phi_{\mathrm{i}} &= \sum_{\alpha}^{\mathrm{AO}} c_{\alpha\mathrm{i}}\chi_{\alpha} \\ \phi_{\mathrm{i}}^2 &= \sum_{\alpha\beta}^{\mathrm{AO}} c_{\alpha\mathrm{i}}c_{\beta\mathrm{i}}\chi_{\alpha}\chi_{\beta} \end{aligned} \tag{8.39}$$

The total number of electrons N may be obtained by integrating and summing over all occupied MOs

$$\mathrm{N} = \sum_{i}^{\mathrm{MO}} \int \phi_{\mathrm{i}}^2 \mathrm{d}\boldsymbol{r} = \sum_{\mathrm{i}}^{\mathrm{MO}} \sum_{\alpha\beta}^{\mathrm{AO}} c_{\alpha\mathrm{i}}c_{\beta\mathrm{i}} \int \chi_{\alpha}\chi_{\beta}\mathrm{d}\boldsymbol{r} = \sum_{\mathrm{i}}^{\mathrm{MO}} \sum_{\alpha\beta}^{\mathrm{AO}} c_{\alpha\mathrm{i}}c_{\beta\mathrm{i}}S_{\alpha\beta} \tag{8.40}$$

where an AO is an atomic orbital. This may be generalised by the introduction of an occupation number, n, for each MO. This is either 0, 1 or 2 for a single determinant wavefunction, or fractional for a correlated wavefunction. N is then represented by

$$\mathrm{N} = \sum_{\mathrm{i}}^{\mathrm{MO}} \mathrm{n}_{\mathrm{i}} \int \phi_{\mathrm{i}}^2 \mathrm{d}\boldsymbol{r} = \sum_{\alpha\beta}^{\mathrm{AO}} \left(\sum_{\mathrm{i}}^{\mathrm{MO}} n_{\mathrm{i}}c_{\alpha\mathrm{i}}c_{\beta\mathrm{i}} \right) S_{\alpha\beta} = \sum_{\alpha\beta}^{\mathrm{AO}} D_{\alpha\beta}S_{\alpha\beta} \tag{8.41}$$

where S is the overlap matrix and the density matrix D is the sum of the product of the MO coefficients and the occupation numbers.

Mulliken population analysis uses this DS matrix to distribute electrons into atomic contributions. The diagonal elements are the number of electrons in the AO, the off-diagonal elements are half the number of electrons shared by AOs. The contributions from the various AOs to an atom A may be summed to give the number of electrons associated with that atom. The contributions from basis functions on different atoms can be divided in a number of ways. The Mulliken method divides the contribution equally between the atoms involved.

The Mulliken electron population is defined as

$$\rho_{\mathrm{A}} = \sum_{\alpha\varepsilon\mathrm{A}}^{\mathrm{AO}} \sum_{\beta}^{\mathrm{AO}} D_{\alpha\beta}S_{\alpha\beta} \tag{8.42}$$

with the gross charge on the atom a sum of the nuclear and electronic contributions

$$Q_A = Z_A - \rho_A \tag{8.43}$$

8.6.5. Vibrational frequencies

ADF may also be used to calculate the vibrational frequencies of a geometry optimised molecule.[3] This is accomplished by numerical differentiation of energy gradients in slightly displaced geometries. Comparison of the computed gradients allows force constants and hence frequencies to be calculated.

The absence of imaginary frequencies is indicative of true energy minima, rather than transition state structures.

8.6.7. Application of ADF

The ADF calculations were conducted on an IBM RS/6000 43P workstation, on UCL's "Plato", a SUN Ultra Enterprise 3000, and on the Royal Institution's "Strutt" Cluster of four Compaq ES40 machines, each with four EV68 processors. A number of different versions of the code were used, from ADF 2.3 to ADF 2000.02. However these differ only by the inclusion of additional features in each successive version.

[3] SCM request the following references be mentioned [Fan, Fan1]

Chapter 9: The Structures and Isomerization of Tetra-Arsenic Tetra-Sulfide

We should have shotguns for this.

Vincent Vega
Pulp Fiction
1994

The use of realgar (As_4S_4) as a pigment has long been recognised. [Fitz] It has also been noted that realgar undergoes an apparently light-induced transformation from red-orange to yellow – display samples in geological collections being particularly at risk. Until relatively recently it was erroneously believed that the result of this decay was orpiment, As_2S_3. However, studies have revealed the existence of another polymorph of As_4S_4, called pararealgar. [Doug] This has since been identified in use as an artists' pigment on a Byzantine/Syriac Gospel lectionary [Cla3] and "The Dreams of Men", a 16th century painting by the Venetian master Tintoretto, [Tren] raising interesting questions as to whether its use was deliberate or an unfortunate consequence of the transformation. This chapter examines the process by which realgar transforms to pararealgar.

9.1: The Polymorphs of Realgar and Its Transformation to Pararealgar

Several different polymorphs of As_4S_4 exist. [Bona, Doug, Muni, Tren] These have been classified with a number of different labels but will be hereafter referred to as follows [Doug]: the low temperature formation polymorph of realgar (formed at temperatures below approximately 250°C) with D_{2d} symmetry is α-As_4S_4, (figure 9.1) β-As_4S_4 is the higher temperature polymorph and has the same molecular symmetry but different crystal packing, pararealgar has a different molecular structure from realgar and C_s symmetry. (Figure 9.2) Another polymorph has been identified experimentally, As_4S_4(II), formed by re-crystallising a quenched AsS melt. It has a molecular structure identical to that of pararealgar. [Muni]

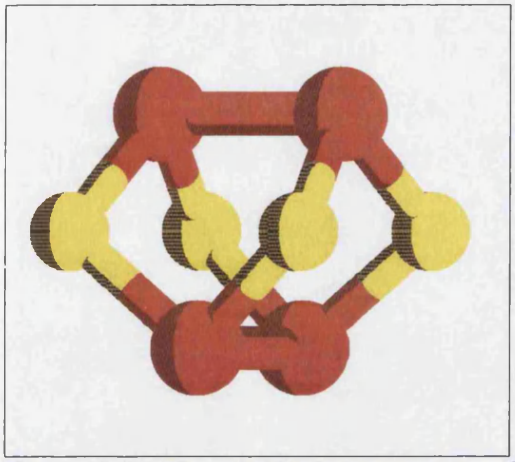

Figure 9.1: The molecular structure of α-As_4S_4. As atoms are depicted in red, S in yellow

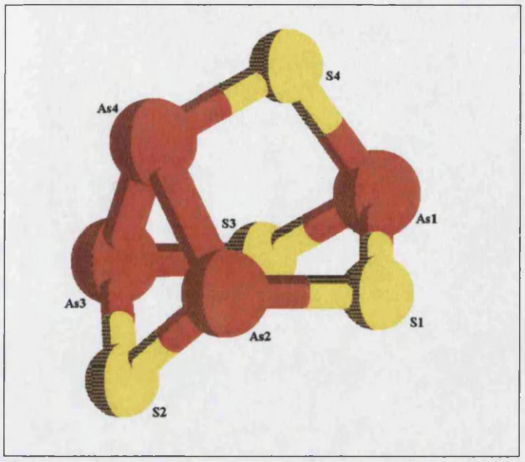

Figure 9.2: The molecular structure of pararealgar.

A further phase, χ-As_4S_4, has also been identified during the transformation of realgar to pararealgar. Various physical techniques have been employed to study this transformation, including X-ray diffraction, scanning electron microscopy, UV/Visible and Raman spectroscopy. [Bona, Doug, Muni, Tren]

The transformation of α-realgar to pararealgar is generally accepted to be light-induced, with transformation speeds varying in response to visible wavelengths. No alteration appears to occur at wavelengths shorter 500 nm. Up to 575 nm there is zero transmission through realgar, so the reaction occurs more quickly, but wavelengths longer 610 nm are almost entirely transmitted so alteration only occurs here very slowly. [Doug] Examination of the UV/Vis spectra of realgar as wavelength decreases [Muni, Fig. 3] reveals an inflection point in the absorption edge at around 550 nm, when the absorbance begins to increase sharply.

The mechanism of the transformation of realgar to pararealgar is investigated computationally in this chapter. Comparisons are made with the experimentally derived data, including that from the as yet unidentified χ-As_4S_4 phase.

9.2: Computational Details

The calculations were conducted on an IBM RS/6000 43P workstation and on UCL's Plato, a SUN Ultra Enterprise 3000, using the Amsterdam Density Functional program suite, versions 2.3, 1999 and 2000, described in chapter 8. The frozen core approximation was employed, S (2p) and As (3p). Triple-zeta uncontracted Slater-type orbital valence basis sets were used, supplemented with a single d-type polarisation function (ADF Type IV). The local density parameterisation of Vosko, Wilk and Nusair [Vosk] was used in conjunction with the exchange and correlation gradient corrections of Perdew and Wang (PW91). [Perd]

9.3: The Structures, Energies and Vibrations of the Phases of As_4S_4

The molecular structures of realgar and pararealgar are shown in figures 9.1 and 9.2. Selected bond lengths and angles are compared with experiment in table 9.1.

The agreement between experimental and calculated bond lengths and angles for both structures is very good. The bond lengths are all slightly overestimated but the maximum discrepancy in with experiment is 0.08 Å

Pararealgar is found to be a metastable form of molecular As_4S_4, having a calculated total bonding energy 18 $kJmol^{-1}$ less stable than realgar.

The calculated and experimental vibrational wavenumbers and assignments of realgar and pararealgar are given in tables 9.2 and 9.3. The agreement between the experimental and calculated wavenumbers for realgar is very good, with a maximum discrepancy of only 26 cm^{-1}.

Structure, symmetry	Bond	**Calculated,** Experimental Bond Length/Å	Bond Angle	**Calculated,** Experimental Angle/°
Realgar[a] D_{2d}	As-As	**2.65** 2.59	S-As-As	**99.1** 97.8
	As-S	**2.27** 2.24	S-As-S	**95.7** 92.8
			As-S-As	**100.9** 101.5
Pararealgar[b] C_s	As1-S1	**2.29** 2.25	S1-As1-S3	**105.0** 103.6
	As1-S4	**2.31** 2.26	S1-As1-S4	**98.4** 96.2
	As2-S1	**2.28** 2.25	As1-S4-As4	**102.7** 104.4
	As2-S2	**2.31** 2.25	S4-As4-As2	**102.1** 101.4
	As2-As4	**2.56** 2.48	As2-S2-As3	**95.1** 95.9
	As4-S4	**2.23** 2.19	As1-S1-As2	**108.6** 109.2
			S1-As2-S2	**108.3** 105.5
			S1-As2-As4	**100.1** 100.0
			As2-As4-As3	**83.8** 83.4

Table 9.1: Selected bond lengths and angles of α-As_4S_4 and pararealgar.

[a]Experimental data from [Doug].

[b]Experimental data from [Bona].

Experimental		Calculated	Assignment
Raman α and *β* phase	IR α and *β* phase	(difference from α-Raman)	
		86	a_2
144 *144*		139 (5)	b_1
167 *164*	168 *167*	151 (16)	e
173 *177*		184 (11)	b_2
184 *187*	183 *185*	187 (3)	a_1
196 *193*	193	222 (26)	a_1
210,214 *211*	204,209,211 *207,210*	211 (1)	e
222 *217*	224 *226*	217 (5)	b_2
330 *332*	329	331 (1)	a_2
341 *343*	341 *345*	357 (16)	e
345 *352*	*350*	365 (20)	b_1
355 *362*	360 *368*	380 (25)	a_1
370 *376*	368 *376*	389 (19)	e
376 *383*	375	387 (11)	b_2

Table 9.2: The calculated and experimental wavenumbers (cm^{-1}) of the vibrations of realgar (D_{2d}). Experimental data from [Muni].

The agreement between the experimental and calculated data is less good for pararealgar. The largest discrepancy in vibrational wavenumber is 46 cm^{-1}. Although the calculated data generally support the experimental symmetry assignment, agreement between theory and experiment could be substantially improved by revising the experimental assignment in one or two areas, for example the ordering of the a'', a' and a' modes at 214, 195 and 211 cm^{-1}.

Experimental		Calculated (difference from Raman)	Assignment
Raman	IR		
118	118	105 (13)	a"
135	134	98 (37)	a'
142		131 (11)	a'
152,158	156	146 (9)	a"
167	164	162 (5)	a'
172,175	169,173	175 (2)	a"
191	190	214 (23)	a"
198,204	198,210	195 (6)	a'
230,236	231,236	211 (22)	a'
275	275	229 (46)	a'
316	316	300 (16)	a'
322	319	276 (46)	a"
340		325 (15)	a"
334	328	327 (7)	a'
346	349	339 (7)	a'
364	358	354 (10)	a'
370	365	349 (21)	a"
383	384	378 (5)	a'

Table 9.3: The calculated and experimental wavenumbers (cm^{-1}) of the vibrations of pararealgar (C_s). Experimental data from [Muni].

9.4: The Transformation from Realgar to Pararealgar

The five lowest energy electronic excitations of realgar were calculated at the equilibrium geometry using the time-dependant approach of ADF 1999. These excitations were found to occur between the highest occupied (HOMO) and lowest unoccupied (LUMO) molecular orbitals. (Table 9.4)

MO	Eigenvalue/eV	Occupation	Character
$5b_1$	-2.527	0	As-As, As-S antibonding
$8a_1$	-2.608	0	As-As bonding, As-S antibonding
11e (LUMO)	-3.108	0	As-As antibonding, As-S bonding
$4a_2$ (HOMO)	-5.836	2	S-S antibonding
$7b_2$	-6.025	2	As-localised non-bonding

Table 9.4: Ground state eigenvalues and characters of the highest occupied and lowest unoccupied molecular orbitals of realgar.

However, it is apparent from table 9.5 that the energies of the transitions are far higher, at shorter wavelengths, than suggested by the experimental results.

Final State Symmetry	Principal Orbital Contribution	Energy/eV	Wavelength/nm	Oscillator Strength
^1E	$4a_2 \rightarrow 11e$	2.84	437	0.5×10^{-2}
^1E	$7b_2 \rightarrow 11e$	3.09	401	0.1×10^{-1}
$^1A_2$	$4a_2 \rightarrow 8a_1$	3.36	369	0
$^1B_2$	$4a_2 \rightarrow 5b_1$	3.41	364	0.7×10^{-3}
$^1B_2$	$7b_2 \rightarrow 8a_1$	3.66	339	0.3×10^{-1}

Table 9.5: The five lowest energy singlet-singlet transitions of realgar.

The agreement between the calculated results and experiment is not good, providing no obvious indication as to which transition is significant. Only one of the transitions is symmetry forbidden and the oscillator strengths of the remaining four give no further indication of which transition might be favoured.

The geometries of the four allowed excited states were optimised. All essentially reflected the ground state geometry with the exception of the $7b_2^1 11e^1$ configuration. In this case there was a noticeable lengthening of the As-As bonds – to 2.97 Å as opposed to 2.65 Å in realgar, to be expected from the As-As antibonding character of the newly populated orbital. (Table 9.4) Since the formation of pararealgar from realgar must involve the breaking of As-As bonds (compare the bonding of the As atoms in figures 9.1 and 9.2) this is a highly possible first step in that transformation.

The excited state is 249 kJ/mol less stable than the ground state but it remains in D_{2d} symmetry. Having an orbitally degenerate electronic state (^1E) it was found to be susceptible to Jahn-Teller distortion [Shri] when the geometry was re-optimised in C_s symmetry. The resulting basket-like structure is formed (figure 9.3) with only one broken As-As bond. Its energy is 215 kJ/mol above the realgar ground state, 34 kJ/mol more stable than the D_{2d} symmetry structure, and some alteration has occurred to the other geometric parameters. (Table 9.6)

Bond	Bond Length/Å	Bond Angle	Bond Angle/°
As1-As4 Distance	4.60	As1-S1-As2	109.7
As1-S1	2.25	S1-As1-S2	100.1
S1-As2	2.30	S1-As2-As3	101.5
As2-As3	2.55	S1-As2-S3	107.8

Table 9.6: Selected bond lengths, distances and angles of the intermediate C_s basket-like structure.

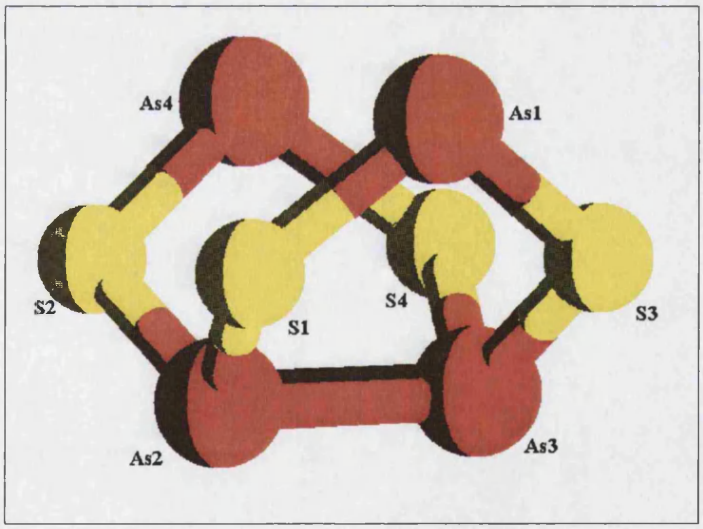

Figure 9.3: The Jahn-Teller distorted basket-like structure.

The calculated vibrational wavenumbers of the basket structure are given in table 9.7. An imaginary frequency occurs in the basket structure, which would seem to indicate that this is a transition state. However, it is a very low frequency mode and so is more likely to be an artefact than an indicator of a genuine transition state. Unfortunately, the lack of agreement between the wavenumbers of this structure and those experimentally derived for the χ-As_4S_4 phase appear to indicate that the basket structure, although an intermediate state, is not the intermediate state identified experimentally.

Experimental		Calculated	
X-phase	Assignment	Basket structure	Assignment
63	Lattice	39i	a"
118	a_2	35	a'
137	a_2	69	a'
146	b_1	98	a"
155	b_1	124	a"
167	e	151	a'
176	b_2	174	a'
188	a_1	182	a'
202	e	187	a"
222	b_2	206	a'
235	b_2	263	a"
274	b_2	301	a'
315	b_2	305	a'
326	a_2	316	a"
345	e	328	a"
351	b_1	347	a"
363	a_1	359	a'
380	b_2	374	a'

Table 9.7: The vibrational wavenumbers of the χ-phase and the basket-like structure. Experimental results from [Bona]

The next step in the degradation process is not obvious. If the geometry of the basket-like structure is re-optimised in the ground electronic state it returns to realgar, with a full compliment of As-As bonds, so it is reasonable to assume that the molecule remains in an excited state at least temporarily. It would also be logical to assume that the next structure should have lower energy than the excited basket-like structure, since no energy is added.

Given the positions of the atoms in the pararealgar molecule, if the process is uni-molecular, one of the As atoms that does not have an As-As bond needs to be re-positioned in closer proximity to the bonded As-As pair. This chair-like structure was constructed (figure 9.4) and its geometry optimised in both the excited and ground state.

The excited state structure is found to be 15 kJ/mol more stable than the basket-like structure, while the ground-state structure, which has a slightly different geometry, is 63 kJ/mol more stable. Unfortunately, the calculated frequencies of both the excited and ground states of this structure also do not correspond to those of the intermediate χ-phase. (Table 9.8)

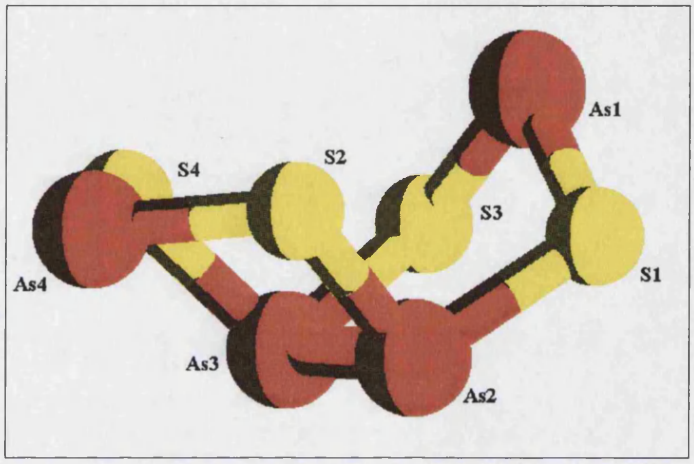

Figure 9.4: The chair-like structure.

From this structure there is again no obvious route to pararealgar. If the positions of various atoms are changed, for example S4 moved closer to As1 to facilitate bonding between them, and the geometry re-optimised then pararealgar will result. However, as with the previous chair-like structure, there is no energetically sound reason for these adjustments to occur. It is feasible that a single excitation of the molecule is insufficient to cause the complete transition from realgar to pararealgar. However, excitations of the ground-state chair–like structure and further excitations of the excited-state chair-like structure do not produce any significant change of structure or bonding.

Experimental		Calculated	
X-phase	Assignment	Chair structure	Assignment
63	Lattice	25	a"
118	a_2	45	a'
137	a_2	76	a'
146	b_1	100	a"
155	b_1	123	a"
167	e	143	a'
176	b_2	175	a"
188	a_1	180	a'
202	e	181	a'
222	b_2	199	a'
235	b_2	281	a"
274	b_2	304	a'
315	b_2	328	a'
326	a_2	332	a"
345	e	339	a"
351	b_1	346	a"
363	a_1	367	a'
380	b_2	370	a'

Table 9.8: The vibrational wavenumbers of the χ-phase and the chair-like structure. Experimental results from [Bona]

9.5: Conclusions

It is clear that the exact nature of the transformation from realgar to pararealgar is far from simple. It involves an intermediate phase, χ, that has been recognised experimentally but whose structure has not been elucidated. From this work it appears that the light-induced excitation of a $7b_2$ electron to the 11e LUMO, creating a geometrically distorted $7b_2^1 11e^1$ state, is the most likely first step in the transformation. However, although the next, chair-like, structure is energetically feasible it has no obvious genesis, indicating that realgar may not follow this route.

Identification of the first step in the transformation appears to be the limit of the application of DFT to this problem. Further excitations have yielded no further substantial changes of geometry, suggesting that this may not be the way forward. An important alternative could be the suggestion that the transformation of realgar to pararealgar is not a uni-molecular process, occurring only through direct interaction between each molecule and its neighbours within a crystal. This falls outside the limits of ADF – a molecular formulism of DFT, so the problem was reluctantly abandoned.

Chapter 10: The Structures of Dihalogendiorganoselenium Compounds

I may not have gone where I intended to go, but I think I have ended up where I needed to be.
The Long Dark Tea-Time of the Soul
Douglas Adams
1988

It has been experimentally demonstrated by X-ray crystallography [Godf] that the products of reactions between diorganoselenium compounds and dihalogens can adopt one of two conformations. For example, the dimethyl-derivatives of chlorine and bromine (Me_2SeCl_2 and Me_2SeBr_2) adopt the ψ-trigonal-bipyramidal structure while the diiodine derivative adopts a charge-transfer 'spoke' structure (Me_2Se-I-I). See figures 10.1 and 10.2.

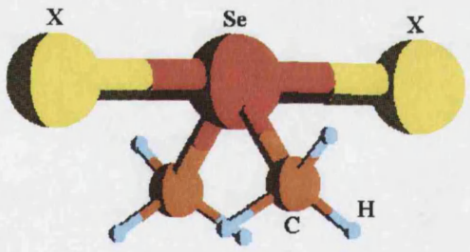

Figure 10.1: Ball-and-stick representation of the ψ-trigonal-bipyramidal structure of R_2SeX_2. In this case R = Me.

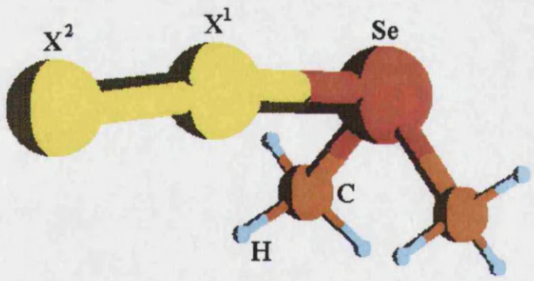

Figure 10.2: Ball-and-stick representation of the charge-transfer structure of R_2SeX_2. In this case R = Me.

This phenomenon is also found in some triorgano- Group 15 compounds, R_3EX_2 (R = Me, Ph, or ^{t}Bu). For example R_3AsI_2 and Me_3AsBr_2 adopt the charge-transfer spoke structure while Ph_3AsBr_2 is trigonal-bipyramidal. [Bric] It has been suggested that the structure adopted in the case of R_3EX_2 may depend on the acidity of E, the Group 15 element. [Bric] A trigonal-bipyramidal structure occurs if E is more acidic than X, the halogen, and a charge-transfer spoke structure if the opposite is true. However, the

nature of the R-group has a significant effect on the acidity of E. Electron-donating R-groups favour a charge-transfer geometry by decreasing the acidity of E. These arguments could in principle be valid for $R_2Se_2X_2$.

In $R_2Se_2X_2$ in the ψ-trigonal-bipyramidal conformation, the Se atom is hyperco-ordinate, being surrounded by five electron pairs (four bonding pairs and one lone pair in valence bond (VSEPR) terms). The stability of molecules centred around hyperco-ordinate p-block elements beyond the second period is related to the polarity of the bonds to that element. [Coop] Significantly, polar bonds that shift electron density away from the central atom favour hyperco-ordinate structures. Since the halogens have a considerable range of electronegativities [SICD] it might be expected that variation of the halogen would lead to a change in the favoured geometry.

A computational study of Me_2SeX_2 reproduced the structural change from ψ-trigonal-bipyramidal to charge-transfer at X = I. [Kal1] Analysis of bond strengths found a much greater difference between Se–X and X–X for the lighter halogens. The Se–X bonds make a much more significant contribution to the stabilisation of the ψ-trigonal-bipyramidal structure than the halogen-halogen bond does to the charge-transfer conformation. With descent of the halogen group, however, the difference between the strengths of these bonds is reduced and the stabilising effect of the Se–X bond diminished. The structural change is thus attributed to the relative strength of one Se–X bond and one X–X bond over two Se–X bonds.

The polarity of the Se – X bond also decreases with increasing halogen atomic number, as anticipated on the grounds of electronegativity. This adds considerable support to the proposed explanation for the change in structure given above [Coop] since the ψ-trigonal-bipyramidal structure is believed to be stabilised by the shift in electron density caused by polar bonds to the central atom. Decreasing polarity of the Se – X bond and increased basicity of Se favour the charge-transfer spoke structure.

This study continues the computational exploration of these systems and investigates the effect of altering the nature of the R-group. The polarity of the selenium-halogen bond and the effect of electron withdrawal by and size of the R-group are all found to be factors affecting the minimum energy structure.

10.1: Computational Details

The calculations were conducted on an IBM RS/6000 43P workstation and the Royal Institution's "Strutt" Cluster of four Compaq ES40 machines, each with four EV68 processors, using the Amsterdam Density Functional program suite described in chapter 8.

Quasi-relativistic frozen cores were used for all atoms except H: C (1s), F (1s), Cl (2p), Se (3d), Br (3d), I (4d) and At (5d). DIRAC, an ADF auxiliary program, was used to calculate the relativistic core potentials. An uncontracted triple-zeta Slater-type orbital valence basis set was used for all atoms, with a single p polarisation function for H and a d function for all other atoms (ADF Zora Type IV). For I and At no polarisation function is provided and hence a d function with an exponent of 1.74 was added to I and a p function with an exponent of 2.08 to At.

The molecular geometries were optimised using the pure-exchange electron gas formula for the local density approximation [Jens, Sla1] in conjunction with Becke's gradient correction to the exchange formula [Beck] and the Lee-Yang-Parr correlation correction. [Lee]

10.2: Results and Discussion

Initially four R-groups were selected on the basis of their electron-donating/withdrawing properties; carbon tri-fluoride (CF_3), hydrogen (H), methyl (CH_3) and tertiary-butyl ($C(CH_3)_3$). The total bonding energies of the optimised geometries were calculated for all halogens from fluorine to astatine with identical pairs of R-groups in both charge transfer and ψ-trigonal-bipyramidal conformations. As a result of these calculations, four further R-groups of intermediate strength of electron donation, CF_2H, CH_2F, CH_2CH_3 and $CH(CH_3)_2$, were added to explore more closely the point in the halogen group at which the transfer from the ψ-trigonal-bipyramidal to the charge-transfer structure takes place.

10.2.1. Optimised geometries

Unfortunately, very little experimental data exist for these types of structures – only Me_2SeX_2 with X = Cl, Br or I have been examined experimentally. [Godf] Tables 10.1 and 10.2 contain the bond lengths and angles for the ψ-trigonal-bipyramidal and charge transfer conformations of the Me_2SeX_2 molecules studied, with the results of previous calculations and X-ray crystallographic data. The previous study [Kal1] also used DFT methodology, but with a smaller basis set (ADF Type III), using the Local Density Approximation (LDA).

Bond Length	Me_2SeF_2	Me_2SeCl_2	Me_2SeBr_2	Me_2SeI_2	Me_2SeAt_2
Se-X	1.923	2.411	2.579	2.810	2.866
	1.978	**2.500**	**2.691**	**2.940**	**3.051**
		2.379	*2.549*		
Se-C	1.953	1.968	1.971	1.977	1.977
	2.023	**2.037**	**2.041**	**2.046**	**2.045**
C-H (ave)	1.100	1.100	1.101	1.101	1.100
	1.091	**1.090**	**1.090**	**1.090**	**1.090**
Bond Angle					
X-Se-X	172.0	178.1	178.6	178.6	178.3
	175.1	**177.6**	**176.4**	**172.8**	**172.7**
		177.8	*177.7*		
X-Se-C	87.4	89.4	90.5	90.5	90.6
	88.4	**90.8**	**91.2**	**92.4**	**92.4**
		91.7	*90.8*		
C-Se-C	96.9	96.0	95.7	95.7	95.4
	96.6	**96.8**	**97.3**	**96.1**	**96.8**
		98.6	*98.0*		
Se-C-H (ave)	106.2	106.1	106.3	106.3	106.2
	106.2	**105.8**	**105.7**	**106.0**	**106.0**

Experimental data (*italic*) from [Godf], calculated data from [Kal1] and this study (**bold**).

Table 10.1: Calculated and experimental bond lengths (Å) and angles (°) for the ψ-trigonal-bipyramidal structures of Me_2SeX_2 (X = F, Cl, Br, I or At).

Bond Length	Me_2SeF_2	Me_2SeCl_2	Me_2SeBr_2	Me_2SeI_2	Me_2SeAt_2
Se-X^1	2.031	2.553	2.693	2.932	3.014
	2.055	**2.694**	**2.834**	**3.086**	**3.169**
				2.916	
X^1-X^2	1.775	2.225	2.502	2.846	2.956
	1.869	**2.268**	**2.579**	**2.951**	**3.115**
				2.768	
Se-C	1.954	1.963	1.966	1.967	1.967
	2.021	**2.029**	**2.031**	**2.032**	**2.033**
C-H (ave)	1.101	1.100	1.101	1.101	1.100
	1.092	**1.092**	**1.092**	**1.092**	**1.091**
Bond Angle					
X^2-X^1-Se	171.3	174.0	174.5	174.0	175.2
	169.3	**177.2**	**174.4**	**175.9**	**176.9**
				174.3	
X^1-Se-C	89.8	91.7	93.4	92.8	93.7
	90.1	**95.3**	**94.1**	**95.8**	**97.4**
				96.2	
C-Se-C	95.1	95.0	95.1	94.9	95.3
	96.6	**96.1**	**95.9**	**95.9**	**95.9**
				99.0	
Se-C-H (ave)	107.4	107.7	107.8	107.9	107.9
	106.9	**107.5**	**107.5**	**107.6**	**107.6**

Experimental data (*italic*) from [Godf], calculated data from [Kal1] and this study (**bold**).

Table 10.2: Calculated and experimental bond lengths (Å) and angles (°) for the charge-transfer structures of Me_2SeX_2 (X = F, Cl, Br, I or At).

There is a reasonably close match between the results of this study and the experimental data, although the bond lengths are somewhat over-estimated by both sets of calculations. The results of the Generalised Gradient Approximation (GGA) calculations have produced a greater discrepancy than the previous LDA calculations. The LDA tends to somewhat over-bind molecules and can lead to calculated bond lengths that are shorter than experimental values. [Zieg] In this case, however, the bond lengths are slightly longer than the experimental values. The inclusion of the

GGA reverses any over-binding effect and has produced even longer bonds. However, the difference between experimental and calculated values is only 0.183Å at its greatest – the I-I bond in the charge-transfer Me_2SeI_2 molecule.

The agreement between calculated and experimental bond angles is very good in both ψ-trigonal-bipyramidal and charge-transfer cases and generally better in the GGA than the LDA case for these molecules. In general, the agreement between the calculated and experimental geometries is good, although further experimental data would be valuable to test the model further.

The purpose of this study is the consideration of the relative energies of the ψ-trigonal-bipyramidal and charge-transfer structures. The more accurate energies generally produced by GGA calculations [Jens] make this methodology more appropriate even given the slight disparity produced in the molecular geometries.

10.2.2. Molecular energies and electron donation

The following figures (figures 10.3–6) show the total energy of the optimised geometries of both molecular conformations with combinations of all four initial R-groups and all five halogens. The preferred molecular geometry in each case is the one with lowest energy – the lower of the two lines. The change in preferred structure occurs where these lines intersect.

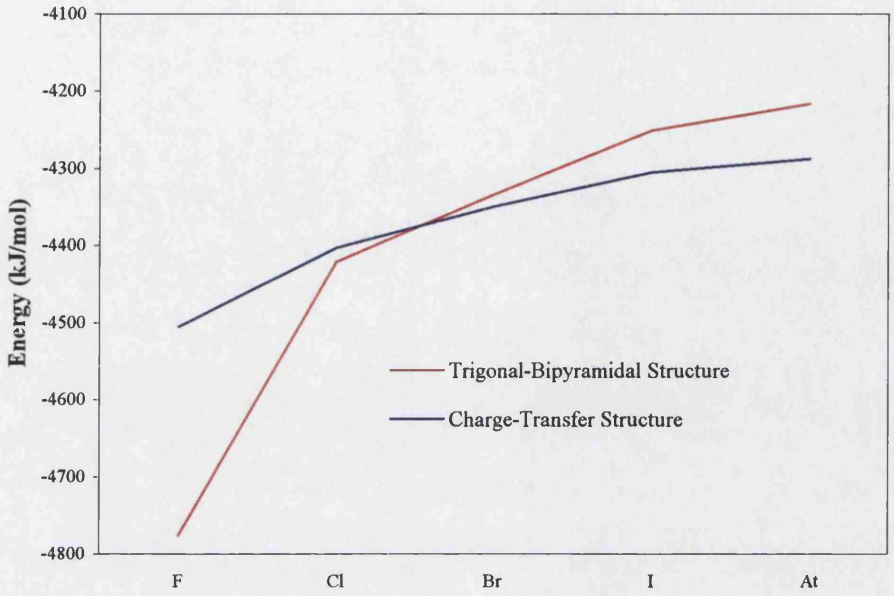

Figure 10.3: The energies of the $(CF_3)_2SeX_2$ (X = F, Cl, Br, I, At) ψ-trigonal-bipyramidal and charge-transfer structures.

Figure 10.3 shows clearly the structural change from the ψ-trigonal-bipyramidal structure to the charge-transfer structure that occurs between X = Cl and X = Br. The ψ-trigonal-bipyramidal structure is favoured for chlorine and the charge-transfer structure for bromine.

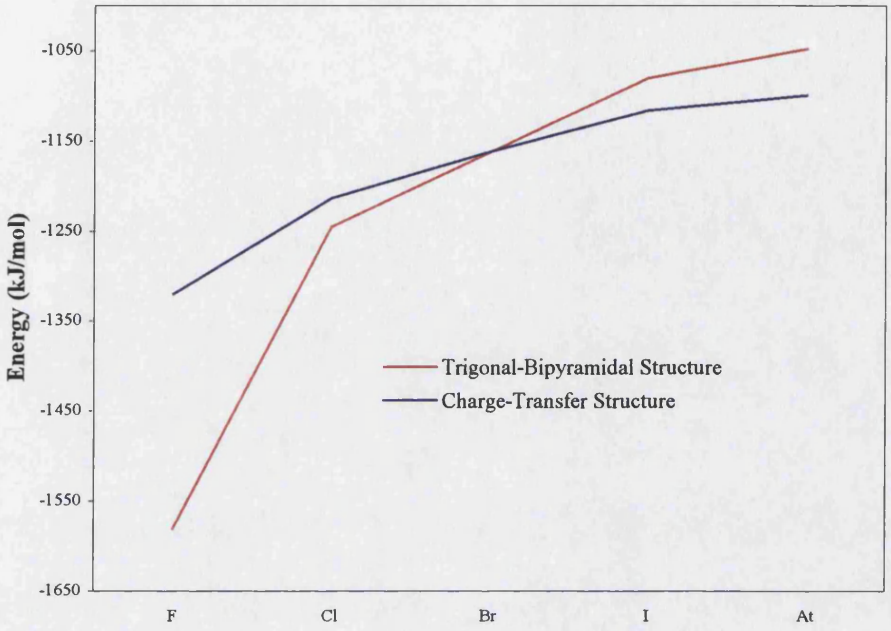

Figure 10.4: The energies of the H_2SeX_2 (X = F, Cl, Br, I, At) ψ-trigonal-bipyramidal and charge-transfer structures.

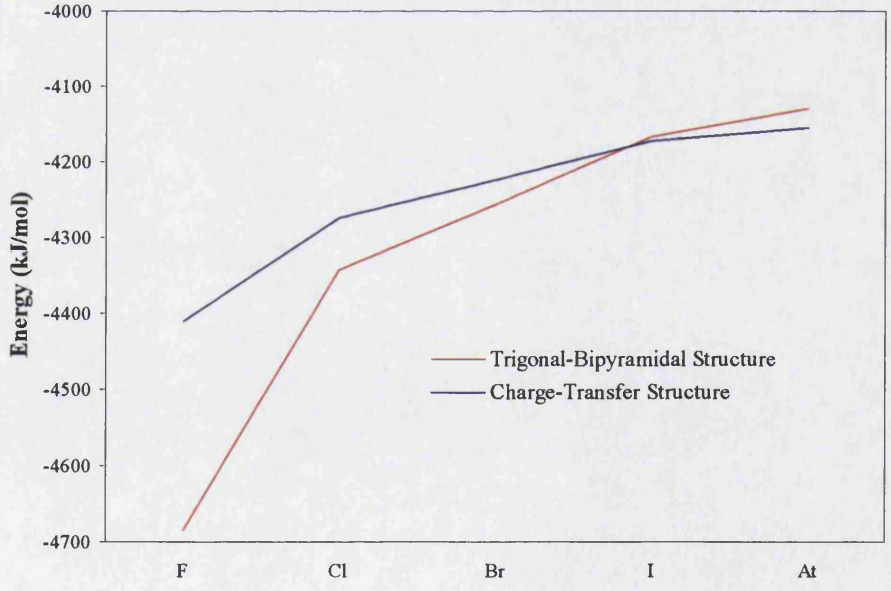

Figure 10.5: The energies of the $(CH_3)_2SeX_2$ (X = F, Cl, Br, I, At) ψ-trigonal-bipyramidal and charge-transfer structures.

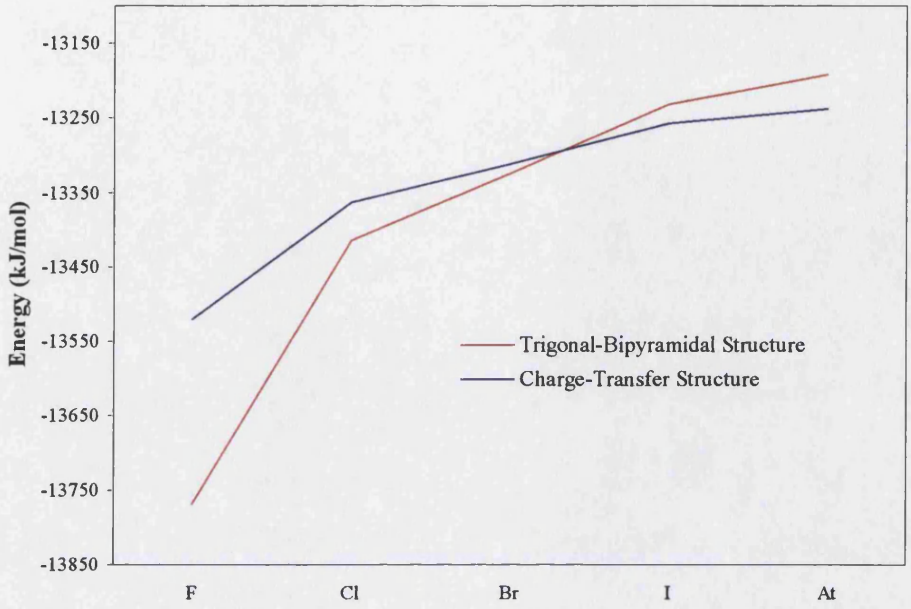

Figure 10.6: The energies of the (t-butyl)$_2$SeX$_2$ (X = F, Cl, Br, I, At) ψ-trigonal-bipyramidal and charge-transfer structures.

Figures 10.3 to 10.6 are in order of decreasing strength of electron withdrawal of the R-groups. The change in the energetically favoured structure, from ψ-trigonal-bipyramidal to charge-transfer, is seen for all four of these R-groups. However, the point at which the change of structure occurs is variable, although it always lies between Cl and I for these R-groups.

The difference in energy between the lowest energy structure and its higher energy counterpart is a measure of how strongly one structure is favoured over the other. From the graphs above, figure 10.7 and tables 10.3 and 10.4, it can be seen that the selection of the minimum energy structure does not have a simple relationship to the electron donation of the R-group since the most electron withdrawing, CF_3, favours the charge-transfer structure more than does R = tertiary butyl for all halogen pairs except fluorine. Given that a less acidic selenium atom is expected from the less electron withdrawing tertiary butyl, the exact opposite result would be expected.

		F	Cl	Br	I	At
CF_3	T-Bp	-4775.87	-4421.06	-4334.06	-4250.62	-4216.48
	C-T	-4505.22	-4403.14	-4349.78	-4304.79	-4287.40
H	T-Bp	-1580.28	-1245.09	-1163.11	-1080.55	-1048.21
	C-T	-1320.11	-1213.65	-1162.42	-1116.13	-1099.59
CH_3	T-Bp	-4683.50	-4342.06	-4256.42	-4166.36	-4128.56
	C-T	-4409.52	-4275.27	-4223.16	-4172.79	-4154.78
t-Butyl	T-Bp	-13768.07	-13414.14	-13324.47	-13231.48	-13192.46
	C-T	-13520.42	-13363.70	-13312.52	-13257.37	-13238.02

Table 10.3: The energies (kJ/mol) of the optimised geometries of the ψ-trigonal-bipyramidal and charge-transfer structures of R_2SeX_2 (R = CF_3, H, CH_3, *t*-Butyl; X = F, Cl, Br, I, At).

	CF_3	H	CH_3	*t*-Butyl
F	270.65	260.17	273.98	247.65
Cl	17.92	31.44	66.79	50.44
Br	-15.72	0.69	33.26	11.95
I	-54.17	-35.58	-6.43	-25.89
At	-70.92	-51.38	-26.22	-45.56

Table 10.4: The difference between the energies (kJ/mol) of the optimised geometries of the ψ-trigonal-bipyramidal and charge-transfer structures of R_2SeX_2 (R = CF_3, H, CH_3, *t*-Butyl; X = F, Cl, Br, I, At). A positive number indicates that the ψ-trigonal-bipyramidal structure is favoured whilst a negative value implies that the charge-transfer structure is preferred.

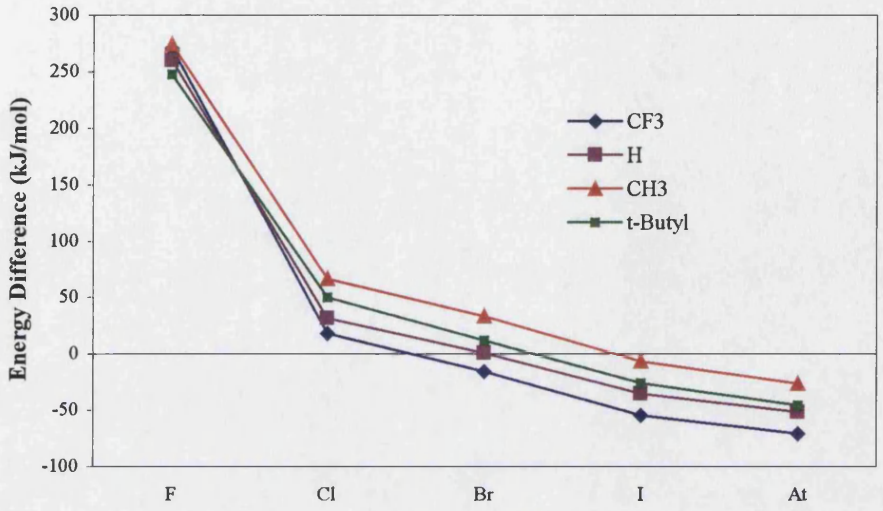

Figure 10.7: The difference in energy between the ψ-trigonal-bipyramidal and charge-transfer structures of R_2SeX_2 (R = CF_3, H, CH_3, *t*-Butyl; X = F, Cl, Br, I, At). The point at which the line Energy Difference = 0 is crossed is the point at which the change from ψ-trigonal-bipyramidal to charge-transfer takes place. The R-groups are listed in order of decreasing electron withdrawal in the legend.

The movement of point of the structural change around bromine but without apparent dependence on the electron donation/withdrawal properties of the R-group was further explored by the inclusion of four additional R-groups, listed in section 10.2 above. As before, geometries were optimised and total bonding energies calculated, although on this occasion only for the key halogens; chlorine, bromine and iodine.

A number of different conformations are possible for pairs of CF_2H, CH_2F, CH_2CH_3 and $CH(CH_3)_2$ R-groups depending on their rotational orientation. The orientations that were expected to have the lowest steric energy, i.e. those with the maximum degree of staggering, were selected.

	ψ-Trigonal-Bipyramidal	Charge-Transfer	Difference
CF_3	-4421.06	-4403.14	17.92
CF_2H	-4377.70	-4328.53	49.17
CH_2F	-4317.22	-4253.41	63.81
CH_3	-4342.06	-4275.27	66.79
CH_2CH_3	-7386.59	-7312.18	74.38
$CH(CH_3)_2$	-10414.20	-10344.90	69.32
t-Butyl	-13385.30	-13363.70	21.60

Table 10.5: The minimum energies (kJ/mol) of the optimised geometries of the structures of R_2SeCl_2, in order of decreasing electron withdrawal of the R-group.

	ψ-Trigonal-Bipyramidal	Charge-Transfer	Difference
CF_3	-4334.06	-4349.79	-15.73
CF_2H	-4290.53	-4276.76	13.77
CH_2F	-4230.30	-4203.46	26.84
CH_3	-4256.42	-4223.16	33.26
CH_2CH_3	-7300.24	-7261.49	38.75
$CH(CH_3)_2$	-10325.77	-10294.85	30.92
t-Butyl	-13324.47	-13312.52	11.95

Table 10.6: The minimum energies (kJ/mol) of the optimised geometries of the structures of R_2SeBr_2, in order of decreasing electron withdrawal of the R-group.

	ψ-Trigonal-Bipyramidal	Charge-Transfer	Difference
CF_3	-4250.62	-4304.79	-54.17
CF_2H	-4201.2	-4230.39	-29.19
CH_2F	-4141.45	-4155.49	-14.04
CH_3	-4166.36	-4172.79	-6.43
CH_2CH_3	-7210.61	-7209.47	1.14
$CH(CH_3)_2$	-10233.9	-10242.4	-8.5
t-Butyl	-13231.5	-13257.37	-25.89

Table 10.7: The minimum energies (kJ/mol) of the optimised geometries of the structures of R_2SeI_2, in order of decreasing electron withdrawal of the R-group.

Tables 10.5, 10.6 and 10.7 show the difference in energy between the ψ-trigonal-bipyramidal and charge-transfer structures for all of the R-groups, excluding hydrogen, with chlorine, bromine and iodine. As can easily be seen from figure 10.8 below, the minimum energy structure does is not solely determined by the electron withdrawal of the R-group.

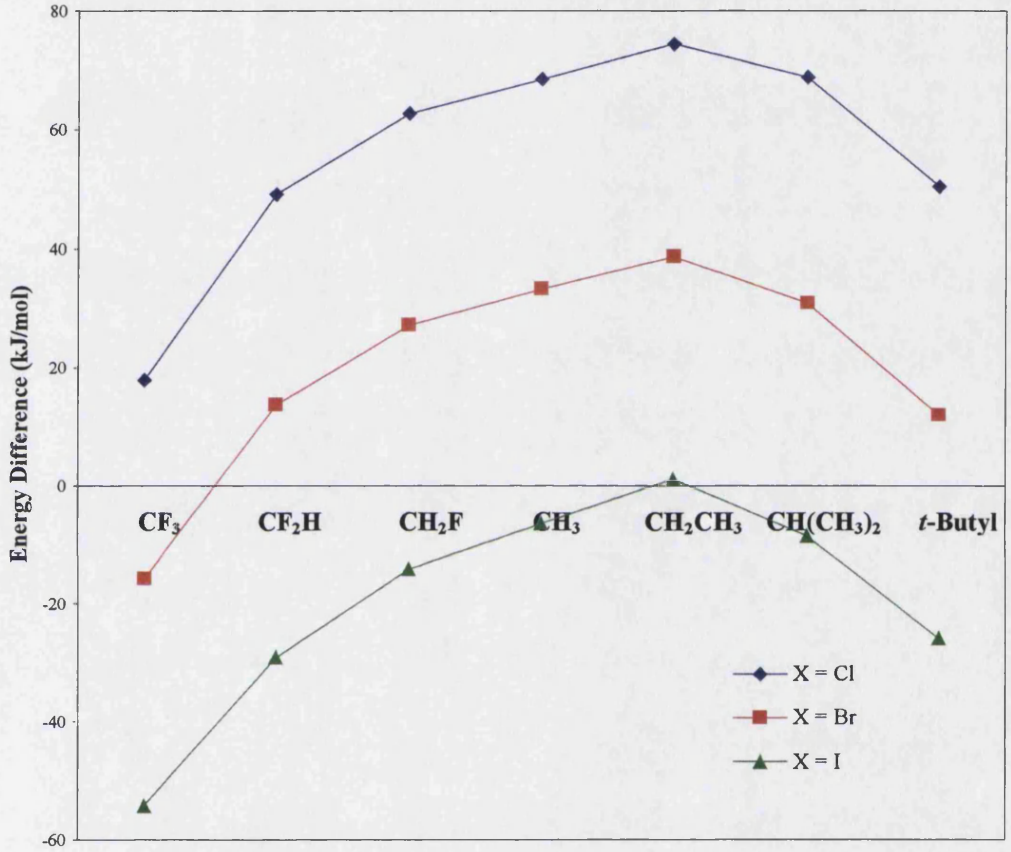

Figure 10.8: The difference between the ψ-trigonal-bipyramidal and charge-transfer structure total bonding energies for the structures R_2SeX_2.

When the difference between the total energies of the structures is positive this indicates that the ψ-trigonal-bipyramidal structure is favoured; negative and the charge-transfer structure is preferred.

It is interesting to note that the same trend is reproduced for all three halogens, although it is shifted, as expected, according to the electronegativity of the halogen. As the halogen becomes less electronegative the polarity of the Se-X bond decreases and the charge-transfer structure becomes more strongly favoured.

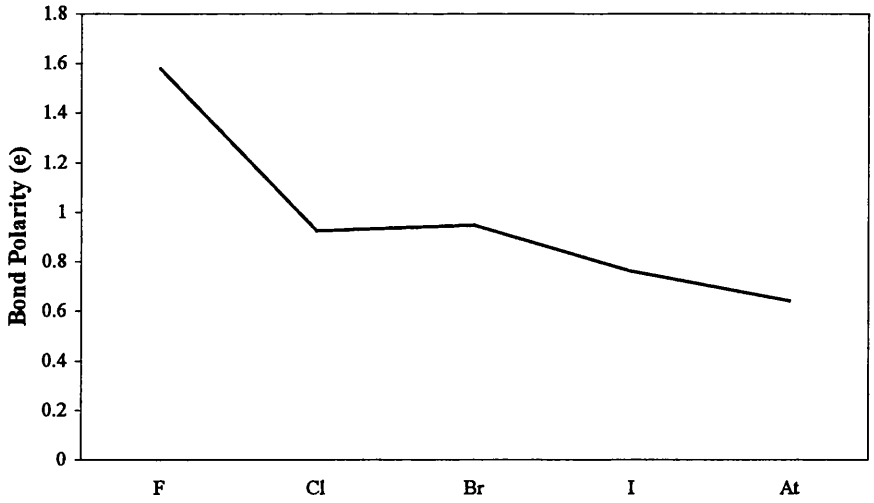

Figure 10.9: The variation in bond polarity of the Se – X bond for the ψ-trigonal-bipyramidal structure of the $Me_2Se_2X_2$ molecule (X = F, Cl, Br, I, At).

The variation in bond polarity with descent of the halogen group for the ψ-trigonal-bipyramidal structures of Me_2SeX_2 is shown in figure 10.9, with the corresponding Mulliken charges on the atoms in table 10.8. The difference between these two charges is a measure of the polarity of the bond between them.

	Charge on Se	Charge on X	Δ(Se-X)
Me_2SeF_2	0.98	-0.60	1.58
Me_2SeCl_2	0.53	-0.40	0.92
Me_2SeBr_2	0.54	-0.41	0.95
Me_2SeI_2	0.43	-0.34	0.76
Me_2SeAt_2	0.35	-0.29	0.64

Table 10.8: The Mulliken charges (in units of e) on the selenium and halogen atoms.

The polarity of the selenium halogen bond does, in general, decrease with descent of the halogen group, as expected on the grounds of halogen electronegativity. This coincides with a general trend towards the charge-transfer structure, supporting the suggestion that more polar Se–X bonds stabilise hyperco-ordinate molecules, discussed at the beginning of this chapter.

Figure 10.9 also shows evidence of the halogen alternation effect, with the Se-X bond polarity being slightly less for chlorine than for bromine. This has been attributed to the addition of d orbitals that occurs in the fourth period of the periodic table. However, the effect does not occur in the calculation of bond polarity by other workers [Kal1] and hence it may in this case be due only to the difference in basis sets used, to which Mulliken charges (upon which these calculations are based) can be very sensitive.

The pattern of variation in total energy with R-group is not so simply explained, however. Decreasing electron withdrawal (i.e. moving from CF_3 to CH_2CH_3) initially coincides with an increase in inclination towards the ψ-trigonal-bipyramidal structure, with the exception of the two least withdrawing R-groups, $CH(CH_3)_2$ and *t*-Butyl which increasingly favour the charge-transfer structure. On the basis of the arguments presented at the beginning of this chapter, this trend is unexpected. As electron withdrawal decreases a charge transfer structure should be more strongly favoured. Exactly the opposite trend occurs in the majority here, implying that electron withdrawal by the R-group is not the dominant influence in determining the most stable molecular structure.

10.2.3. R-group size

Although CF_3 and *t*-Butyl have very different electron donating/withdrawing properties both favour the charge-transfer conformation more strongly than the R-groups in between. Additionally, they are two of the largest R-groups considered by this study. To properly consider the importance of steric effects on the most stable conformation of the molecules, a measure of the size of the R-groups is required.

To estimate the size of the R-groups, a calculation of the solid angle occupied by the R-group at the central carbon atom, on the axis of the carbon-selenium bond, was made. (figure 10.10) For the full method and results of the calculations see appendix 5.

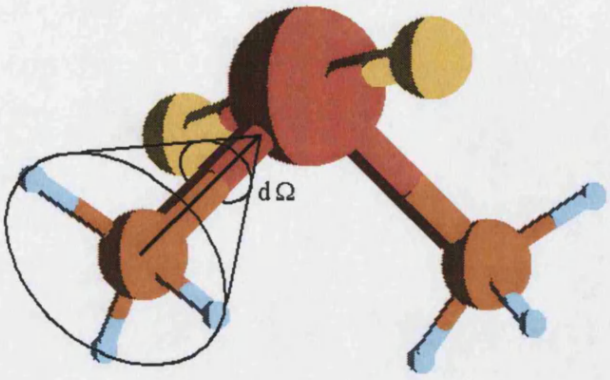

Figure 10.10: The size of the methyl group in terms of the element of solid angle subtended along the Se-C axis at the carbon atom.

R-group	Size, as element of solid angle (steradians)
CF_3	2.107
CF_2H	1.937
CFH_2	1.804
CH_3	1.691
CH_2CH_3	1.930
$CH(CH_3)_2$	2.248
t-Butyl	2.539

Table 10.9: Approximate R-group sizes in order of decreasing strength of electron withdrawal.

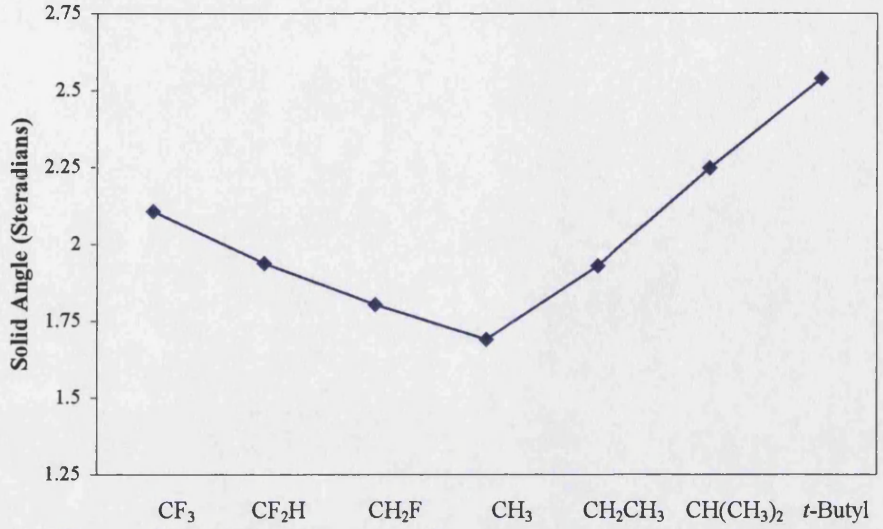

Figure 10.11: The variation of approximate R-group size, in order of decreasing strength of electron withdrawal.

Figure 10.11, above, to a large extent demonstrates the same trend as the graphs of energy difference (figure 10.8). Clearly, the larger R-groups favour the charge-transfer structure more than do the smaller ones. For chlorine the energy difference between the structures is smaller, although they remain ψ-trigonal bi-pyramidal. For iodine, all molecules, but for that where R = CH_3, are charge-transfer with the largest R-groups having the greatest energy difference between the structures. In the bromine case the structures are generally somewhere between these two extremes, with CF_3 favouring charge-transfer and *t*-butyl ψ-trigonal-bipyramidal, but with a relatively small difference between the two structures.

The charge-transfer conformation would certainly be more tolerant of a large R-group than the ψ-trigonal-bipyramidal, having fewer bonds to the central selenium atom to accommodate. However, the size of the R-groups cannot entirely explain the shape of the energy difference curves since CF_3, which is notably smaller than *t*-Butyl, favours the charge-transfer structure more strongly. If the size of the R-group were the only crucial variable *t*-Butyl would surely favour charge-transfer more than CF_3.

10.2.4. R-group size and selenium-carbon bond strength

In general terms, the length of a bond between two atoms is inversely related to its strength. Thus as a bond is lengthened it becomes weaker.

In figure 10.12 the total energy of the Me_2SeBr_2 molecule is considered as the Se-C bond is lengthened in a series of single point calculations with fixed molecular geometries. An increase of 0.1 Å in the Se-C bond length in Me_2SeBr_2 molecule causes a destabilisation of approximately 13 kJ/mol.

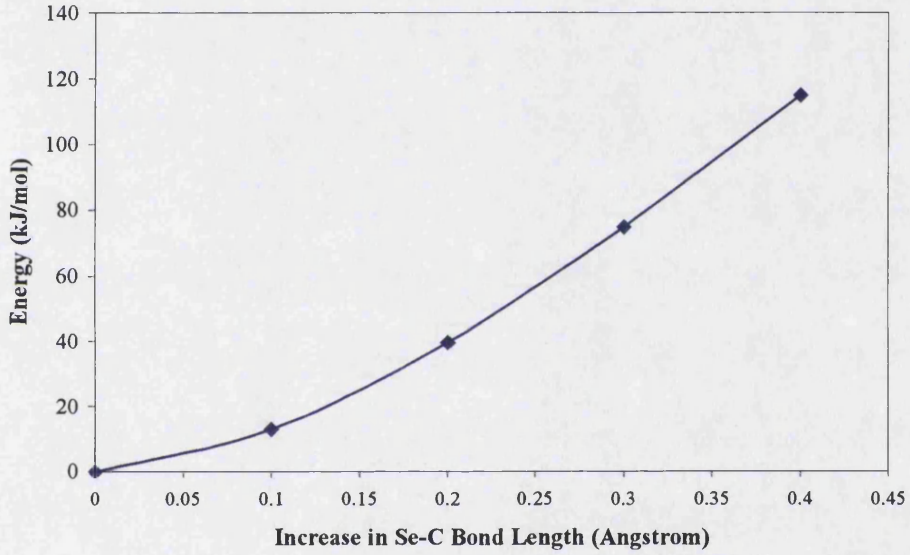

Figure 10.12: Variation in energy of the Me_2SeBr_2 molecule in the ψ-trigonal-bipyramidal conformation, with increase of Se-C bond length from equilibrium value.

A plot of the length of the Se-C bond in the optimised geometries of the R_2SeBr_2 molecules, for all R, shows a distinct variation as R is altered for both ψ-trigonal-bipyramidal and charge-transfer structures. (Figure 10.13)

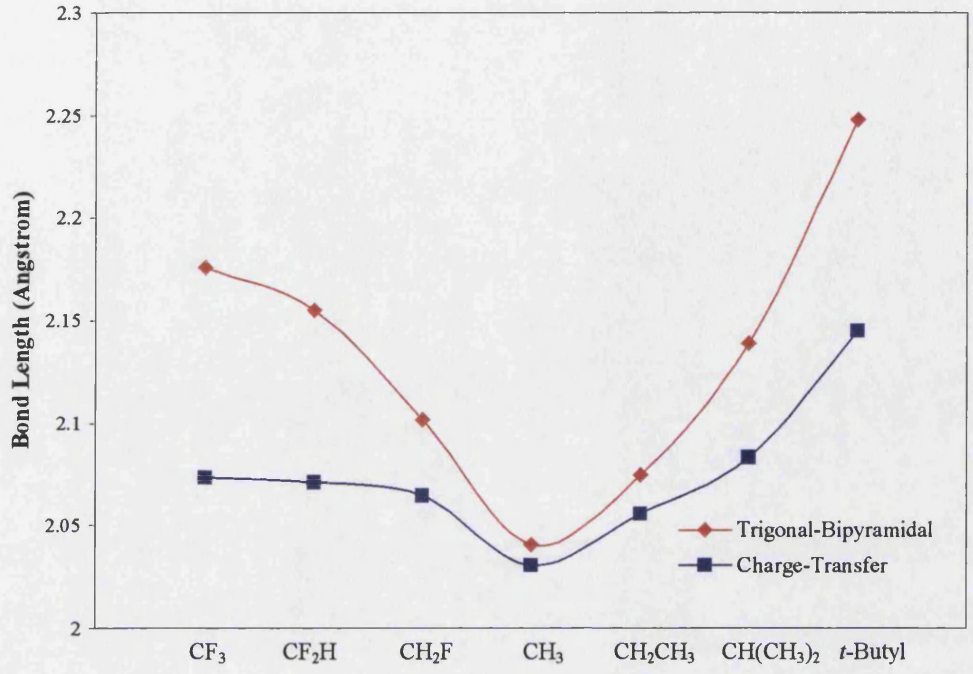

Figure 10.13: The variation of Se-C bond length with R-group, for the R_2SeBr_2 molecule.

This trend is repeated for both chlorine and iodine based molecules.

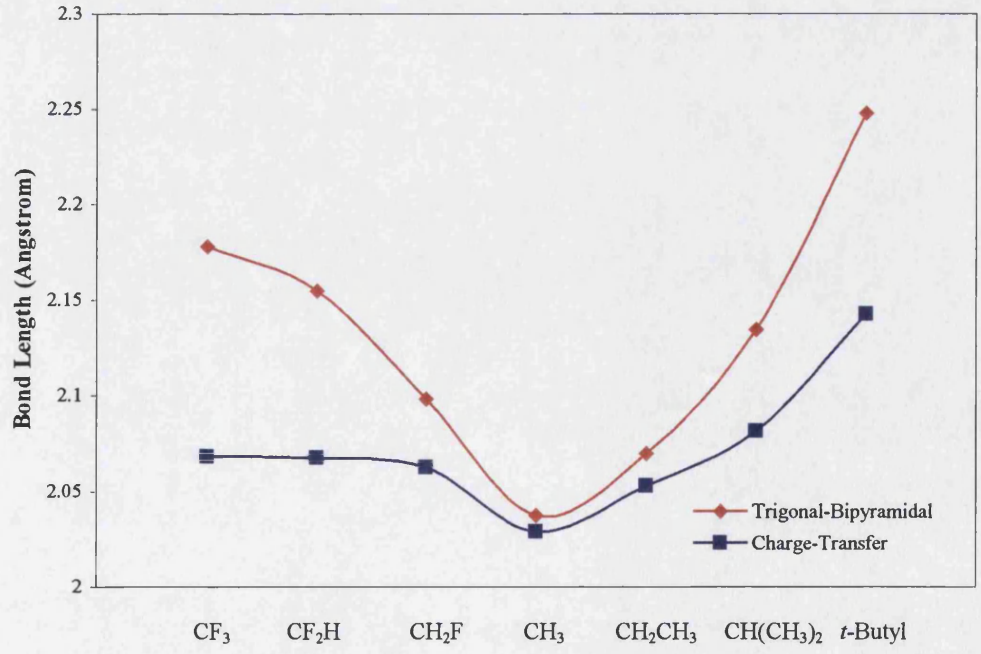

Figure 10.14: The variation of Se-C bond length with R-group, for the R_2SeCl_2 molecule.

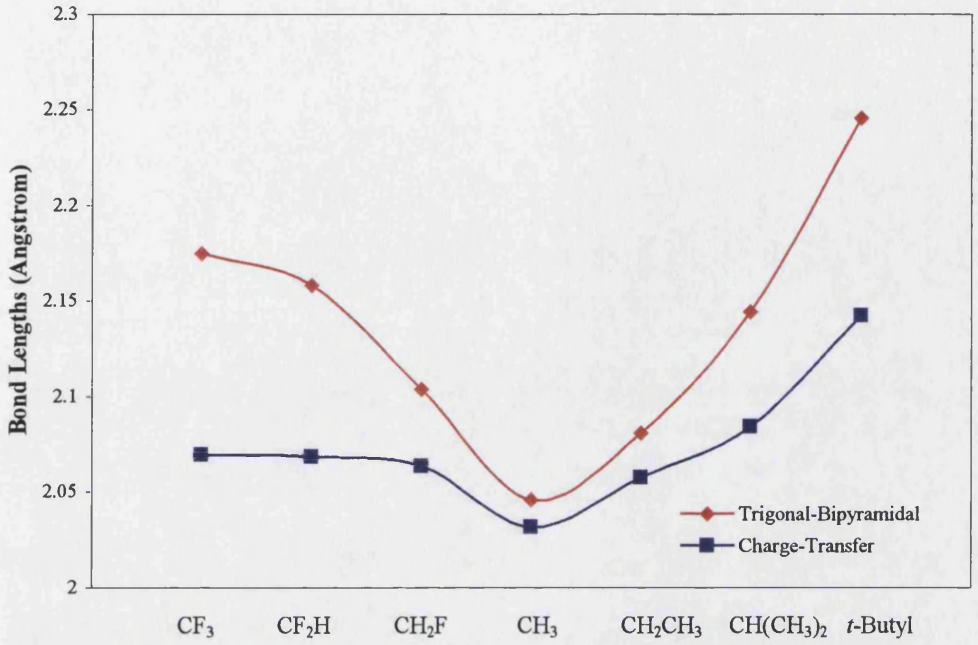

Figure 10.15: The variation of Se-C bond length with R-group, for the R_2SeI_2 molecule.

The least sterically hindered systems, those with the smallest R-groups, are the Me_2SeX_2 molecules. From table 10.10 it can be seen that the Se-C bond lengths for these systems in both the ψ-trigonal-bipyramidal and charge-transfer structures are around 2.04 Å. If this is assumed to be the preferred length for the Se-C bond, in the absence of any steric hindrance, it is apparent that the increase in R-group size causes an increase in the bond length of up to 0.2 Å in the most extreme case. This is of an appropriate order of magnitude, given the results of the single-point energy calculations, to have a significant effect on the favoured structure of the molecule, i.e. the reduction in total bonding energy as a result of the increased Se-C bond length may well influence the preferred molecular geometry.

It is also noticeable in figures 10.13, 10.14 and 10.15 that the increase in Se-C bond length as R gets bigger is far less in the charge-transfer structures than it is in the ψ-trigonal-bipyramidal. The destabilisation of the Se-C bond with increasing R-group size is more significant in the ψ-trigonal-bipyramidal structure. Additionally, the difference between the Se-C bond lengths in the ψ-trigonal-bipyramidal and charge-transfer structures is not linear with R-group size. (Figure 10.16) The charge-transfer structures with the fluorine containing R-groups have shorter (and hence more stable) bonds than those with non-fluorine containing R-groups of similar size. This is

particularly obvious if molecules containing the similarly sized CH_2CH_3 and CF_2H R-groups are examined.

R-group	Se-C bond length (Angstrom)					
	Chlorine		Bromine		Iodine	
	Trig-Bp	C-T	Trig-Bp	C-T	Trig-Bp	C-T
CF_3	2.178	2.068	2.176	2.073	2.175	2.069
CF_2H	2.155	2.067	2.155	2.071	2.158	2.068
CFH_2	2.100	2.063	2.102	2.065	2.104	2.063
CH_3	2.037	2.029	2.041	2.031	2.046	2.032
CH_2CH_3	2.070	2.053	2.075	2.056	2.081	2.057
$CH(CH_3)_2$	2.134	2.081	2.139	2.083	2.144	2.084
t-Butyl	2.248	2.142	2.248	2.145	2.245	2.142

Table 10.10: The variation in the length of the Se-C bond for the various conformations of R_2SeX_2. (R = CF_3, CF_2H, CFH_2, CH_3 CH_2CH_3, $CH(CH_3)_2$, *t*-Butyl) (X = F, Cl, Br, I, At.)

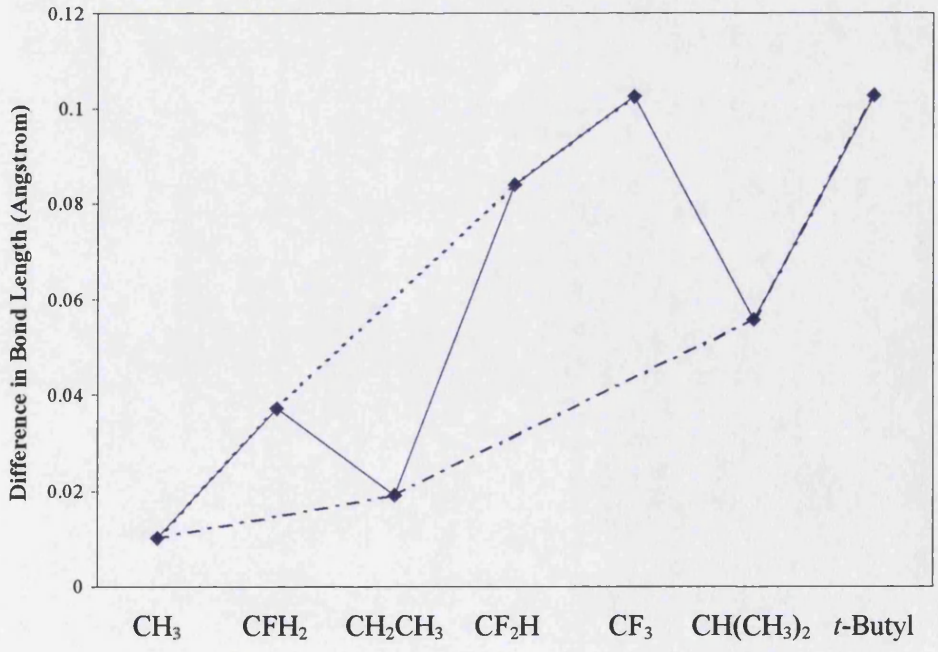

Figure 10.16: The difference between the Se-C bond length in the ψ-trigonal-bipyramidal and charge-transfer structures of R_2SeBr_2 in order of increasing R-group size.

If the Se-C bond lengths of both structures are plotted as a function of R-group size for the R_2SeBr_2 molecule (figure 10.17) it becomes apparent that the increase in bond length for the charge-transfer structure is roughly linear with R-group size. This is not the case for the ψ-trigonal-bipyramidal structures, however, where the spread of values is greater. Referring back to figures 10.13–15 and 10.16, two trends are apparent. The Se–C bond lengths in the charge-transfer conformations with the fluorinated R-groups remain roughly constant, whilst those in the ψ-trigonal-bipyramidal increase substantially. This increase in bond length and concomitant decrease in bond strength causes the ψ-trigonal-bipyramidal molecules with fluorine containing R-groups to become significantly less stable than their charge-transfer counterparts. In the molecules with non-fluorinated R-groups, an increase in the Se–C bond length and consequent destabilisation is seen in both conformations, although the ψ-trigonal-bipyramidal is more strongly affected.

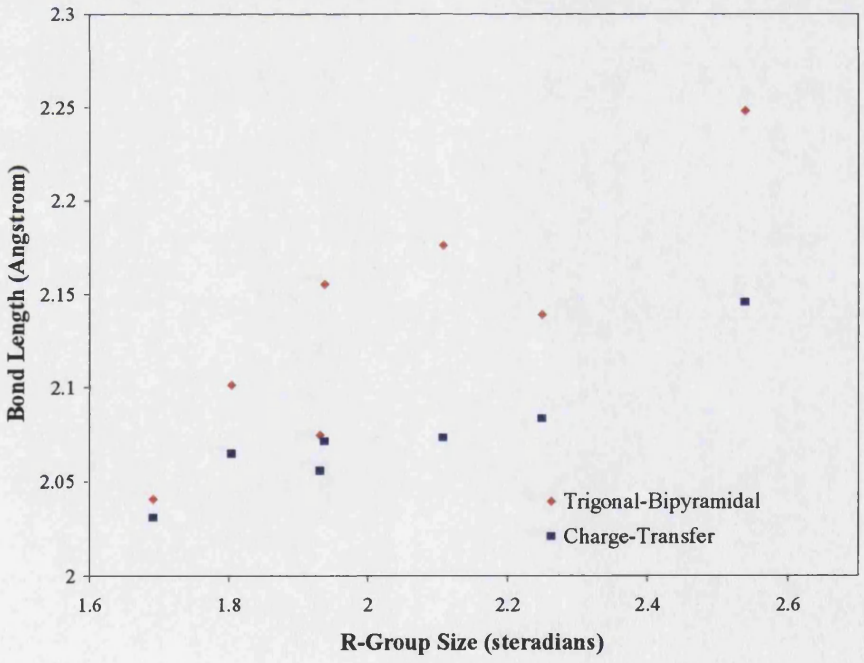

Figure 10.17: The variation of Se-C bond length in the R_2SeBr_2 molecule with R-group size (see table 10.9).

R-group	ψ-Trigonal-Bipyramidal		Charge Transfer	
	Selenium	Carbon	Selenium	Carbon
CF_3	0.41	1.61	0.09	1.55
CF_2H	0.41	1.21	0.09	1.15
CFH_2	0.48	0.79	0.15	0.75
CH_3	0.53	0.35	0.18	0.30
CH_2CH_3	0.51	0.22	0.17	0.20
$CH(CH_3)_2$	0.56	0.08	0.16	0.07
t-Butyl	0.52	-0.04	0.19	-0.06

Table 10.11: The Mulliken charge on the central selenium atom and the carbon atoms bonded to it, in units of e, for X = Cl.

R-group	ψ-Trigonal-Bipyramidal		Charge Transfer	
	Selenium	Carbon	Selenium	Carbon
CF_3	0.44	1.61	0.11	1.55
CF_2H	0.43	1.21	0.10	1.16
CFH_2	0.49	0.80	0.16	0.75
CH_3	0.54	0.33	0.18	0.30
CH_2CH_3	0.53	0.22	0.17	0.20
$CH(CH_3)_2$	0.53	0.08	0.17	0.07
t-Butyl	0.55	-0.05	0.19	-0.06

Table 10.12: The Mulliken charge on the central selenium atom and the carbon atoms bonded to it, in units of e, for X = Br.

R-group	ψ-Trigonal-Bipyramidal		Charge Transfer	
	Selenium	Carbon	Selenium	Carbon
CF_3	0.31	1.62	0.06	1.55
CF_2H	0.30	1.22	0.05	1.16
CFH_2	0.38	0.80	0.10	0.74
CH_3	0.43	0.33	0.12	0.30
CH_2CH_3	0.41	0.22	0.12	0.20
$CH(CH_3)_2$	0.41	0.07	0.11	0.06
t-Butyl	0.43	-0.07	0.12	-0.07

Table 10.13: The Mulliken charge on the central selenium atom and the carbon atoms bonded to it, in units of e, for X = I.

Tables 10.11–13 show the charges on the selenium atoms and the R-group carbon atoms bonded to them. The charges on the carbon atoms are roughly constant for any given R-group in either conformation, taking values ranging from –0.06 e to +1.62 e. The more positive values occur in the fluorine containing R-groups and can be attributed to the electronegativity of the fluorine drawing electrons away from the central carbon atom.

The presence of charge on both the carbon and selenium atoms causes an electrostatic interaction between them. Calculation of the strength of this interaction for the X = Br molecules demonstrates its significance.

R-group	Electrostatic Repulsion (kJ/mol)	
	ψ-Trigonal-Bipyramidal	Charge-Transfer
CF_3	452	114
CF_2H	635	78
CFH_2	509	81
CH_3	141	37
CH_2CH_3	129	23
$CH(CH_3)_2$	28	8
t-Butyl	-17	-7

Table 10.14: The electrostatic repulsion between central selenium atom and the carbon atoms bonded to it, at their equilibrium distance. X = Br.

It is clear from table 10.14 that the strength of the electrostatic repulsion in the ψ-trigonal-bipyramidal conformation is much stronger than in its charge-transfer counterpart. If these values are compared to the strength of the repulsion at the unhindered minimum bond distance found when R = CH_3 (table 10.15) it can also be seen that the strength of the repulsion is considerably reduced in a number of cases by the bond extension found in the ψ-trigonal-bipyramidal molecules. It is also important to notice that the strength of the electrostatic interaction given in tables 10.14 and 10.15 is for one Se–C bond. In fact the overall effect in the molecule is twice this due to the presence of two R-groups and, hence, two Se–C bonds.

R-group	Electrostatic Repulsion (kJ/mol)	
	ψ-Trigonal-Bipyramidal	Charge-Transfer
CF_3	482	116
CF_2H	354	79
CFH_2	267	82
CH_3	121	37
CH_2CH_3	79	23
$CH(CH_3)_2$	29	8
t-Butyl	-19	-8

Table 10.15 The electrostatic repulsion between central selenium atom and the carbon atoms bonded to it at a distance of 2.04Å. X = Br.

If these tables (10.14 and 10.15) are compared with the graphs of Se-C bond length (figures 10.13–15) a number factors become apparent. Firstly, the charge-transfer structures with perfluorinated R-groups (to the left of R = CH_3 in the figures) experience almost no Se–C bond extension, whilst those without fluorine (to the right of R = CH_3) are extended. The ψ-trigonal-bipyramidal structures all experience Se–C bond extension to varying degrees.

The similarly sized CH_2CH_3 and CF_2H R-groups experience a similar degree of bond extension in the charge-transfer structures. The next two non-fluorinated R-groups experience considerably more extension, a trend mimicked in the ψ-trigonal-bipyramidal structures. These two R-groups are the largest in this study and therefore the most prone to steric effects. Since the charges on both the selenium and carbon

atoms in these molecules are small the electrostatic interactions are negligible. It is reasonable to assume that the bond extension seen in both conformations is therefore due to steric hindrance. Since the ψ-trigonal-bipyramidal conformation has an additional lone pair of electrons to accommodate around the central selenium atom, it should experience a greater effect than the charge-transfer molecule, which is seen in the greater extension of the Se–C bond.

In the perfluorinated R-groups two influences are at work. The strength of the electrostatic repulsion in the charge-transfer structures is not high, particularly in comparison with the ψ-trigonal-bipyramidal conformations. Only a very slight increase over the minimum bond length is seen, which does not lead to a significant decrease in the electrostatic repulsion. The slight increase in Se–C bond length, moving to the left away from CH_3, is therefore attributed to the steric hindrance caused by the increasing R-group size.

The bond length extension seen in the perfluorinated ψ-trigonal-bipyramidal structures is significantly greater than that found in the charge-transfer structures. The difference between the two conformations is also rather more in CF_2H than in the similarly sized CH_2CH_3 and so cannot be attributed to sterics alone as it is in the non-fluorinated ligands. The selenium atoms in the perfluorinated ψ-trigonal-bipyramidal structures are much more positively charged than those in the charge-transfer structures, which, in combination with the high charge on the carbon atoms in the R-groups, leads to a high electrostatic repulsion between the selenium and carbon atoms. This electrostatic repulsion is significantly reduced by the extension of the Se–C bond from 2.04Å to the equilibrium position. The longer bonds found in the perfluorinated ψ-trigonal-bipyramidal molecules are attributable to the comparatively high charges on the selenium and carbon atoms.

10.3: Conclusions

Only one of the explanations for the observed structural behaviour of R_2SeX_2 molecules discussed at the beginning of this chapter is reliably demonstrated by the present theoretical results. That polar bonds stabilise a hyperco-ordinate central selenium atom is clearly seen in the increasing tendency towards ψ-trigonal-bipyramidal structures with ascent of the halogen group.

It is less straightforward to explain the other trends in the structural behaviour of this group of molecules. A combination of two factors, electron withdrawal by and size of the R-groups, and the effect that they have on the strength of the carbon-selenium bond, are essential to describe the changes in structure. The charge-transfer structure is favoured by the larger R-groups, regardless of the strength of electron withdrawal of the R-groups themselves: the acidity of the selenium does not dictate the positions of the halogens and neither is the position solely due to steric effects.

Although the larger R-groups favour a charge-transfer structure, this is only purely due to the steric hinderances in the non-fluorinated R-groups. If no other factor had influence then tertiary-butyl compounds would favour the charge-transfer structure more than the smaller carbon tri-fluoride compounds. This is not found to be the case and hence at least one other factor must play a role. A key variable was found to be the strength of the carbon-selenium bond. This is certainly affected by sterics since the larger R-groups produce longer Se-C bonds that are weaker, hence destabilising the molecule. However, the charges on the bonded Se and C atoms also have a considerable influence on the length of the Se-C bond.

In the charge-transfer molecules the positive charge on the selenium atom is relatively small and so the bond lengths in these molecules are principally influenced by sterics. In the ψ-trigonal-bipyramidal conformation the effect of the electronegativity of the Se-bound halogens leads to a larger Se positive charge. When this is coupled with a charge on the carbon atom of the R-group it produces a strong electrostatic interaction that affects the carbon-selenium bond strength. The fluorine containing R-groups have a larger positive charge on the bonding carbon atom than those that do not contain fluorine because electrons are withdrawn by the fluorine atoms. This results in

increased Se-C repulsion, a lengthening of the Se–C bond length and hence a reduction of the carbon-selenium bond strength and a destabilisation of the ψ-trigonal-bipyramidal structures with fluorine containing R-groups with respect to their charge-transfer analogues. Consequently the molecules with fluorine-containing R-groups favour the charge-transfer structure more strongly than they would if influenced by sterics alone.

Chapter 11: Future Research Directions

All he'd wanted were the same answers the rest of us want. Where did I come from? Where am I going? How long have I got?

Deckard
Blade Runner
1982

This thesis has presented work in a number of areas, all of which have scope for considerable further development.

11.1: Studies with Density Functional Theory

Although this was only a minor component of the total research, it presents a number of interesting opportunities for further work. Establishing a route for the transformation of realgar would be a contribution to both our understanding of the basic chemistry and its application to conservation and preservation. The initial stages of that transformation have been explored but the process does not appear to be uni-molecular. A DFT-based study of this system using a non-molecular formulism would allow potential interactions between molecules to be investigated. This could elucidate the final steps in the transformation, and may allow the χ-phase to be identified by comparison of vibrational wavenumbers with experimental results.

Studies of the di-halogen mixed R-group selenium compounds have shown that their structural behaviour is dominated by the strength of the carbon-selenium bond within the context of the polarity of the halogen-selenium bonds and the nature of the R-group. If the R-group is large then steric effects will weaken the carbon-selenium bond, favouring the charge-transfer structure. If small, then the ψ-trigonal-bipyramidal structure is more stable. However, if the selenium atom is partially charged as a result of electron withdrawal by the halogens, then the charge on the carbon of the R-group becomes significant. If this is also large as a result of electron withdrawal in the R-group then the selenium-carbon bond is weakened favouring the charge-transfer

structure more than would be expected according to sterics alone. This is particularly seen in the case of R-groups containing electron withdrawing fluorine.

The behaviour of these molecules with homogeneously paired halogens and R-groups is now entirely predictable. However, the effect of mixed halogens and R-groups, with varying electron-withdrawing properties and size, has not been explored. The first step in extending the present results to more complex systems would to calculate the minimum energy optimised geometries of systems with the same homogeneous pairs of R-groups, but with heterogeneous halogen pairs, and vice versa. This would allow predictions of the behaviour that would be expected with entirely hetrogeneous molecules, and an investigation into the applicability of these present results to systems such as the triorgano-Group 15 compounds experimentally characterised by Bricklebank et al. [Bric]

11.2: Raman Microscopy in Art, Archaeology and Conservation

The stated aim of this research was the production of a historico-geographical pigment distribution map to cover all pigment materials, everywhere, from pre-history to the current day. Studies in this thesis have been limited to a very few historico-geographical areas: early western manuscripts, oriental manuscripts and modern art with one or two archaeological artefacts. Other workers have completed studies in areas such as medieval miniatures or American rock art but in general these have been one-off examinations rather than coherent programs of study. This leaves pigment use in a range of different media, including wall painting, furniture, ceramics and works of art on wood or canvas, from a variety of different places and periods still unexamined. In addition although studies of, for example, English Anglo Saxon manuscript illustration have been in depth, they are not as yet exhaustive – all manuscripts of known provenance have not yet been examined. In the same way, studies of Islamic material presented here represent a brief overview of a huge area both historically and geographically.

The immediate challenge for the future is how to proceed. As far as manuscript illumination is concerned, research could be directed in one of two obvious directions:

depth or breadth. Continued studies in the areas commenced in this thesis would add to our understanding of the fine structure of pigment use, charting more closely the geographical or historical variations in the areas currently under investigation. Extension of the studies to adjacent geographical areas or historical periods would put the present results into a much wider context in terms of pigment use on a larger scale enabling changing influences to be studied.

In the case of the Anglo Saxon manuscript studies more is to be gained by broadening the selection of materials for study. Although the analysis of English Anglo Saxon material has not been exhaustive, a significant amount of material has been examined. It is already clear from these results that pigment use across Europe as a whole is subject to geographical influence as far as availability is concerned. This has led to a demonstrable historical variation in the use of pigments in English manuscripts. Widening the study to include schools of French, German, Dutch and Italian illumination would allow these variations to be examined and their influence seen.

For the study of Islamic manuscripts the reverse is true. The present results are an overview with large geographical and historical coverage in which only very broad trends were seen. The sample size for each different type of manuscript was small and large gaps exist between samples. It would be productive to fill those gaps. For example, all of the Mughal manuscripts examined come from the reign and court atelier of the Emperor Akbar but the physical extent of his empire was such that there were several schools of manuscript illumination scattered, in principal cities, across a large geographical area. Further, the artistic innovations, and possible changes in materials, of his successors have not been examined. The same is true of all of the Islamic material studied – filling the gaps would bring to light historically or geographically local variations in technique and materials.

The application of Raman microscopy to art authentication has been demonstrated comprehensively in this research and can only benefit from the extension of pigment mapping to a wider range of materials. In general there is no further research required into the authenticity of the Vinland Map since the present results are conclusive. However the controversy still rages, so further examination of the materials, perhaps

with a more sophisticated Raman microscope such as that used for the majority of the rest of this research, can only be beneficial.

The application of Raman microscopy to modern pigments is so far largely unexplored. However the potential for development in forensic sciences is immense. Pigments are used extensively in modern life, from automobile paint through to ball-point pen ink. The ability to identify tiny evidential traces of these materials and relate them to specific sources is a powerful tool for law enforcement.

However, as with art analysis and pigment analysis in general, the application of Raman microscopy to forensic science relies on the quality of its databases. Although it is relatively unusual to encounter a new pigment in the study of historical materials, the range of modern pigments is large and expanding. Few Raman spectra of modern pigments have been recorded and databases of Raman spectra are also extremely deficient in the area of organic (that is plant or animal derived) pigments and dyes.

The solution to the first problem is simply to analyse, systematically, as extensive a range of modern pigments as possible and publish these both in scientific literature and in a publicly accessible forum such as on the internet. The second problem is more difficult since the impediment to the analysis of organic materials is technical. Some organic pigments, such as indigo, carmine and kermes, have given reasonable Raman spectra but many others suffer from acute fluorescence that makes them difficult to analyse with visible laser wavelengths. However, recent developments such as remote fibre optic probes for FT-Raman systems offer the possibility of non-destructive in situ analysis with fluorescence avoidance that may allow substances such as Tyrian purple or plant derived pigments to be identified.

The production of an historico-geographical map of the use of pigments globally through history is a substantial undertaking attainable only in stages through inter-disciplinary collaboration. However, this work is a step towards that aim.

References

ADF ADF2.3 – 2002.01, SCM, Theoretical Chemistry, Vrije Universiteit, Amsterdam, The Netherlands, http://www.scm.com

Addi Catalogue of Additions, an ongoing publication, British Museum Press, London

Alex Insular Manuscripts, 6th to the 9th Century, J. J. G. Alexander in A Survey of Manuscripts Illuminated in the British Isles I, J. J. G. Alexander (Ed.), 1978, Harvey Miller, London

Back The Lindisfarne Gospels, Janet Backhouse, 1992, Phaidon Press Ltd., London

Bac1 The Golden Age of Anglo-Saxon Art 966 – 1066, Janet Backhouse, D. H. Turner and Leslie Webster (Eds.), 1984, British Museum Publications Limited, London

Baer Indian Yellow, N. S. Baer et al. in Artists' Pigments; a Handbook of Their History and Charateristics, Robert L. Feller (Ed.), 1986, Cambridge University Press, Cambridge

Bae1 Relativistic Atomic Orbital Contractions and Expansions: Magnitudes and Explanations, E. J. Baerends et al., Journal of Physics B, 1990, 23, pg 3225 - 3240

Banw Fundamentals of Molecular Spectroscopy, Colin N. Banwell and Elaine M. McCash, 4th Edition, 1994, McGraw-Hill Book Company Europe, Maidenhead

Beck Density-Functional and Exchange-Energy Approximation with Correct Asymptotic Behaviour, A. D. Becke, Physical Review A, 1998, 38, pg 3098 – 3100

Beis Concepts of Modern Physics, Arther Beiser, 5th Edition, 1995, McGraw-Hill Inc., New York

Bell Raman Spectroscopic Library of Natural and Synthetic Pigments (pre ~ 1850 AD), Ian M. Bell, Robin J. H. Clark and Peter J. Gibbs, Spectrochimica Acta, 1997, A53, pg 2159 - 2179

Best Non-Destructive Pigment Analysis of Artefacts by Raman Microscopy, Stephen P. Best, Robin J. H. Clark and Robert Withnall, Endeavour, 1992, 16, pg 66 – 73

Bind William Blake; His Art and Times, David Bindman, 1982, Thames and Hudson Ltd., London

Bish Latin Palaeography, Antiquity and Middle Ages, Bernard Bishcoff, translated by D. O. Cronin and D. Ganz, 1990, Cambridge University Press, Cambridge

Blai An Introduction to Anglo-Saxon England, Peter Hunter Blair, 1956, Cambridge University Press, Cambridge

Bona Light-Induced Variations in Realgar and β-As_4S_4: X-Ray Diffraction and Raman Studies, P. Bonazzi et al., American Mineralogist, 1996, 81, pg 874 – 880

Bric Synthesis and Structural Characterisation of R_3AsX_2 Compounds (R = Me, Ph, p-FC_6H_6 or p-$MeOC_6H_4$; X_2 = Br_2, I_2 or IBr); Dependency of Structure on R, X and the Solvent of Preparation, Neil Bricklebank et al., Journal of the Chemical Society, Dalton Transactions, 1995, pg 3873 - 3879

Brow Anglo-Saxon Manuscripts, Michelle P. Brown, 1991, The British Library, London

Bro1 A guide to Western Historical Scripts from Antiquity to 1600, Michelle P. Brown, 1993, The British Library, London

Bro2 Mercian Manuscripts? The 'Tiberius Group' and its Historical Context, Michelle P. Brown, in Mercia, an Anglo-Saxon Kingdom in Europe, M. P. Brown and C. Farr (Eds.), 2001, University of Leicester Press, Leicester

Bro3 "In the Beginning was the Word": Books and Faith in the Age of Bede, Michelle P. Brown, The Jarrow Lecture 2000, J. & P. Bealls Ltd., Newcastle upon Tyne

Burg Library of FT-Raman Spectra of Pigments, Minerals, Pigment Media and Varnishes, and Supplement to Existing Library of Raman Spectra of Pigments With Visible Excitation, L. Burgio and R. J. H. Clark, Spectrochimica Acta, 2001, A57, pg 1491 - 1521

Burn Interference Measurements in the Spectra of Neon and Natural Mercury, Kevin Burns, Kenneth B. Adams and Jean Longwell, Journal of The Optical Society of America, 1950, 40, pg 339 - 344

Butl William Blake 1757 – 1827, Martin Butlin, 1990, Tate Gallery Publications, London

But1 William Blake, Martin Butlin, 1978, Tate Gallery, London

Caha Private communication, Noa Cahaner McManus, 2002, formerly of the Tate Gallery, London

Cahi The Vinland Map, Revisited: New Compositional Evidence on Its Inks and Parchment, T. A. Cahill et al., Analytical. Chemistry, 1987, 59, pg 829 – 833

Cah1 Compositional and Structural Studies of the Vinland Map and Tartar Relation, T. A. Cahill, B. H. Kusko in The Vinland Map and The Tartar Relation, R. A. Skelton, T. E. Manston and G. D. Painter, (Eds.), 1995, Yale University Press, New Haven and London, 1995, pg xxix – xxxix

Canb Persian Painting, Sheila R. Canby, 1993, British Museum Press, London

Chan The Technique of Mughal Painting, Moti Chandra, 1949, The U. P. Historical Society, Lucknow

Chap Unpublished data, private communication, Tracey Chaplin, 2002, University College London

Clar Simplification of Near-Infrared Visualisation Techniques for Identifying Blue Pigments In-Situ on Manuscripts, Mark Clarke and Marieke Meijers, Proceedings of the Sixth International Seminar on The Care and Conservation of Manuscripts, The Royal Library, Copenhagen, 19 – 20 October 2000

Cla1 Non-Destructive Pigment Analysis of Artefacts by Raman Microscopy, Stephen P. Best, Robin J. H. Clark and Robert Withnall, Endeavour, 1992, 16, pg 66 - 73

Cla2 Analysis of 16th Century Qazwini Manuscripts by Raman Microscopy and Remote Laser Raman Microscopy, R. J. H. Clark and P. J. Gibbs, Journal of Archaeological Chemistry, 1998, 25, pg 621 – 62

Cla3 Raman Microscopy of a 13th Century Illuminated Text, Robin J. H. Clark and Peter J. Gibbs, Analytical Chemistry, 1998, 70, pg 99A – 104A

Coop Chemical Bonding to Hypercoordinate Second-Row Atoms: d Orbital Participation Versus Democracy, David L. Cooper et al., Journal of the American Chemical Society, 1994, 116, pg 4414 – 4426

Delh Raman Microprobe and Microscope with Laser Excitation, M. Delhaye and P. Dhamelincourt, Journal of Raman Spectroscopy, 1975, 3, pg 33 - 43

Dodw On Divers Arts by Theophilus, Edited and Translated by C. R. Dodwell, 1986, Oxford University Press, Oxford

Dod1 The Canterbury School of Illumination 1066 – 1200, C. R. Dodwell, 1954, Cambridge University Press, Cambridge

Dona Determination of the Radioncarbon Age of the Parchment of the Vinland Map, D. J. Donahue, J. S. Olin and G. Harbottle, Radiocarbon, 2002, 44, pg 45 - 52

Dorm Drawing in English Manuscripts c. 950 – c. 1385: Technique and Purpose, Sally Dormer, 1991, Thesis: (PhD) University of London (Courtauld Institute of Art)

Doug The Light-Induced Transformation of Realgar to Pararealgar, D. L. Douglass, Chichang Shing and Ge Wang, American Mineralogist, 1992, 77, pg 1266 - 1274

Down Adhesive Testing at the Canadian Conservation Institute – An Evaluation of Selected Poly(Vinyl Acetate) and Acrylic Adhesives, Jane L. Down et al., Studies in Conservation, 1996, 41, pg 19 - 44

Edlė The Dispersion of Standard Air, Bengt Edlėn, Journal of the Optical Society of America, 1953, 43, pg 339 – 344

Edwa FT Raman Microscopy of Untreated Natural Plant Fibres, H. G. M. Edwards, D. W. Farwell and D. Webster, Spectrochimica Acta, 1997, A 53, pg 2383 – 2392

Emme Art of India – Paintings and Drawings in the Victoria and Albert Museum, Anna Emmett, 1992, Emmett Publishing, UK

Eppe Applications of Charge Transfer Devices in Spectroscopy, Patrick M. Epperson et al., Analytical Chemistry, 1988, 60, pg 327A – 335A

EQCL Evangelium Quattuor Codex Lindisfarnensis, T. D. Kendrick et al. (Eds.): Volume 1, 1956, full facsimile, UrsGrafVerlag; Volume 2, 1960, commentary, Olten

Ethe Catalogue of Persian Manuscripts in the India Office Library, Hermann Ethé, 1903, Horace Hart, Oxford

Fan Application of Density Functional Theory to Infrared Absorption Intensity Calculations on Main Group Molecules, Liangyou Fan and Tom Ziegler, Journal of Chemical Physics, 1992, 96, pg 9005 - 9012

Fan1 Application of Density Functional Theory to Infrared Absorption Intensity Calculations on Transition-Metal Carbonyls, Liangyou Fan and Tom Ziegler, 1992, Journal of Physical Chemistry, 96, pg 6937 - 6941

Feil A History of England, Keith Feiling, 1950, Macmillan and Co., London

Ferr Introductory Raman Spectroscopy, John R. Ferraro and Kazuo Nakamoto, 1994, Academic Press Limited, London

Fitz Orpiment and Realgar, Elisabeth West Fitzhugh in Artists' Pigments; a Handbook of Their History and Charateristics III, Elisabeth West Fitzhugh (Ed.), 1997, Oxford University Press, Oxford

Gett Painting Materials – A Short Encyclopedia, Rutherford J. Gettens and George L. Stout, 1966, Dover Publications Inc., New York

Get1 Vermilion and Cinnabar, Rutherford J. Gettens, Robert L. Feller and W. T. Chase in Artists' Pigments – a Handbook of Their History and Characteristics, Vol. 2, Ashok Roy (Ed.), 1993, Oxford University Press, Oxford

Godf Crystallographic Characterisation of Dihalogenodimethylselenium Compounds, Me_2SeX_2 (X = CL, Br or I) and the Dependance of Their Structures on the Nature of the Halogen, Stephen M. Godfrey et al., Journal of the Chemical Society, Dalton Transactions, 1997, pg 1031 – 1035

Grab Art and Culture in the Islamic World, Oleg Grabar in Islam: Art and Architecture, Marcus Hattstein and Peter Delius (Eds.), 2000, Könemann Verlagsgesellscaft mbH, Cologne

Hall England, A Concise History, F. E. Halliday, 1989, Thames and Hudson Ltd., London

Hame A History of Illuminated Manuscripts, Christopher de Hamel, 1994, Phaidon Press Limited, London

Ham1 Medieval Craftsmen: Scribes and Illuminators, Christopher de Hamel, 1992 British Museum Press, London

Hatt Glossary of Dynasties, Markus Hattstein in Islam: Art and Architecture, Marcus Hattstein and Peter Delius (Eds.), 2000, Könemann Verlagsgesellscaft mbH, Cologne

Hat1 History of the Safavids and Qajars, Markus Hattstein in Islam: Art and Architecture, Marcus Hattstein and Peter Delius (Eds.), 2000, Könemann Verlagsgesellscaft mbH, Cologne

Hat2 History of the Ottomans: The Rise and Fall of a World Empire, Markus Hattstein in Islam: Art and Architecture, Marcus Hattstein and Peter Delius (Eds.), 2000, Könemann Verlagsgesellscaft mbH, Cologne

Hill Conservation, Mounting and Storage Solutions for Two Hamzanama Folios, Anna Hillcoat-Imanishi, Pauline Webber and Michael Wheeler, The Paper Conservator, 1999, 23, pg 26 – 35

Hohe Inhomogeneous Electron Gas, P. Hohenberg and W. Kohn, Physical Review B, 1965, 136, pg 864 - 871

Ings The Norse Settlement at L'Anse Aux Meadows, Newfoundland, A. S. Ingstan, Acta Archaeologica, 1970, 41, pg 109 – 154

Jens Introduction to Computational Chemistry, Frank Jensen, 1999, John Wiley and Sons, London

Kalt Evidence For Actinide Metal to Ligand π Backbonding. Density Functional Investigations of the Electronic Structure of $[\{(NH_2)_3(NH_3)U\}_2(\mu^2\text{-}\eta^2\text{: }\eta^{2\text{-}N}{}_2)]$, Nikolas Kaltsoyannis and Peter Scott, Chemical Communications, 1998, pg 1665 - 1666

Kal1 Computational Study of the Electronic and Geometric Structures of the Dihalogenodimethylselenium Compounds, Me_2SeX_2 (X = F, Cl, Br, I or At), Nikolas Kaltsoyannis, Journal of the Chemical Society, Dalton Transactions, 1997, pg 4759 – 4764

Kloc Analysis of Pigments and Inks on Oil Paintings and Historical Manuscripts Using Total Reflection X-Ray Fluorescence Spectroscopy, R. Klockenkämper, A. von Bohlen and L. Moens, X-Ray Spectrometry, 2000, 29, pg 119 – 129

Koch A Chemist's Guide to Density Functional Theory, Wolfram Koch and Max C. Holthausen, 2001, Wiley-VCH Verlag GmbH, Weinheim

Kohn Self-Consistent Equations Including Exchange and Correlation Effects, W. Kohn and L. J. Sham, Physical Review A, 1965, 140, pg 1133 - 1138

Krah The Chemistry of Synthetic Dyes and Pigments, S. E. Krahler (Ed.), 1955, Reinhold Publishing Corporation, New York

Kühn Verdigris and Copper Resinate, Hermann Kühn in Artists' Pigments – a Handbook of Their History and Characteristics, Vol. 2, Ashok Roy (Ed.), 1993, Oxford University Press, Oxford

Küh1 Lead-Tin Yellow, Hermann Kühn in Artists' Pigments – a Handbook of Their History and Characteristics, Vol. 2, Ashok Roy (Ed.), 1993, Oxford University Press, Oxford

Laid Physical Chemistry, Keith J. Laidler and John H. Meiser, 1999, Houghton Mifflin Company, Boston

Lamb Traces of the Past, J. B. Lambert, 1997, Pegasus Books, Reading, MS., pg 150

Lee Development of the Colle-Salvetti Correlation-Energy Formula Into a Functional of the Electron-Density, Chengteh Lee, Weitao Yang and Robert G. Parr, Physical Review B, 1988, 37, pg 785 - 789

Long Early History of the Raman Effect, D. A. Long, International Reviews in Physical Chemistry, 1988, 7, pg 317 – 349

Lon1 Raman Spectroscopy, D. A. Long, 1977, McGraw-Hill, Inc., London

Lost The Art of the Book in India, Jeremiah P. Losty, 1982, The British Library, London

Los1 Indian Book Painting, Jeremiah P. Losty, 1986, The British Library, London

Lowe Codicies Latini Antiquiores Part III, Great Britain and Ireland, E. A. Lowe, 1935, Clarendon Press, Oxford

Macn A World in Transition: Early Cartography of the North Atlantic, D. McNaughton, in Vikings: The North Atlantic Saga, W. W. Fitzhugh and E. I. Ward, (Eds.), 2000, Smithsonian Institution Press, Washington, pg 257 - 269

Mart Reaction of a Mo Atom with H_2, N_2 and O_2: A Density Functional Study, Ana Martínez, Andreas M. Köster and Dennis R. Salahub, Journal of Physical Chemistry, 1997, A 101, pg 1532 - 1541

Mccr Chemical Analytical Study of the Vinland Map; Report to Yale University Library, W. C. McCrone, 1974, New Haven

Mcc1 The Vinland Map, W. C. McCrone, Analytical. Chemistry. 1988, 60, pg 1009 – 1018

Mcc2 Judgement Day for the Turin Shroud, W. C. McCrone, 1996, McCrone Research Institute, Chicago, pg 38 – 48

Mcc3 Vinland Map 1999, W. C. McCrone, Microscope, 1999, 47, pg 71 - 74

Mere Handlist of Persian Manuscripts 1895 – 1966, G. M. Meredith-Owens, 1968, The Trustees of the British Museum, London

Moon A Note on the Use of False-Color Infrared Photography in Conservation, Thomas Moon, Michael R. Schilling and Sally Thirkettle, Studies in Conservation, 1992, 37, Pg 42 –52

Morg Early Gothic Manuscripts [II] 1250 – 1285, Nigel Morgan in A Survey of Manuscripts Illuminated in the British Isles IV, J. J. G. Alexander (Ed.), 1982, Harvey Miller, London

Mull Electronic Population Analysis on LCAO-MO Molecular Wave Functions. I., R. S. Mulliken, Journal of Chemical Physics, 1955, 23, pg 1833 - 1840

Muni Spectroscopic Investigation and Normal Mode Analysis of As_4S_4 Polymorphs, M. Muniz-Miranda et al., Spectrochimica Acta, 1996,

Olin Without Comparative Studies of Inks, What Do We Know About the Vinland Map?, J. S. Olin, Pre-Columbiana, 2000, 2, pg 27 – 36

Orna Pigment Analysis of The Glajor Gospel Book of U. C. L. A., Mary Virginia Orna O. S. U. and Thomas F. Mathews, Studies in Conservation, 1981, 26, pg 57 – 72

Perd Accurate and Simple Analytic Representation of the Electron-Gas Correlation Energy, John P. Perdew and Yue Wang, Physical Review B, 1992, 45, pg 13244 - 13249

Per1 Density-Functional Approximation for the Correlation Energy of the Inhomogeneous Electron Gas, John P. Perdew, Physical Review B, 1986, 33, pg 8822 - 8824

Pykk Calculated Structures of MO_2^{2+}, MN_2 and MP_2 (M = Mo, W), Pekka Pyykkö and Toomas Tamm, Journal of Physical Chemistry, 1997, A 101, pg 8107 - 8114

Port Painters, Paintings and Books, An Essay on Indo-Persian Technical Literature, 12^{th} – 19^{th} Centuries, Yves Porter, 1994, Manohar, New Delhi

Rama A New Type of Secondary Radiation, C. V. Raman and K. S. Krishnan, Nature, 1928, 121, pg 501

Rieu Catalogue of Turkish Manuscripts in the British Museum, Charles Rieu, 1888, Longmans and Co., London

Roge Mughal Miniatures, J. M. Rogers, 1993, The Trustees of the British Museum, London

Rous Complex of Dinitrogen with Trivalent Uranium, Paul Roussel and Peter Scott, Journal of the American Chemical Society, 1998, 120, pg 1070 - 1071

Sand Gothic Manuscripts [II] 1286 – 1385, Lucy Freeman Sandler in A Survey of Manuscripts Illuminated in the British Isles V, J. J. G. Alexander (Ed.), 1986, Harvey Miller, London

Scot Later Gothic Manuscripts [II] 1390 – 1490, Kathleen L. Scott in A Survey of Manuscripts Illuminated in the British Isles VI, J. J. G. Alexander (Ed.), 1996, Harvey Miller, London

Sell 1066 And All That, Walter Sellar and Robert Yeatman, 1933, Methuen and Co., London

Shri Inorganic Chemistry, D. F. Shriver and P. W. Atkins, 3rd Edition, 1999, Oxford University Press, Oxford

SICD S. I. Chemical Data, Gordon Aylward and Tristan Findlay, 3rd Edition, 1994, John Wiley and Sons, Brisbane

Skel The Vinland Map and The Tartar Relation, R. A. Skelton, T. E. Manston and G. D. Painter, 1995, Yale University Press, New Haven and London

Slat Atomic Shielding Constants, J. C. Slater, Physical Review, 1930, 36, pg 57 - 64

Sla1 A Simplification of the Hartree-Fock Method, J. C. Slater, Physical Review, 1951, 81, pg 385 - 390

Stre Calculation of the Raman Shift in Vacuum, G. Strey, Spectrochimica Acta, 1968, 25A, pg 163 – 167

Suma Miniature Painting Technique, Dr. Sumahendra, 1990, Rootprang Publications, Jaipur

Tate Tate collections, general collection, at www.tate.org.uk, as of August 2002.

Temp Anglo-Saxon Manuscripts 900 – 1066, Elzbieta Temple in A Survey of Manuscripts Illuminated in the British Isles II, J. J. G. Alexander (Ed.), 1976, Harvey Miller, London

teVe Chemistry with ADF, G. te Veld et al., Journal of Computational Chemisty, 2001, 22, pg 931 - 967

Thom Il Libro dell'Arte by Cennino D'Andrea Cennini, translated by Daniel V. Thompson JR., 1933, Dover Publications Ltd., New York

Thol Catalogue of Ancient Manuscripts in the British Museum Part II, Latin, E. M. Thompson, 1884, British Museum, London

Titl Miniatures From Turkish Manuscripts: A Catalogue and Subject Index of paintings in the British Library and the British Museum, Norah M. Titley, 1981, The British Library, London

Tit1 Miniatures from Persian Manuscripts, Norah M. Titley, 1997, The British Library, London

Tops Indian Court Painting, Andrew Topsfield, 1994, Her Majesty's Stationery Office, London

Towe The Vinland Map: Still a Forgery, K. M. Towe, Accounts of Chemical Research, 1990, 23, pg 84 – 87

Town Joyce Townsend of the Tate Gallery, London, quoted in Blake's Heaven, Tim Radford, 12th October 2000, Science, The Guardian

Trea Treasures of the Earth – the Minerals and Gemstone Collection, 1995, Orbis Publishing Ltd., London

Tren Characterisation of Pararealgar and Other Light-Induced Transformation Products of Realgar by Raman Microspectroscopy, Karen Trentelman, Leon Stodulski and Mark Pavlosky, Analytical Chemistry, 1996, 68, pg 1755 - 1761

USPa US Patent 2,383,762 28th August, 1945

Vand Raman Spectroscopic Database of Azo Pigments and Application to Modern Art Studies, P. Vandenabeele et al., Journal of Raman Spectroscopy, 2000, 31, pg 509 – 517

Van1 Analysis with Micro-Raman Spectroscopy of Natural Organic Binding Media and Varnishes Used in Art, P. Vandenabeele et al., Analytica Chimica Acta, 2000, 407, pg 261 – 274

vanL Relativistic Regular Two-Component Hamiltonians, E. van Lenthe, E. J. Baerends and J. G. Snijders, Journal of Chemical Physics, 1993, 99, pg 4597 – 4605

van1 Relativistic Total Energy Using Regular Approximations, E. van Lenthe, E. J. Baerends and J. G. Snijders, Journal of Chemical Physics, 1994, 101, pg 9783 – 9792

van2 Geometry Optimizations in the Zero Order Regular Approximation for Relativistic Effects, E. van Lenthe, A. Ehlers and E. J. Baerends, Journal of Chemical Physics, 1999, 110, pg 8943 - 8953

Vaug History of Islam in the Indian Subcontinent, Philippa Vaughan in Islam: Art and Architecture, Marcus Hattstein and Peter Delius (Eds.), 2000, Könemann Verlagsgesellscaft mbH, Cologne

Vau1 Decorative Arts, Philippa Vaughan in Islam: Art and Architecture, Marcus Hattstein and Peter Delius (Eds.), 2000, Könemann Verlagsgesellscaft mbH, Cologne

Vau2 William Blake, William Vaughan, 1977, Thames and Hudson Ltd., London

Vosk Accurate Spin-Dependent Electron Liquid Correlation Energies for Local Spin Density Calculations: A Critical Analysis, S. H. Vosko, L. Wilk and M. Nusair, Canadian Journal of Physics, 1980, 58, pg 1200 – 1211

Wale Supplementary Handlist of Persian Manuscripts, 1966 – 1998, Muhammad Isa Waley, 1998, The British Library, London

Wall The Viking Settlement at L'Anse aux Meadows, B. L. Wallace, in Vikings: The North Atlantic Saga, W. W. Fitzhugh and E. I. Ward (Eds.), 2000, Smithsonian Institution Press, Washington, pg 208 – 216

Wal1 The Strange Case of The Vinland Map, H. Wallis et al., The Geographical Journal, 1974, pg183 – 214

Wash The Case of The Vinland Map, W. E. Washburn, in The Vinland Map and The Tartar Relation, R. A. Skelton, T. E. Manston and G. D. Painter, 1995, Yale University Press, New Haven and London, xxi - xxvii

Webs The Making of England – Anglo-Saxon Art and Culture AD 600 – 900, Leslie Webster and Janet Backhouse (Eds.), 1991, British Museum Publications Ltd, London

Whee Private Communication, Michael Wheeler, Senior Paper Conservator, Victoria and Albert Museum, March 2001

Zeig Approximate Density Functional Theory as a Practical Tool in Molecular Energetics and Dynamics, Tom Zeigler, Chemical Reviews, 1991, 91, pg 651 – 667

Appendix 1: Anglo Saxon and Later Manuscripts in the British Library

Figure A1.1: The Evangelist portrait of St. Mark - Cotton Ms Nero D IV f. 93v.

Figure A1.2: The Initial page of the Gospel of St. Luke – Cotton Ms Nero D IV f. 139.

Figure A1.3: The First Page of Canon Tables – Royal Ms 1 B VII f. 9.

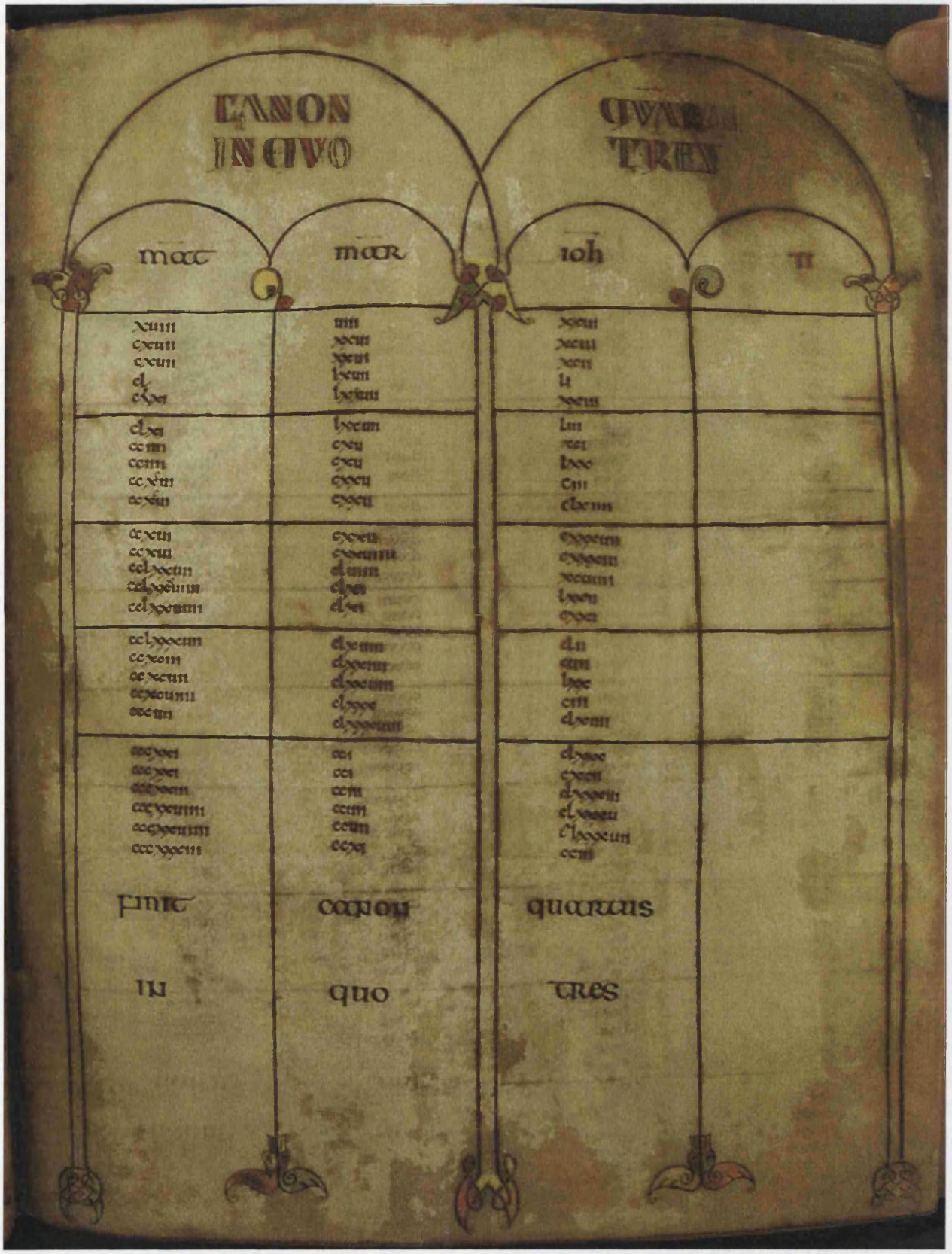

Figure A1.4: The Seventh Page of Canon Tables – Royal Ms 1 B VII f. 12.

Figure A1.5: The St Luke Miniature - Add. Ms. 40618 f. 21v.

Figure A1.6: The pigments of the Second St Luke Miniature - Add. Ms. 40618 f. 22v.

Figure A1.7: The Initial of the Gospel of St Luke - Add. Ms. 40618 f. 23.

Figure A1.8: The St John Miniature - Add. Ms. 40618 f. 49v.

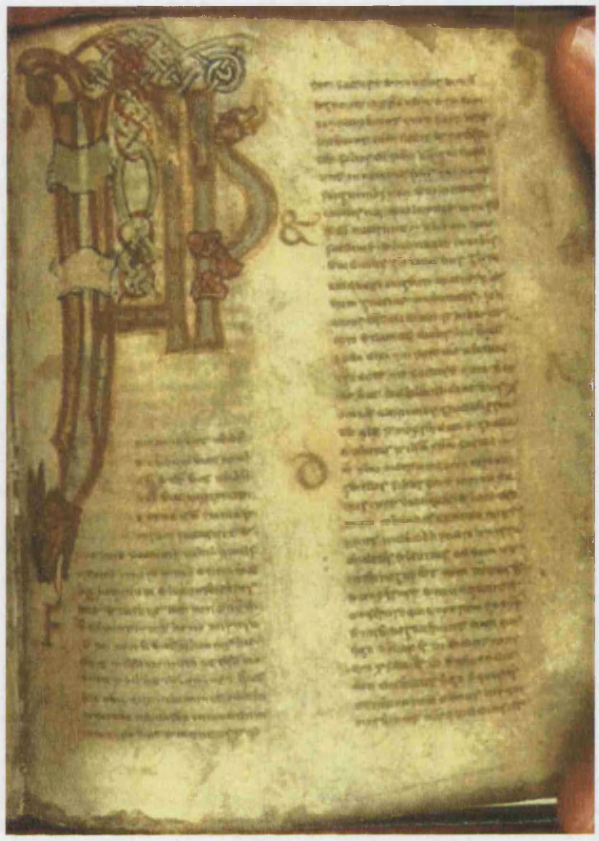

Figure A1.9: The Initial to the Gospel of St John - Add. Ms. 40618 f. 50.

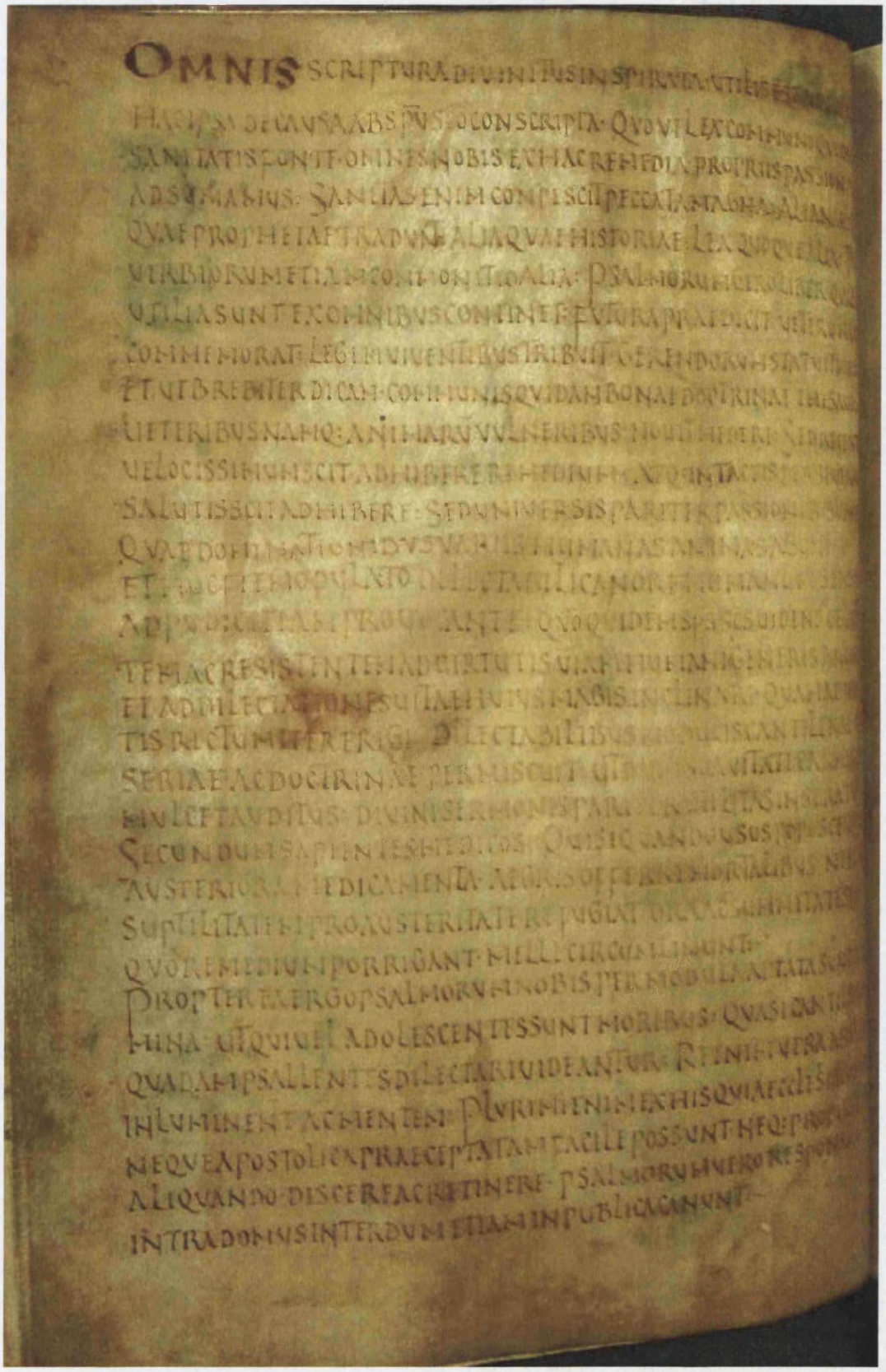

Figure A1.10: A rubricated page - Cotton Ms. Vespasian A1 f. 2v.

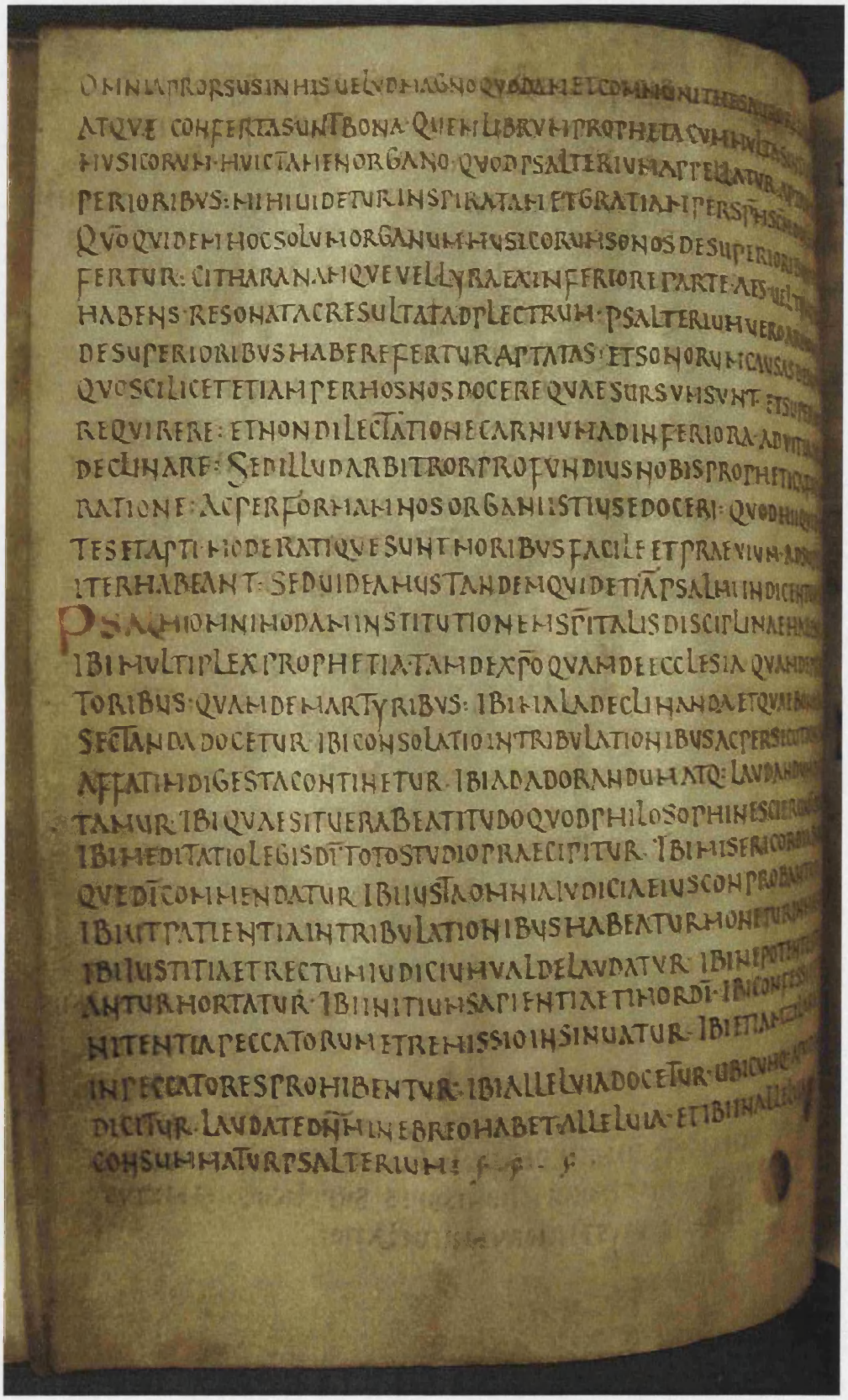

Figure A1.11: A rubricated page - Cotton Ms. Vespasian A1 f. 3v.

Figure A1.12: David and his musicians - Cotton Ms. Vespasian A1 f. 30v.

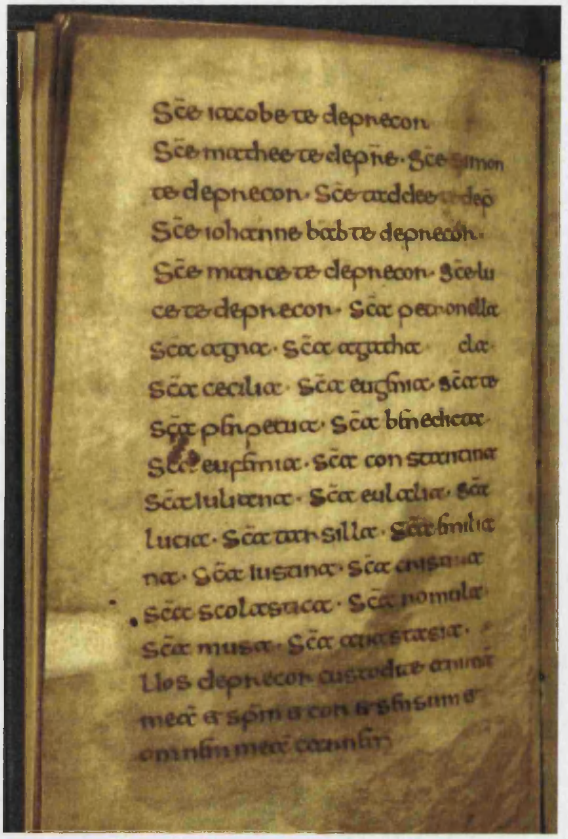

Figure A1.13: A rubricated text page - Harley Ms 7653 f. 1v.

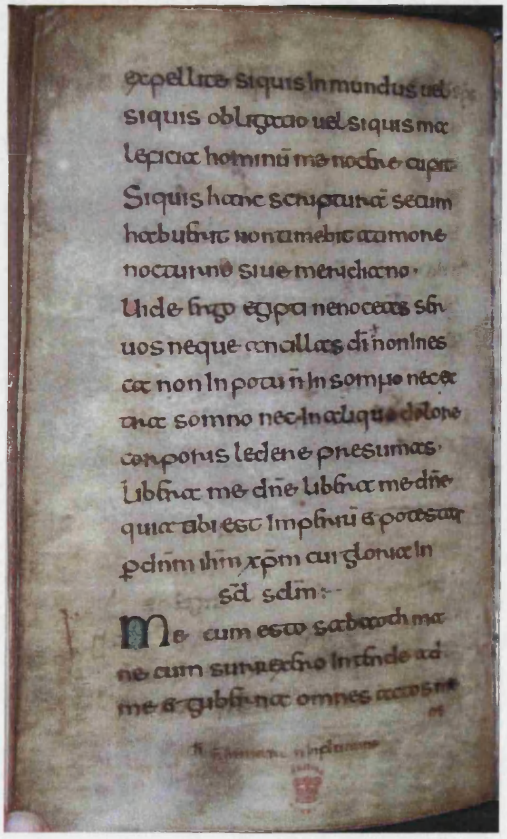

Figure A1.14: A rubricated text page - Harley Ms 7653 f. 2v.

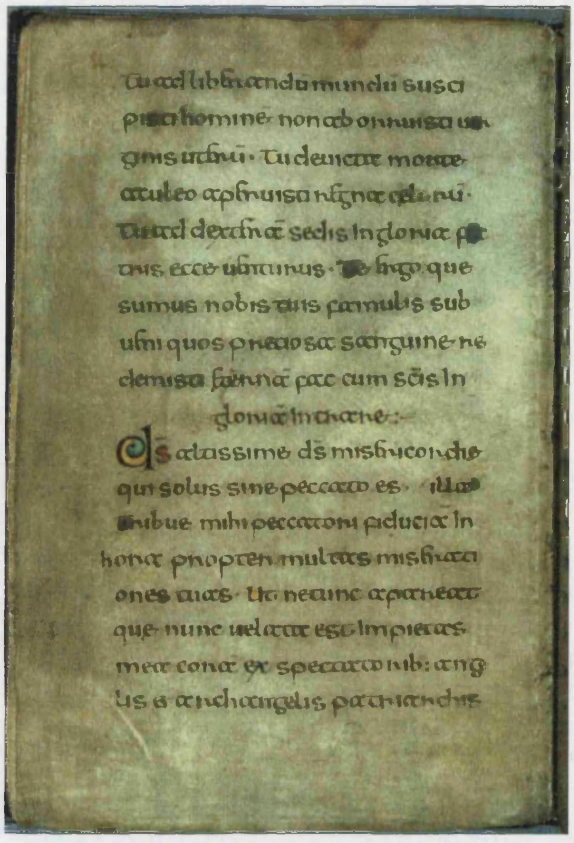

Figure A1.15: A rubricated text page - Harley Ms 7653 f. 6v.

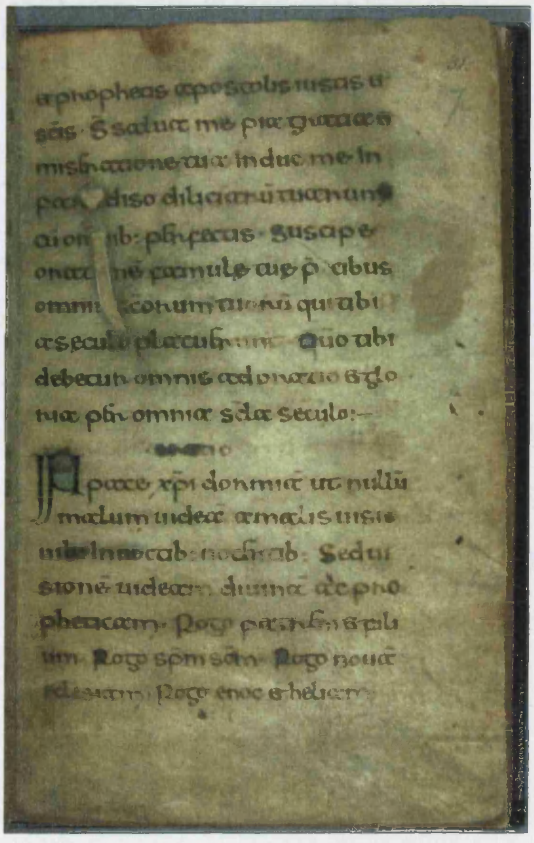

Figure A1.16: A rubricated text page - Harley Ms 7653 f. 7.

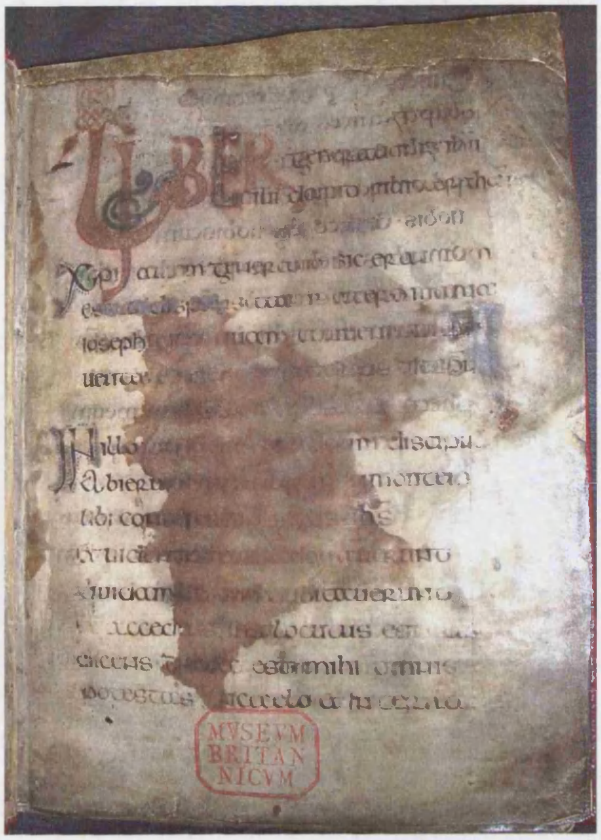

Figure A1.17: A rubricated text page - Royal Ms 2 A XX f2.

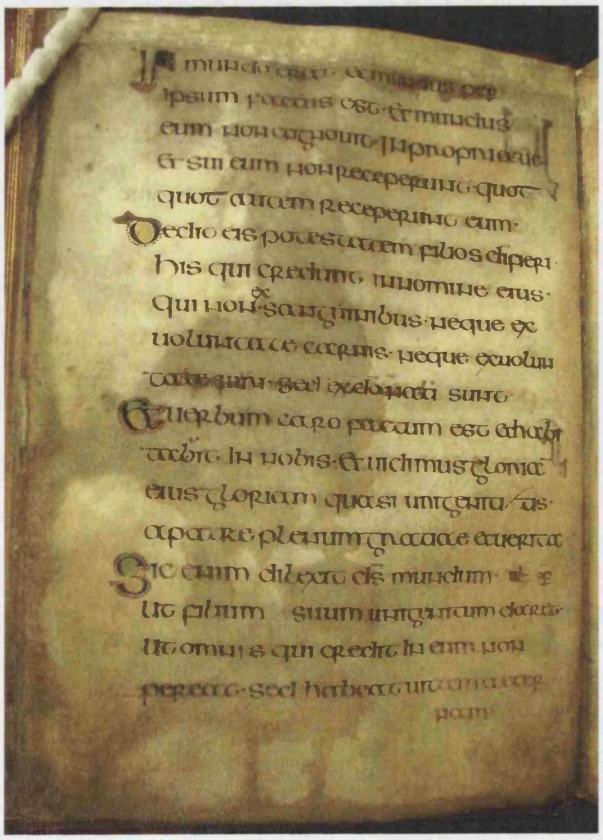

Figure A1.18: A rubricated text page - Royal Ms 2 A XX f4v.

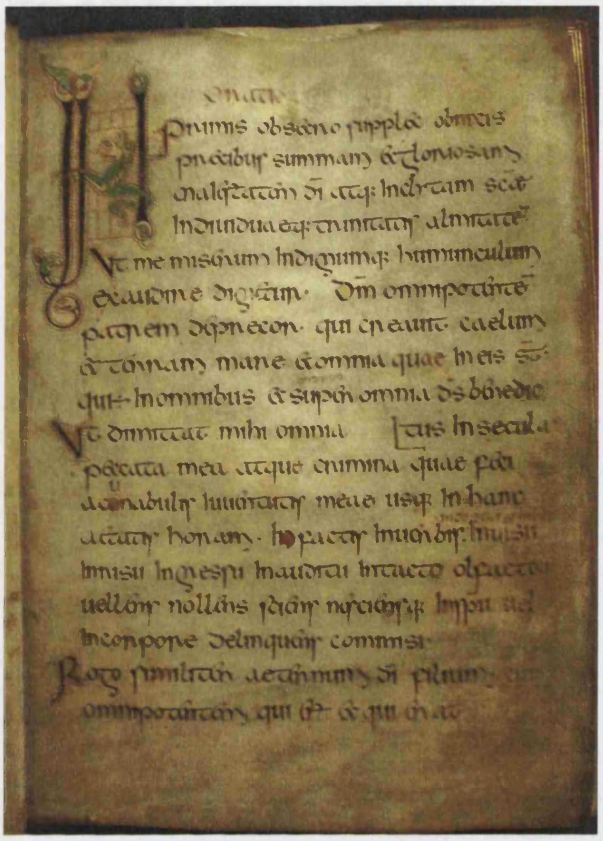

Figure A1.19: A zoomorphic initial page - Royal Ms 2 A XX f17.

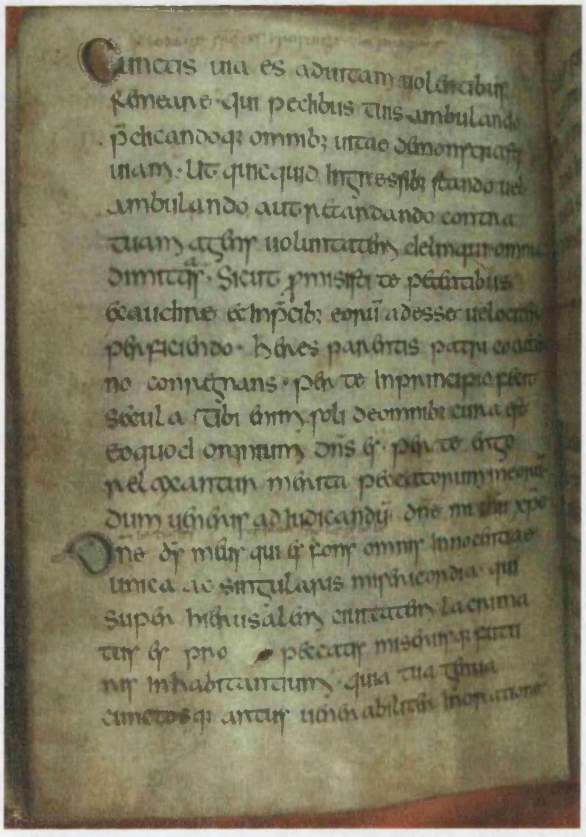

Figure A1.20: A rubricated text page - Royal Ms 2 A XX f29v.

Figure A1.21: The first page of Canon Tables - Royal Ms I E VI f. 4.

Figure A1.22: The second page of Canon Tables - Royal Ms I E VI f. 4v.

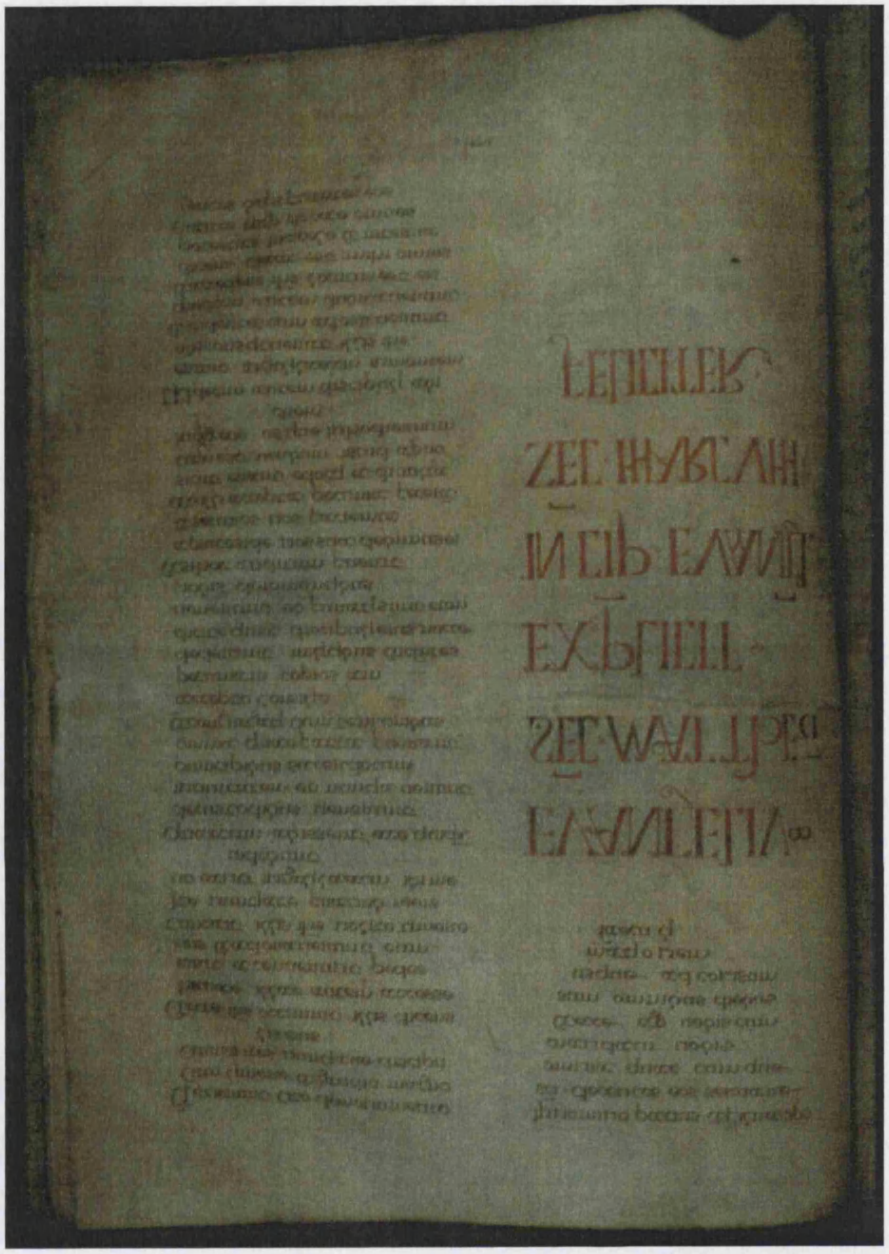

Figure A1.23: The Explicit Page of St. Matthews Gospel - Royal Ms I E VI f. 28v.

Figure A1.24: The Evangelist Miniature of the Gospel of St. Mark - Royal Ms I E VI f. 30v.

Figure A1.25: The Incipit Page of the Gospel of St. Luke - Royal Ms I E VI f. 43.

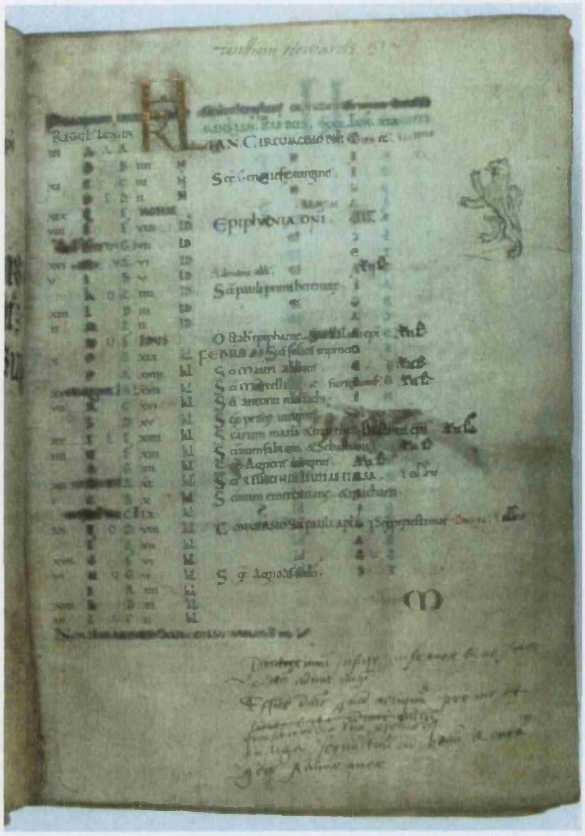

Figure A1.26: The first page of the Calendar - Arundel Ms 155 f. 2.

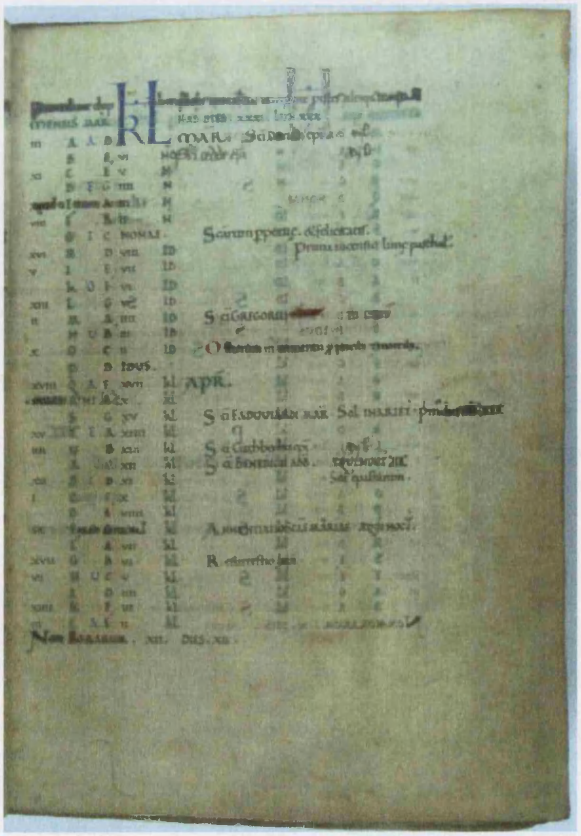

Figure A1.27: The third page of the Calendar - Arundel Ms 155 ff. 3.

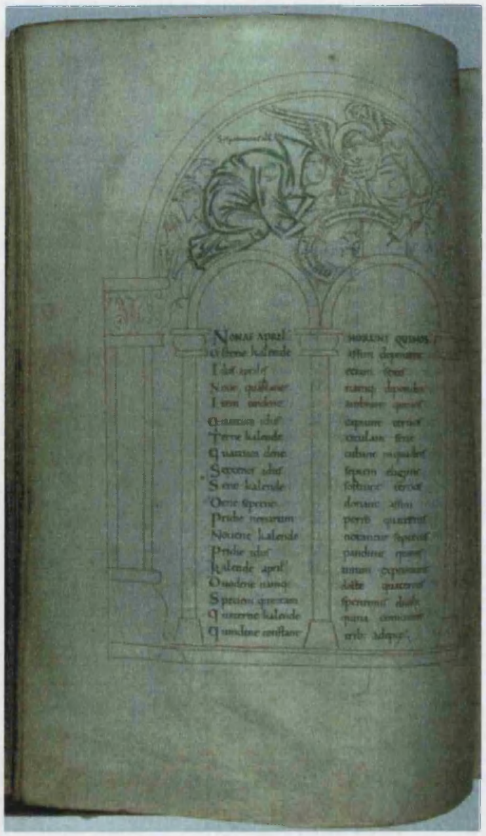

Figure A1.28: From the Computistical Tables - Arundel Ms 155 f. 9v.

Figure A1.29: The Opening of Psalm 1 - Arundel Ms 155 f. 12.

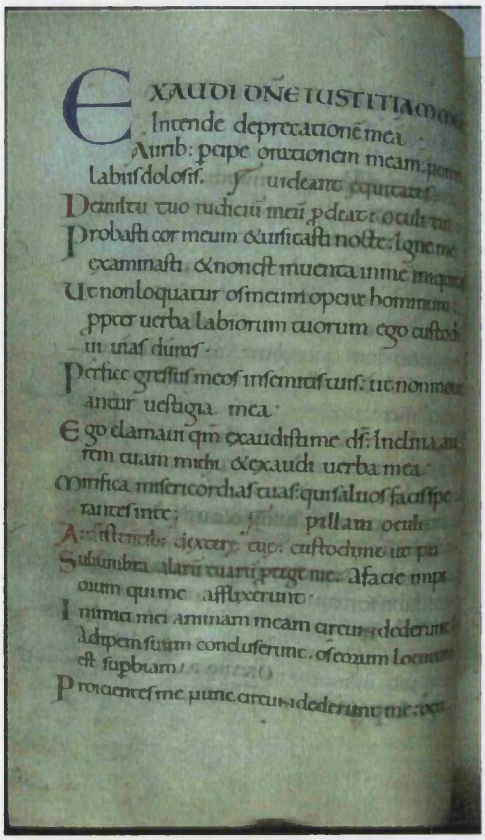

Figure A1.30: A rubricated page - Arundel Ms 155 f. 21v.

Figure A1.31: The Miniature of St. Benedict - Arundel Ms 155 f. 133.

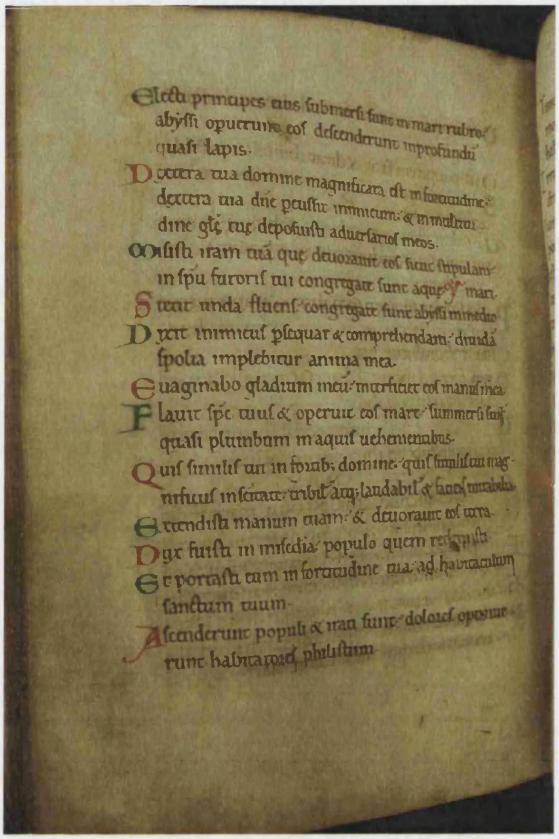

Figure A1.32: A rubricated page - Arundel Ms 155 f. 135v.

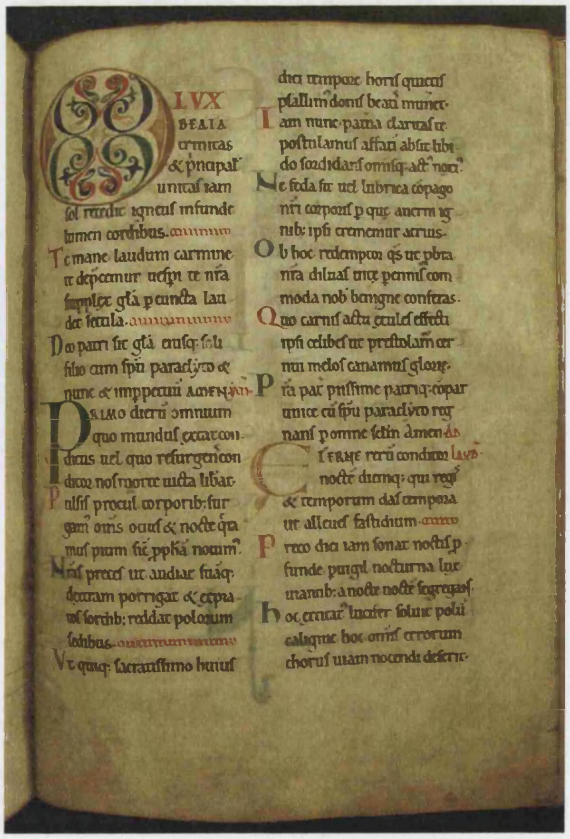

Figure A1.33: A 12th century addition - Arundel Ms 155 f. 147.

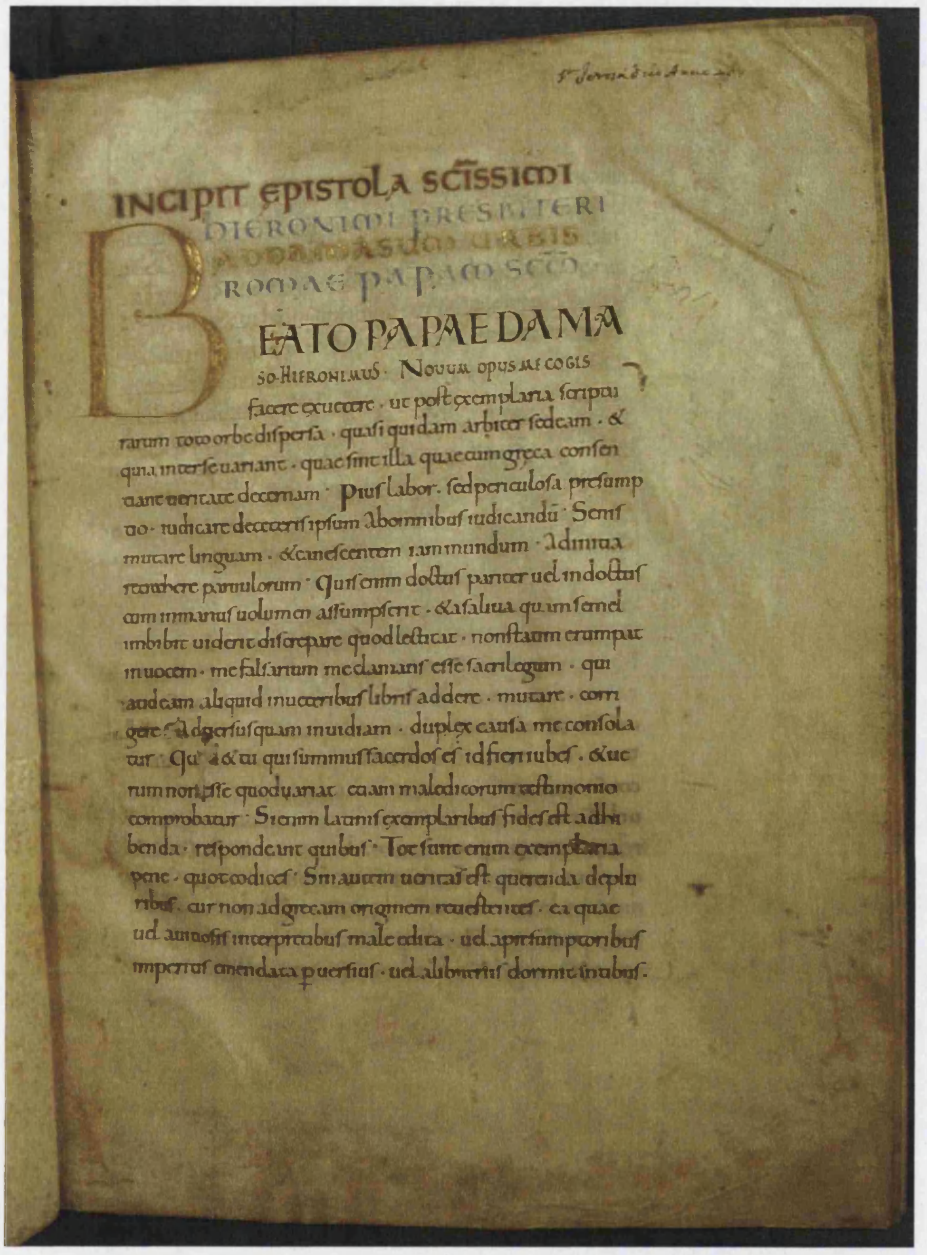

INCIPIT EPISTOLA SCISSIMI
HIERONIMI PRESBITERI
ROMAE PAPAM SCO
BEATO PAPAE DAMA
SO HIERONIMUS Nouum opus me cogis
facere exigere ut post exemplaria scriptu
rarum toto orbe dispersa quasi quidam arbiter sedeam &
quia inter se uariant quae sint illa quae cum greca consen
tiant ueritati decernam Prius labor sed periculosa presump
tio iudicare de ceteris ipsum a omnibus iudicandu Semi
mutare linguam & canescentem iam mundum admitta
reuocare paruulorum Quis enim doctus pariter uel indoctus
cum immanus uolumen assumpserit & a fatua quam semel
imbibit uiderit discrepare quod lectitat nonstatim erumpat
in uocem me falsarium me clamans esse sacri legum qui
audeam aliquid in ueteribus libris addere mutare cor
rigere Adgersus quam in diam duplex causa me consola
tur Qui & ei qui summus sacerdos est id fieri iubet & ue
rum non esse quod uariat ea iam maledicorum testimonio
comprobatur Si enim latinis exemplaribus fides est adhi
benda respondeant quibus Tot sunt enim exemplaria
pene quot codices Si autem ueritas est quaerenda de plu
ribus cur non ad graecam origenem reuertimur ea quae
ud antiqui interpretes male edita ud a prisumptoribus
imperiti emendata pueriliter ud a librariis dormitantibus

Figure A1.34: A text page - Add. Ms. 34890 f. 1.

Figure A1.35: The Evangelist Miniature of St. Matthew - Add. Ms. 34890 f. 10v.

A1.36: The Evangelist Miniature of St. Luke - Add. Ms. 34890 f. 73v.

Figure A1.37: The Evangelist Miniature of St. John - Add. Ms. 34890 f. 114v.

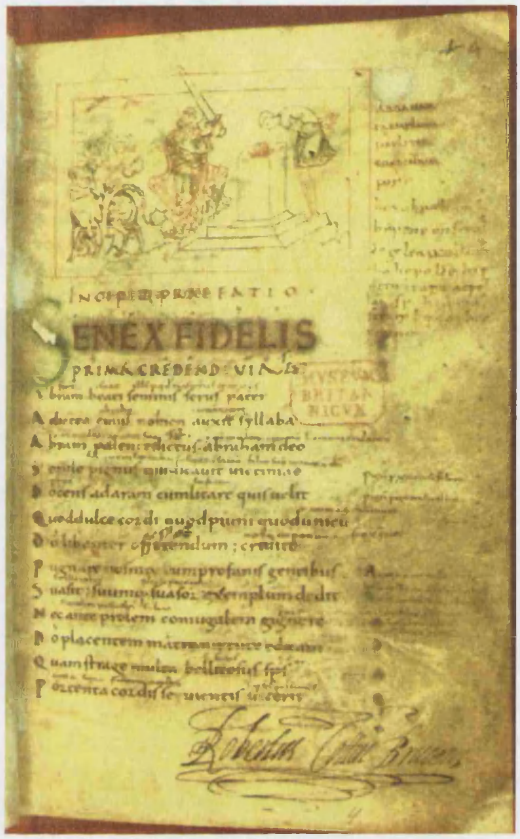

Figure A1.38: An illustrated page - Cotton Cleopatra C VIII f. 4.

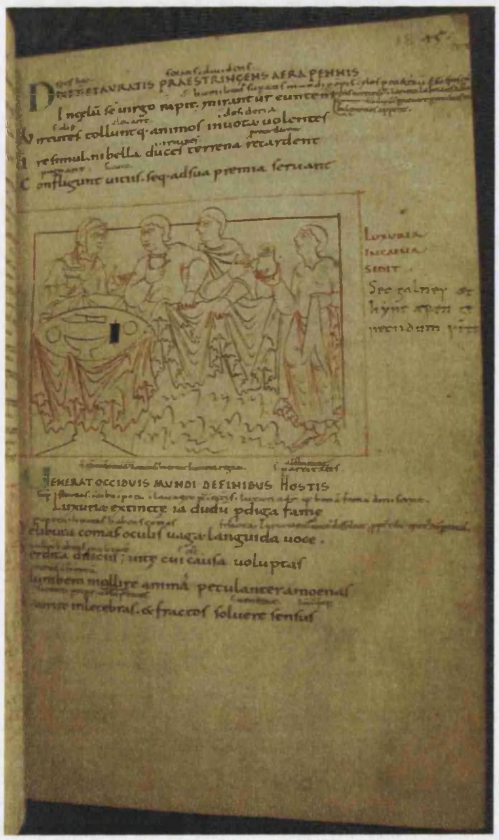

Figure A1.39: An illustrated page - Cotton Cleopatra C VIII f. 18.

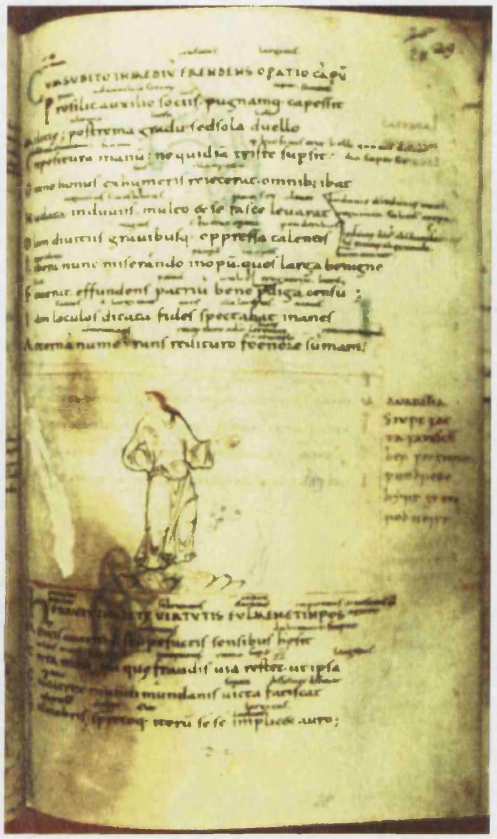

A1.40: An illustrated page - Cotton Cleopatra C VIII f. 28.

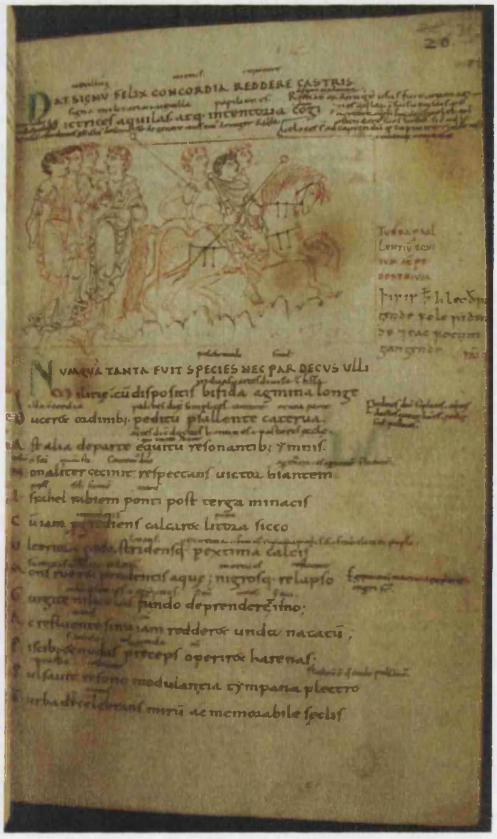

Figure A1.41: An illustrated page - Cotton Cleopatra C VIII f. 31.

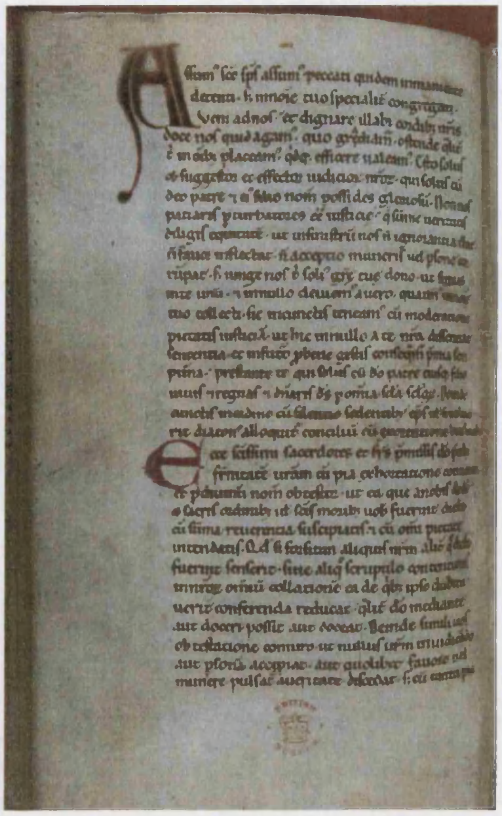

Figure A1.42: A decorated page from the second manuscript - Cotton Cleopatra C VIII f. 38v.

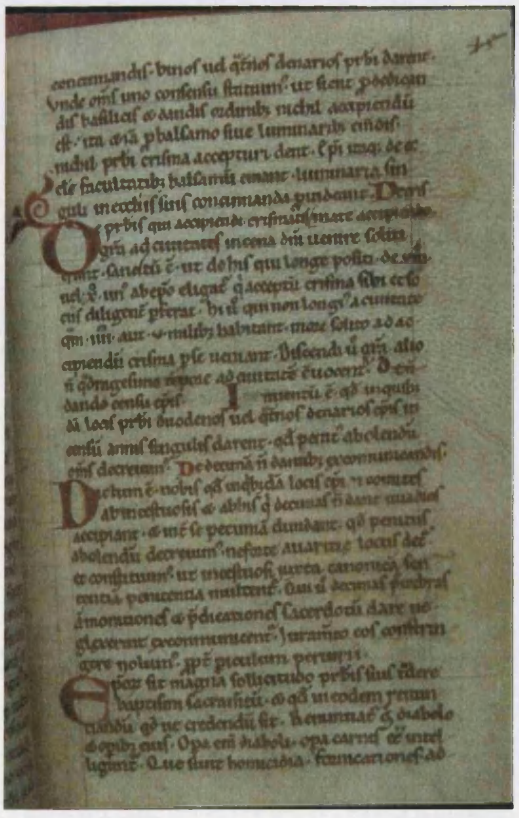

Figure A1.43: A decorated page from the second manuscript - Cotton Cleopatra C VIII f. 48.

Figure A1.44: St John on Patmos – Add. Ms 42555 f. 5.

Figure A1.45: Christ in Mandorla with Evangelist Symbols and Clerics – Add Ms 42555 f.6.

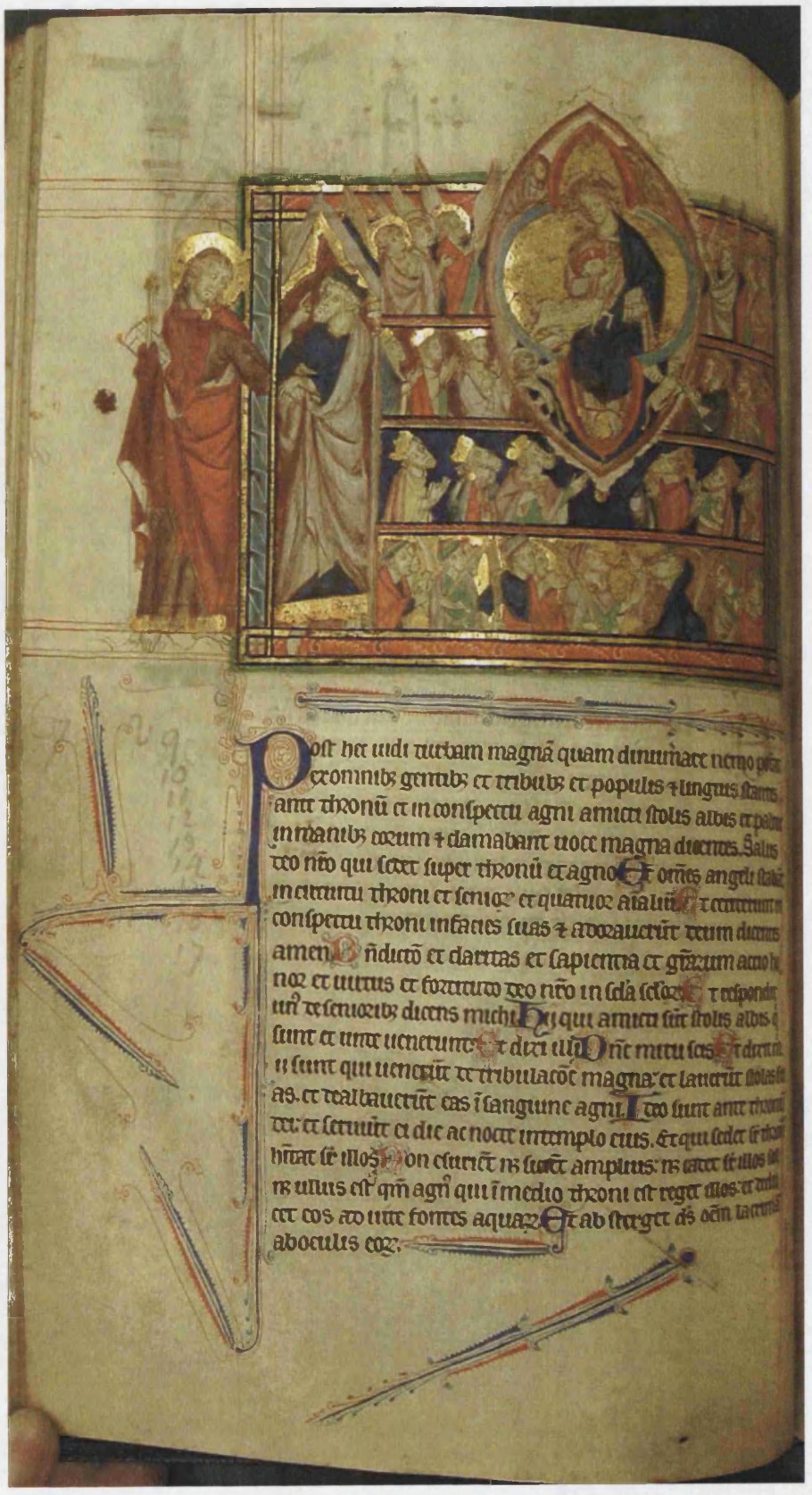

Figure A1.46: St. John with Christ and Agnus Dei – Add Ms 42555 f. 18v.

Figure A1.47: Moses Receiving the Law With Souls in Peril on the Sea - Add Ms 42555 f. 22.

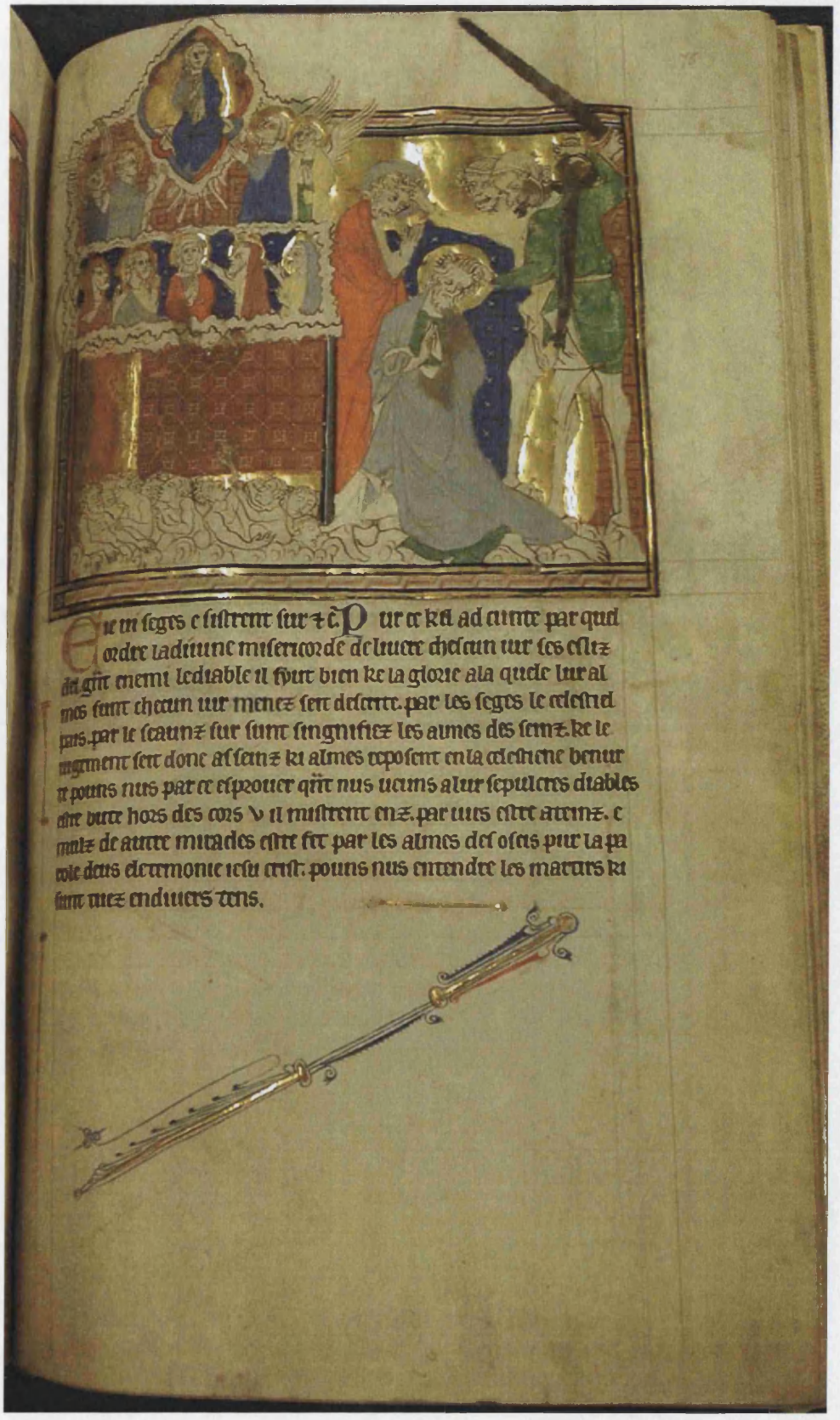

Figure A1.48: Decapitation of Martyrs – Add Ms 42555 f. 75.

Figure A1.49: The 14th century miniatures of saints – Add Ms 24686 f. 2.

Figure A1.50: The late 13th century miniatures of the passion- Add Ms 24686 f. 4.

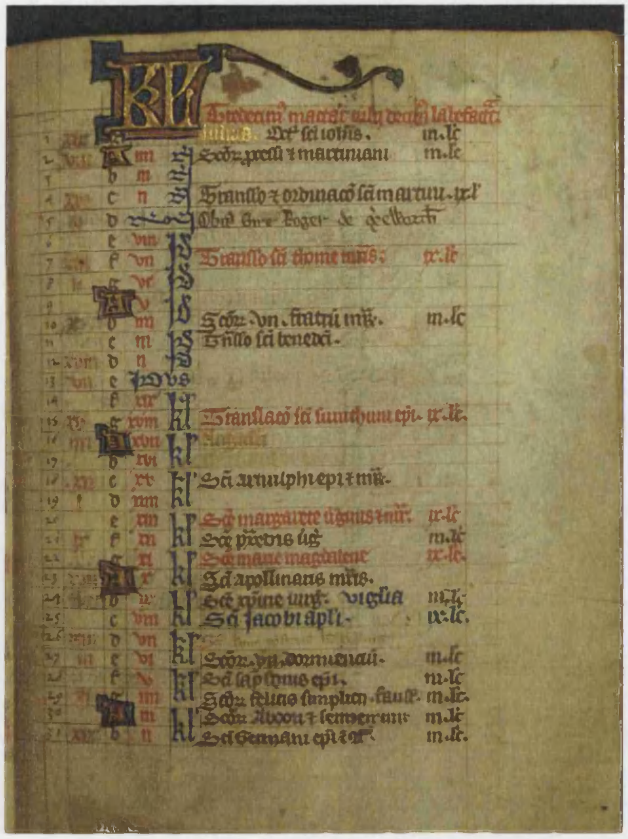

Figure A1.51: A decorated calendar page – Add Ms 24686 f. 8.

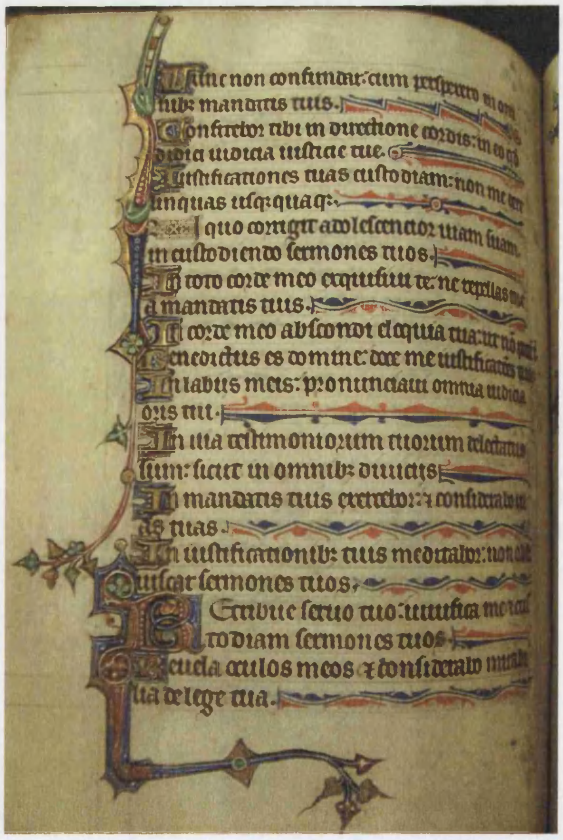

Figure A1.52: A Psalter division page – Add Ms 24686 f. 71v.

Figure A1.53: A decorated text page – Add Ms 24686 f. 111v.

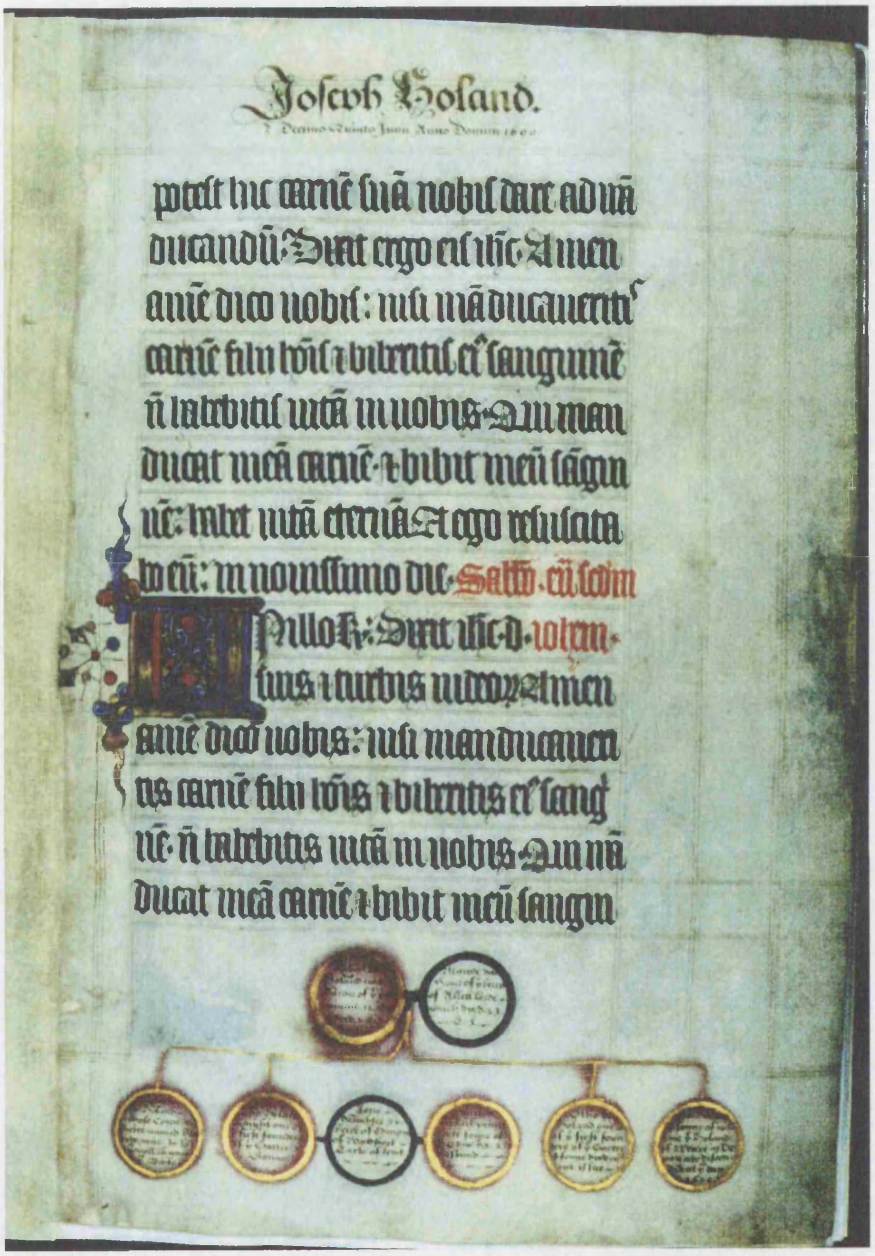

Figure A1.54: The genealogical inscription page - Harley Ms 7026 f. 4.

Figure A1.55: The Presentation Miniature frontispiece - Harley Ms 7026 f. 4v.

Figure A1.56: The Edict of Caesar Augustus - Harley Ms 7026 f. 5.

Figure A1.56: The Adoration of the Magi - Harley Ms 7026 f. 7v.

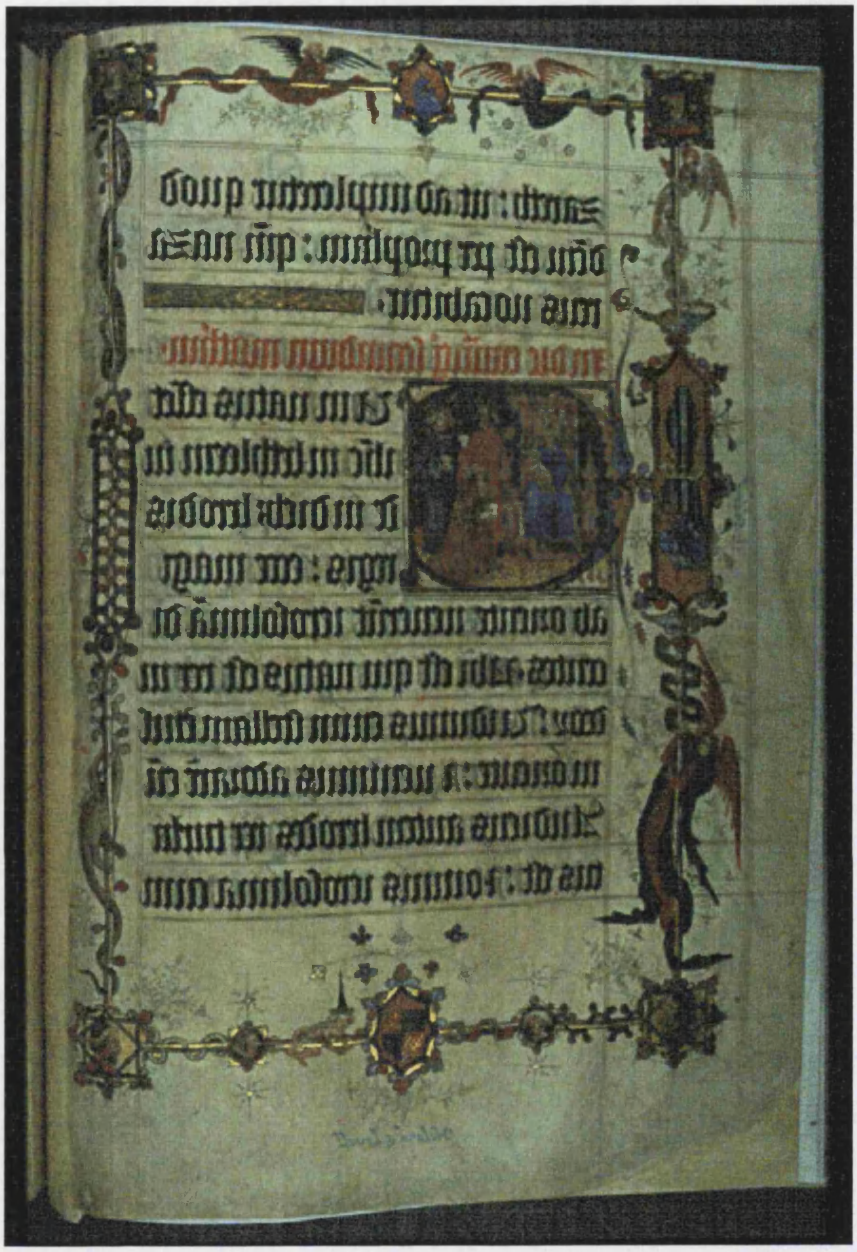

Figure A1.58: The Presentation in the Temple - Harley Ms 7026 f. 12.

Figure A1.59: The Corpus Christi Procession - Harley Ms 7026 f. 13.

Figure A1.60: A decorated text page from the additional missal fragment - Harley Ms 7026 f. 21.

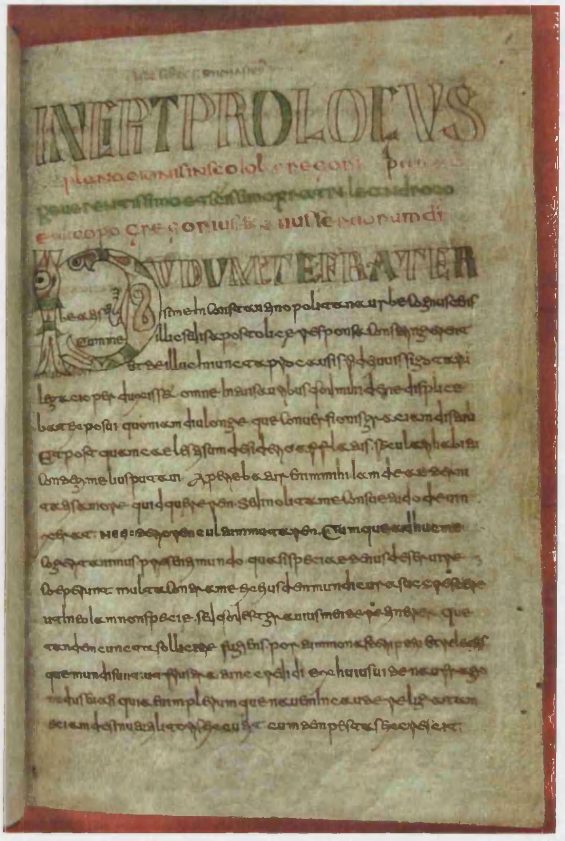

Figure A1.61: A decorated initial page - Add 31031 f. 1.

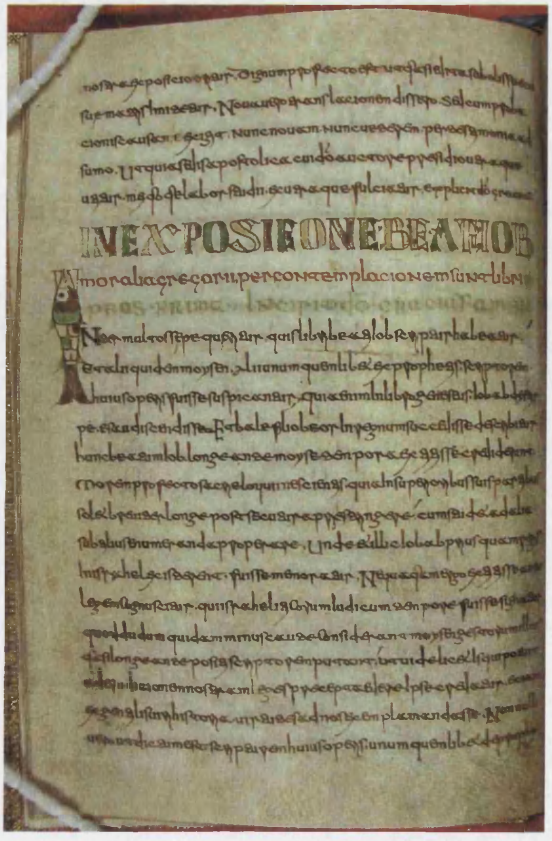

Figure A1.62: A rubricated page - Add 31031 f. 5v.

Figure A1.63: Pigment staining through to the blank page - Add Ms 33241 f. 1.

Figure A1.64: Queen Emma Receiving the Encomium - Add Ms 33241 f. 1v.

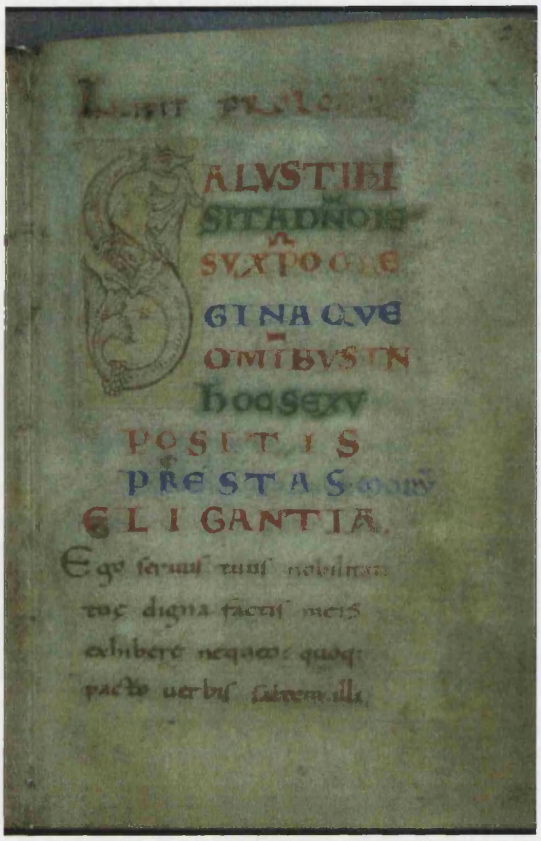

Figure A1.65: A decorated text page - Add Ms 33241 f. 2.

Figure A1.66: An illuminated page - Add Ms 16413 f. 23v.

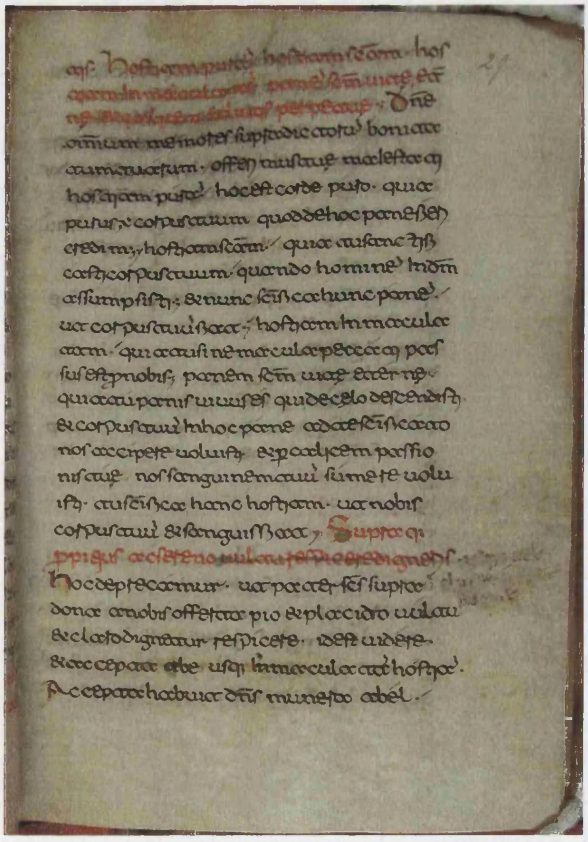

Figure A1.67: A rubricated page - Add Ms 16413 f. 29.

Appendix 2: The Use of Polyvinyl Acetate in Manuscript Conservation

The selection and use of materials in a conservation setting has always been a subject of considerable controversy. Unfortunately, the materials chosen have not always had appropriate properties.

Most manuscripts have suffered some wear and tear and have had to endure a variety of environmental conditions. A common side effect of this is that the pigment layer begins to lift from the substrate, eventually flaking off and being lost.

To combat this kind of decay a variety of consolidation techniques have been used over many years, with adhesives ranging from wheat starch paste and gelatin to a variety of modern polymers. Unfortunately, it is often the case that conservation techniques in common use are not documented. It is also often the case that fairly large institutions have only small conservation departments, such that the vast majority of, for example, western manuscript conservation over a period of 50 years may be done by a single person in the duration of a single career. Under these circumstances the need for exhaustive documentation may not be immediately apparent and any variations to treatments or techniques that may have been developed are lost when their developer retires.

A2.1: The Vespasian Psalter

Short notes appended to the records of a number of manuscripts in the British Library suggest that for a period during the 1970s, consolidation using a solution of polyvinyl acetate (PVAc) in methanol was attempted. Difficulties with the analysis of the Vespasian Psalter (Cotton Vespasian A1, see chapter 3) suggested that such a record should be sought for this manuscript, and one was found that confirmed that PVAc had indeed been used.

A2.2: Polyvinyl Acetate

Polyvinyl acetate has the formula $(CH_3COOCHCH_2)_n$ and is a chain of acetate groups bridged by methyl groups. Commercially, it forms the basis of a number of adhesive preparations with the addition of plasticisers, fillers, stabilisers or other additives to alter its properties.

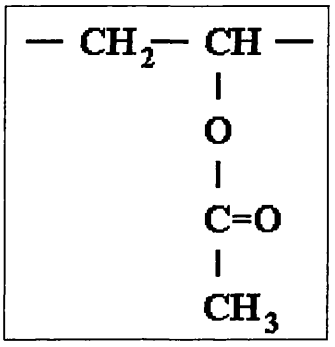

Figure A2.1: The monomer of polyvinyl acetate.

A2.3: PVAc in conservation

There is considerable anecdotal evidence to suggest that PVAc is not a suitable material for conservation purposes: yellowing, embrittlement, adhesion of treated surfaces and colour changes in pigments have all been discussed although they are not often formally reported.

A recent large-scale study [Down] reports the aging properties of a number of commercially available adhesives with various additives. A number of properties are common to all of the PVAc adhesives on aging.

In general the PVAc adhesives are acidic and become more so on aging in both dark and, especially, light conditions. They emit acetic acid vapour from one of two sources: free acetic acid in the formulation in the initial stages after application and acetic acid from hydrolysis of the acetate group upon aging. Acetic acid is known to decrease paper pH and to attack pigments. Again the amount released is greater if the material is light aged. Other additives to the adhesive also release volatile materials such as esters, which may be hydrolysed to acids in the presence of an acid and water. All of the

PVAc adhesives tested also showed a tendency to yellow, again particularly in the light aged samples.

A2.4: Conclusions

It is clear from the study that there are very few occasions when any form of PVAc adhesive could be considered ideal in a conservation setting. Its continued application in the light of this information would be unwise. However, the implications for objects that have already been treated are more serious. In particular, light appears to be a key factor in the rate at which changes in the adhesive occur; combined with water, inducing hydrolysis of both PVAc and the associated volatiles, it appears to be particularly harmful.

These particular points (the damage caused by the action of light on PVAc, the materials produced as a result and the effect of moisture on these materials) must be taken into account in the care of a treated object. Such objects should be considered unsuitable for display except in very carefully controlled conditions and for very short periods of time. In addition special attention should be paid to ensure that they are stored in dark, dry and, particularly, well ventilated conditions to prevent the build-up of volatile emissions.

Appendix 3: Islamic Manuscripts

Note: Since Islamic manuscripts are read from the "back", the designations of recto and verso are reversed.

Figure A3.1: Two seated figures - OR 1403 f. 8.

Figure A3.2: Dancing figures - OR 1403 f. 9v.

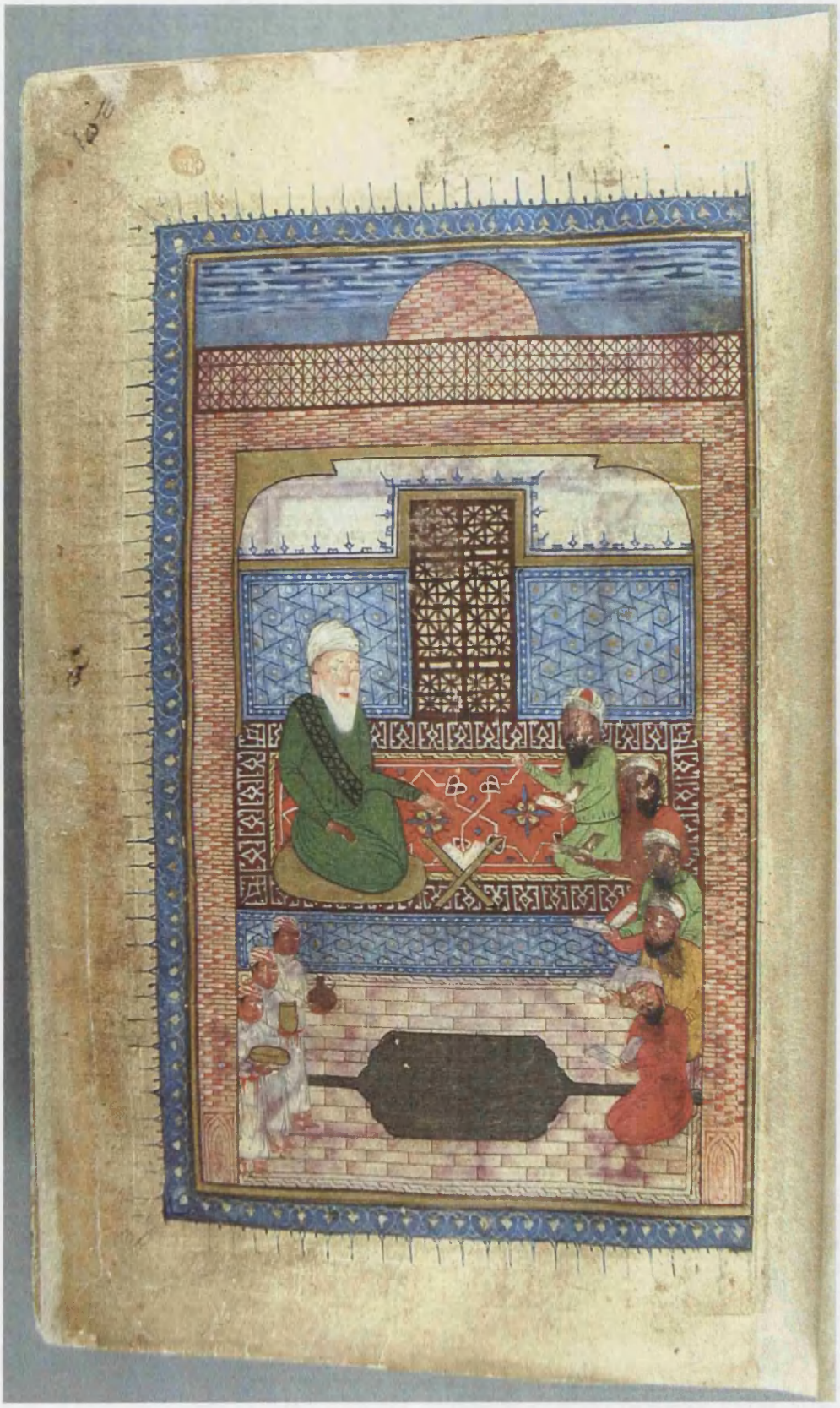

Figure A3.3: A teacher and students - OR 1403 f. 10.

Figure A3.4: A ruler addressing two subjects - OR 1403 f. 13.

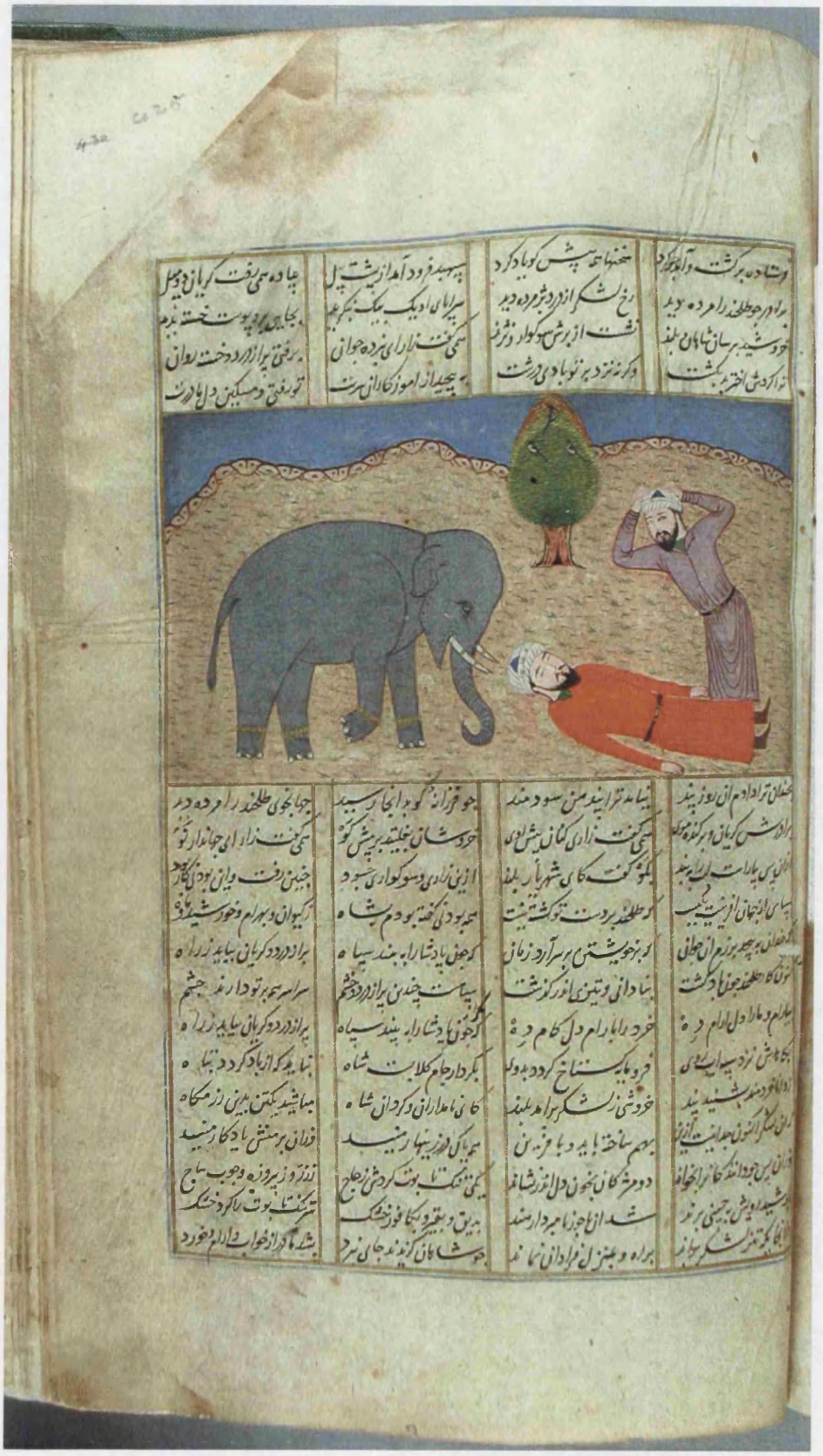

Figure A3.5: Two men and an elephant - OR 1403 f. 425.

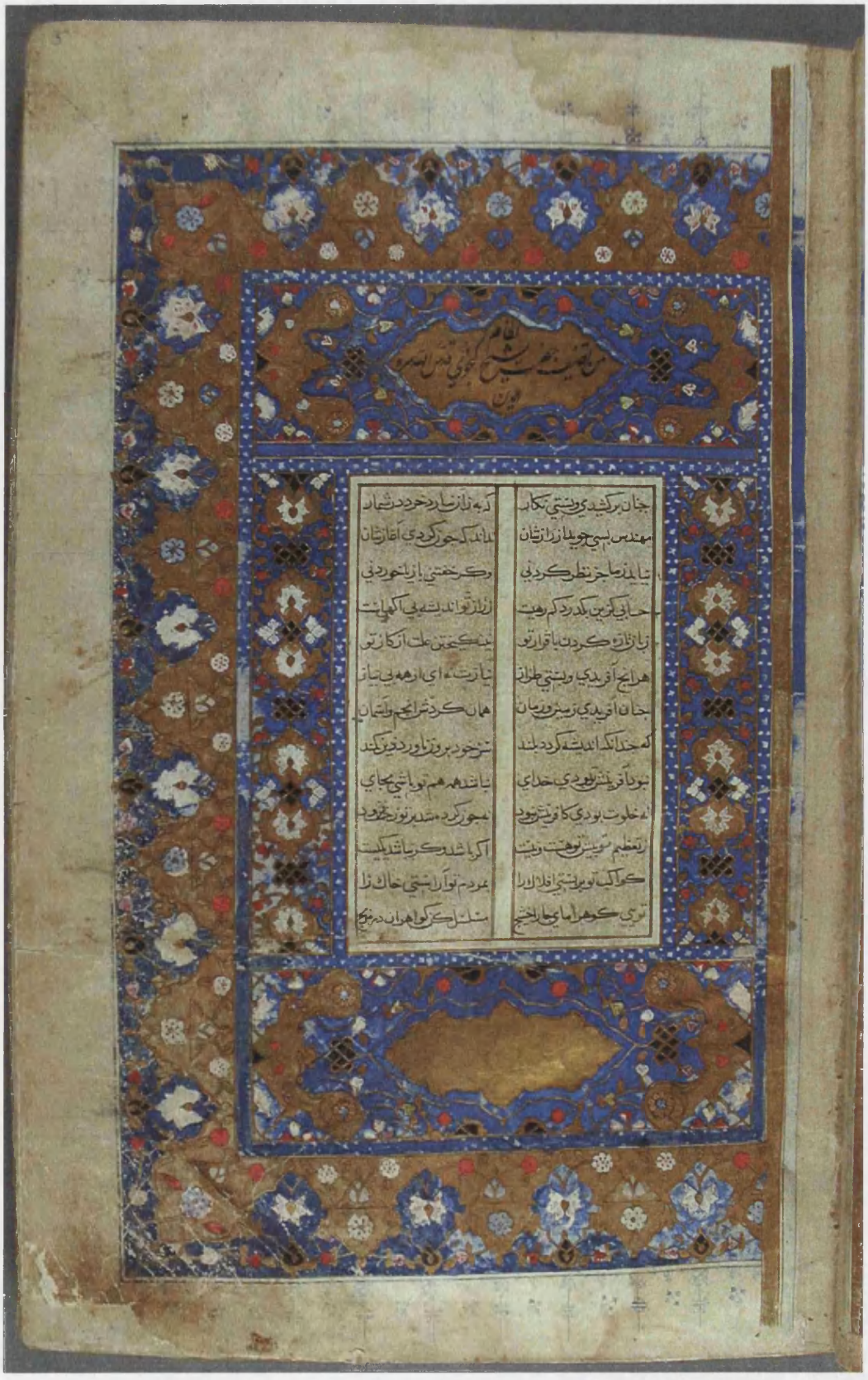

Figure A3.6: Double page unvan - OR 13836 f. 5.

Figure A3.7: A battle scene - OR 13836 f. 17v.

Figure A3.8: A ruler addressing his subjects - OR 13836 f. 21v.

Figure A3.9: A decorated page - OR 11676 f. 2.

Figure A3.10: The Court of a King - OR 11676 f. 4v.

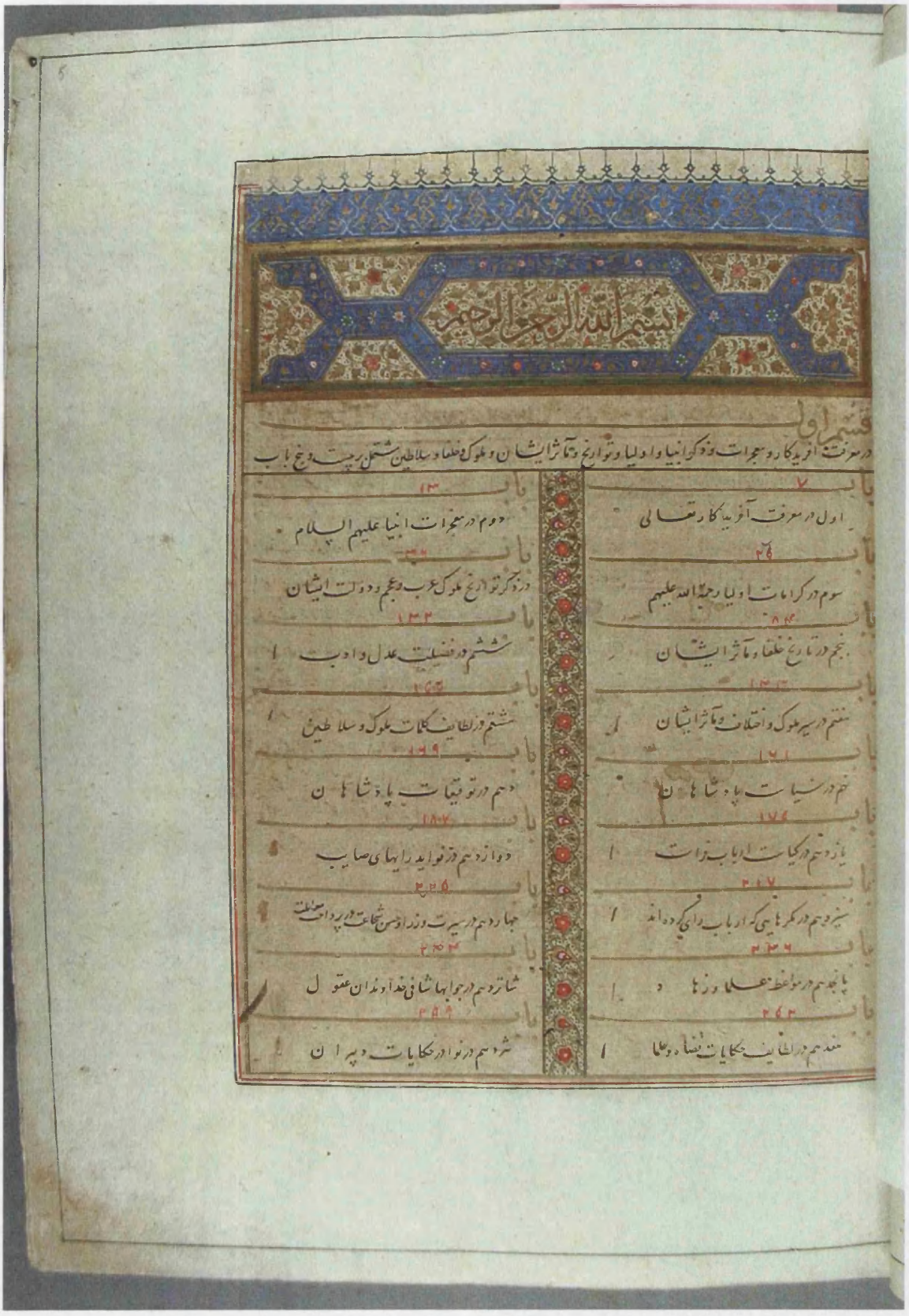

Figure A3.11: A decorated sutra heading - OR 11676 f. 5.

Figure A3.12: Men meeting in a mosque - OR 11676 f. 113.

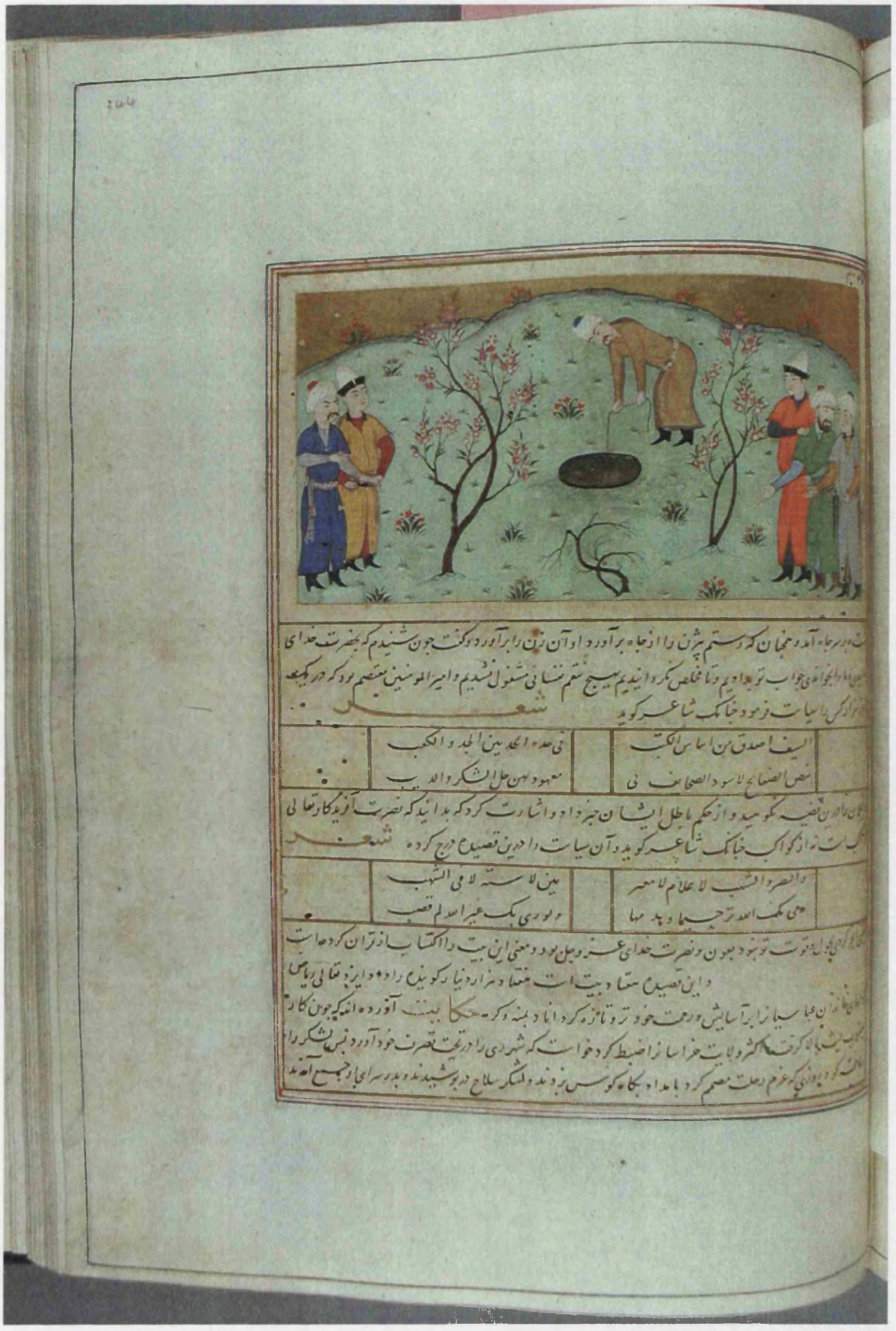

Figure A3.13: Men at a well - OR 11676 f. 344.

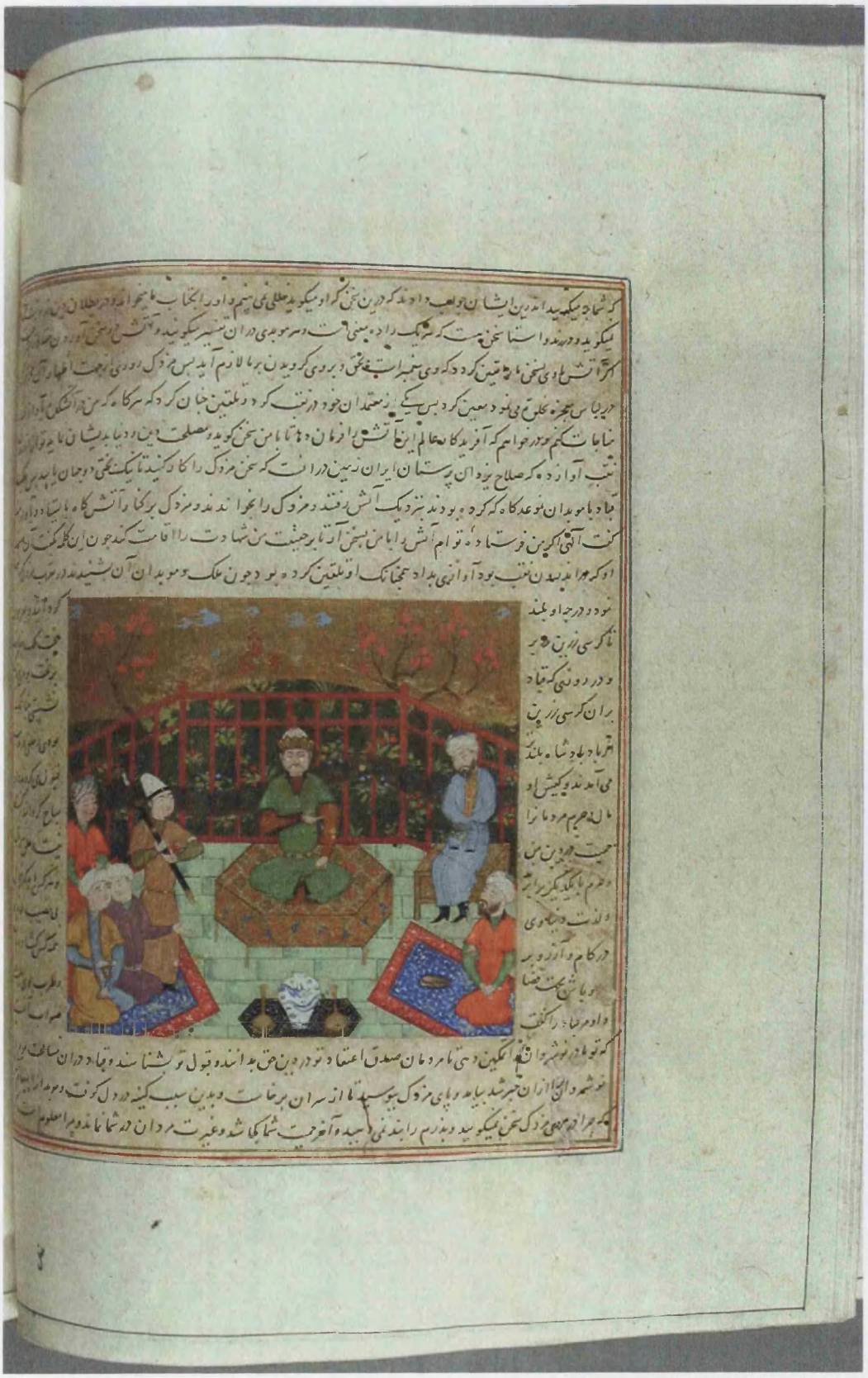

Figure A3.14: A garden pavilion - OR 11676 f. 405v.

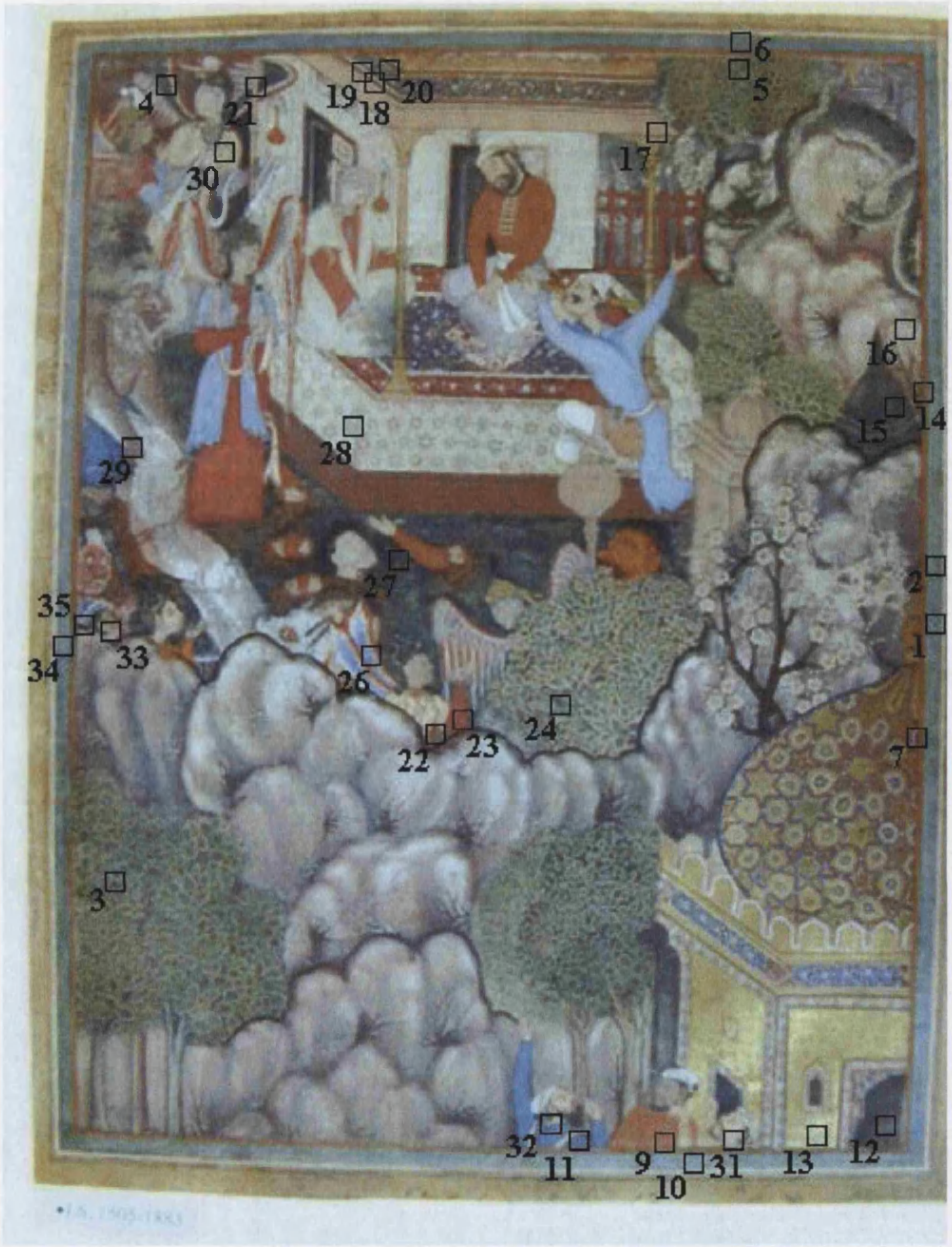

Figure A3.15: Hamza approached by fairies - IS 1505-1883.

Figure A3.16: The murder of Qibad - IS 1508-1883.

Figure A3.17: Amar Ayaz witnessing the death of Qamir - IS 1513-1883.

Figure A3.18: Image of IM2-1896-65 under UV light.

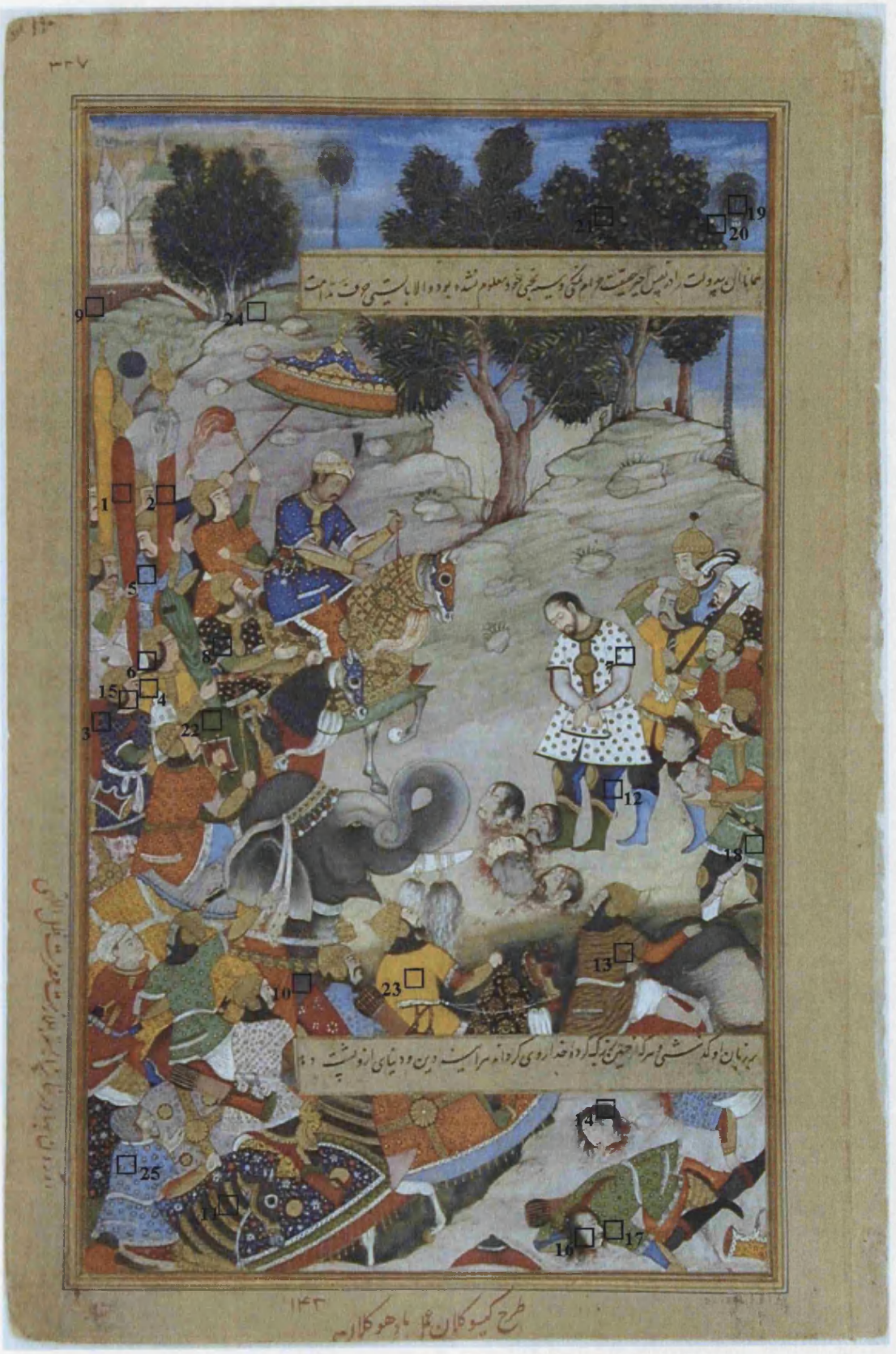

Figure A3.19: A single folio from the Akbarnama - IM2-1896-65.

Figure A3.20: Maulānā Husain Khvārazm, being read to by a youth - OR 11837 f. 148.

Figure A3.21: Pegasus - OR 7315 f. 11v.

Figure A3.22: Draco - OR 7315 f. 12v.

Figure A3.23: Angels that support God's throne - OR 7315 f. 26v.

Figure A3.24: Hārūt and Mārūt hanging upside-down - OR 7315 f. 30.

Figure A3.25: A decorated page - OR 13935 f. 1v.

Figure A3.26: Conjoined twins - OR 13935 f. 15v.

Figure A3.27: Winged figures - OR 13935 f. 17.

Figure A3.28: Winged figure holding a trumpet - OR 13935 f. 43v.

Figure A1.29: Man with a torch - OR 13935 f. 273.

Figure A3.30: Two men in combat - OR 13935 f. 306v.

Figure A3.31: Men in battle - ISL 3442 f. 354.

Figure A3.32: Unvan - OR 7073 f. 3v.

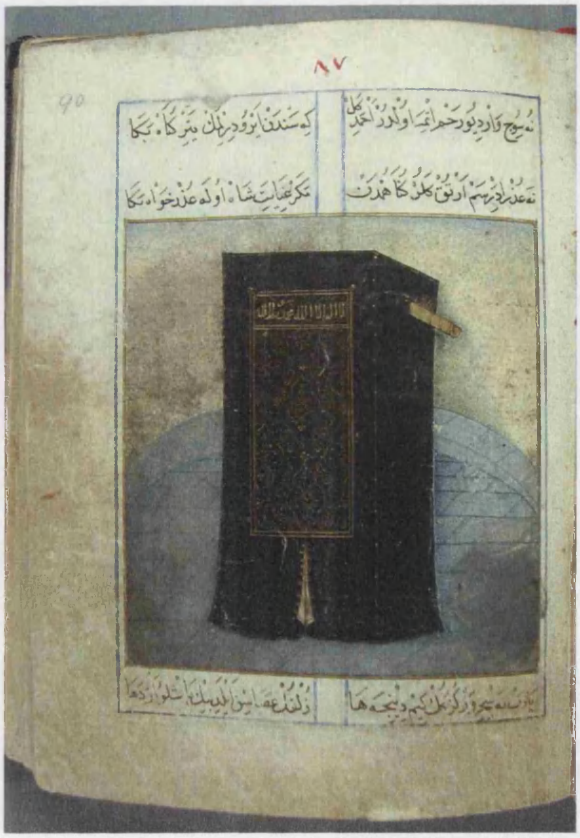

Figure A3.33: The Kâbe - OR 7073 f. 90.

Figure A3.34: An interior scene - OR 7073 f. 108v.

Figure A3.35: A landscape - OR 7073 f. 149v.

Figure A3.36: An illuminated page - OR 7354 f. 1.

Figure A3.37: The fox that outwitted the launderer's ass - OR 7354 f. 6v.

Figure A3.38: The man who thought his baby had been attacked - OR 7354 f. 9v.

Figure A3.39: The cat that was caught in the snarer's net - OR 7354 f. 13.

Figure A3.40: The King talking to a bird - OR 7354 f. 19.

Figure A3.41: Unvan - OR 405 f. 2v.

Figure A3.42: Unvan - OR 405 f. 3v.

Figure A3.43: The Prophet rides through the heavens - OR 405 f. 11.

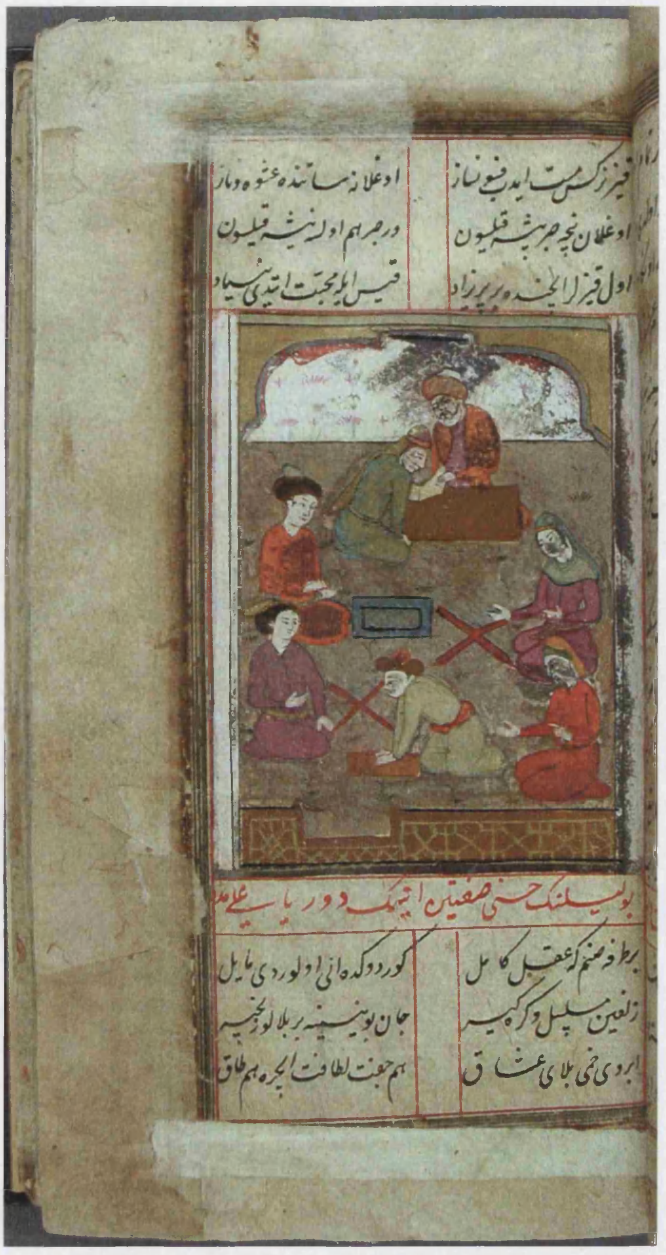

Figure A3.44: Leila and Mecnun at school - OR 405 f. 19.

Figure A3.45: Mecnun visited in the desert - OR 405 f. 30.

Figure A3.46: Leila visiting Mecnun in the desert - OR 405 f. 83.

Appendix 4: The Work of William Blake

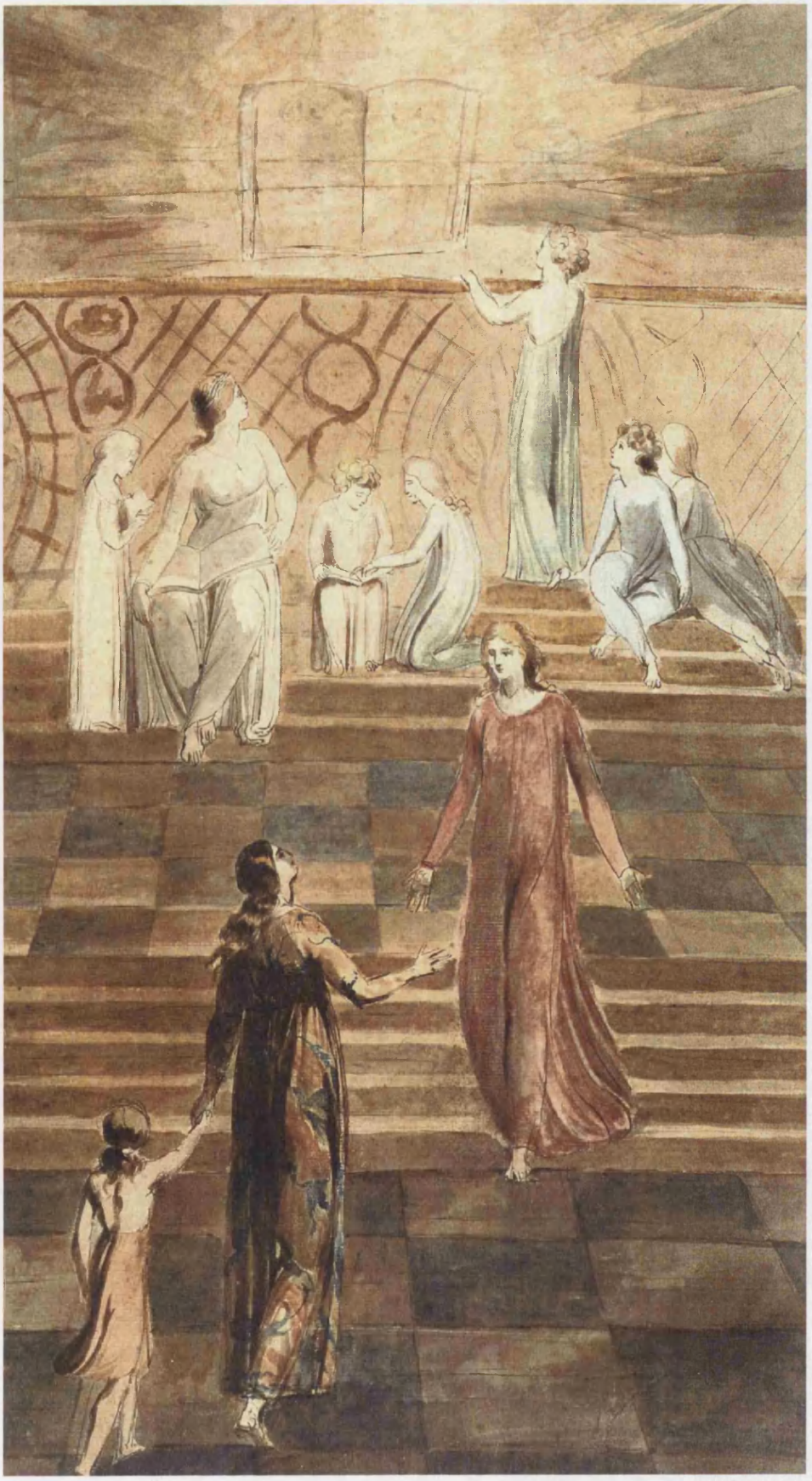

Figure A4.1: An Allegory of the Bible.

Figure A4.2: Age Teaching Youth.

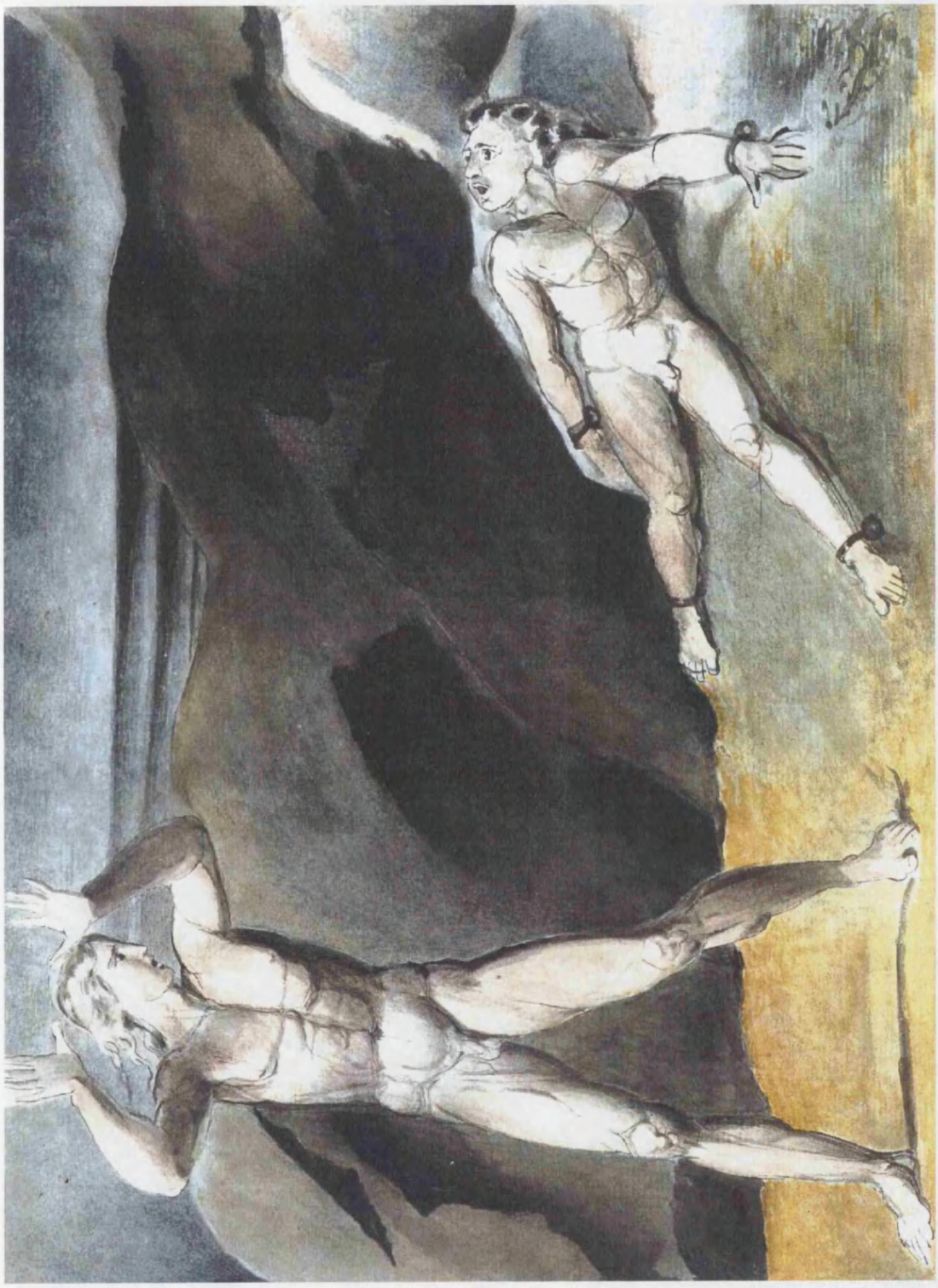

Figure A4.3: Los and Orc.

Figure A4.4: Visions of the Daughters of Albion, Plate 4.

Figure A4.5: Satan Exulting Over Eve.

Figure A4.6: God Judging Adam.

Figure A4.7: Newton:

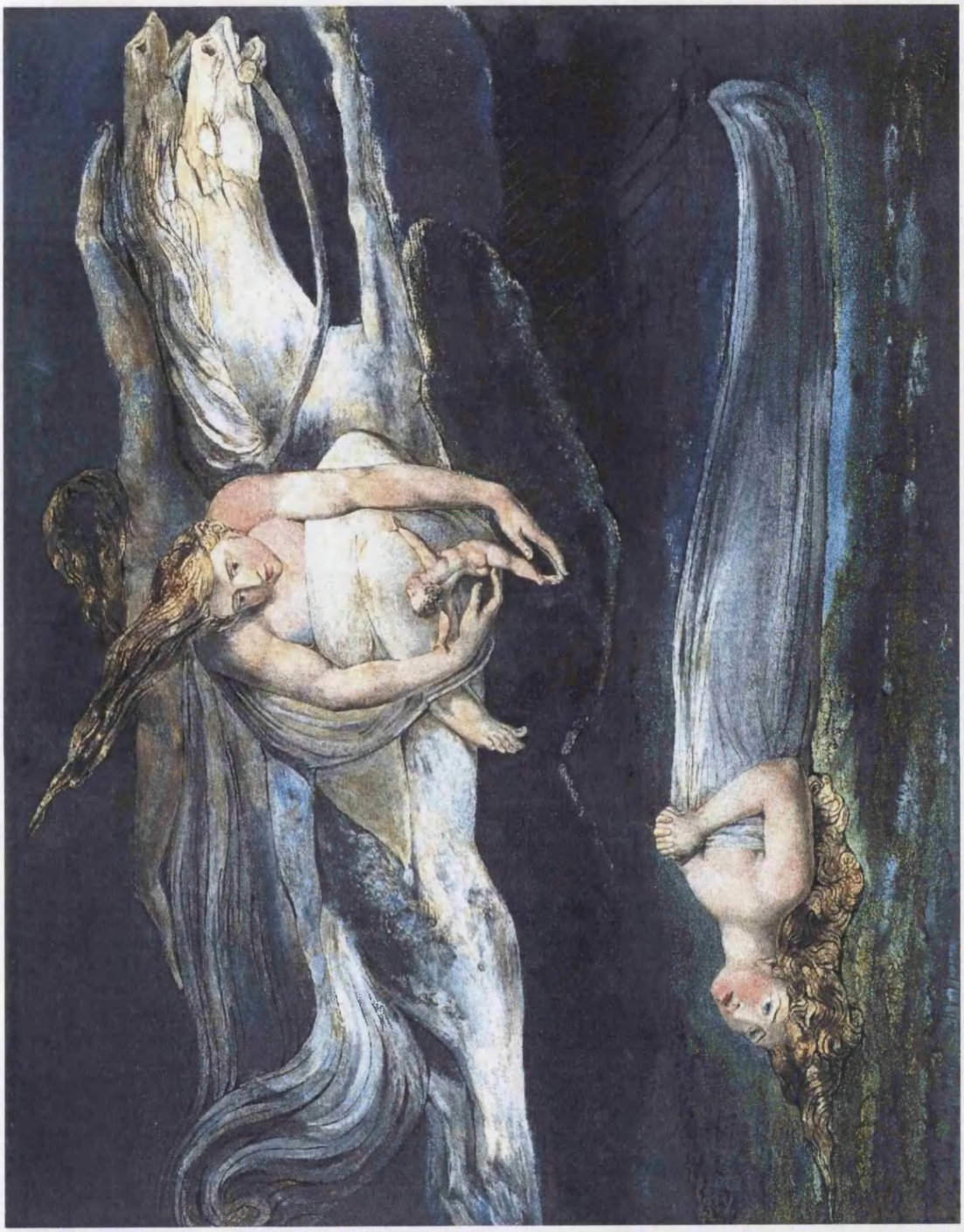

Figure A4.8: Pity.

Figure A4.9: The Night of Enitharmon's Joy.

Figure A4.10: The Body of Christ Bourne to the Tomb.

Figure A4.11: The River of Life.

Figure A4.12: Dante and Virgil Penetrating the Forest.

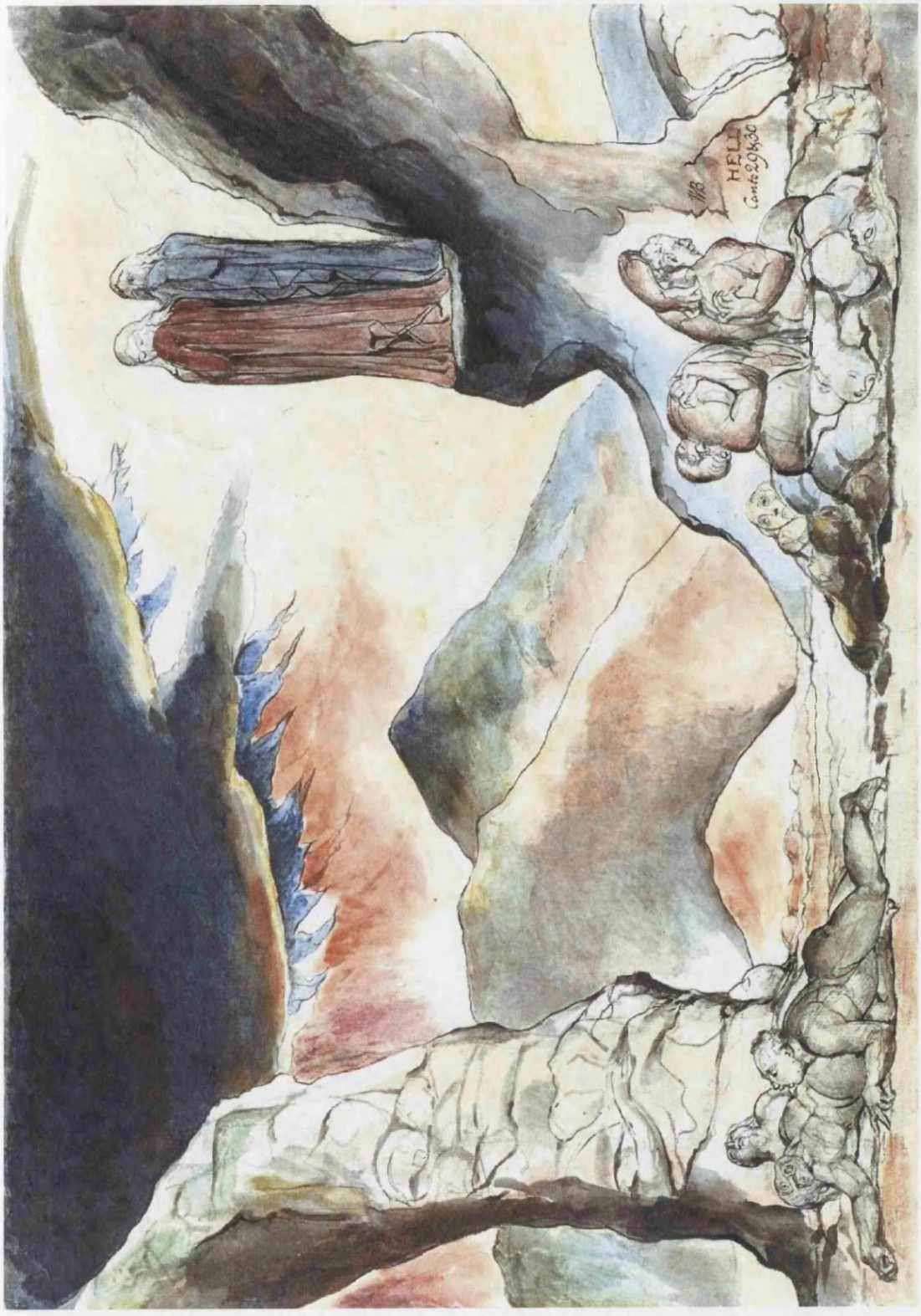

Figure A4.13: The Pit of Disease: The Falsifiers.

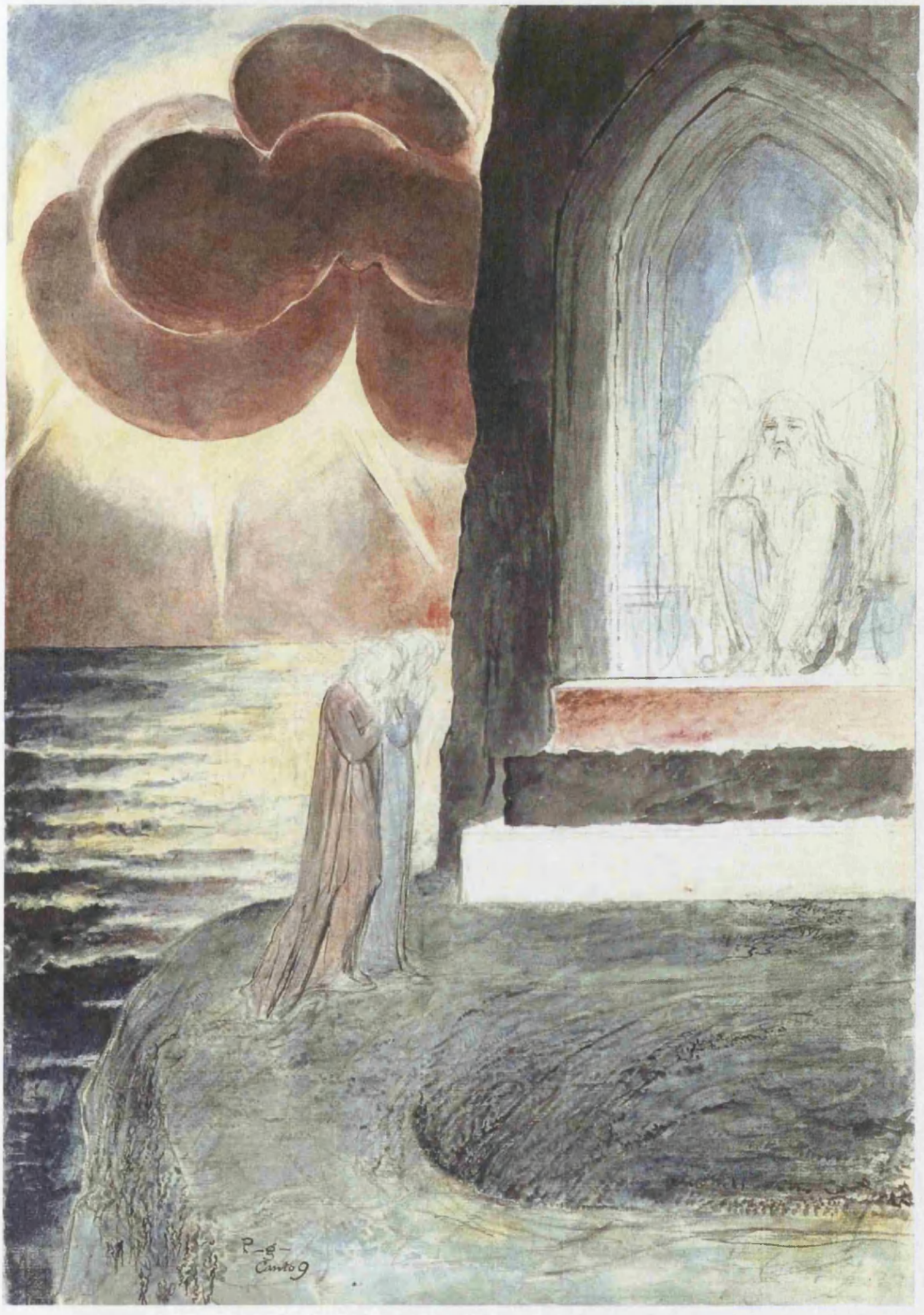

Figure A4.14: Dante and Virgil Approaching the Angel who Guards the Entrance of Purgatory.

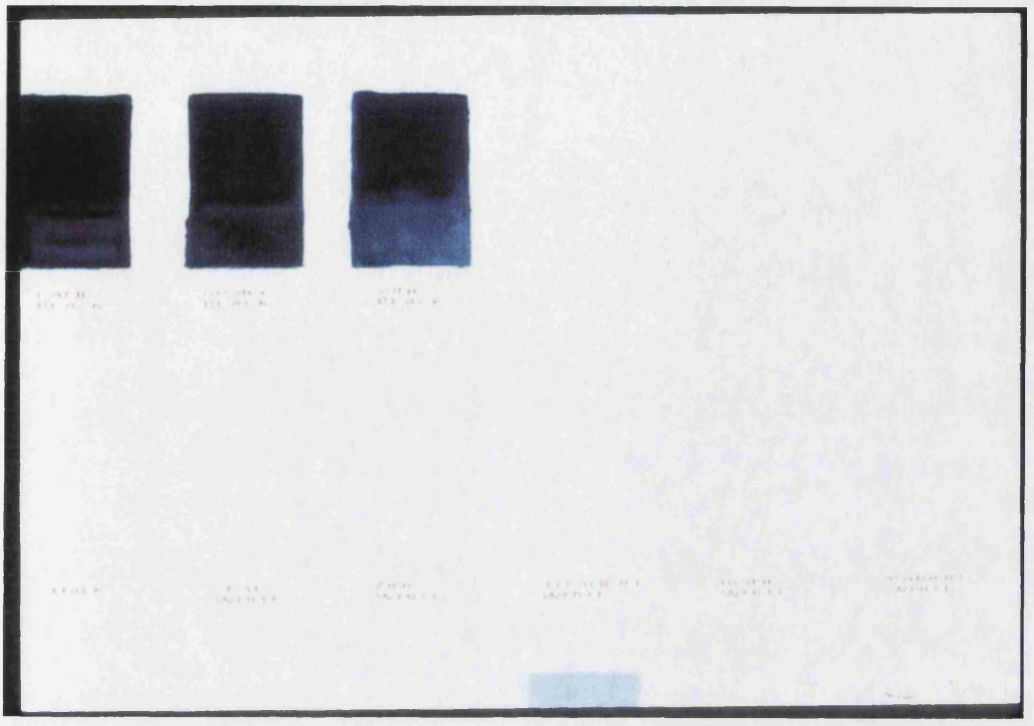

Figure A4.15: Pigment swatch 1, normal photography.

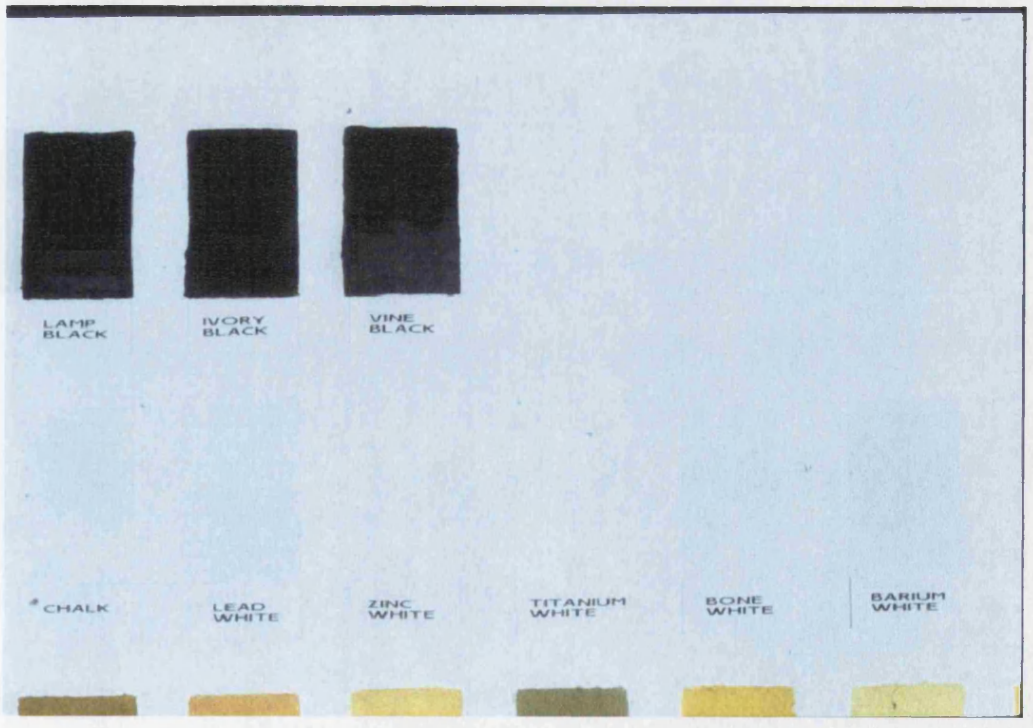

Figure A4.16: Pigment swatch 1, false colour photography.

Figure A4.17: Pigment swatch 2, normal photography.

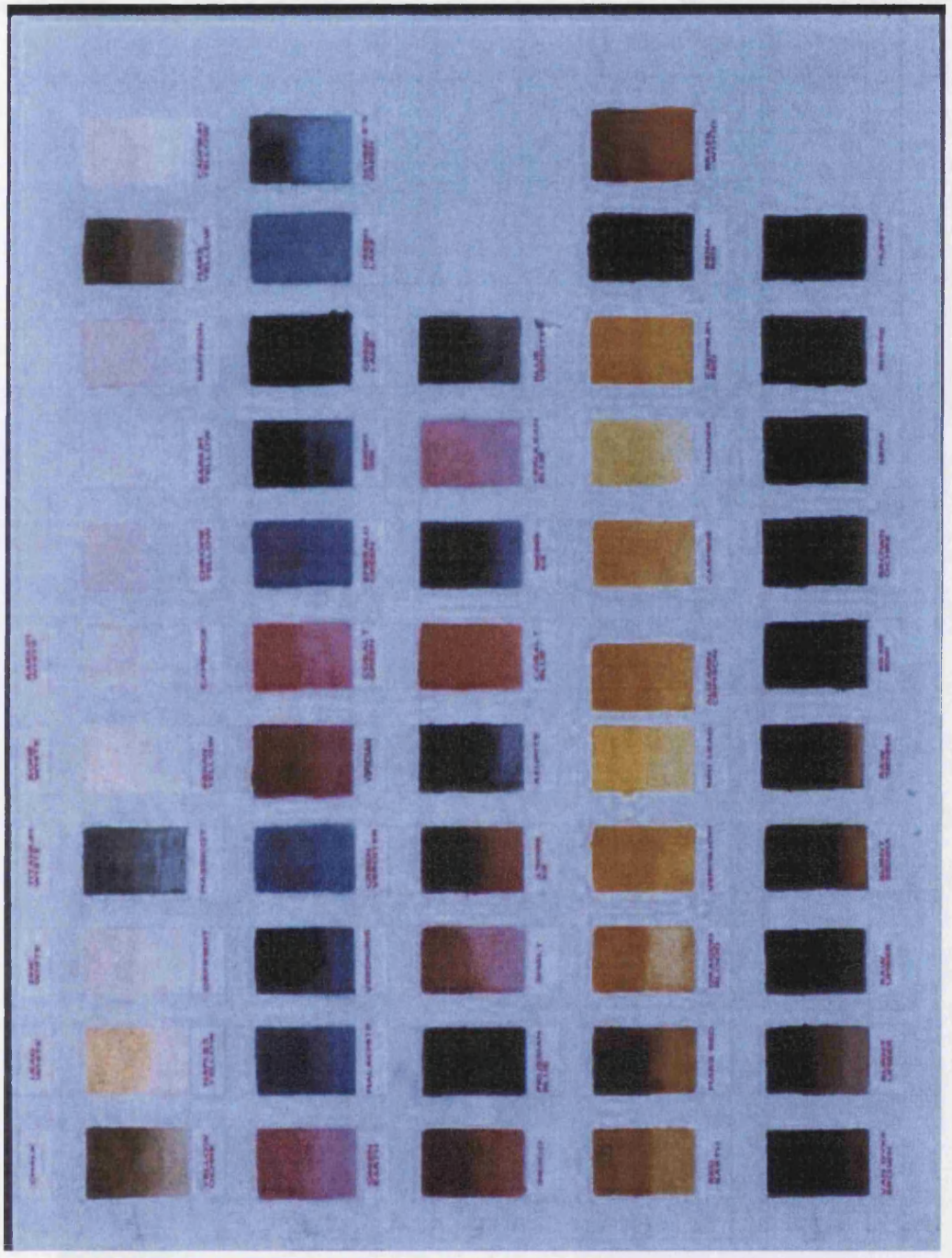

Figure A4.18: Pigment swatch 2, false colour photography.

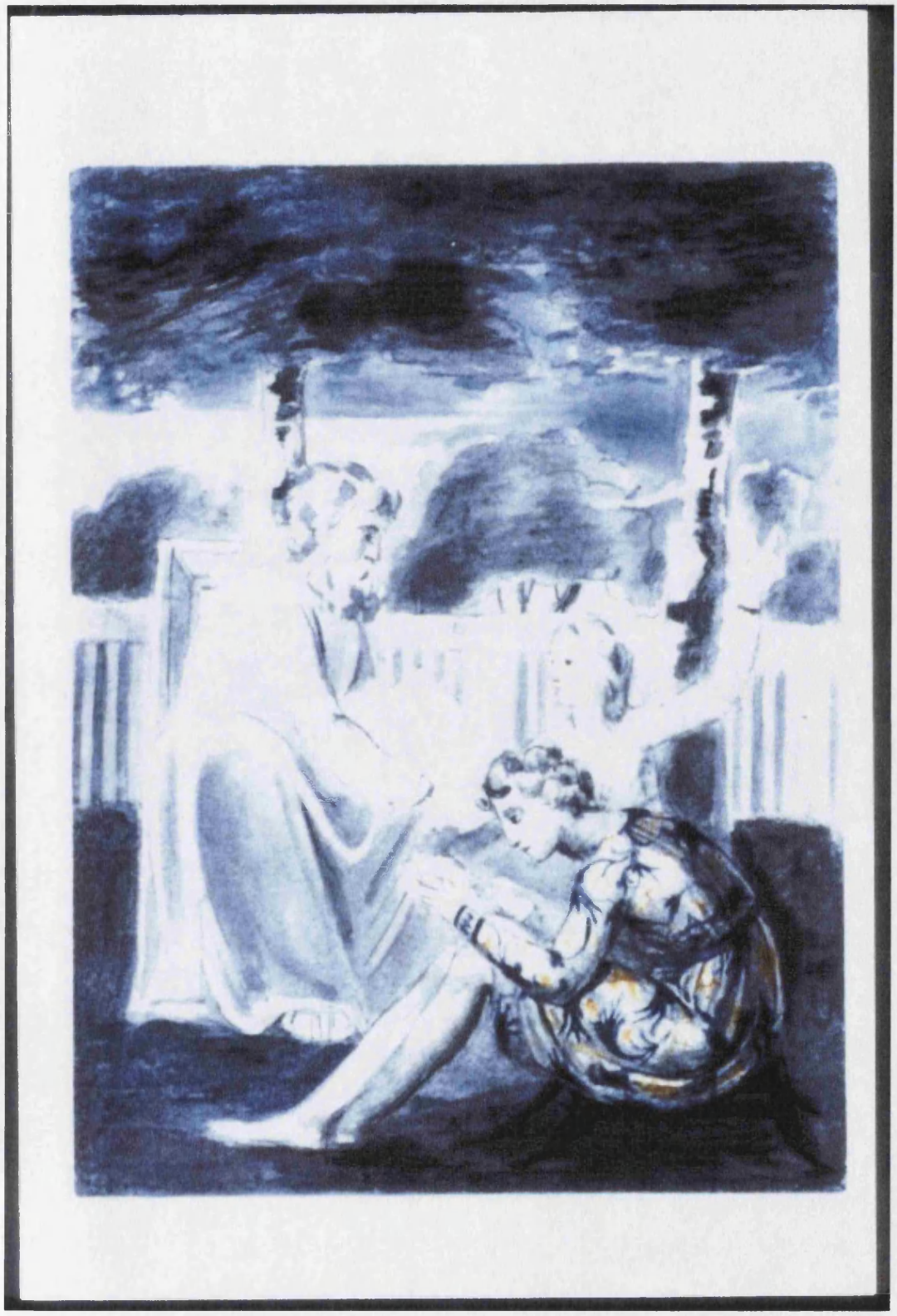

Figure A4.19: The false colour image of Age Teaching Youth

Figure A4.20: The false colour image of Los and Orc.

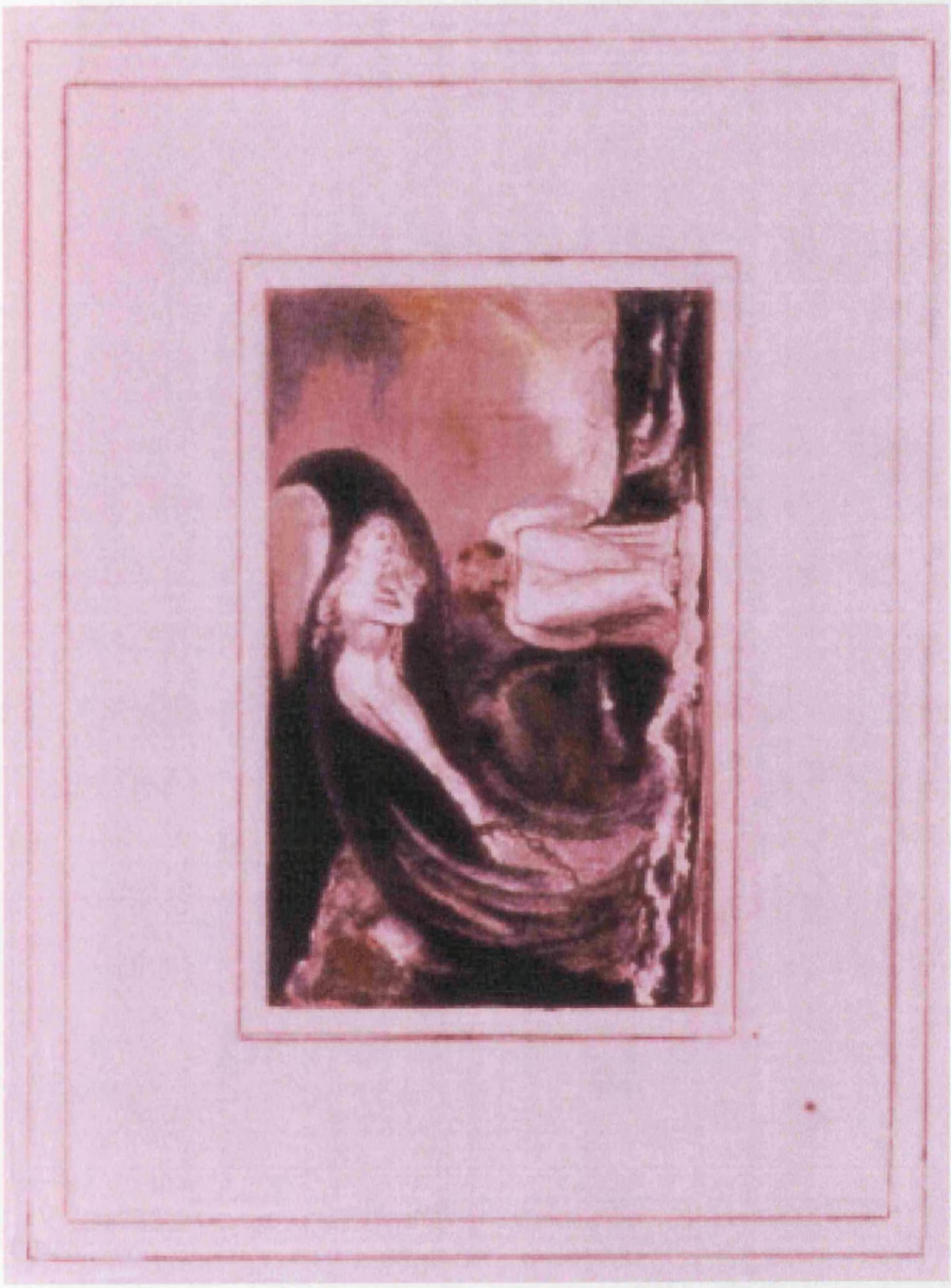

Figure A4.21: The false colour image of Visions of the Daughters of Albion, Plate 4.

Figure A4.22: The false colour image of God Judging Adam.

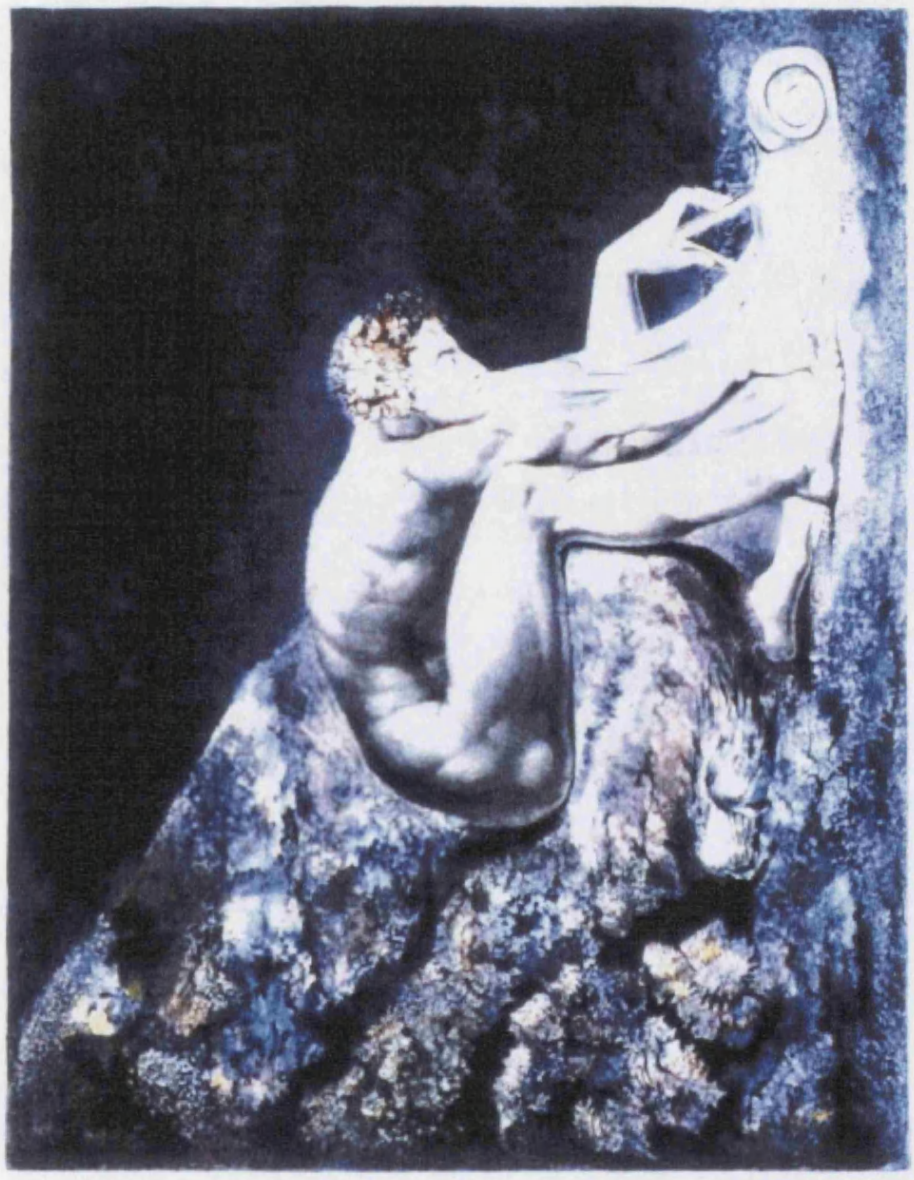

Figure A4.23: The false colour image of Newton.

Figure A4.24: The false colour image of Pity.

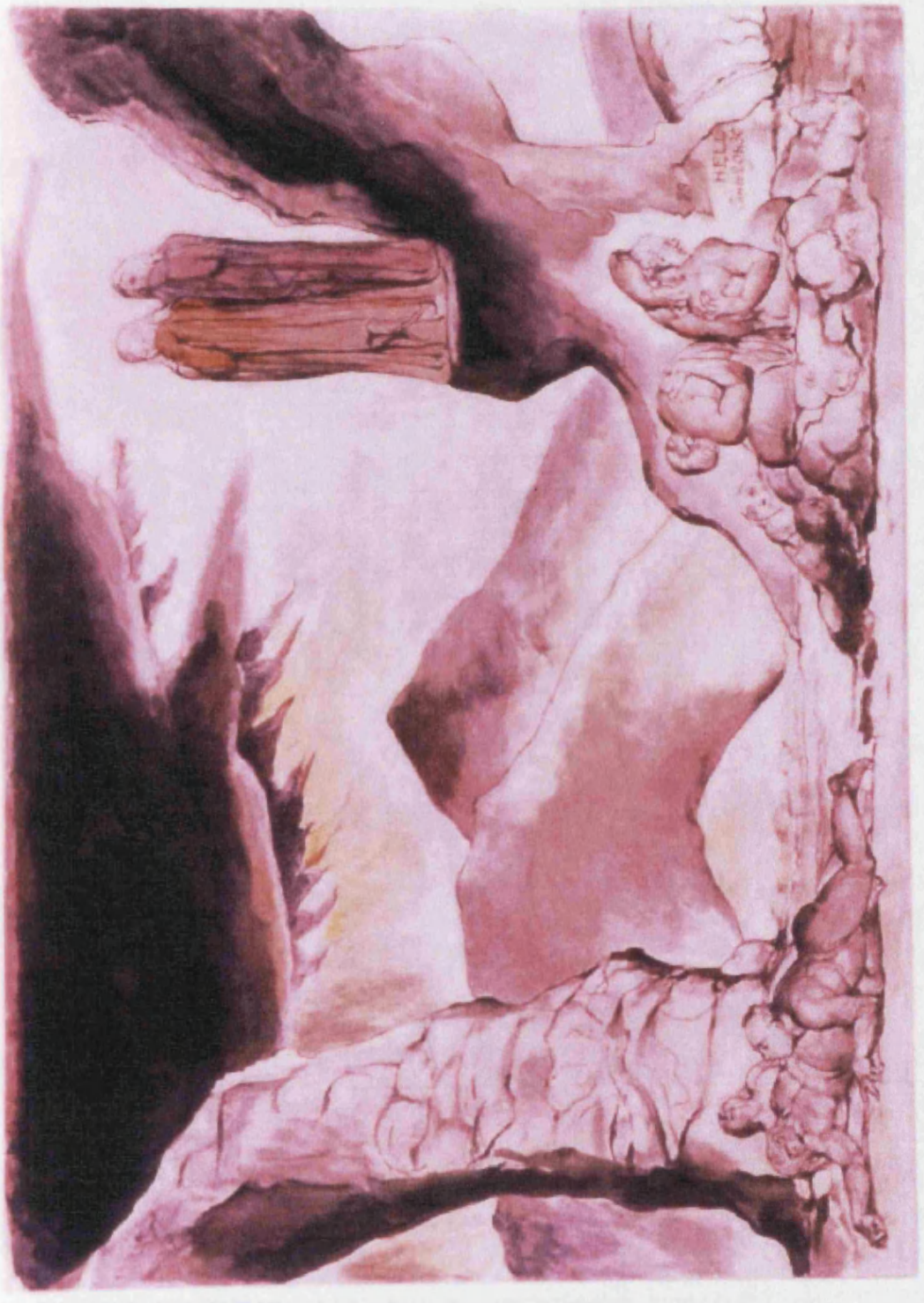

Figure A4.25: The false colour image of The Pit of Disease: The Falsifiers.

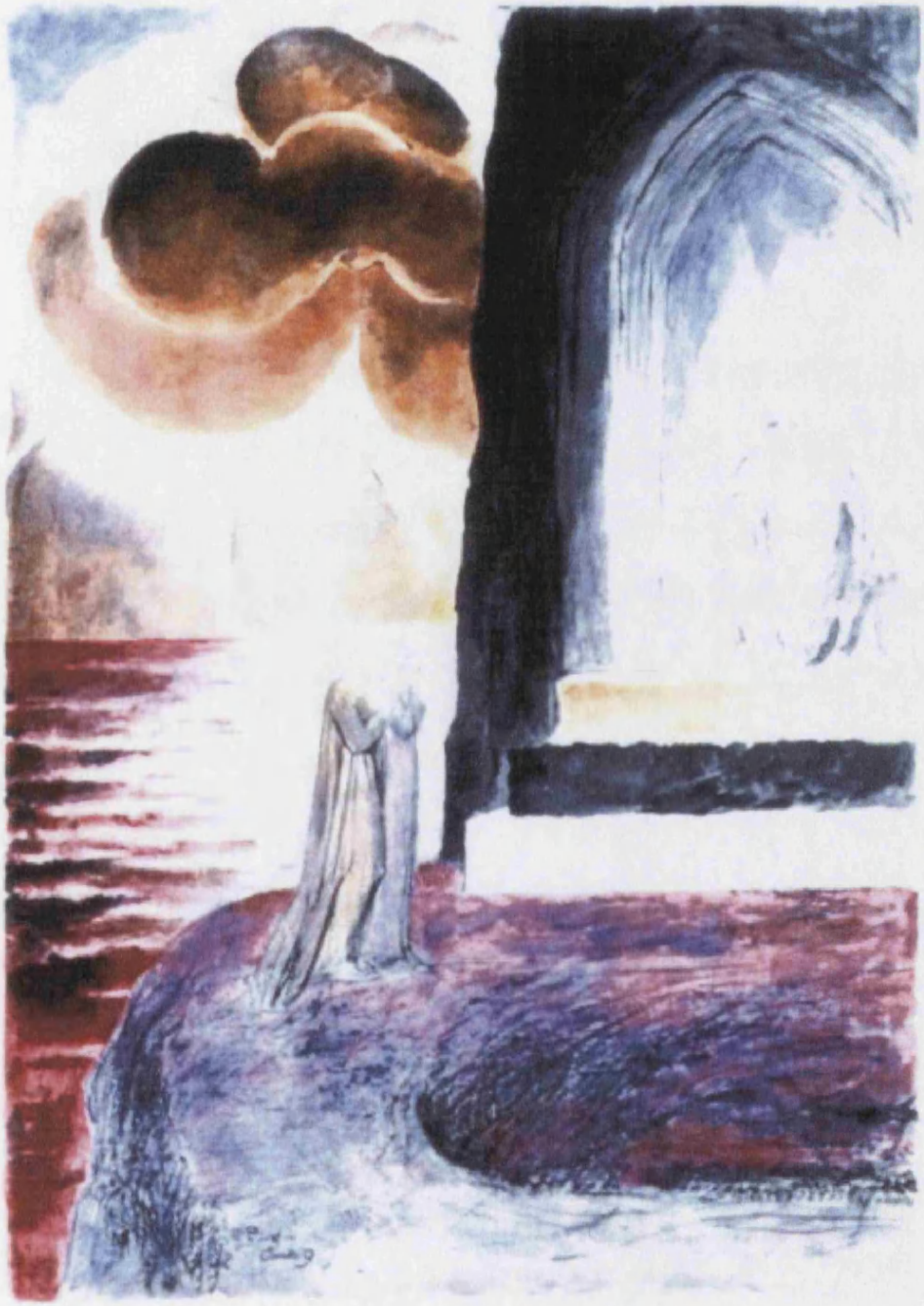

Figure A4.26: The false colour image of Dante and Virgil Approaching the Angel who Guards the Entrance of Purgatory.

Appendix 5: The Calculation of R-Group Size

An estimate of the size of the R-groups is required for chapter 10 to allow the steric effects to be properly considered. Rather than simply being a measure of the size of the R-group itself, this value needs to take account of the amount of space that the R-group occupies and prevents other atoms from using. This would need to include a measure of how far away from the central selenium atom the R-group is: a large R-group with a long bond to the carbon could produce less of a steric hindrance than a smaller R-group, much closer.

This idea is captured in solid angle theory – a measurement of the element of the sphere surrounding a central point that is occupied.

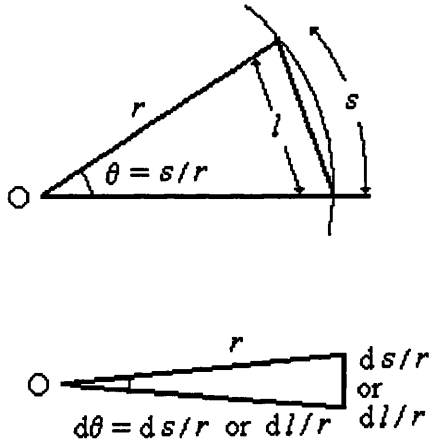

Figure A5.1: Plane angles, in radians.

If s is the length of an arc of a circle centred at O, with radius r, the plane angle θ subtended by this arc is given by the ratio s/r. For a small angle $d\theta$, the cord (l) and the arc differ in length only in the second order of smallness and so $d\theta$ is given by ds/r or by dl/r.

Solid angles extend the above into three-dimensional space. A sphere of radius r is centred at the apex of the angle O. The solid angle, in units of steradians, is given by

$$\Omega = S / r$$

where S is the area cut off on the surface of the sphere by the angle. Therefore, the solid angle around a point is 4π since the surface of a sphere is $4\pi r^2$.

For a small solid angle $d\Omega$, the plane area dA differs from dS again by a second order of smallness so that $d\Omega = dS / r^2$ or dA / r^2. However, this relies on the area dS lying normal to the radius r. If this is not the case, then dS must be projected onto a plane which is normal to r as an area $dS \cos \theta$.

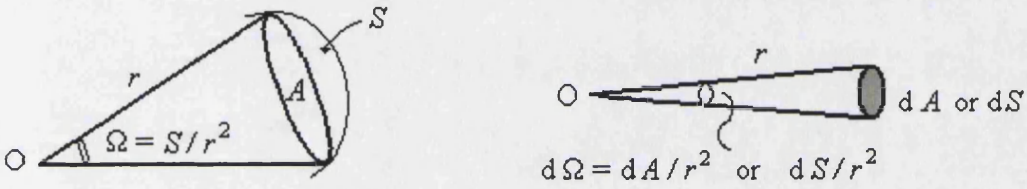

Figure A5.2: Solid angles in steradians.

If certain assumptions are made this can easily be extended to calculate an approximate R-group size. The R-groups are treated most simply as in figure A5.3 below. The calculation is performed for a solid angle centred on the axis of the selenium – carbon bond, delimited by the radius from the centre of the selenium atom to the centre of the R-group atom furthest from the bond. The solid angle is then arrived at by simple geometry.

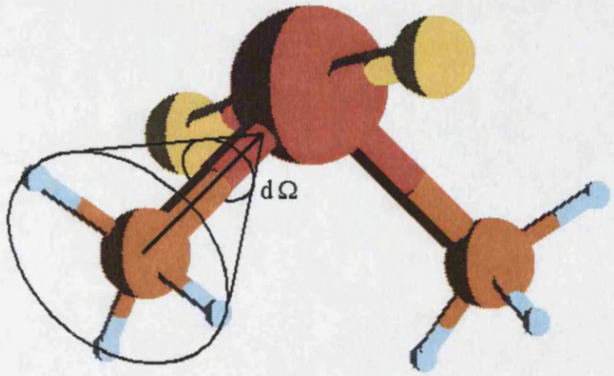

Figure A5.3: The size of the methyl R-group in terms of the element of solid angle subtended along the Se-C axis at the carbon atom.

However, this assumes that the atom furthest from the bond is situated in the plane at right-angles to the selenium-carbon bond, which is clearly not the case, and takes no account of the size of the terminal atom. From figure A5.4 it can be seen that these variations can easily be included.

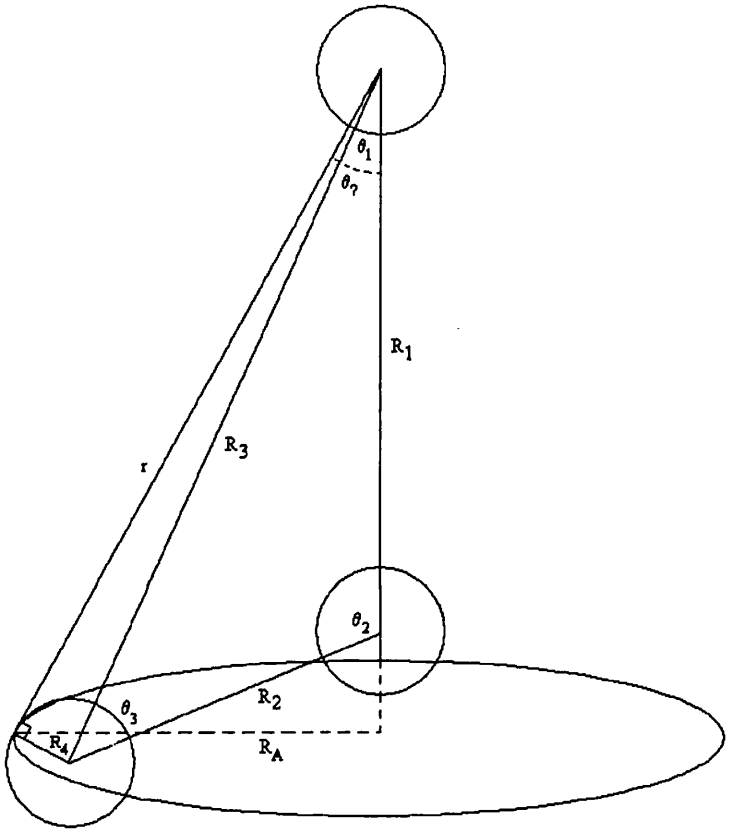

Figure A5.5: The geometry of the calculation of R-group size. R_1 is the radius from the centre of the selenium atom to the centre of the bonded carbon atom. R_2 is the distance from the centre of the carbon atom to the centre of the furthest atom from the carbon in the R-group. R_3 is the radius from the centre of the selenium to the centre of the furthest atom. R_4 is the radius of the furthest atom. r is, therefore, the radius from the centre of the selenium atom to the furthest extent of the furthest atom of the R-group. R_A is the radius of the notional area *dA* on which the furthest atom sits, at 90° to the axis R_1. R_1, R_2 and R_3 are found from the graphical interpretation of the atomic position matrix given in the results of the ADF calculations. R_4, which depends on the atom in question, is taken from a standard reference. [SICD]

From the description of solid angle given above, and referring to figure A5.4

$$d\Omega = dA / r^2$$

The area is given by $dA = \pi R_A^2$

where $R_A = r\sin\theta_?$

and the angle $\theta_?$ is given by $\theta_? = \theta_1 + \sin^{-1}(R_4/R_3)$

The unknown radius $r = (R_3^2 - R_4^2)^{½}$

So dA becomes $dA = \pi (R_3^2 - R_4^2)^{½} \sin(\theta_1 + \sin^{-1}(R_4/R_3))$

and $d\Omega = \pi \sin(\theta_1 + \sin^{-1}(R_4/R_3))$

Since only two atoms appear as outliers to the R-groups, R_4 is either 0.37Å for hydrogen or 0.71Å for fluorine. [SICD]

However, this method of calculation would give the same solid angle for both CF_3 and CH_2F, which is clearly not the case, since the furthest atom from the central axis in both cases is fluorine, but the other outliers are of different size. To compensate for this approximately, the other atoms at the edges of the R-group must be considered. Thus the size of the R-group was calculated for CH_2F, for example, using the fluorine atom and then again with the hydrogen and the results averaged with a 2:1 hydrogen to fluorine weighting.

R-group	Size, as element of solid angle (steradians)
CF_3	2.107
CF_2H	1.937
CFH_2	1.804
CH_3	1.691
CH_2CH_3	1.930
$CH(CH_3)_2$	2.248
t-Butyl	2.539

Table A5.1: Approximate R-group sizes in order of decreasing electron withdrawal.

Appendix 6: Reference Raman Spectra

Reference spectra are taken from [Bell] and [Burg].

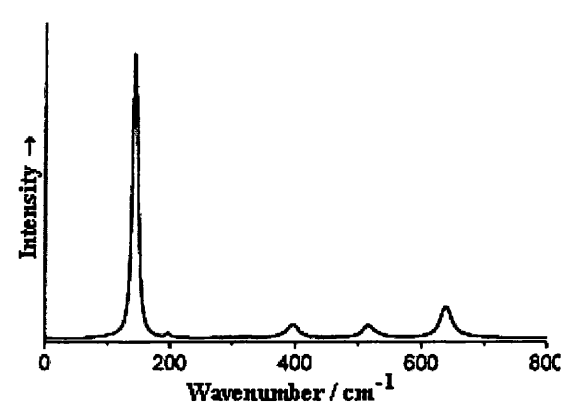

a)

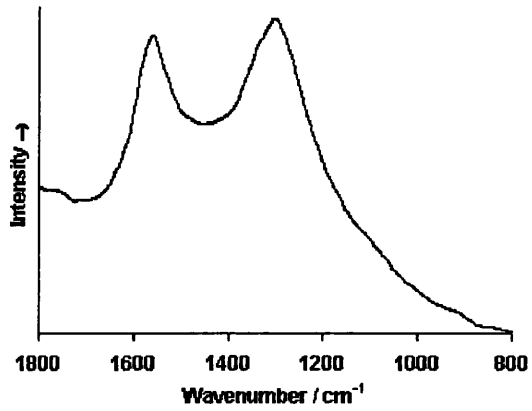

d)

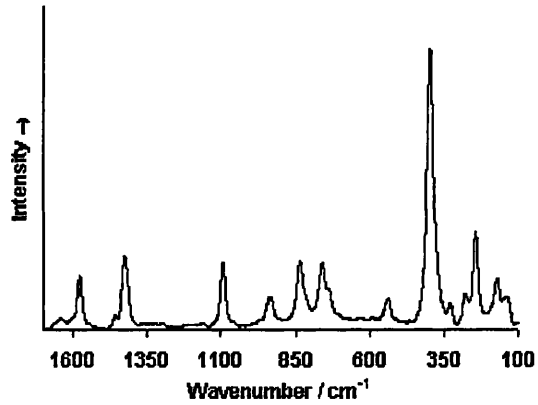

b)

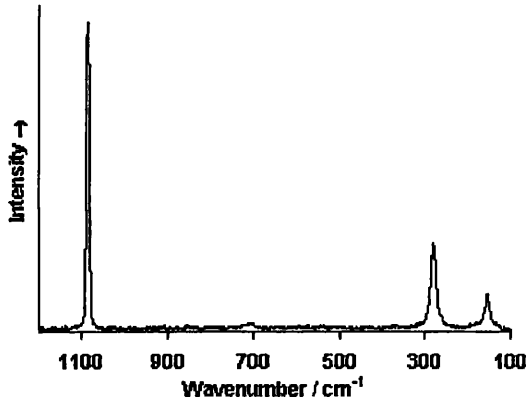

e)

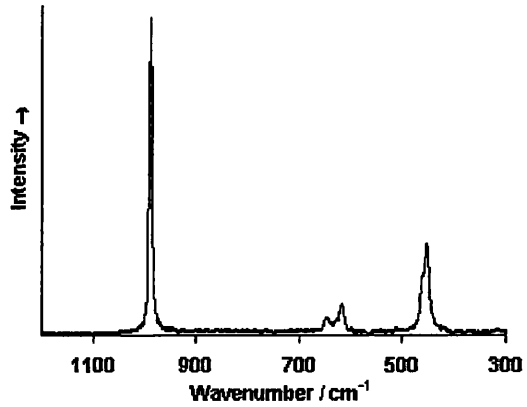

c)

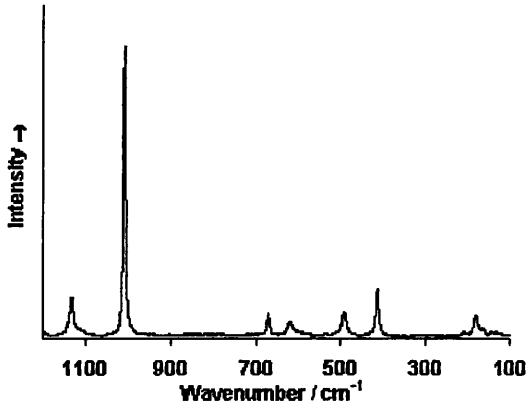

f)

Figure A6.1: The reference Raman spectra of a) anatase, b) azurite, c) barites, d) carbon, e) chalk, f) gypsum.

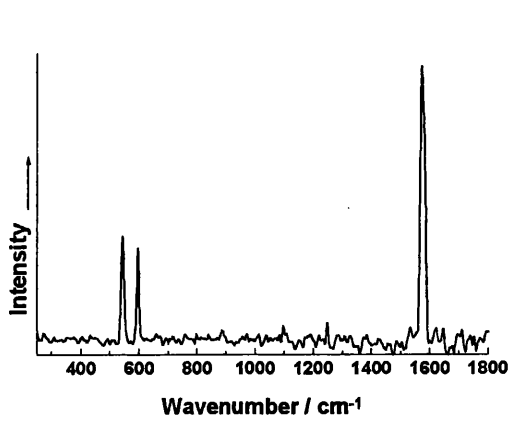

a)

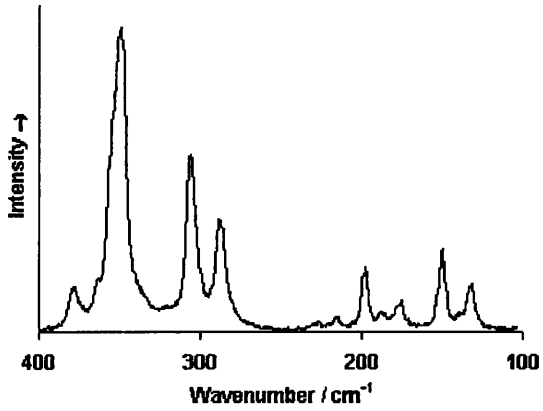

d)

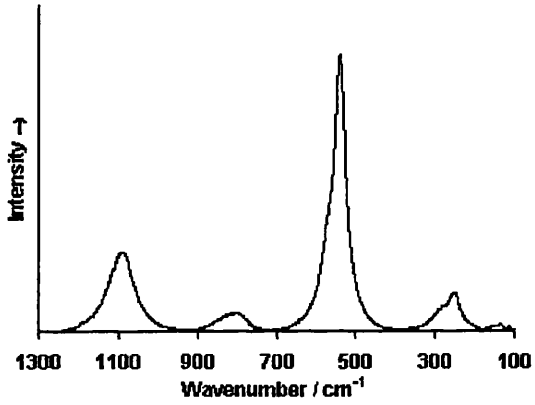

b)

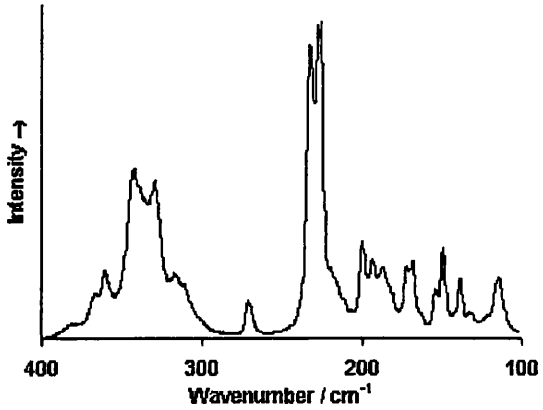

e)

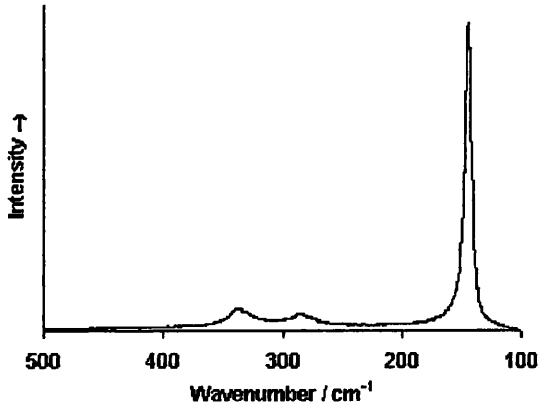

c)

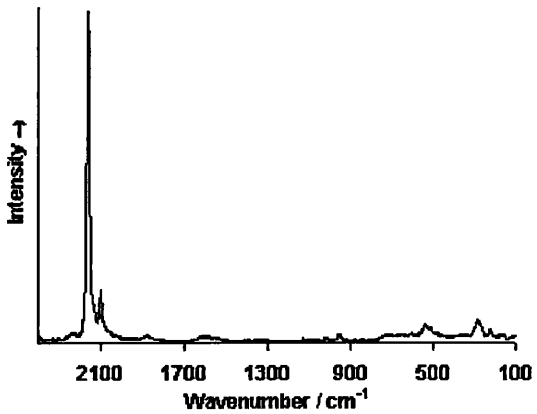

f)

Figure A6.2: The reference Raman spectra of a) indigo, b) lazurite, c) litharge, d) orpiment, e) pararealgar, f) Prussian blue.

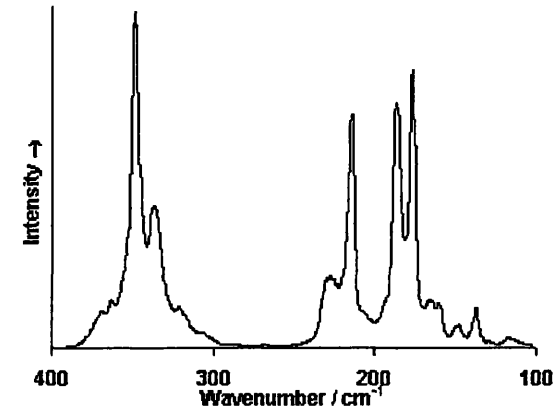

a)

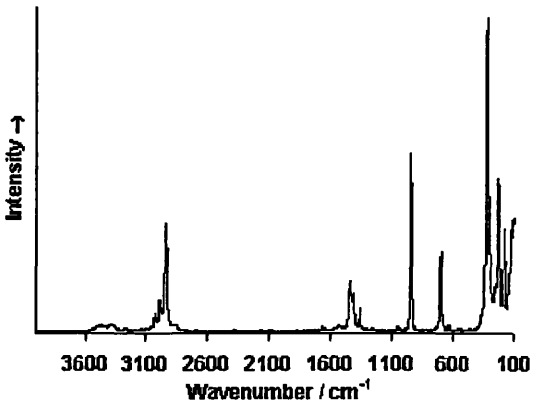

d)

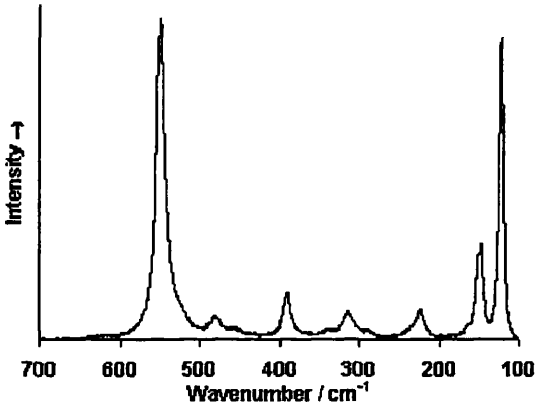

b)

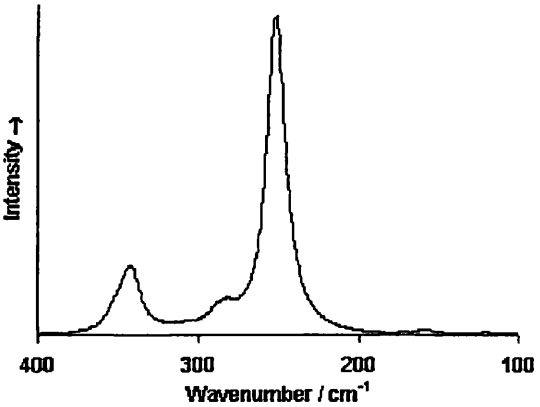

e)

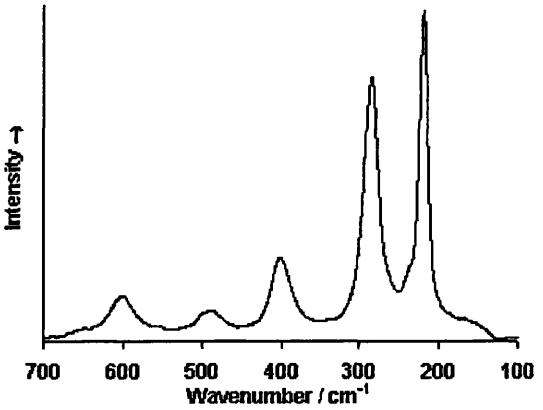

c)

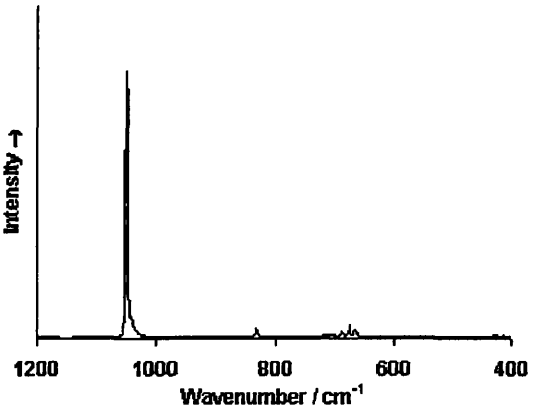

f)

Figure A6.3: The reference Raman spectra of a) realgar, b) red lead, c) red ochre, d) verdigris, e) vermilion, f) white lead.

Time is to clock as mind is to brain. The clock or watch somehow contains the time. And yet time refuses to be bottled up like a genie stuffed in a lamp. Whether it flows as sand or turns on wheels within wheels, time escapes irretrievably, while we watch. Even when the bulbs of the hourglass shatter, when darkness withholds the shadow from the sundial, when the mainspring winds down so far that the clock hands hold still as death, time itself keeps on. The most we can hope a watch to do is mark that progress. And since time sets its own tempo, like a heartbeat or an ebb tide, timepieces don't really keep time. They just keep up with it, if they're able.

Dava Sobel,
Longitude,
1995